

# **Synthetic, Biosynthetic and Biological Studies of Specialized Pro-resolving Mediators: Novel Leads in Drug Discovery**

Dissertation for the degree of *Philosophiae Doctor*

By

Jannicke Irina Nesman



Faculty of Mathematics and Natural Sciences

University of Oslo

2020

© **Jannicke Irina Nesman, 2020**

*Series of dissertations submitted to the  
Faculty of Mathematics and Natural Sciences, University of Oslo  
No. 2328*

ISSN 1501-7710

All rights reserved. No part of this publication may be  
reproduced or transmitted, in any form or by any means, without permission.

Cover: Hanne Baadsgaard Utigard.  
Print production: Representralen, University of Oslo.

## **Preface**

The work presented in this thesis was undertaken at the School of Pharmacy, University of Oslo in the period from December 2017 to September 2020. During this time, a sojourn of five weeks was carried out at Barts and The London School of Medicine and Dentistry at Queen Mary University of London, in Professor Jesmond Dalli's group, in 2018. My supervisors through this period have been Professor Trond Vidar Hansen, Associate Professor Anders Vik and Dr. Karoline Gangestad Primdahl. Financial support for my doctorate was given by the School of Pharmacy, University of Oslo, and a travel grant for a research stay abroad was funded by the Norwegian PhD School of Pharmacy.

The thesis is a collection of two papers and one manuscript, presented in a non-chronological order of writing. The papers and manuscript are preceded by an introductory chapter that provides background information and motivation for the work.

## **Acknowledgements**

As this three-year journey at the School of Pharmacy seems to be drawing near to a close, I would like to take the opportunity to express my deepest gratitude to those who have contributed to this work in many ways.

First, I would like to thank my supervisors Professor Trond Vidar Hansen and Associate Professor Anders Vik for welcoming me to the LIPCHEM-group and giving me the opportunity and your trust to take on this challenge. Professor Trond Vidar Hansen's in-depth knowledge of organic chemistry, biology, and the field that we are working in has been invaluable and inspiring. Associate Professor Anders Vik has been a great supporter and contributed with helpful advice throughout this process. Dr. Karoline Gangestad Primdahl deserves a special gratitude, not only as an appreciated supervisor, but over the years we have got to know each other quite well and become friends. I am grateful for all the fun days together in the lab, all the trips we have had together and for all her support.

Dr. Marius Aursnes and Dr. Jørn Tungen deserve a special mention for their contribution to this work. Their outstanding knowledge of organic chemistry, retrosynthetic analysis, and experimental skills have been vital to the scientific work presented herein. The more I have learned over the years, the more questions have arisen along the way, and your time set aside for fruitful discussions and explanations has been highly appreciated.

I would like to thank Dr. Renate Kristianslund, my dear friend and former colleague, for all the work- and non-work-related discussions, for her infinite help and support no matter what, and all

the good times spent together, especially all the wining and dining. Renate is also acknowledged for proof-reading this thesis.

Additionally, I wish to thank other current and former colleagues, all of which have contributed to a fun and motivating work environment: Elvar, Alexander, Amalie, Lars-Inge, Åsmund, Vegard, Nora, Iuliana, Anne and Gunnar.

I sincerely thank Professor Jesmond Dalli for the collaboration and for the opportunity to be a part of his research group and their warm welcome during my stay in London. Gaining new knowledge in the field of biology and experience with several new techniques has been highly educational and appreciated. A travel grant funded by the Norwegian PhD School of Pharmacy making this stay possible is also greatly acknowledged.

Professor Emeritus Karl Egil Malterud is thanked for his help and explanations considering enzymatic incubation studies.

Professor Frode Rise and Dirk Petersen deserves special thanks for maintaining an outstanding NMR-facility.

It is also impossible not to mention Head of Department Henrik Schultz, Professor Rigmor Solberg, Professor Pål Rongved and Halvor Aandal. Thank you all.

I would like to express my appreciation to all my former colleagues at the Norwegian Museum of Science and Technology for the fantastic work environment, your support, and the great times together inside and outside of the museum over the past six years. My supervisors Anne and Laila deserve a special mention for always facilitating my work hours so that I could prioritize my doctoral work whenever needed. Curator Phil Loring is greatly acknowledged for proof-reading this thesis.

I am also very grateful and incredibly privileged to have so many close friends who have always listened and provided their support despite not always understanding what I do for a living. “Syklubben” in Fredrikstad, Nora Kazaale, Vigdis, Linn and Mona should be mentioned for their encouragement throughout my studies and in life.

Lastly, I would like to thank my beloved family in Norway and Finland, especially my mother and father, “bonuspappa” Steinar, and my brother for your never-ending support, your patience and love, which have kept me motivated throughout the years of this work.

Oslo, September 2020

*Jannicke Irina Nesman*

Jannicke Irina Nesman

## Contents

Preface.....	I
Acknowledgements.....	I
List of Papers and Manuscript .....	VII
Abstract.....	IX
Graphical abstracts.....	XI
Abbreviations.....	XIII
Chapter 1 Introduction .....	1
1.1 Introduction to polyunsaturated fatty acids.....	1
1.1.1 Eicosapentaenoic acid, docosahexaenoic acid and n-3 docosapentaenoic acid: chemical structures and biological significance.....	2
1.1.2 Polyunsaturated fatty acids as substrates for lipoxygenase and cyclooxygenase enzymes .....	3
1.1.3 Enzymatic and biochemical oxidations of polyunsaturated fatty acids .....	4
1.2 Inflammation and resolution of inflammation .....	6
1.3 Introduction to oxygenated lipid mediators in inflammation.....	8
1.3.1 Prostaglandins .....	8
1.3.2 Leukotrienes.....	9
1.3.3 Lipoxins .....	10
1.4 Specialized pro-resolving lipid mediators .....	12
1.4.1 E-class resolvins.....	13
1.4.2 Protectins.....	14
1.4.3 N-3 docosapentaenoic acid derived protectins .....	16
1.4.4 Other protectins: the sulfido-conjugates .....	17
1.4.5 Biosynthesis of protectins .....	17
1.4.6 Enzymatic and biochemical oxidations of protectins .....	20
1.5 Receptors activated by specialized pro-resolving lipid mediators.....	21
1.5.1 Resolvin E1 .....	22
1.5.2 Protectin D1 .....	23
1.6 Drug development using specialized pro-resolving mediators .....	23
1.7 Synthetic methods employed in total synthesis of specialized pro-resolving lipid mediators .....	25

1.7.1 Wittig and <i>Z</i> -selective Wittig reactions .....	26
1.7.2 Cross-coupling reactions.....	27
1.7.3 <i>Z</i> -selective reduction of alkynes .....	28
1.7.4 Aldol reactions .....	29
1.8 Literature syntheses of resolvin E1 .....	32
1.9 Literature syntheses of protectins .....	38
1.10 Aim of study .....	43
References.....	44
Chapter 2 Results and discussion.....	52
2.1 Paper I: Synthesis, Structural Confirmation, and Biosynthesis of 22-OH-PD1 <sub>n-3</sub> DPA.....	52
2.1.1 Synthetic strategy towards 22-OH-PD1 <sub>n-3</sub> DPA .....	53
2.1.2 Total synthesis of 22-OH-PD1 <sub>n-3</sub> DPA .....	54
2.1.3 Matching experiments and biosynthetic investigations .....	58
2.1.3 Conclusion .....	60
2.2 Paper II: The synthetic protectin D1 analog 3-oxa PD1 <sub>n-3</sub> DPA reduces neuropathic pain and itching.....	62
2.2.1 Retrosynthetic analysis and strategy.....	63
2.2.2 Total synthesis of 3-oxa PD1 <sub>n-3</sub> DPA and the 17 <i>R</i> -epimer .....	64
2.2.4 Total synthesis of PD1 <sub>n-3</sub> DPA .....	68
2.2.5 Biological evaluations.....	69
2.2.6 Conclusion .....	72
2.3 Biosynthetic studies of 3-oxa PD1 <sub>n-3</sub> DPA .....	73
2.3.1 Initial biosynthetic studies using 3-oxa n-3 DPA .....	73
2.4 Paper III: Stereoselective synthesis of the specialized pro-resolving and anti-inflammatory mediator resolvin E1 .....	75
2.4.1 Retrosynthetic analysis of resolvin E1.....	75
2.4.2 Total synthesis of resolvin E1 .....	76
2.4.3 Matching experiments.....	80
2.4.4 Conclusion .....	80
Chapter 3 Summary and future outlook.....	82
Chapter 4 Conclusions .....	85
References.....	86
Chapter 5 Experimental procedures.....	88

Appendix..... 120





## List of Papers and Manuscript

### Paper I:

*Synthesis, Structural Confirmation, and Biosynthesis of 22-OH-PDI<sub>n-3</sub> DPA*

Jannicke Irina Nesman, Karoline Gangestad Primdahl, Jørn Eivind Tungen, Fransesco Palmas, Jesmond Dalli and Trond Vidar Hansen.

*Molecules*, **2019**, 24 (18), 3228.

### Paper II:

*The synthetic protectin analog 3-oxa-PDI<sub>n-3</sub> DPA reduces neuropathic pain and itching*

Jannicke Irina Nesman, Sangsu Bang, Yul Huh, Ru-Rong Ji, Charles N. Serhan, and Trond Vidar Hansen.

Manuscript

### Paper III:

*Stereoselective synthesis of the specialized pro-resolving and anti-inflammatory mediator resolvin E1*

Jannicke Irina Nesman, Jørn Eivind Tungen, Anders Vik and Trond Vidar Hansen.

*Tetrahedron*, **2020**, 76 (3), 130821.

### Paper not included in the dissertation:

### Paper IV:

*Total synthesis of (-)-Mucosin and Revision of Structure*

Jens Mortansson Nolsøe, Simen Antonsen, Carl Henrik Gørbitz, Trond Vidar Hansen, Jannicke Irina Nesman, Åsmund Kjendseth Røhr and Yngve Stenstrøm.

*J. Org. Chem.* **2018**, 83 (24), 15066.



## Abstract

Over the last decades, extensive efforts have been devoted to gaining knowledge on the cellular and chemical details of the inflammatory process. These efforts have established that resolution of inflammation is regulated by actively and strictly controlled biosynthesis of several distinct families of oxygenated polyunsaturated fatty acids, collectively termed specialized pro-resolving lipid mediators. The potent ability of these compounds to initiate pro-resolving pathways of an active inflammatory process and to promote the return to homeostasis have opened up important new research areas.

Knowledge of the metabolism of the lipid mediators and their structural assignment is necessary when it comes to developing new treatment strategies for inflammatory-related disorders. For this reason, we wanted to investigate the  $\omega$ -oxidation, as part of the metabolism, of the specialized pro-resolving lipid mediator PD1<sub>n-3</sub> DPA. To establish the formation and structure of a C<sub>22</sub> mono-hydroxylated metabolite of PD1<sub>n-3</sub> DPA, a stereoselective synthesis of 22-OH-PD1<sub>n-3</sub> DPA was performed. Biological experiments involving matching between our synthetic material and biosynthetic material confirmed the structure of 22-OH-PD1<sub>n-3</sub> DPA. Additionally, cellular studies showed that 22-OH-PD1<sub>n-3</sub> DPA is produced by  $\omega$ -oxidation of PD1<sub>n-3</sub> DPA in human neutrophils and human monocytes.

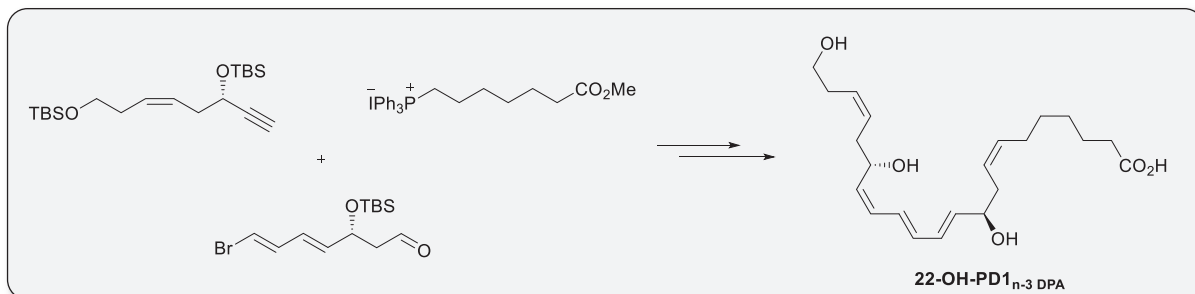
In a continuation of the above work, structural modifications made on PD1<sub>n-3</sub> DPA resulted in the design and synthesis of two analogues, termed 17*S*-3-oxa-PD1<sub>n-3</sub> DPA and 17*R*-3-oxa-PD1<sub>n-3</sub> DPA. These modifications were made on the basis of developing synthetic analogues with increased metabolic stability while still retaining the desirable biological activity of PD1<sub>n-3</sub> DPA. Initial biological experiments showed that 17*S*-3-oxa-PD1<sub>n-3</sub> DPA relieved neuropathic pain and itching *in vivo* with similar potency to PD1<sub>n-3</sub> DPA. Further biological testing of both synthetic analogues is currently ongoing. In addition, a slightly modified total synthesis of PD1<sub>n-3</sub> DPA was achieved.

Several of the synthetic methodologies employed in the above syntheses were used to develop a convergent and stereoselective synthesis of the anti-inflammatory and pro-resolving lipid mediator RvE1. The key steps in this synthesis were the Nagao acetate-aldol reaction, a *Z*-selective Boland reduction and a *Z*-selective Wittig reaction. In addition, the structure of our synthetic material was confirmed by matching experiments with authentic RvE1. Biological evaluations of this material are ongoing.

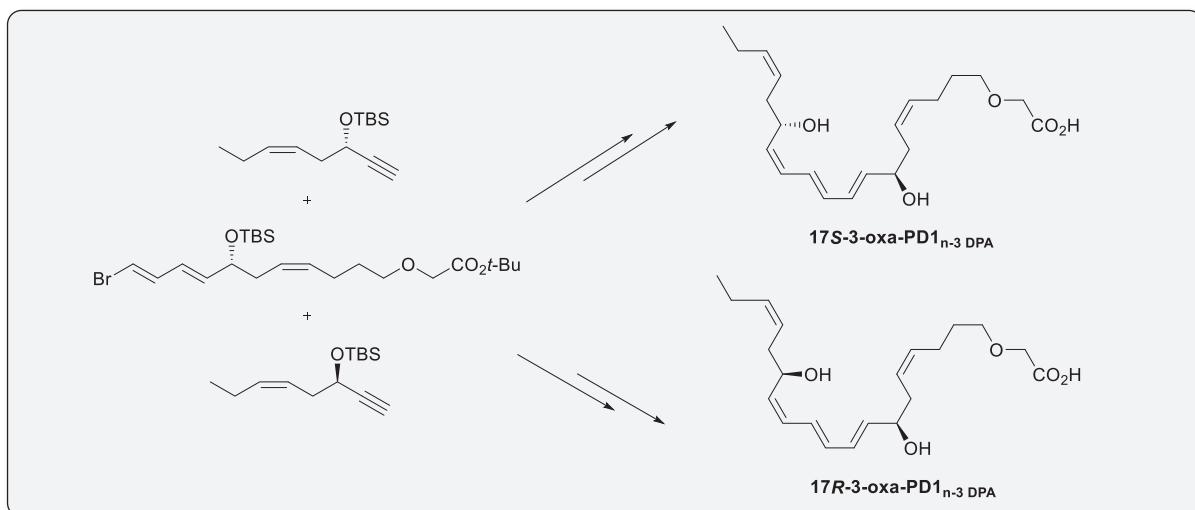


## Graphical abstracts

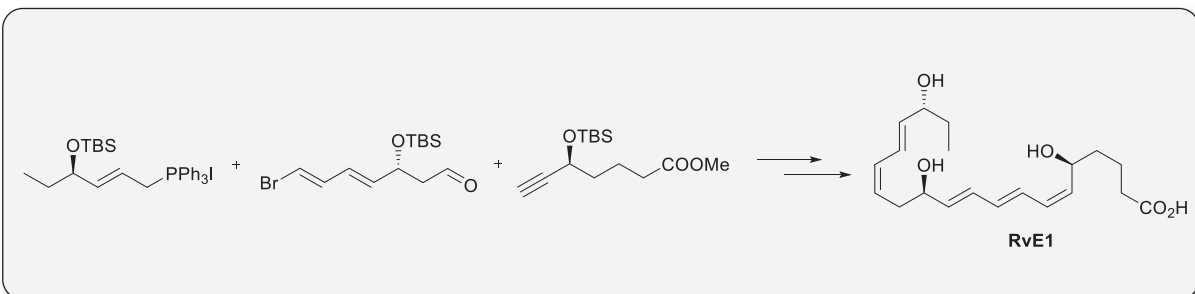
### Paper I:



### Paper II:



### Paper III:





## Abbreviations

9-BBN	9-borabicyclo[3.3.1]nonane
AA	Arachidonic acid ((5Z,8Z,11Z,14Z)-eicosatetraenoic acid)
ALA	Alpha-linolenic acid ((9Z,12Z,15Z)-octadecatrienoic acid)
ALX	A lipoxin receptor
ASA	Acetylsalicylic acid
AT-LX	Aspirin-triggered lipoxin
AT-PD	Aspirin-triggered protectin
BLT	B leukotriene receptor
CAM	Cerium ammonium molybdate
ChemR	Chemerin receptor
CoA	Coenzyme A
COX	Cyclooxygenase
CSA	Camphorsulfonic acid
CTLC	Cutaneous T-cell lymphoma
CYP450	Cytochrome P450 monooxygenase
DDQ	Dichloro-dicyano-benzoquinone
DHA	Docosahexaenoic acid ((4Z,7Z,10Z,13Z,16Z,19Z)-docosahexaenoic acid)
DIAD	Diisopropyl azodicarboxylate
DIBAL-H	Diisobutyl aluminium hydride
DIPT	Diisopropyl tartrate
DMAP	Dimethylaminopyridine
DMP	Dess-Martin periodinane
DMSO	Dimethyl sulfoxide
DPA	Docosapentaenoic acid ((7Z,10Z,13Z,16Z,19Z)-docosapentaenoic acid)
dr	Diastereoselective ratio
EC	Effective concentration
<i>ee</i>	Enantiomeric excess
EPA	Eicosatetraenoic acid ((5Z,8Z,11Z,14Z,17Z)-eicosapentaenoic acid)
<i>epi</i> -PD1	epimer of protectin D1
FAD	Flavin adenine dinucleotide
GPCR	G-protein coupled receptor
GPR	G-protein receptor
HEPE	Hydroxy eicosatetraenoic acid
HMPA	Hexamethylphosphoramide
<i>Hp</i> DHA	Hydroperoxydocosahexaenoic acid
<i>Hp</i> ETE	Hydroperoxyeicosatetraenoic acid
HPLC	High-performance liquid chromatography
IL	Interleukin
IP	Intraperitoneal
IT	Intrathecal

LA	Linoleic acid ((9Z,12Z)-octadecadienoic acid)
LC-MS/MS	Liquid-chromatography tandem mass spectrometry
LDA	Lithium diisopropyl amide
LGR	Leucine G-protein receptor
LLS	Longest linear sequence
LOX	Lipoxygenase
LT	Leukotriene
LX	Lipoxin
Mar	Maresin
MCTR	Maresin conjugates in tissue regeneration
MRM	Multiple reaction monitoring
NAD	Nicotinamide adenine dinucleotide
NaHMDS	Sodium <i>bis</i> (trimethylsilyl)amide
NBS	<i>N</i> -Bromosuccinimide
NPD1	Neuroprotectin D1
NSAID	Non-steroidal anti-inflammatory drug
PCC	Pyridinium chlorochromate
PCTR	Protectin conjugates in tissue regeneration
PD1	Protectin D1
PG	Prostaglandin
PMB	<i>para</i> -Methoxy benzyl
PMN	Polymorphonuclear neutrophil
PPTS	Pyridinium <i>para</i> -toluenesulfonate
PUFA	Polyunsaturated fatty acid
RedAl®	Sodium <i>bis</i> (2-methoxyethoxy)aluminiumhydride
RCTR	Resolvin conjugates in tissue regeneration
RvD	Resolvin of the D-class
RvE	Resolvin of the E-class
RvE1	Resolvin E1
Sia	<i>sec</i> -Isoamyl
SPM	Specialized pro-resolving lipid mediator
TBAF	Tetrabutylammonium fluoride
TBDBS	<i>tert</i> -Butyldiphenylsilyl
TBS	<i>tert</i> -Butyldimethylsilyl
TES	Triethylsilyl
THF	Tetrahydrofuran
TMS	Trimethylsilyl
TsCl	Toluenesulfonyl chloride
TsOH	Toluenesulfonic acid



## Chapter 1 Introduction

### 1.1 Introduction to polyunsaturated fatty acids

Polyunsaturated fatty acids (PUFAs) are important molecules that participate in a number of physiological processes. In addition to being essential structural components of biological membranes, PUFAs serve as precursors to a variety of biologically active signaling molecules.<sup>1-4</sup>

Two major classes of PUFAs are the n-6 and the n-3 unsaturated fatty acids. This classification refers to the position of the first double bond relative to the terminal methyl (n) carbon in the fatty acid chain (Figure 1.1). Linoleic (LA, **1**) and  $\alpha$ -linolenic acid (ALA, **2**) are the simplest n-6 and n-3 PUFAs, respectively. These are essential nutrients that cannot be synthesized by the human body, and thus have to be obtained through the diet.<sup>5, 6</sup>

Once consumed in the diet, the above-mentioned fatty acids can be converted to the longer chain PUFAs. LA (**1**) is a precursor to arachidonic acid (AA, **3**), whereas ALA (**2**) is a precursor to other important n-3 fatty acids, such as eicosapentaenoic acid (EPA, **4**) and docosahexaenoic acid (DHA, **5**).<sup>1</sup>

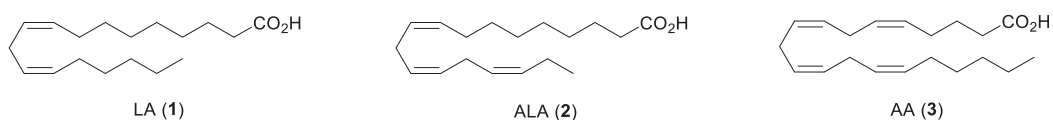
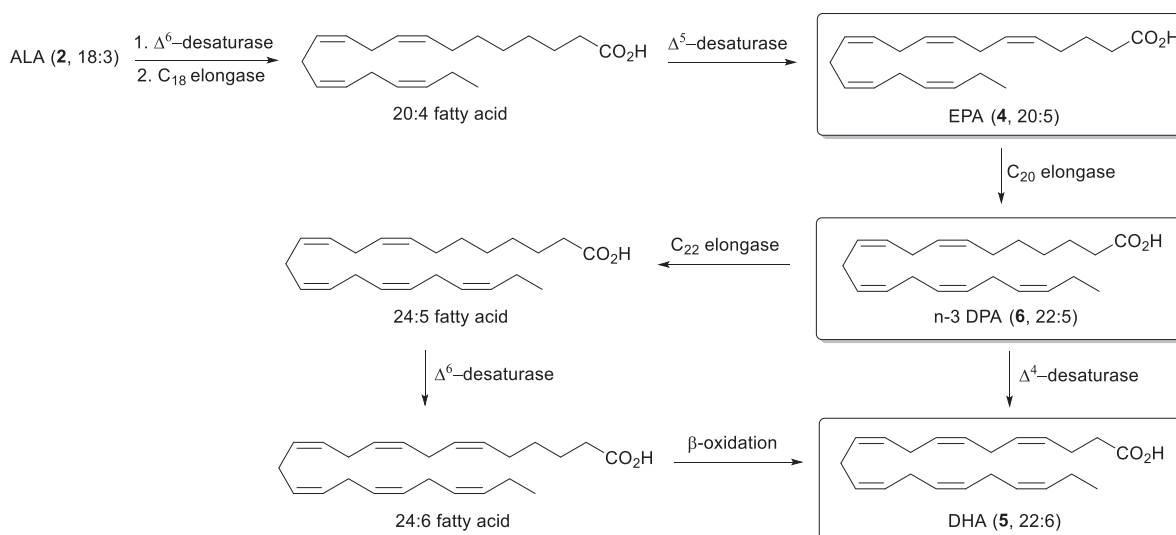


**Figure 1.1** Chemical structure of LA (**1**), ALA (**2**) and AA (**3**).

### 1.1.1 Eicosapentaenoic acid, docosahexaenoic acid and n-3 docosapentaenoic acid: chemical structures and biological significance

In humans, the longer chain n-3 PUFAs are biosynthesized from ALA (**2**) by a consecutive series of enzymatic desaturation and elongation steps. A simplified outline of this process is illustrated in Scheme 1.1. Elongation and desaturation of ALA (**2**) generates EPA (**4**). This fatty acid is further converted to DHA (**5**) via n-3 docosapentaenoic acid (n-3 DPA, **6**) as an intermediate.<sup>7-9</sup> Each elongation step, catalyzed by elongase enzymes, increases the hydrocarbon chain by two carbon units, and the desaturase enzymes introduce *cis* double bonds at specific positions towards the carboxyl end of the fatty acid chain.<sup>10, 11</sup> From PUFA **6**, two alternative pathways for DHA (**5**) biosynthesis have been identified (Scheme 1.1). However, strong evidence suggests that the longest pathway occurs in mammals to give **5** via subsequent elongation and desaturation followed by one cycle of retro-conversion ( $\beta$ -oxidation, see Section 1.4.6).<sup>10</sup>



**Scheme 1.1** Chemical structures and a brief outline of the conversion of EPA (**4**) to DHA (**5**) where n-3 DPA (**6**) is an intermediate.

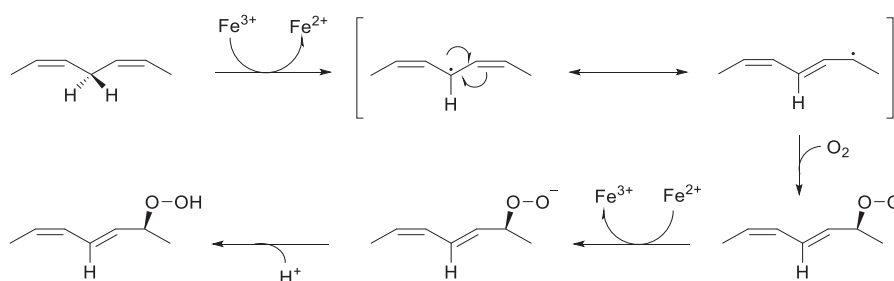
The critical roles of nutritional PUFAs, such as LA (**1**), were first demonstrated in 1929 when the exclusion of fat from the diet of rats led to impaired function and increased mortality.<sup>12, 13</sup> These studies, conducted by George Burr and his wife Mildred Burr, led to the discovery of essential fatty acids.<sup>14</sup> Since then, several studies on humans have documented the importance of consuming n-3 PUFAs, such as EPA (**4**) and DHA (**5**), in treatment and prevention of several inflammatory-related diseases,<sup>1</sup> including cardiovascular disease,<sup>15</sup> rheumatoid arthritis,<sup>16</sup> diabetes type 2,<sup>17</sup> and neurodegenerative diseases.<sup>18</sup> The observed beneficial health effects are associated with the production of, and relationship between, oxygenated n-6 and n-3 PUFAs – compounds that can

regulate inflammatory processes.<sup>19</sup> Enzymes involved in the biosynthetic conversion of PUFAs during inflammatory conditions are discussed in the next section.

### 1.1.2 Polyunsaturated fatty acids as substrates for lipoxygenase and cyclooxygenase enzymes

Two central enzyme groups responsible for the production of physiologically important lipid mediators are lipoxygenases (LOX) and cyclooxygenases (COX), which catalyze the stereoselective incorporation of molecular oxygen in PUFAs.<sup>20-22</sup>

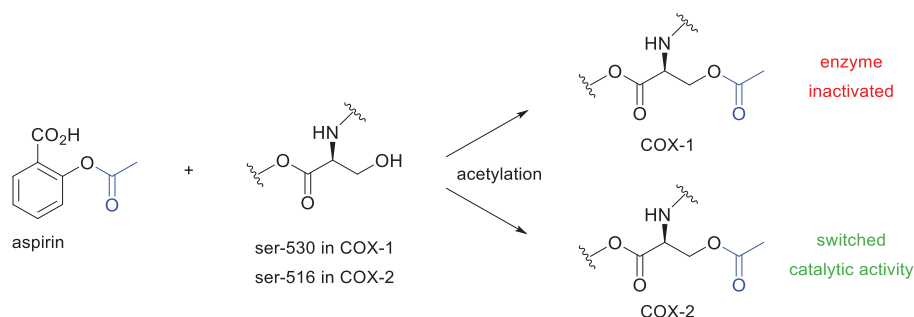
Unlike the two established COX enzymes, which are expressed in most cells, lipoxygenases are primarily active in cells of the immune system.<sup>23</sup> LOX enzymes constitute a family of iron-containing isozymes that catalyze the stereoselective incorporation of molecular oxygen in PUFAs with one or more *cis,cis*-1,4-pentadiene systems to yield predominantly *S*-configured products (Scheme 1.2).<sup>24, 25</sup> The lipoxygenation step is initiated by stereoselective hydrogen radical abstraction, followed by rearrangement via resonance stabilization, oxygen insertion and finally reduction to form a hydroperoxy product.<sup>20</sup> The hydroperoxy products formed can be further enzymatically converted into a variety of biologically active lipid mediators, including leukotrienes, lipoxins, resolvins, maresins and protectins.<sup>26</sup>



**Scheme 1.2** Free radical mechanism for lipoxygenation of a *cis,cis*-1,4-pentadiene system in a PUFA.<sup>20</sup>

There are several different LOX isoforms expressed in humans, including 5-LOX, 12-LOX, 12*R*-LOX, 15-LOX and 12/15-LOX.<sup>22, 23</sup> The different isoforms are classified according to the position where oxygen is incorporated into the chain of AA (**3**).<sup>22, 23</sup> However, for scientists not working in the LOX field, this nomenclature may turn out to be confusing and misleading. To clarify, the human genome contains six functional LOX genes that encode for six different LOX-isoforms, and gene nomenclature is increasingly being employed when referring to a specific isoenzyme.<sup>22</sup>

Cyclooxygenases are enzymes involved in the conversion of AA (**3**) into the endoperoxide prostaglandin H<sub>2</sub> (PGH<sub>2</sub>, **14**, Section 1.3.1), which is an intermediate in the biosynthesis of various eicosanoids, including the prostaglandins (PGs) and thromboxanes.<sup>27</sup> COX-1 and COX-2 are two COX isoforms identified. COX-1, which is expressed in most cells, catalyzes the formation of PGs that are important for normal cellular functions, whereas COX-2 is expressed as a response to inflammation and are involved in the formation of the pro-inflammatory PGs.<sup>27</sup> Selective inhibition of COX-2 by non-steroidal anti-inflammatory drugs (NSAIDs) is therefore preferable to relieve inflammatory symptoms like fever and pain. However, recent studies have shown that inhibition of COX-2 with NSAIDs delays resolution of inflammation due to the important roles of certain PGs in the lipid mediator class switch, a process further explained in Section 1.3.3.<sup>28</sup> For this reason, many NSAIDs are considered toxic to this crucial process (i.e. resolution toxic). On the contrary, treatment with the NSAID aspirin, also known as acetylsalicylic acid (ASA), is different. The mechanism of action by ASA is illustrated in Scheme 1.3, and involves covalent modification of the serine residues 530 and 516 in the active site of COX-1 and COX-2, respectively. Acetylation of these side-chains prevents the correct alignment of AA (**3**) within the enzymes' active site, and thus inhibits the formation of AA-derived eicosanoids. Unlike COX-1, the catalytic region of COX-2 remains active to produce lipoxygenase-like products from PUFA **4-6** (Scheme 1.1), but with the oxygen insertion in the opposite *R*-configuration rather than *S*, resulting in oxygenated lipid mediators with anti-inflammatory and pro-resolving properties.<sup>29-31</sup>



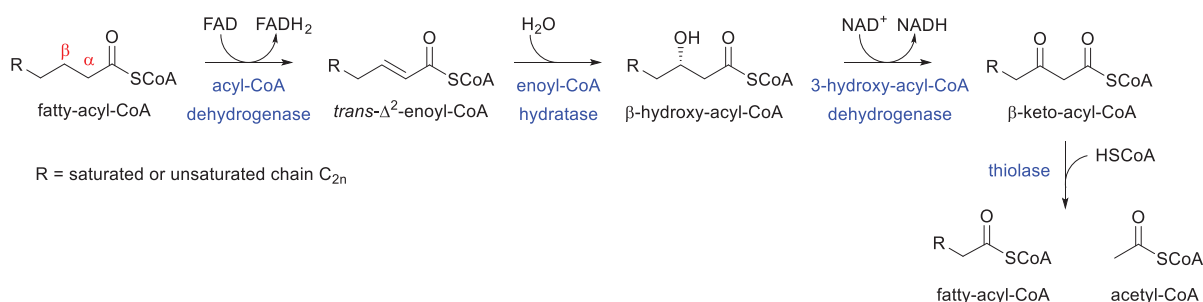
**Scheme 1.3** Illustration of aspirin-acetylation of serine residues in the catalytic site of COX-1 and COX-2.

### 1.1.3 Enzymatic and biochemical oxidations of polyunsaturated fatty acids

Fatty acids are stored in the body as triglycerides or phospholipids, which are released upon enzymatic hydrolysis and can be degraded to produce energy. Fatty acid degradation mainly occurs through a process called  $\beta$ -oxidation.<sup>11, 32</sup>

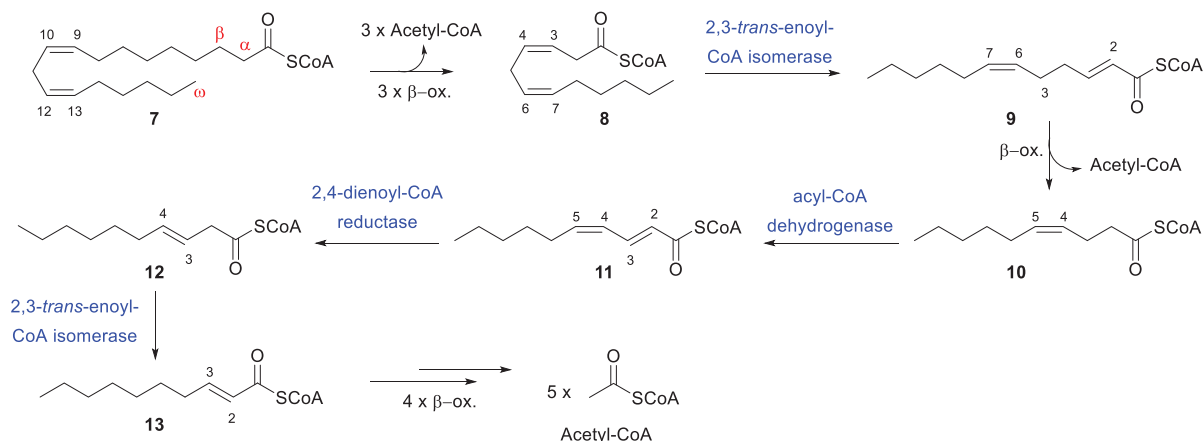
In this process, the fatty acid is activated as a fatty-acyl-coenzyme A (CoA) and transported from the cytosol to the inner matrix of the mitochondria where  $\beta$ -oxidation occurs. The four steps in the

oxidation cycle with associated catalyzing enzymes are outlined in Scheme 1.4. Following dehydrogenation and stereoselective hydration, the fatty acyl-CoA is oxidized at the  $\beta$ -carbon to form a ketone. In the final step, addition of coenzyme A (HSCoA) cleaves the bond between the  $\alpha$ - and  $\beta$ -carbons in  $\beta$ -keto-acyl-CoA, catalyzed by a thiolase, resulting in a fatty-acyl-CoA shortened by two carbon units and acetyl-CoA. Other products formed from one cycle of  $\beta$ -oxidation are the reduced form of the coenzymes flavin adenine dinucleotide (FAD) and nicotinamide adenine dinucleotide (NAD).<sup>32</sup>



**Scheme 1.4** Outline of one cycle of  $\beta$ -oxidation of a fatty-acyl-CoA.

For saturated fatty acids, the cycle in Scheme 1.4 is repeated until only two acetyl-CoA units are produced in the final step. When the fatty-acyl-chain is unsaturated, the location of a *cis*-double bond may occur at three-carbon intervals, whereas the substrates in the  $\beta$ -oxidation cycle have *trans*-double bonds in conjugation to the carbonyl group.<sup>32</sup> In these situations, two additional enzymes are required in the process, namely 2,3-*trans*-enoyl-CoA isomerase and 2,4-dienoyl-CoA reductase, as illustrated in Scheme 1.5. These enzymes catalyze the transformation of a *cis*-double bond into a *trans*-double bond in the correct position for the  $\beta$ -oxidation to continue. When the oxidation cycle eventually reaches a new *cis*-double bond in  $C_3$ -position, the additional steps in Scheme 1.4 are repeated.<sup>33</sup>



**Scheme 1.5**  $\beta$ -oxidation of linoleoyl-CoA (7).<sup>33</sup>

## 1.2 Inflammation and resolution of inflammation

Inflammation is an innate, protective response by the body's immune system to harmful stimuli or invading pathogens.<sup>34</sup> The function of inflammation is to remove the cause of injury, followed by tissue repair and restoration of function of the affected tissue.<sup>35</sup>

The inflammatory response is a highly complex and strictly coordinated biochemical cascade of events.<sup>36</sup> Figure 1.2 illustrates the duration of an acute inflammatory response and the resolution process. Following a microbial infection or tissue injury, pro-inflammatory mediators, such as chemokines, cytokines and AA-derived eicosanoids (i.e. leukotriene B<sub>4</sub> and prostaglandin E<sub>2</sub>), are produced by resident cells. These mediators stimulate vasodilation and vessel wall permeability with concomitant recruitment and influx of leukocytes from the blood by chemotaxis, causing edema.<sup>26, 34, 36</sup> Polymorphonuclear neutrophils (PMNs) are the predominant first responders of white blood cells required to eliminate invading pathogens and to remove damaged tissue by phagocytosis. Nonetheless, destructive agents from the PMNs, intended to kill or neutralize invaders, can accidentally spill into the surrounding tissue and cause collateral damage, which further increases the pro-inflammatory response in the stage known as acute inflammation.<sup>37</sup> This biochemical response causes the classic signs of inflammation known as redness, heat, swelling and pain.<sup>38</sup>

Once the injuring stimulus has been removed, the inflammatory response needs to be terminated. Termination of ongoing inflammation is initiated by lipid mediator class switching.<sup>26, 39</sup> This involves a transition in the biosynthesis of pro-inflammatory eicosanoids towards anti-inflammatory and pro-resolving mediators that effectively promote resolution. The time between peak inflammatory cell infiltration and the clearance of these cells and cellular debris from the tissue site, leading to restoration of tissue homeostasis, is defined as resolution (Figure 1.2).<sup>36</sup> This

phase is characterized by the limitation of neutrophil infiltration and the removal of apoptotic PMNs and debris through efferocytosis by monocyte-derived macrophages.<sup>39, 40</sup>

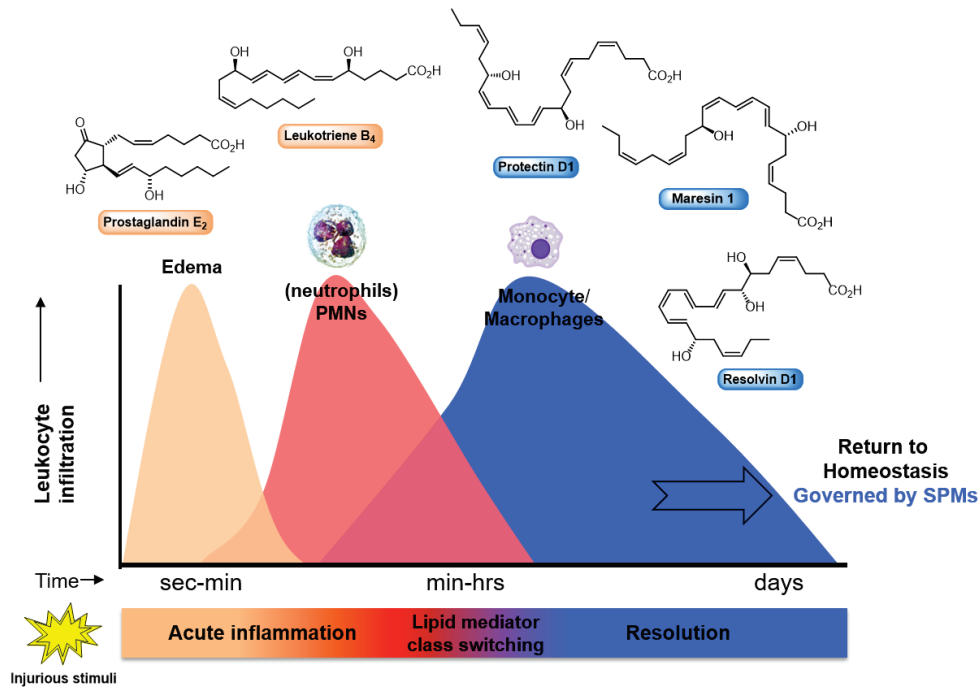


Figure 1.2 Outline of an acute inflammatory response from initiation to resolution.<sup>41</sup>

Non-resolving inflammation results in an ongoing immune response that may develop into chronic inflammatory disorders.<sup>3, 41</sup> It has been recognized that chronic inflammation is an underlying factor in the progression of a variety of diseases, including cardiovascular disease, diabetes, asthma and neurodegenerative diseases. Several reviews have been published on this subject during the last years.<sup>26, 28, 42-45</sup>

Like the onset, resolution of inflammation is an active and highly regulated process controlled by locally produced mediators.<sup>28, 46</sup> Several distinct families of anti-inflammatory and pro-resolving mediators derived from n-3 PUFAs have been discovered, such as the resolvins, protectins and maresins, collectively termed specialized pro-resolving lipid mediators (SPMs). These compounds are agonists in resolution and mediate their actions through G-protein coupled receptors (GPCRs), thereby actively stimulating resolution programs to limit the inflammatory response, promote tissue restoration and enable regaining of physiology or function.<sup>28</sup> Thus, advances in the understanding of the mechanisms in resolution pathways and the lipid mediators involved can provide new insight into the cause of chronic disorders and may contribute to the development of pro-resolution therapeutics in treatment of chronic inflammatory diseases.<sup>28, 36</sup>

## 1.3 Introduction to oxygenated lipid mediators in inflammation

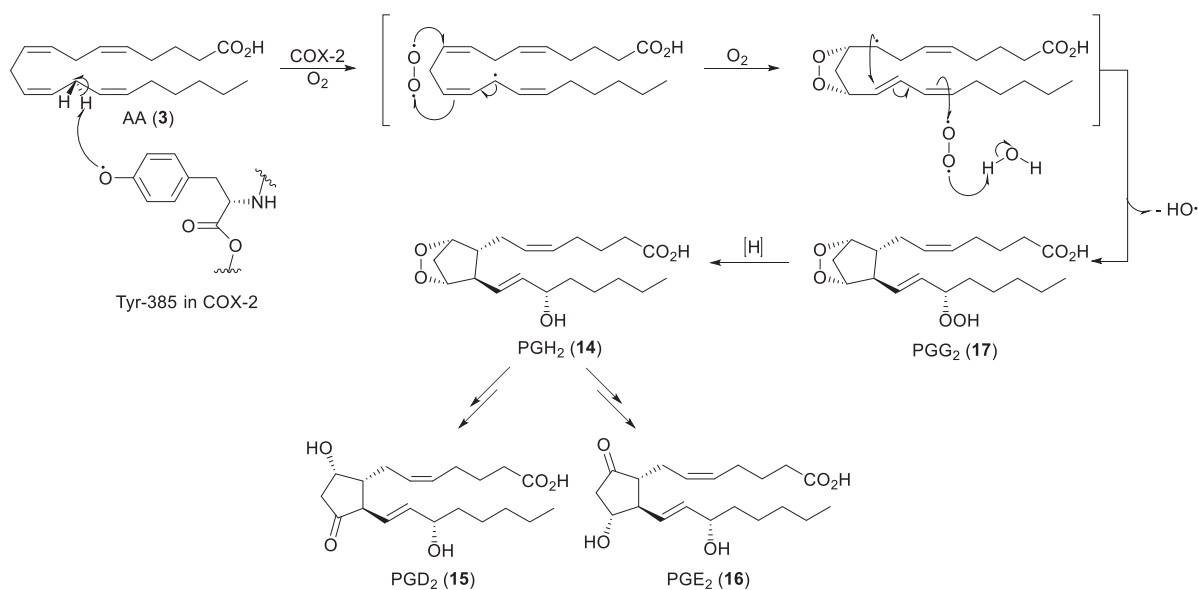
Inflammatory processes are regulated by several types of signaling compounds derived from the oxygenation of PUFAs. As previously stated, PUFAs are key components of biological membranes, and they are stored as esters in the phospholipid barrier of cells and organelles. During the course of an inflammatory response, stored PUFAs are released from the membrane and enzymatically converted into different classes of oxygenated bioactive lipid metabolites.<sup>47-49</sup> This section will discuss metabolites derived from AA (**3**), namely the prostaglandins (PGs), leukotrienes (LTs) and lipoxins (LXs), collectively known as the classical eicosanoids. Metabolites derived from n-3 PUFAs are presented in the subsequent section.

### 1.3.1 Prostaglandins

Prostaglandins are formed by most cells in human tissue and are synthesized locally in order to sustain homeostatic functions. At very low concentrations, PGs act as vasodilators, suppress blood platelet aggregation, inhibit gastric acid secretion and regulate contractions of smooth muscle, in addition to playing a key role in modulation of the inflammatory response.<sup>2, 27, 50, 51</sup>

Biosynthesis of the PGs is significantly increased during the early stages of inflammation, and involves the sequential oxidation and reduction of membrane released AA (**3**) by COX-2 (Scheme 1.6).<sup>27, 52</sup> In the cyclooxygenase pathway, a phenol radical on tyrosine residue 385 in the enzyme's active site removes a hydrogen atom from the 13-position in AA (**3**), resulting in a radical that combines with molecular oxygen to form a cyclic endoperoxide.<sup>53, 54</sup> Insertion of another oxygen molecule at C<sub>15</sub> followed by reduction of the resulting hydroperoxy group forms PGH<sub>2</sub> (**14**). This short lived intermediate can then be converted to all the 2-series of prostaglandins, including PGD<sub>2</sub> (**15**) and PGE<sub>2</sub> (**16**), via cell-specific prostaglandin synthases.<sup>55</sup>



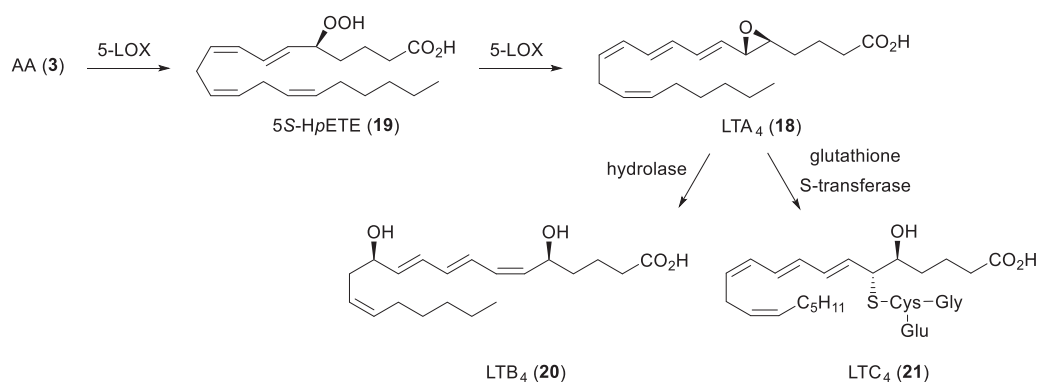


**Scheme 1.6** Outline of the biosynthesis of PGD<sub>2</sub> (**15**) and PGE<sub>2</sub> (**16**) catalyzed by COX-2.

Once produced, the pro-inflammatory PGs elicit the cardinal signs of inflammation, such as redness and edema, which are caused by an increased blood flow to the inflamed tissue and infiltration of leukocytes with the blood stream.<sup>27</sup> Later on in the inflammatory process, PGE<sub>2</sub> (**16**) and PGD<sub>2</sub> (**15**) are able to upregulate the expression of enzymes necessary for LX biosynthesis, thereby inducing the lipid mediator class switching and initiating the termination of acute inflammation (see Section 1.3.3).<sup>56</sup>

### 1.3.2 Leukotrienes

The leukotrienes are a class of pro-inflammatory mediators produced in the early stage of inflammation (Scheme 1.7). In this process, AA (**3**) is transformed into the epoxide leukotriene A<sub>4</sub> (LTA<sub>4</sub>, **18**) via 5*S*-HpETE (**19**) as an intermediate by the sequential actions of 5-LOX.<sup>2, 57</sup> Intermediate **18** can then undergo hydrolysis to yield leukotriene B<sub>4</sub> (LTB<sub>4</sub>, **20**), or conjugation with glutathione to form leukotriene C<sub>4</sub> (LTC<sub>4</sub>, **21**), catalyzed by a hydrolase and LTC<sub>4</sub> synthase (glutathione S-transferase), respectively.<sup>2</sup> Unlike the prostaglandins, LTs are predominantly produced by inflammatory cells, such as polymorphonuclear leukocytes, and were hence given the name *leukotrienes*.<sup>2</sup> The last part of the name refers to the conjugated triene moiety in these compounds.<sup>58</sup>



**Scheme 1.7** Outline of the biosynthesis of the leukotrienes LTA<sub>4</sub> (**18**), LTB<sub>4</sub> (**20**) and LTC<sub>4</sub> (**21**).

The LTs mediate their pro-inflammatory actions by interacting with distinct G-protein coupled receptors (GPCRs) on the cell surface of leukocytes. Upon receptor binding, LTB<sub>4</sub> (**21**) elicits a chemotactic response in addition to inducing adhesion of leukocytes on endothelial cells, thus facilitating rapid recruitment and transmigration of white blood cells, primarily neutrophils, into the inflamed tissue. The cysteinyl-containing leukotrienes induce increased vascular permeability, smooth muscle contraction and recruitment of eosinophils in inflammatory diseases, such as asthma.<sup>2, 59-61</sup>

### 1.3.3 Lipoxins

A third class of bioactive AA-derived eicosanoids is the lipoxins. These mediators were the first of a growing number recognized to have anti-inflammatory and pro-resolving properties,<sup>62</sup> initially identified in 1984 as a product formed by the actions of 15-LOX on AA (**3**).<sup>63, 64</sup> Unlike PGs and LTs that accelerate inflammatory processes, LXs are known to counter-regulate this process and to initiate resolution of ongoing inflammation. Lipoxins, including lipoxin A<sub>4</sub> (LXA<sub>4</sub>, **22**) and lipoxin B<sub>4</sub> (LXB<sub>4</sub>, **23**, Figure 1.3), are able to prevent neutrophil migration and accumulation to inflamed tissue and to induce neutrophil apoptosis.<sup>65, 66</sup> LXs have also proved to recruit and activate macrophages to phagocytize dead cells and debris, which is essential to avoid tissue damage and to resolve ongoing inflammation.<sup>66</sup> Similar bioactions have been reported for the aspirin-triggered lipoxins, which are formed in the presence of aspirin-acetylated COX-2 (AT-LXA<sub>4</sub>, **24** and AT-LXB<sub>4</sub>, **25**, Figure 1.3).<sup>67-69</sup>

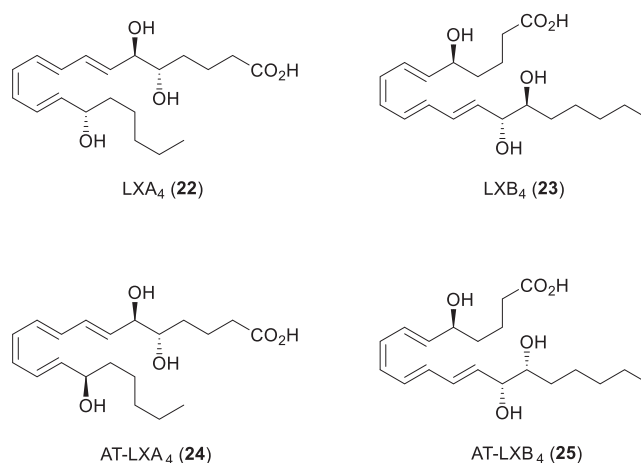


**Figure 1.3** Structures of LXA<sub>4</sub> (22) and LXB<sub>4</sub> (23) and their aspirin-triggered forms (AT-LXA<sub>4</sub> (24) and AT-LXB<sub>4</sub> (25)).

Lipoxins are the first SPMs locally produced during the onset of an inflammatory process.<sup>70</sup> Notably, they are formed as a consequence of PGE<sub>2</sub> (16) and PGD<sub>2</sub> (15) promoting the expression of 15-LOX, which is a key initiating enzyme in LX biosynthesis.<sup>39, 56</sup> PGE<sub>2</sub> (16) also has the ability to inhibit COX-activity and thus counteract the enhancement of acute inflammation by blocking PG synthesis. This process ultimately results in a switch from the production of pro-inflammatory to pro-resolving lipid mediators.<sup>56</sup> In this way, physiological inflammation programs its own resolution. Inhibition of COX-2 with NSAIDs leading to inhibition of PG biosynthesis therefore delays resolution due to the important roles of certain PGs in the lipid mediator class switch.<sup>28</sup>

## 1.4 Specialized pro-resolving lipid mediators

Extensive research over the last two decades has established the inflammatory response to be an active self-limited process, and not passive as previously believed.<sup>37, 46, 71, 72</sup> In 2000, Professor Charles N. Serhan and co-workers at Harvard Medical School were the first to demonstrate that resolution of inflammation is characterized by active biosynthesis of n-3 PUFA-derived lipid mediators, the SPMs.<sup>73, 74</sup> The discovery of SPMs is of particular interest, since these mediators provide the first molecular basis for the many health beneficial effects associated with n-3 PUFA consumption.<sup>26</sup> Resolvins, maresins and protectins are three chemically distinct SPM-families formed by stereoselective enzymatic oxygenation of PUFA 4-6 (Figure 1.4). The E-class of resolvins are derived from EPA (4), whereas the D-class of resolvins, protectins, and maresins as well as the recently described sulfido-conjugated-resolvins, -protectins, and -maresins (RCTRs, PCTRs and MCTRs) are all derived from DHA (5). SPMs that originate from n-3 DPA (6) include n-3 DPA-resolvins, -protectins, and -maresins.<sup>75</sup>

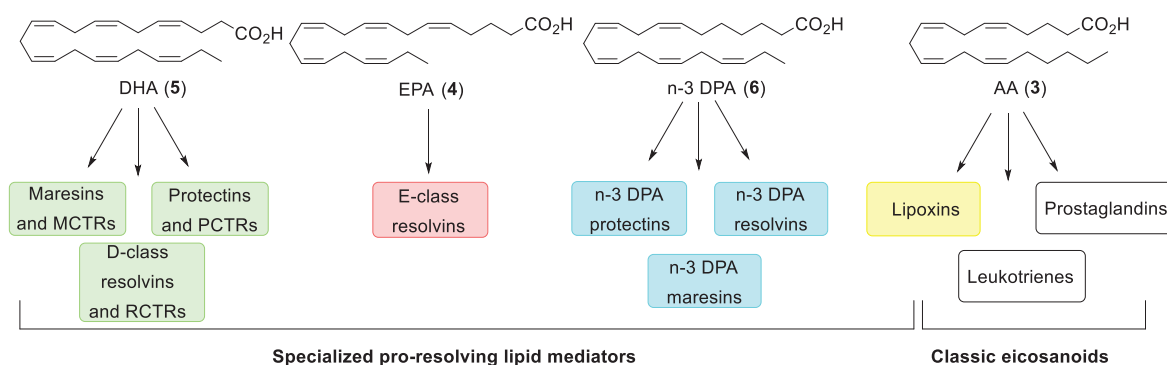


**Figure 1.4** Overview over the distinct SPM-families and classical eicosanoids derived from DHA (5), EPA (4), n-3 DPA (6) and AA (3).<sup>75, 76</sup>

The SPMs are locally produced with the leukocyte exudate traffic and regulate the resolution phase of ongoing inflammation. The key defined biological functions for all SPMs include cessation of neutrophil infiltration to the site of inflammation and thereby reducing PMN-mediated tissue damage, and increasing clearance of apoptotic cells and debris by activated macrophages through efferocytosis. Moreover, the SPMs act via specific receptors as potent agonists in a stereoselective fashion, thus minor differences in the configuration of these lipid mediators can result in considerable changes in their potency.<sup>77</sup>

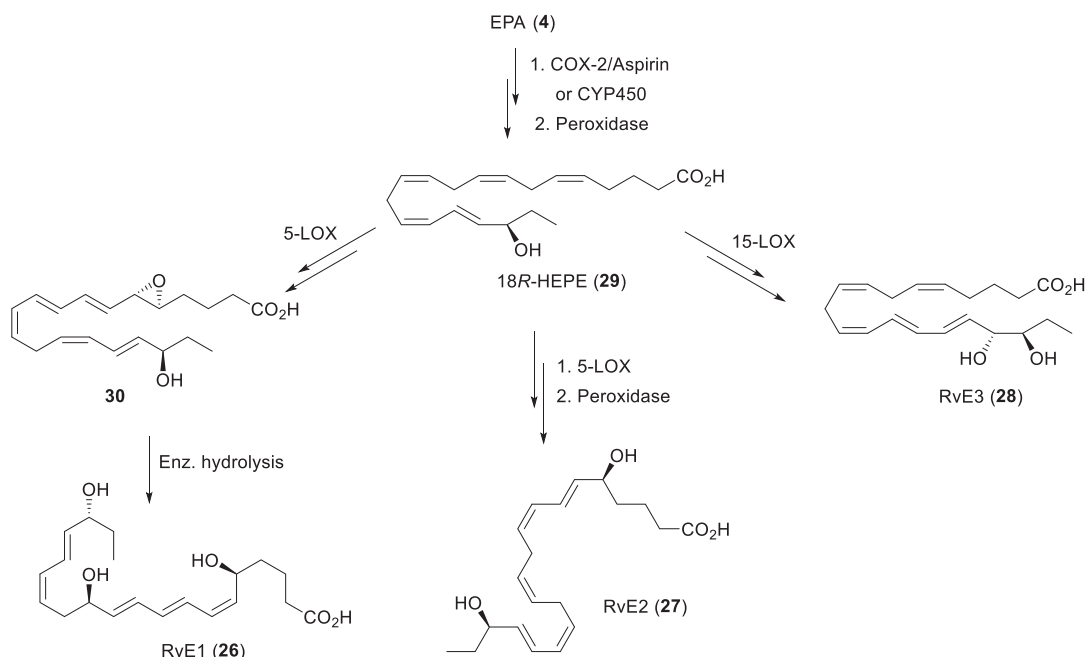
To gain knowledge of biological functions that may be therapeutically beneficial, exact determination of each SPM chemical structure is essential. Liquid-chromatography tandem mass spectrometry (LC-MS/MS) based lipidomics is an extensively used method for the structure elucidation of lipid metabolites isolated from inflammatory exudates, human cells and human

tissue.<sup>19, 29, 77, 78</sup> Matching retention times and fragmentation patterns of biological material with material prepared by stereoselective synthesis has enabled the exact structure assignment and biological evaluations of a number of SPMs, including those presented in the following sections.

#### 1.4.1 E-class resolvins

In 2000, resolvin E1 (RvE1, **26**) was the first n-3 PUFA derived SPM reported.<sup>79</sup> This compound was found to be biosynthesized in resolving inflammatory exudates from mice that were treated with EPA (**4**) and aspirin, which provided the first evidence of the beneficial health effects of EPA on a molecular level.<sup>74, 79</sup> The name resolvin was assigned to this compound due to its pro-resolving actions in the resolution phase of inflammation.<sup>74</sup> Matching experiments with synthetic standards have later confirmed the potent anti-inflammatory and pro-resolving bioactions of RvE1 (**26**), and the absolute configuration of the carbinols present in the structure was assigned 5*S*,12*R*,18*R*.<sup>80</sup> After the discovery of RvE1 (**26**), two EPA-derived resolvins were later identified and termed RvE2 (**27**) and RvE3 (**28**).<sup>81, 82</sup>

The three resolvins can be generated from the common precursor 18*R*-HEPE (**29**), which is formed from EPA (**4**) in the presence of aspirin acetylated COX-2 or cytochrome P450 (CYP450) as illustrated in Scheme 1.8.<sup>83, 84</sup> In human PMNs, the sequential actions of 5-LOX on intermediate **29**, followed by enzymatic hydrolysis of the resulting epoxide **30** on C<sub>12</sub> produce RvE1 (**26**), whereas RvE2 (**27**) can be formed by the action of 5-LOX on **29** followed by reduction.<sup>85</sup> In the case of RvE3 (**28**) formation, insertion of molecular oxygen at C<sub>17</sub> in **29** via the 15-LOX pathway results in a *R*-configured hydroperoxy intermediate that is reduced to the corresponding alcohol.<sup>84</sup> The enantiomer of intermediate **29**, 18*S*-HEPE, has also proved to be endogenously produced and subsequently converted to the 18*S*-epimers of RvE1-RvE3 in parallel biosynthetic pathways as those presented below.<sup>82, 84, 85</sup>



**Scheme 1.8** Outline of the biosynthesis of the E-class resolvins.

In addition to the collectively defined bioactions of the SPMs, the E-class of resolvins has shown potent actions in reducing inflammatory pain, and RvE1 (**26**) has effectively treated periodontal inflammation in animal models.<sup>81, 86</sup> For example, RvE1 (**26**) both diminished inflammation and promoted tissue restoration in a rabbit model of periodontitis, which is a chronic bacterial-induced gum condition that results in loss of connective tissue attached to the teeth and subsequent tooth loss.<sup>87, 88</sup> There are two additional series of resolvins identified, which include mediators derived from DHA (**5**) known as the D-class resolvins (RvD) and n-3 DPA-derived resolvins that possess anti-inflammatory and pro-resolving properties.<sup>74, 89</sup>

### 1.4.2 Protectins

In 2002, a new family of DHA-derived SPMs formed in murine inflammatory exudates and human PMNs was discovered by the Serhan group.<sup>74, 90</sup> In this study, the most prominent product identified was consistent with a dihydroxylated fatty acid termed protectin D1 (PD1, **31**). The name was given this compound due to its highly protective properties during inflammation, its DHA-origin and the number 1 for its originality. PD1 is also referred to as neuroprotectin (NPD1) when it is produced in the nervous system.<sup>91</sup> PD1 (**31**) has been found in many tissues, such as the retina, the lungs and the brain, and its biological properties have been widely investigated.<sup>26, 92</sup> In

addition to the fundamental anti-inflammatory and pro-resolving actions defined for the SPMs, PD1 (**31**) are able to promote regeneration of corneal nerves and restoration of corneal sensitivity in eye inflammation,<sup>93</sup> to protect against diabetic kidney disease,<sup>94</sup> and to effectively prevent neuropathic pain induced by nerve trauma (e.g. surgery).<sup>95</sup> Additionally, PD1 (**31**) has been found to be generated in pulmonary tissue and to dampen airway inflammation.<sup>96</sup>

The protectin family of SPMs is chemically characterized by a conjugated *E,E,Z*-triene moiety flanked by two chiral secondary allylic alcohols positioned at C<sub>10</sub> and C<sub>17</sub>, and this molecular template has proved to be critical for potent functions (Figure 1.5).<sup>97</sup> The exact structure of PD1 (**31**) was elucidated by matching endogenously produced material with several related isomers prepared by organic synthesis. Consequently, the structure was determined as 10*R*,17*S*-dihydroxydocosa-4*Z*,7*Z*,11*E*,13*E*,15*Z*,19*Z*-hexaenoic acid.<sup>92</sup> In subsequent investigations, the  $\Delta^{15}$ -*trans* isomer of PD1 demonstrated to be inactive towards reducing human PMN transmigration *in vitro*, and the 10*S*,17*R*-enantiomer of PD1 was inactive towards regulating neutrophil infiltration in murine peritonitis, which emphasizes the important role of the double bond geometry and absolute configurations of the carbinols in maintaining biological activity.<sup>26, 92</sup> Aspirin-triggered PD1 (AT-PD1, **32**) is a 17*R*-epimer of PD1 (Figure 1.5) produced from DHA (**5**) in the presence of aspirin-acetylated COX-2. AT-PD1 (**32**) shares many of the anti-inflammatory and pro-resolving properties with its isomer PD1 (**31**), including reduction of PMN infiltration, and enhanced apoptotic cell clearance by macrophage efferocytosis.<sup>29, 98</sup>

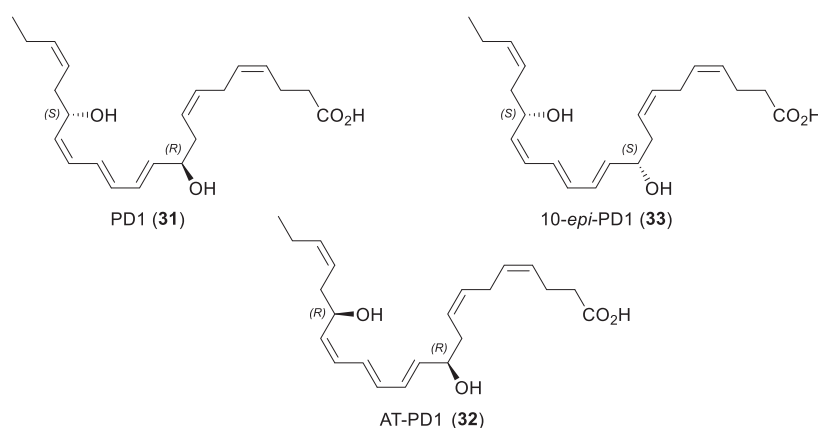


**Figure 1.5** Chemical structures of PD1 (**31**), AT-PD1 (**32**) and 10-*epi*-PD1 (**33**).

Another PD1-epimer with a 10*S*-configuration was synthesized during the stereochemical assignment of PD1 (**31**), depicted as 10-*epi*-protectin D1 (10-*epi*-PD1, **33**) in Figure 1.5. Although this compound was a minor product found in human PMN extracts, it is interesting to note that 10-*epi*-PD1 (**33**) was the most potent down-regulator of PMN infiltration in murine peritonitis experiments compared to several synthetic isomers tested *in vivo*, including PD1 (**31**).<sup>92</sup>

### 1.4.3 N-3 docosapentaenoic acid derived protectins

In 2013, Dalli and co-workers reported that n-3 DPA (**6**) was converted by human leukocytes to a novel class of SPMs during inflammation and resolution of inflammation.<sup>99</sup> The structures of these SPMs were elucidated based on UV and LC-MS/MS-based profiling and reported to share the same structural features as the D-class resolvins, protectins and maresins, except the Z-double bond between C<sub>4</sub> and C<sub>5</sub> (Figure 1.6).<sup>99</sup> Although minor changes in the structural properties of the SPMs can be of functional significance, the n-3 DPA-derived lipid mediators have proved to exert the same potent bioactions as reported for the corresponding DHA-derived analogues.<sup>75, 99</sup> The structures of some of these compounds are presented in Figure 1.6, including resolvin RvD1<sub>n-3</sub> DPA, **34**), maresin 1 n-3 DPA (Mar1<sub>n-3</sub> DPA, **35**), protectin D1 n-3 DPA (PD1<sub>n-3</sub> DPA, **36**) and protectin D2 n-3 DPA (PD2<sub>n-3</sub> DPA, **37**). Our group has reported total syntheses of SPM **34**, **35**, **36** and **37**.<sup>100-103</sup> Of note, the stereochemical assignment for naturally occurring **37** is proposed based on biogenic evidence and has not yet been confirmed by matching studies between endogenous and synthetic material.<sup>104</sup>

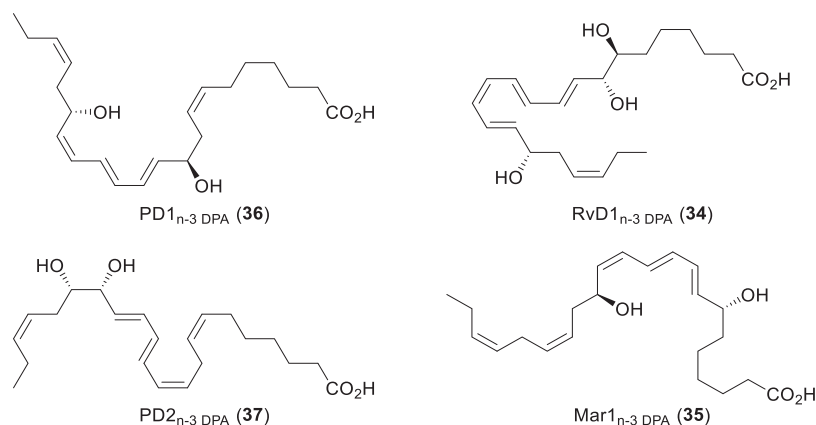


**Figure 1.6** Chemical structures of RvD1<sub>n-3</sub> DPA (**34**), Mar1<sub>n-3</sub> DPA (**35**), PD1<sub>n-3</sub> DPA (**36**) and PD2<sub>n-3</sub> DPA (**37**).

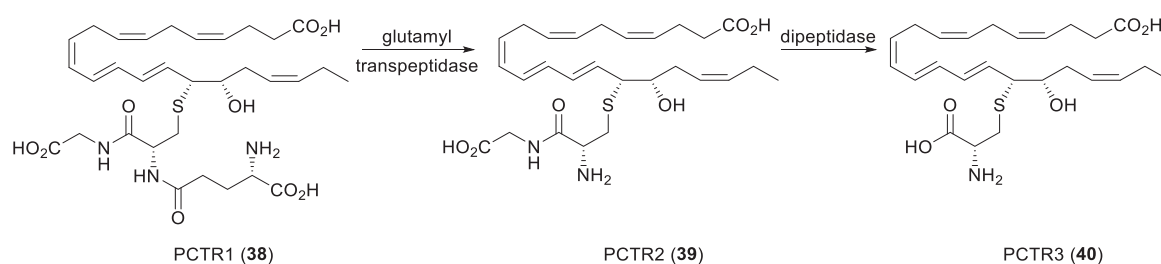
PD1<sub>n-3</sub> DPA (**36**) and PD2<sub>n-3</sub> DPA (**37**) are members of the n-3 DPA-derived protectin family of SPMs. The latter compound was identified as an anti-inflammatory and pro-resolving lipid mediator formed from the same biosynthetic intermediate as SPM **36** and named accordingly.<sup>99</sup> PD1<sub>n-3</sub> DPA (**36**) was prepared by organic synthesis in 2014, and the two carbinol atoms were assigned to be 10*R* and 17*S* configured by matching studies.<sup>101</sup> Additionally, the potent anti-inflammatory and pro-resolving actions of PD1<sub>n-3</sub> DPA (**36**) were confirmed, including significant attenuation of neutrophil recruitment to inflamed tissue and stimulation of human macrophage phagocytosis and efferocytosis.<sup>101</sup> Moreover, the first evidence that PD1<sub>n-3</sub> DPA (**36**) regulates neuroinflammation was recently published.<sup>105</sup> In this study, using a mice model of epilepsy, SPM **36** demonstrated to



promote resolution of neuroinflammation and to arrest epileptogenesis, resulting in a significant reduction in the number of and time spent in epileptic seizures.<sup>105</sup>

#### 1.4.4 Other protectins: the sulfido-conjugates

In 2014 and 2015, Serhan and collaborators identified three new classes of peptide-conjugated SPMs in *Escherichia coli* (*E.coli*) infected mice, human spleen and human blood from sepsis patients.<sup>106, 107</sup> These compounds, coined the resolvin- (RCTR), maresin- (MCTR) and protectin- (PCTR) conjugates in tissue regeneration, were shown to accelerate tissue repair and tissue regeneration on injured planarian (a type of flatworm), in addition to possessing anti-inflammatory and pro-resolving bioactions with human cells *in vitro*.<sup>106, 107</sup> The protectin conjugates involved in tissue regeneration include PCTR1-PCTR3 (**38-40**).<sup>107</sup> The proposed biosynthetic conversion of peptide conjugate **39** and **40** from **38** is outlined in Scheme 1.9. PCTR1 (**38**) in the presence of  $\gamma$ -glutamyl transpeptidase generates PCTR2 (**39**), which is further converted to PCTR3 (**40**) by a dipeptidase.<sup>107</sup> The structure of PCTR1 (**38**) has been established through matching experiments of biogenic **38** with material prepared by stereoselective synthesis.<sup>108</sup>

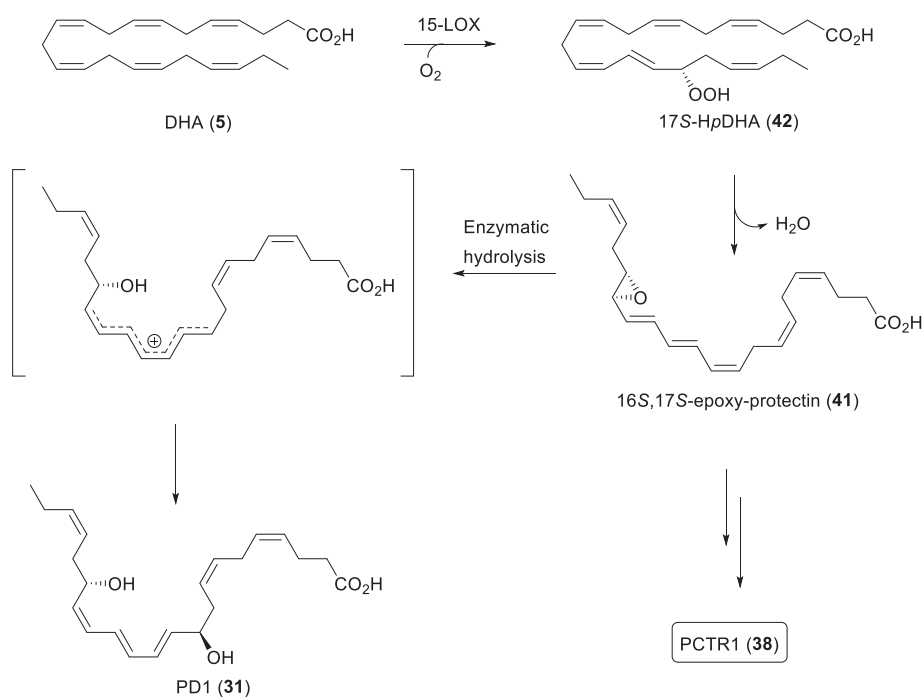


**Scheme 1.9** Proposed enzymatic conversion of PCTR1 (**38**) to produce PCTR2 (**39**) and PCTR3 (**40**).

#### 1.4.5 Biosynthesis of protectins

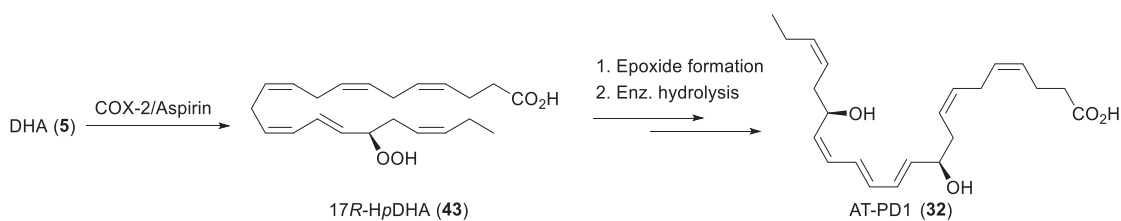
The biosynthesis of the DHA-derived protectins takes place in inflammatory exudates, resulting in the formation of PD1 (**31**) and PCTR1 (**38**), as outlined in Scheme 1.10.<sup>97</sup> Each pathway to the formation of mediator **31** and **38** involves the generation of epoxy-protectin **41**, which was initially disclosed as an intermediate in the formation of PD1 (**31**).<sup>90</sup> Later, the structure of epoxide **41** was confirmed by matching endogenous and synthetic material. Additional incubation and matching studies revealed that synthetic **41** was converted into both PD1 (**31**) and PCTR1 (**38**) by human macrophages, further implying epoxide **41** as a common intermediate in the production of these two protectins.<sup>108, 109</sup>

The biosynthesis of PD1 (**31**) commences with an oxygenation of the C<sub>17</sub>-position on DHA (**5**), promoted by 15-LOX, into 17*S*-hydroperoxy DHA (17*S*-HpDHA, **42**). This short-lived intermediate is further converted by human leukocytes into epoxide **41**, which by enzymatic hydrolysis by the attack of water on C<sub>10</sub> provides PD1 (**31**).<sup>92, 109</sup> The latter step is likely to occur through a carbocation intermediate, formed by enzymatic ring opening of intermediate **41** (Scheme 1.10). This has been evidenced by the formation of the *E,E,Z*-triene under enzymatic actions whereas the *E,E,E*-triene in addition to the formation of two diastereomeric water adducts on C<sub>10</sub> is formed under non-enzymatic conditions.<sup>104, 109, 110</sup> Furthermore, conjugation of intermediate **41** with glutathione, catalyzed by a glutathione *S*-transferase, affords the 16*R*,17*S*-conjugate **38**, which can be converted to PCTR2 (**39**) and PCTR3 (**40**) as discussed in the preceding section.<sup>107, 108</sup>



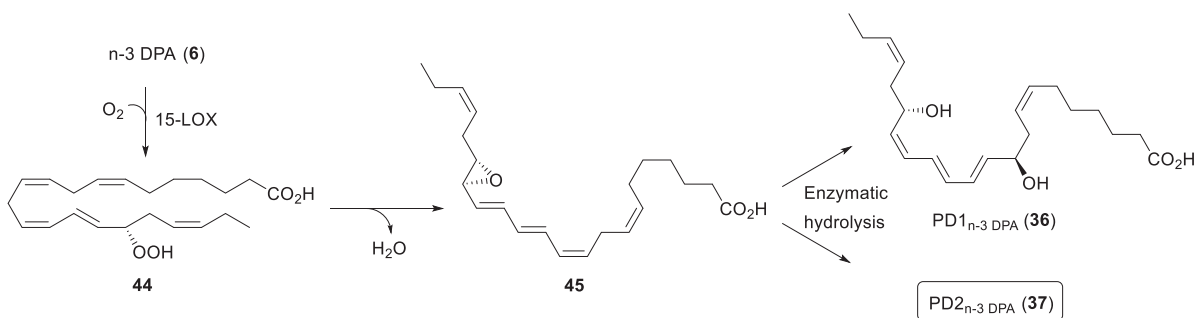
**Scheme 1.10** Outline of the biosynthesis of PD1 (**31**) and PCTR1 (**38**) from DHA (**5**).

The biosynthetic pathway towards AT-PD1 (**32**) has been elucidated and is essentially the same as the pathway outlined for PD1 (**31**) above.<sup>29</sup> In the first step, COX-2 in the presence of aspirin catalyzes the stereoselective incorporation of oxygen at C<sub>17</sub> in DHA (**5**) to yield 17*R*-HpDHA (**43**). This intermediate is then further enzymatically transformed through an epoxide intermediate and hydrolysis into the 17*R*-epimer **32** (Scheme 1.11).<sup>111</sup>



**Scheme 1.11** Outline of the biosynthesis of AT-PD1 (32) from DHA (5).

The biosynthetic pathway producing the n-3 DPA-derived protectins was initially proposed by Dalli and co-workers in 2013, as outlined in Scheme 1.12.<sup>99</sup> In this route, oxygen insertion at C<sub>17</sub> in n-3 DPA (6), catalyzed by 15-LOX, affords hydroperoxide 44 that can be converted to epoxide 45 via intramolecular oxygen attack on C<sub>16</sub> and loss of water. Intermediate 45 can then undergo enzymatic hydrolysis, either at C<sub>10</sub> or C<sub>17</sub>, to generate PD1<sub>n-3</sub> DPA (36) or PD2<sub>n-3</sub> DPA (37), respectively.



**Scheme 1.12** Outline of the biosynthesis of PD1<sub>n-3</sub> DPA (36) and proposed biosynthesis of PD2<sub>n-3</sub> DPA (37).<sup>104</sup>

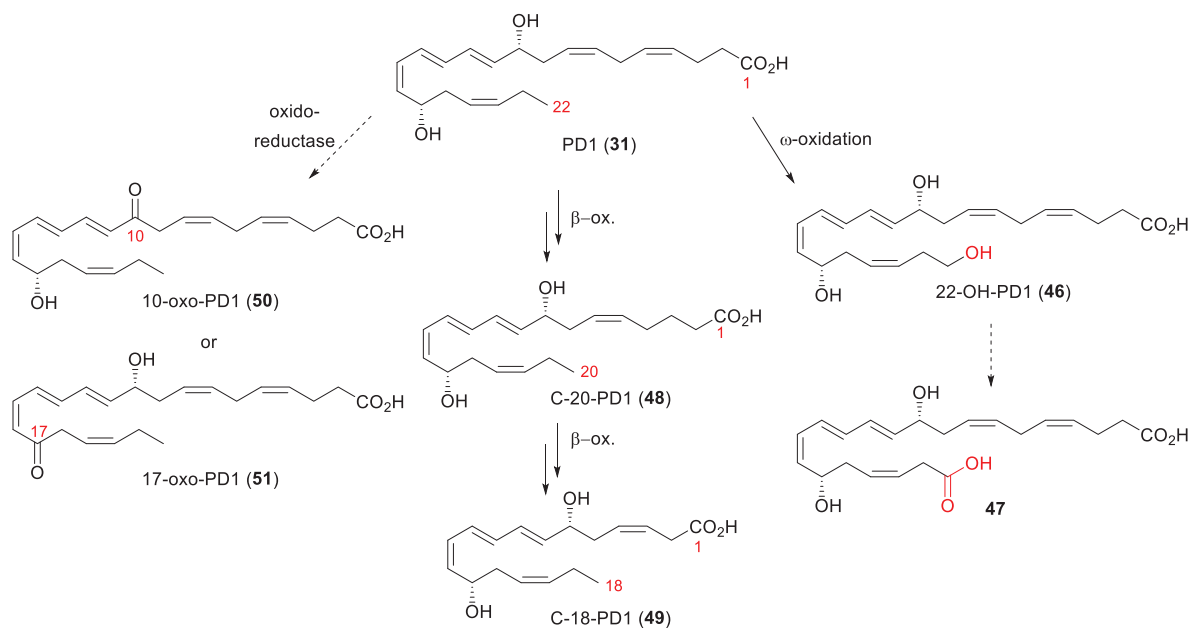
The involvement of epoxide 45 as an intermediate in the formation of PD1<sub>n-3</sub> DPA (36) was recently confirmed by matching studies. In these investigations, enzymatic incubations demonstrated that n-3 DPA (6) was converted to epoxide 45 by 15-LOX, and that synthetic 45 was converted to PD1<sub>n-3</sub> DPA (36) by human neutrophils.<sup>104</sup> Moreover, when synthetic 45 was incubated with denatured neutrophils or phosphate buffered saline, a significant lower amount of SPM 36 was produced, which supports the presence of a hydrolytic enzyme in the conversion of 45 to PD1<sub>n-3</sub> DPA (36).<sup>104</sup>

#### 1.4.6 Enzymatic and biochemical oxidations of protectins

PD1 (**31**), like other lipid mediators such as LTB<sub>4</sub> (**20**), undergoes  $\omega$ -hydroxylation to generate an  $\omega$ -hydroxylated metabolite.<sup>90, 112</sup> While omega oxidation of LTB<sub>4</sub> (**20**) results in loss of biological activity, the resulting metabolite of PD1, termed 22-OH protectin D1 (22-OH-PD1, **46**), has been found to retain the ability of PD1 (**31**) to attenuate LTB<sub>4</sub>-induced chemotaxis in human PMNs, and thus decrease leukocyte recruitment *in vivo*.<sup>112, 113</sup> Given the major known metabolic pathways for oxygenated eicosanoid metabolites, 22-OH-PD1 (**46**) might be further oxidized to dicarboxylic acid **47**, followed by prospective  $\beta$ -oxidation (Scheme 1.13).<sup>114-116</sup> However, further studies are needed to investigate this hypothesis.

The first evidence that SPMs are subjected to biochemical  $\beta$ -oxidation was recently published.<sup>117</sup> In this study, PD1 (**31**) was incubated with human hepatoma cell lines to investigate potential hepatic biotransformations in humans. In these incubations, sequential formation of two prominent metabolites was identified with concomitant decrease in PD1 (**31**) concentration. The metabolites were identified as C-20-PD1 (**48**) and C-18-PD1 (**49**), which is consistent with products formed by one and two rounds of  $\beta$ -oxidation of PD1 (**31**), respectively (see Scheme 1.13). The identities of compound **48** and **49** were additionally confirmed by comparison of biologic material with standards obtained through chemical synthesis. Nonetheless, only trace amounts of 22-OH-PD1 (**46**) were detected in the incubations, and the dicarboxylic acid **47** was not observed. These initial findings suggest that, contrary to eicosanoids, the main metabolic pathway for PD1 (**31**) is not from the  $\omega$ -end, but from the polar head. Interestingly, C-18-PD1 (**49**) was able to inhibit LTB<sub>4</sub>-induced chemotaxis in human PMNs comparable with PD1 (**31**), whereas C-20-PD1 (**48**) was ineffective.<sup>117</sup>

Scheme 1.13 outlines the different metabolic and proposed metabolic pathways for PD1 (**31**).<sup>117</sup> Other plausible oxidations may be through the actions of oxidoreductase enzymes on one of the two allylic alcohols to produce the corresponding ketones 10-oxo-PD1 (**50**) or 17-oxo-PD1 (**51**), which is known to occur in a number of SPMs.<sup>118-121</sup>



**Scheme 1.13** Metabolic and proposed metabolic pathways for PD1 (**31**).<sup>117</sup>

Other protectins are likely to share the same metabolic fate as PD1 (**31**) or other lipid mediators, although further studies are needed to substantiate this suggestion. Towards drug development efforts, elucidating the biochemical pathways involved in the metabolic inactivation of protectins can be useful to provide a basis for the design and synthesis of metabolically stable analogues that mimic their potent bioactions.

## 1.5 Receptors activated by specialized pro-resolving lipid mediators

G-protein coupled receptors, also referred to as seven transmembrane proteins, are a large group of membrane proteins that regulate an array of physiological responses such as vision, smell and taste, among others.<sup>122, 123</sup> Activation of a GPCR by an external signaling molecule (i.e. agonist), results in a conformational change of the receptor, which in turn activates internal downstream signaling pathways, ultimately resulting in cellular responses.<sup>124</sup> As briefly mentioned, the SPMs have been shown to exert their beneficial actions through GPCRs, and several SPM receptors have been reported to date (see Figure 1.7).<sup>125-130</sup> The A lipoxin and formyl peptide receptor 2 (ALX/FPR2) was the first of these receptors to be identified, which transduce the signals initiated by LXA<sub>4</sub> (**22**), and the D-class resolvins, such as RvD1, and RvD3. Additionally, the listed SPMs signal through the GPCR termed GPR32, which is also activated by RvD5.<sup>131, 132</sup> Furthermore, the leucine G-protein coupled receptor 6 (LGR6) was recently identified to be specifically activated

by the SPM maresin 1 (Mar1).<sup>127, 129</sup> The SPM-receptor interactions reported for RvE1 (**26**) and PD1 (**31**) are discussed in the following sections.

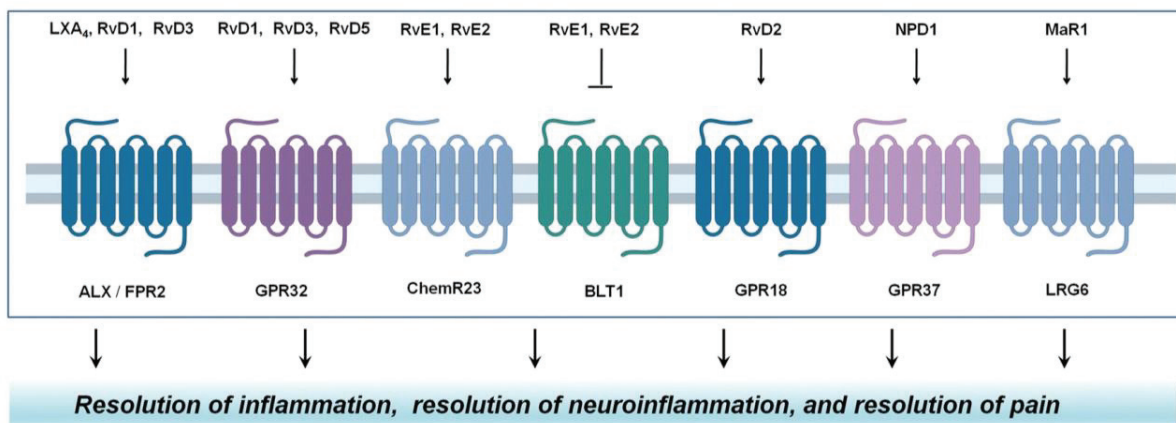


Figure 1.7 Illustration of SPM activation of respective GPCRs in regulating inflammatory processes.<sup>133</sup>

### 1.5.1 Resolvin E1

Resolvin E1 (**26**) exerts its bioactions through the Chemerin receptor 23 (ChemR23), which is mainly expressed on immune cells, such as monocytes and macrophages.<sup>86, 125</sup> ChemR23 is a high affinity RvE1-receptor (equilibrium dissociation constant,  $K_d = \sim 11.3$  nM) that elicits pro-resolution pathways upon binding.<sup>80</sup> Stimulation of ChemR23 by RvE1 (**26**) has shown to down-regulate the production of pro-inflammatory cytokines, including tumor necrosis factor- $\alpha$  (TNF- $\alpha$ ).<sup>80</sup> Moreover, RvE1-receptor binding has demonstrated to signal phosphorylation of two proteins (Akt and ribosomal protein S6), which is a signaling pathway that ultimately results in enhanced human macrophage phagocytosis.<sup>134</sup> In addition to activating the ChemR23 receptor, RvE1 (**26**) has been shown to regulate the activity of the B leukotriene receptor 1 (BLT1, see Figure 1.7 above), which is highly expressed on human PMNs.<sup>135, 136</sup> BLT1 is a high-affinity receptor for the chemoattractant LTB<sub>4</sub> (**20**). However, it's been reported that RvE1 (**26**) compete with LTB<sub>4</sub> (**20**) for BLT1-binding by acting as a partial agonist while attenuating the pro-inflammatory signals promoted by LTB<sub>4</sub> (**20**), thus limiting LTB<sub>4</sub>-mediated PMN infiltration during an inflammatory response.<sup>125, 136</sup> These findings indicate that RvE1-receptor interactions counteract the production and action of pro-inflammatory mediators in addition to stimulating clearance of inflammatory lesions, which are all critical features in the resolution of inflammation.<sup>134, 136</sup>

### 1.5.2 Protectin D1

Initial investigations of PD1-receptor binding interactions, using radiolabeled-PD1, provided evidence for cell type specific binding of PD1 (**31**) to human retinal pigment epithelial cells and leukocytes. It was reported that radiolabeled PD1 (**31**) displayed high affinity and stereoselective binding in these cells with  $K_d$ -values in the low nanomolar range.<sup>137</sup> Furthermore, in these experiments, radiolabeled PD1 (**31**) did not compete with RvE1 (**26**) or LXA<sub>4</sub> (**22**) for specific binding with human PMNs, which provided the first evidence for interactions of PD1 (**31**) with specific high affinity receptors that is not shared by ALX/FPR2, BLT1, or ChemR23. In 2018, it was discovered that PD1 (**31**) elicits signaling responses *via* specific binding to the G-protein coupled receptor 37 (GPR37), which is highly expressed in the brain.<sup>126, 138, 139</sup> In this report, PD1 (**31**) activation of GPR37 on human macrophages resulted in marked enhancement of macrophage phagocytosis of fluorescent-labelled particles *in vitro*.<sup>126</sup> Moreover, PD1-GPR37 interactions in macrophage cultures suppressed the production of pro-inflammatory cytokines critically involved in inflammatory pain, such as interleukin-1 $\beta$  (IL-1 $\beta$ ), and increased the expression of anti-inflammatory cytokines, including interleukin-10 (IL-10). Additional *in vivo* experiments using mouse models confirmed the role of GPR37 in regulating macrophage phagocytosis and resolving inflammatory induced pain.<sup>126</sup> These findings suggest that PD1 (**31**) contributes to the resolution of inflammation and inflammatory pain by interacting with the GPR32 receptor.

### 1.6 Drug development using specialized pro-resolving mediators

Drug development refers to the process of bringing a new drug molecule into clinical practice once a lead compound has been identified through the process of drug discovery.<sup>140, 141</sup> Drug development is a complex, expensive and time-consuming process that requires extensive interdisciplinary scientific collaboration – it is dependent on organic chemistry and synthesis, pharmacology as well as comprehensive knowledge of biological systems.<sup>142</sup>

In drug discovery, initial basic research often occurs in academia, where research data generated may propose that the inhibition or activation of a biological target, such as a protein or a pathway, will result in a therapeutic effect in a disease of study.<sup>143</sup> Thus, collaborations to identify potential drug targets are not uncommon between academic researchers with expert knowledge of specific biological pathways and scientists in the pharmaceutical industry.<sup>144, 145</sup> Since new drug molecules are rarely discovered directly, drug discovery includes various approaches to identify new substances, so-called lead compounds (or leads). A lead compound is a chemical compound that exerts a desired biological activity by affecting a specific biological target. The lead is usually optimized with respect to potency (pharmacodynamic effects), absorption, distribution, metabolism, elimination and toxicity (pharmacokinetic effects) for safe and effective therapeutic use in humans.<sup>146</sup>

Interaction of a drug or a ligand with receptors resulting in biochemical and physiological effects is known as pharmacodynamics. Upon receptor binding, an agonist activates the receptor to produce a biological response, and the potency of that agonist is defined as the concentration necessary to produce a defined level of a given biological activity (e.g. stimulating macrophage efferocytosis in inflamed tissue). A potent agonist stimulates the activity at low concentrations, which is often specified as the concentration necessary to produce half of the maximum response (EC<sub>50</sub>-values). Nevertheless, for a drug or a ligand to be therapeutically useful, it must have additional properties in addition to high potency to allow for absorption of the ligand into the systemic circulation and/or distribution within the body to reach the target site without inactivation or toxic side effects.<sup>146</sup>

The lead optimization process includes systematic synthetic alterations to the molecular structure of the lead to identify structure-activity relationships (SAR) to the target, resulting in synthetic analogues of the lead. The aim of SAR-studies is to provide structural information essential to producing a biological response (i.e. the pharmacophore), and to show which part of the structure that is not essential to that response. The former may then be altered to enhance potency, whereas the latter can be removed or modified chemically to alter pharmacokinetic effects or to introduce conformational rigidity. These modifications may then result in a drug candidate worthy of extensive biological and pharmacological pre-clinical studies, which might be further developed into a clinical drug ready for clinical trials in humans.<sup>146</sup>

As discussed in earlier sections, the SPMs are highly potent ligands for distinct GPCRs that have shown great potential in pre-clinical animal models in resolving inflammation. Unlike traditional anti-inflammatory drugs, such as COX inhibitors, the SPMs exert their actions with the apparent absence of immunosuppressive effects (see Section 1.1.3 and Section 1.3.3 for details).<sup>125</sup> These dual properties have attracted great interest in the SPMs as novel lead compounds in drug discovery programs towards the development of new resolution-based therapeutics.<sup>75, 125</sup>

Several SPM-analogues with increased metabolic and/or chemical stability have been synthesized, and some of these analogues have entered clinical trial programs.<sup>118, 135, 147-150</sup> A notable example is an analog of RvE1 (**52**, Figure 1.8), which has shown promising results for the treatment of inflammation-based dry-eye disease in a phase 2 clinical trial, findings that are further investigated in a phase 3 trial.<sup>125</sup> Lipoxin analogues with increased metabolic resistance that retain the potent bioactivity of their parent molecule have also been developed.<sup>148, 151, 152</sup> One of these analogues is a benzo-fused ring mimetic of LXA<sub>4</sub> (**53**, Figure 1.8), which has proved to promote tissue repair and tissue regeneration in animal models of periodontitis.<sup>135, 153</sup> Consequently, analog **53** is being investigated in a phase 1 clinical trial for topical treatment of periodontal inflammation.<sup>154</sup>



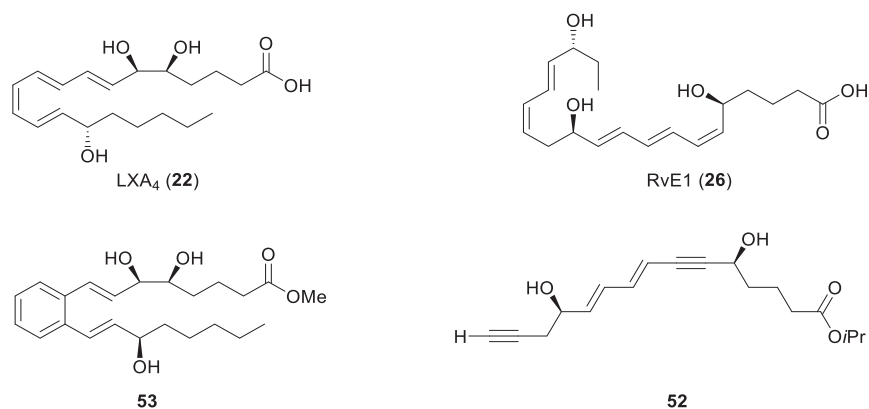


**Figure 1.8** Chemical structures of RvE1 (26) and LXA<sub>4</sub> (22) and the two synthetic analogues 52 and 53 in clinical trial programs.

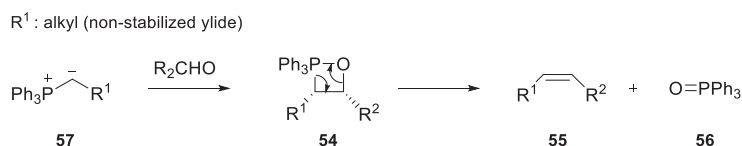
## 1.7 Synthetic methods employed in total synthesis of specialized pro-resolving lipid mediators

Organic synthesis has historically been applied as a tool for elucidating, confirming, and replicating the molecules produced by nature.<sup>155</sup> Since the SPMs are formed in minute amounts from natural sources, organic synthesis is necessary to access larger quantities that will enable exact structural assignments and thorough biological investigations.<sup>156</sup> The chemical structures of the SPMs may seem to be very similar and simple looking. However, the synthesis, purification and spectroscopic analysis of these mediators are demanding. Not to mention, these molecules are sensitive towards chemical decomposition and the conjugated *E,E,Z*-triene moiety present in many of the SPMs is prone to isomerization upon contact with heat, light, and acidity. Furthermore, when a synthesis is performed, possible stereochemical or geometrical isomers can be formed that are difficult to remove from the desired product.<sup>157, 158</sup> For these reasons, reliable stereo- and regio-controlled synthetic approaches are essential to their production. As previously mentioned, the correct stereochemistry and double bond geometry is most often crucial for the SPMs to mediate their bioactions. Multiple double bonds with *E*- and *Z*-configurations are present within these structures, both as skipped *Z*-olefins and alkenes in conjugation. Some key methods applied to construct alkenes and other functional groups are presented in the following sections.

### 1.7.1 Wittig and *Z*-selective Wittig reactions

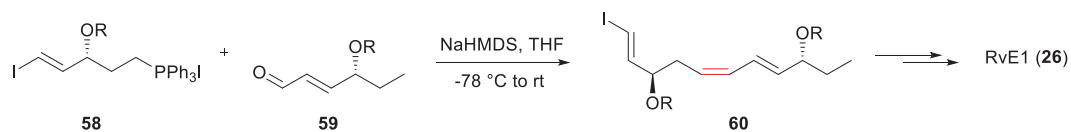
The Wittig reaction, named after the Nobel Laureate Georg Wittig, was discovered in 1954,<sup>159</sup> and is an efficient and widely used method to construct alkenes from aldehydes and ketones.<sup>160</sup> In this reaction, a phosphonium ylide reacts with the carbonyl compound to form an alkene with phosphine oxide as the by-product. A very significant feature of the Wittig reaction is that the stereoselectivity of the reaction is dependent on the substituents on the ylide. The different types of ylides may be classified into three types. Stabilized ylides are those that have anion-stabilizing substituents adjacent to the negative charge. These type of ylides favor the formation of *E*-alkenes. Non-stabilized ylides are those without additional anion-stabilizing substituents, and preferentially form *Z*-alkenes in the Wittig reaction, while semi-stabilized substituents (i.e. aromatic rings) usually produce a mixture of *E*- and *Z*- products.<sup>161</sup> In addition to the choice of ylide, other ways to enhance the selectivity for *Z*-configured alkenes are to perform the reaction at low temperatures, in highly diluted solutions, and to use lithium-free conditions.<sup>160, 162</sup>

The mechanism of the Wittig reaction is a debated subject, but the proposed mechanism illustrated in Scheme 1.14 to form a *Z*-alkene is commonly agreed upon.<sup>160-163</sup> This involves stereoselective formation of a *syn*-oxaphosphetane intermediate (**54**) followed by stereospecific elimination to yield the corresponding *Z*-configured alkene (**55**) with loss of triphenyl phosphine oxide (**56**). The thermodynamic driving force in this reaction is the high affinity of phosphorous towards oxygen to form the remarkably strong phosphorous-oxygen bond in the phosphine-oxide by-product.<sup>164</sup> Under lithium-free conditions, strong evidence suggests that the first step in the Wittig reaction is a [2+2] cycloaddition between the phosphonium ylide (**57**) and the carbonyl compound to form the oxaphosphetane intermediate **54** directly.<sup>162</sup>



**Scheme 1.14** Proposed mechanism for the Wittig reaction.

The Wittig reaction has been employed in the synthesis of numerous SPMs and other unsaturated natural products.<sup>165-168</sup> Scheme 1.15 illustrates how Ogawa and Kobayashi utilized a *Z*-selective Wittig reaction in their synthesis of RvE1 (**26**).<sup>169</sup> The C<sub>14</sub>-C<sub>15</sub> olefin in RvE1 was formed by deprotonating phosphonium salt **58** using sodium *bis*(trimethylsilyl)amide (NaHMDS) to form the corresponding ylide, followed by a Wittig reaction between the ylide and aldehyde **59** to afford the *Z*-configured alkene in intermediate **60**.

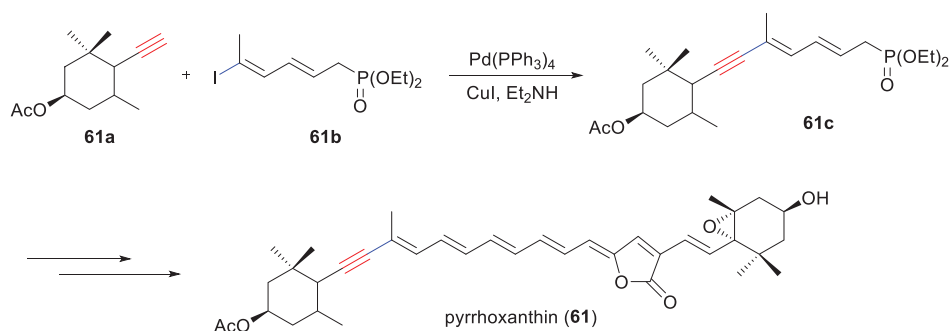


**Scheme 1.15** Formation of a *cis*-olefin utilizing the Wittig reaction in the total synthesis of RvE1 (**26**) by Ogawa and Kobayashi.<sup>169</sup>

### 1.7.2 Cross-coupling reactions

Palladium and nickel catalyzed cross-coupling reactions, such as Heck,<sup>170</sup> Negishi,<sup>171</sup> Suzuki,<sup>172</sup> and the Sonogashira<sup>173</sup> reactions, are valuable carbon-carbon bond forming methods for the synthesis of both *Z*- and *E*-olefins. In these reactions, the stereochemistry of the starting alkenyls is retained in the product as a result of the cross-coupling step being mainly stereospecific.<sup>174</sup> The major impact of these reactions in organic synthesis led to the joint awarding of the 2010 Nobel Prize in Chemistry to Richard F. Heck, Ei-ichi Negishi and Akira Suzuki for their work on palladium-catalyzed cross-coupling reactions.<sup>175</sup>

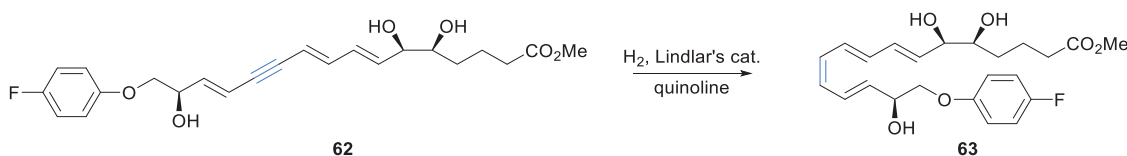
The powerful ability of transition-metal catalyzed cross-coupling reactions to forge carbon-carbon bonds between functionalized substrates under mild conditions has resulted in wide application in natural product synthesis.<sup>174</sup> Due to the highly unsaturated nature of the SPMs, cross-coupling reactions are frequently utilized in their preparation.<sup>102, 157, 158, 176-178</sup> One example of the employment of the Sonogashira reaction in the synthesis of natural product **61** is illustrated in Scheme 1.16.<sup>179</sup>



**Scheme 1.16** Application of the Sonogashira reaction in the total syntheses of pyrroxanthin (**61**).<sup>179</sup>

### 1.7.3 Z-selective reduction of alkynes

Selective hydrogenation of alkynes to create *Z*-alkenes has been extensively employed in the synthesis of unsaturated natural products, and numerous established methods exist. One of the most commonly employed protocols includes palladium-based reagents, such as the Lindlar catalyst.<sup>180</sup> In this catalyst, palladium is deposited on a CaCO<sub>3</sub> support poisoned with lead acetate and quinoline. Additionally, aromatic imine bases, such as quinoline and pyridine, are often added due to their ability to modulate catalyst reactivity and thereby increase selectivity.<sup>181, 182</sup> The selectivity for alkene formation in the Lindlar reaction may be explained by strong adsorption of the reactive alkyne on the catalyst surface, preventing re-adsorption of the resulting alkene product. The latter is proposed to be formed by *syn*-addition of hydrogens from the catalyst to the triple bond. As the concentration of alkyne decreases, competitive adsorption of quinoline on the catalyst surface can prevent binding and further reduction of the alkene product.<sup>183</sup> Nonetheless, over-reduction is still often encountered when this method is applied. To avoid this problem, co-solvents, such as pyridine and 1-octene, or cyclohexene can be added in the reactions.<sup>180</sup> One example of the application of the Lindlar's catalyst is the reduction of intermediate **62**, furnishing the metabolically stable LXA<sub>4</sub>-analog *para*-fluorophenoxy **63** (Scheme 1.17).<sup>65</sup>

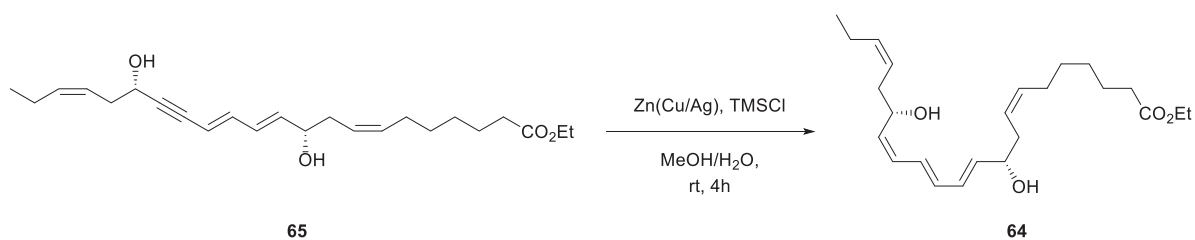


**Scheme 1.17** Application of the Lindlar reduction in the synthesis of *para*-fluorophenoxy lipoxin analog **63**.<sup>65</sup>

Other established methods to obtain *Z*-configured alkenes include Brown's nickel-based catalyst P-2 Ni<sup>184</sup> and the copper (I) hydride reagent known as Stryker's reagent.<sup>185</sup> The former is readily generated *in situ* by the reduction of nickel acetate with sodium borohydride in ethanol, and is one of the most frequently used reducing systems, together with the Lindlar catalyst, for partial hydrogenation of alkynes. The Brown catalyst has a broad functional group tolerance, and may be used in the presence of alkenes, acetals, silylated ethers, and free hydroxyl groups, among others. However, some drawbacks experienced using the methods described include isomerization to *E*-alkenes and over-reduction.<sup>180</sup>

Chemoselective reduction of a conjugated alkyne is challenging due to an increased reactivity of the conjugated system. Thus, unwanted side reactions, such as over-reduction to saturated analogues, may be encountered using the above-mentioned methods.<sup>180</sup> An alternative protocol is the Boland reduction using an activated Zn(Cu/Ag) reagent.<sup>186</sup> This reduction proceeds without an

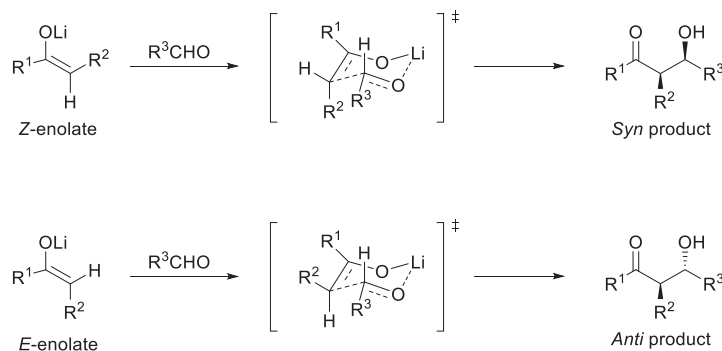
applied hydrogen atmosphere in a MeOH/H<sub>2</sub>O solvent system, and has successfully been utilized for *Z*-selective hydrogenation of conjugated alkynes. Durand and Balas established the conjugated triene, utilizing a modified Boland protocol reported by our group,<sup>187</sup> in their synthesis of 10-*epi*-PD1<sub>n-3</sub> DPA ethyl ester **64** as illustrated in Scheme 1.18.<sup>157</sup>



**Scheme 1.18** Application of the Boland reduction in the synthesis of the PD1<sub>n-3</sub> DPA ethyl ester epimer **64** by Durand and Balas.<sup>157</sup>

### 1.7.4 Aldol reactions

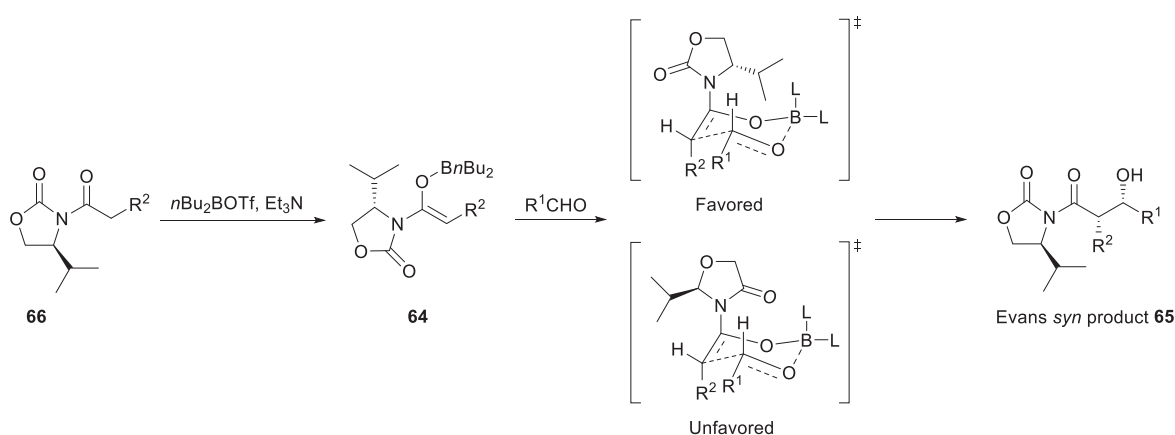
The aldol reaction was discovered independently by Wurtz<sup>188</sup> and Borodin<sup>189</sup> in the 1870s, and is an important and extensively used method for the construction of carbon-carbon bonds and stereogenic centers in organic synthesis.<sup>190</sup> In 1957, Zimmerman and Traxler published a model rationalizing the diastereofacial selectivity observed in the aldol reaction.<sup>191</sup> According to this model, the reaction between an enolate and an aldehyde proceeds through a six-membered chair-like transition state, where an *E*- and a *Z*-metal enolate affords *anti*- and *syn*-adducts, respectively. The controlling factor in this model is based on minimizing steric interactions in the transition state, where the metal-enolate geometry impose the orientation of the R<sup>2</sup>-group to be either *pseudo*-equatorial or axial, whereas the R<sup>3</sup>-substituent of the aldehyde favors the to be oriented in the more stable *pseudo*-equatorial position, as illustrated in Scheme 1.19.<sup>191</sup>



**Scheme 1.19** The Zimmerman-Traxler transition states for *Z*- and *E*-enolates.<sup>191, 192</sup>

If a Zimmerman-Traxler transition state is operative, then controlling the geometry of the enolate formed will also control the stereoselective outcome of the aldol reaction. In practice, the stereochemistry of the resulting adducts can be highly metal dependent. Lithium and boron are often preferred as the metal source, since the relatively short metal-oxygen bond between these two metals are believed to result in a tighter transition state which in turn increase the stereoselectivity.<sup>192</sup> Titanium based Lewis acids are also used in aldol reactions, which is known as the Mukaiyama-aldol reaction in the Lewis acid mediated reaction between silyl enol ethers and an aldehyde.<sup>193</sup>

A successful advancement of the aldol reaction is the stereoselective creation of secondary alcohols using chiral oxazolidinones developed by Evans, known as the Evans-aldol reaction.<sup>192, 194</sup> The chiral auxiliaries applied in this reaction are generally commercially available as either enantiomer. Scheme 1.20 illustrates the Evans-aldol reaction and how the stereoselectivity is rationalized based on the Zimmerman-Traxler model.<sup>191, 192, 195</sup> In this reaction, *n*Bu<sub>2</sub>BOTf and Et<sub>3</sub>N are used to form the *Z*-enolate **64**, controlling the relative stereochemistry, whereas the stereochemistry of the oxazolidinone auxiliary ensures that the nucleophile addition preferentially occurs to one face of the aldehyde through the favored transition state, which in turn controls the absolute configuration of the product. In the favored transition state, the dipoles of the carbonyl group of the auxiliary and the enolate oxygen are oriented in opposite directions, and the aldehyde R<sup>1</sup>-group oriented in *pseudo*-equatorial position, reducing steric interactions. Consequently, the Evans *syn* aldol product **65** is formed selectively.

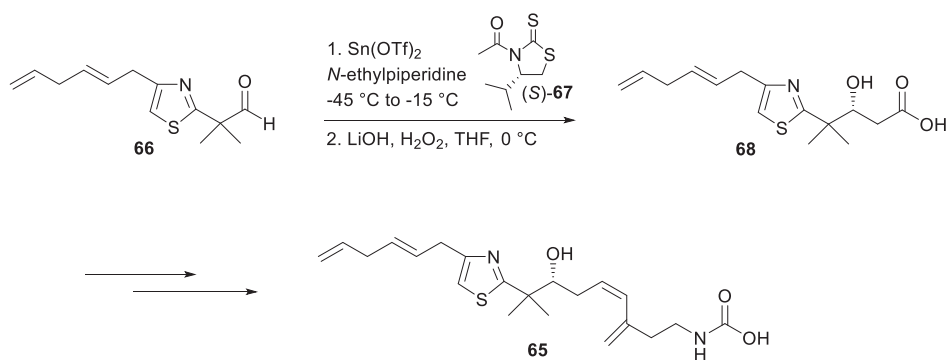


**Scheme 1.20** Stereoselectivity in the Zimmerman-Traxler model of the Evans aldol reaction.

By varying the combination between the Lewis acid and the chiral auxiliary in the Evans-aldol reaction, products of all possible configurations have been prepared, making this reaction an

exceptionally successful and popular approach for asymmetric construction of carbon-carbon bonds.<sup>196-199</sup>

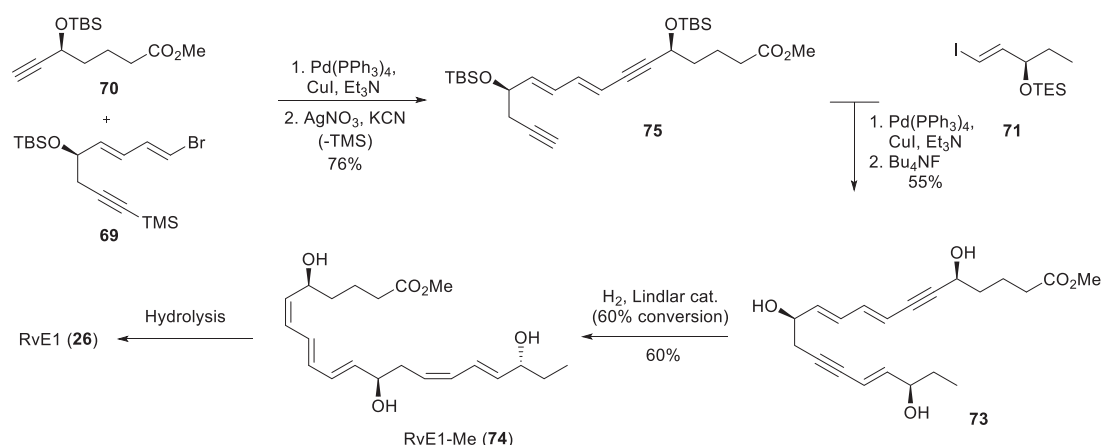
Continuing work related to Evan's findings was reported by Nagao and co-workers in 1986.<sup>200</sup> In this study, it was found that acetylated thiazolidinethiones underwent highly selective acetate aldol reactions to afford aldol products in excellent selectivity, a property that was typically not observed when employing *N*-acetyloxazolidinones.<sup>200, 201</sup> Since its discovery, the reaction referred to as the Nagao acetate aldol reaction, has been widely employed in natural product synthesis. One example of its application in the total synthesis of (-)-mycothiazole (**65**) is illustrated in Scheme 1.21.<sup>202</sup>



**Scheme 1.21** Employment of the Nagao acetate aldol reaction in the synthesis of (-)-mycothiazole (**65**).<sup>202</sup>

## 1.8 Literature syntheses of resolvin E1

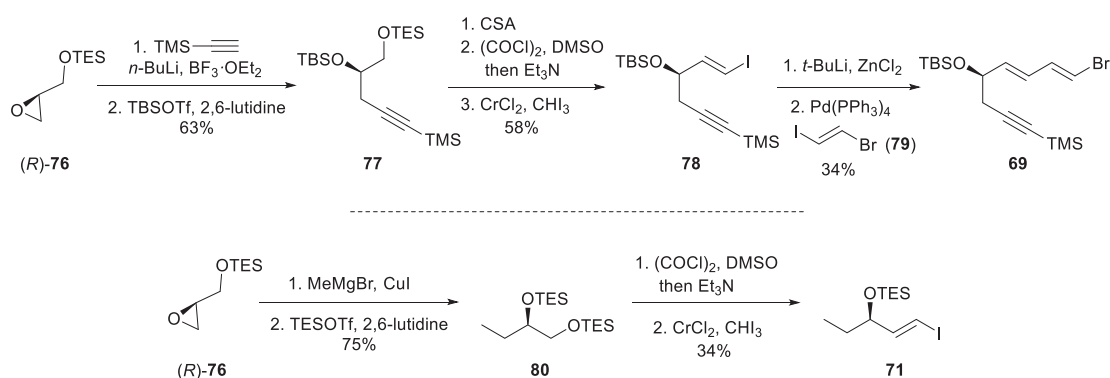
Several research groups have developed synthetic strategies towards RvE1 (**26**). The first strategy was reported in 2005, by Petasis and co-workers.<sup>80, 203</sup> The key reactions applied in this synthesis are shown in Scheme 1.22 and include assembly of the three fragments **69**, **70** and **71** by two subsequent Sonogashira coupling reactions to afford intermediate **73**. Semi-reduction of the two triple bonds in **73** using the Lindlar catalyst provided the methyl ester of RvE1 (**74**) in 13 steps over the longest linear sequence (LLS). In the latter step, the reduction stopped at 60% conversion. Further conversion to RvE1 (**26**) is not mentioned by the authors.



**Scheme 1.22** Petasis' synthesis of RvE1 (**26**) using Sonogashira couplings between the three key fragments **69**, **70** and **71**.<sup>203</sup>

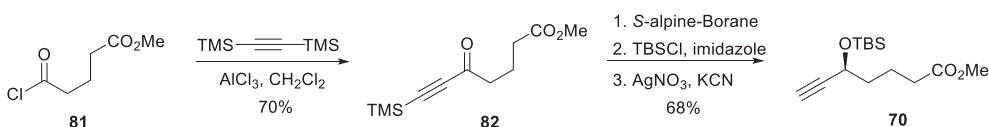
Fragment **69** and **71** were both prepared from the same starting material (*R*)-**76** through ring opening of the epoxide with the anion of TMS-acetylene and MeMgBr, respectively (Scheme 1.23). In the construction of fragment **69**, selective deprotection of the primary silylether in **77** followed by Swern oxidation<sup>204</sup> and Takai olefination<sup>205</sup> afforded intermediate **78**. Then, a Negishi<sup>171</sup> coupling between intermediate **78** and iodide **79** furnished the conjugated *E,E*-dienyl moiety of fragment **69**. Key fragment **71** was prepared in a similar manner, by employing Swern oxidation of intermediate **80** followed by Takai olefination of the resulting aldehyde as outlined in Scheme 1.23.





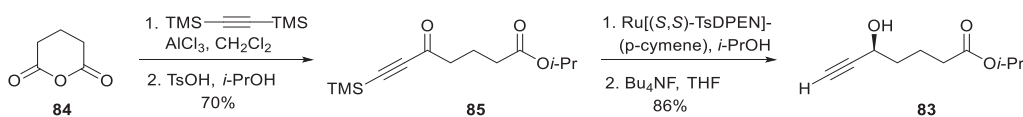
**Scheme 1.23** Preparation of fragment **69** and **71** used in the Sonogashira reaction.<sup>203</sup>

Coupling partner **70** was prepared as illustrated in Scheme 1.24. Transformation of **81** into acetylene **82** followed by an asymmetric Midland reduction<sup>206</sup> using (*S*)-*B*-Isopinocampheyl-9-BBN (*S*-Alpine-Borane) gave the corresponding propargylic alcohol in 90% *ee*. The resulting alcohol was TBS-protected and converted into fragment **70** following removal of the TMS group using AgNO<sub>3</sub> and KCN.



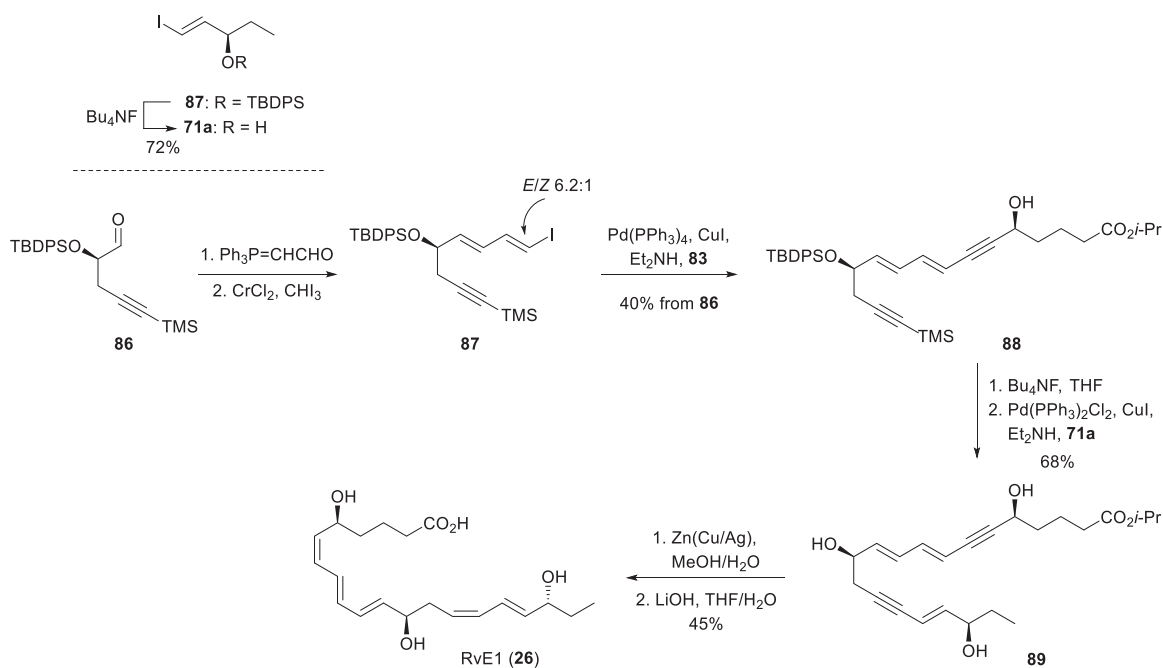
**Scheme 1.24** Preparation of fragment **70** used in the Sonogashira reaction.<sup>203</sup>

The Petasis' synthesis towards RvE1 (**26**) was later re-investigated by Schwartz and co-workers to improve the efficiency with respect to yields, enantiopurity and scale-up.<sup>207</sup> Scheme 1.25 shows an improved enantioselective synthesis of the propargylic alcohol fragment **70** above, resulting in analog **83**. Acetylide ring opening of glutaric anhydride **84**, followed by acid-catalyzed esterification, gave isopropyl ester **85**. Asymmetric reduction of the ketone moiety in **85** by the Noyori<sup>208</sup> catalyst gave the secondary alcohol **83** in excellent enantiomeric purity (>98% *ee*).



**Scheme 1.25** Improved synthetic strategy to obtain the carbonyl end fragment **83**.<sup>207</sup>

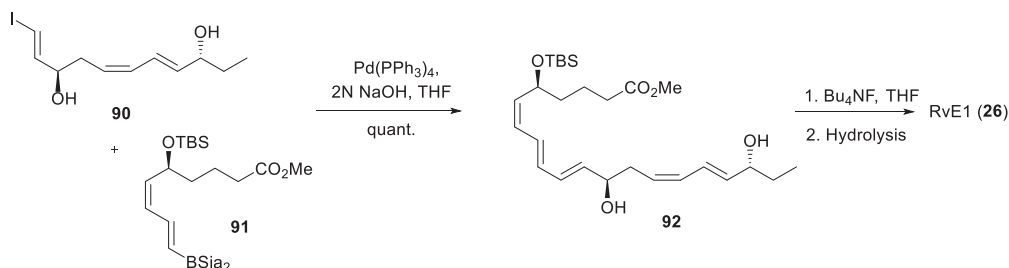
In the Schwartz strategy, aldehyde **86** and key fragment **71a** was prepared according to the Petasis protocol above (Scheme 1.23), affording **86** in 50% yield over 6 steps and **71a** in 33% yield over 6 steps following desilylation. Next, Wittig homologation of aldehyde **86** with triphenylphosphoranylidenacetaldehyde followed by Takai olefination produced intermediate **87** as a mixture of isomers (*E/Z* = 6.2:1, based on <sup>1</sup>H-NMR analysis) in the latter reaction. The mixture was directly subjected to a Sonogashira coupling with alkyne **83** to afford intermediate **88** in 40% yield from **86** after chromatographic purification. Global silyl deprotection of **88** and subsequent Sonogashira coupling with fragment **71a** furnished the carbon skeleton of RvE1 (**89**) in reasonable yield (68%). Reduction of the internal alkynes in **89** provided the corresponding pentaene product without over-reduction or *Z*-alkene isomerization. Resolvin E1 (**26**) was finally obtained after basic hydrolysis in 45% yield over the two last steps. In this synthesis, the target compound was obtained in 13 synthetic steps and 4 % yield over the longest linear sequence (LLS). The purity of the isolated target compound **26** is not provided by the authors.



Scheme 1.26 Improved synthesis of RvE1 (**26**) by Schwartz and co-workers.<sup>207</sup>

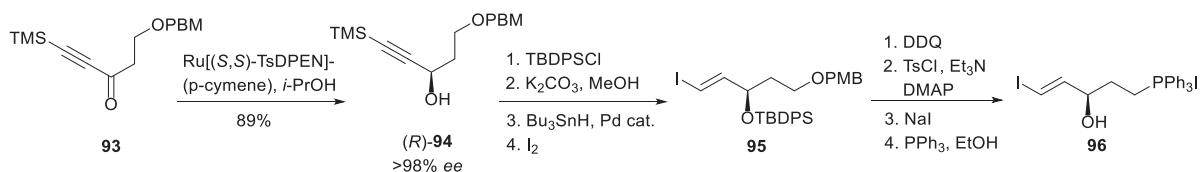
In 2009, Ogawa and Kobayashi reported a third convergent synthesis of RvE1 (**26**).<sup>169</sup> In this strategy, a late Suzuki<sup>172</sup> coupling of fragment **90** and **91** established the conjugated triene in **92**, in which the ester functionality remained intact under the basic conditions (Scheme 1.27). However, if LiOH was used as a base in the Suzuki coupling, the corresponding acid of **92** was obtained in one pot, but chromatographic purification of the crude acid proved difficult. In the final step, intermediate **92** was treated with Bu<sub>4</sub>NF to furnish RvE1 (**26**) in 19 linear steps, but how

the methyl ester of RvE1 was hydrolyzed into **26** is not mentioned by the authors. The total number of steps in this strategy was 33 in comparison with a total of 23 steps in the Schwarts' synthesis. The target compound **26** was isolated in >92% purity based on <sup>1</sup>H-NMR analyses, and the final acid was converted to the methyl ester using diazomethane to confirm the structure by comparing <sup>1</sup>H- and <sup>13</sup>C-NMR spectra with those reported by Petasis.<sup>203</sup>



**Scheme 1.27** Final steps in the synthesis of RvE1 (**26**) by Ogawa and Kobayashi using the Suzuki coupling.<sup>169</sup>

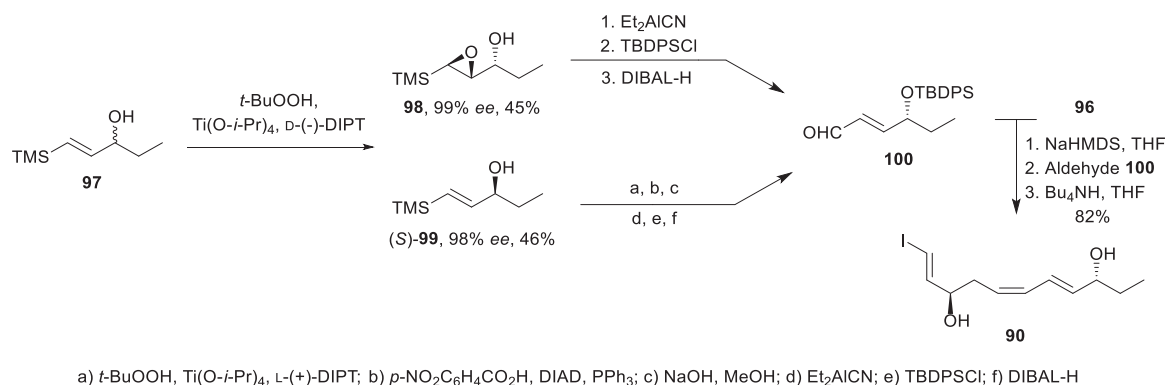
Key fragment **90**, which was used in the Suzuki coupling, was prepared as outlined in Scheme 1.28 and Scheme 1.29. Starting from ketone **93**, obtained over 5 previous steps, asymmetric reduction using the Noyori catalyst afforded (*R*)-**94** in high yield and high enantiomeric purity (>98% *ee*, based on <sup>1</sup>H-NMR of the corresponding Mosher acid<sup>209</sup> derivatives). Protection of the secondary hydroxyl group in (*R*)-**94**, followed by desilylation and palladium catalyzed hydrostannation<sup>210</sup> afforded the *E*-alkene stereoselectively, which upon exposure to I<sub>2</sub> furnished iodide **95**. Through a four-step transformation, including selective deprotection of the primary alcohol, tosylation and halogenation, Wittig-salt **96** was obtained in 34% yield from compound **93** (Scheme 1.28).



**Scheme 1.28** Preparation of intermediate Wittig-salt **96**.<sup>169</sup>

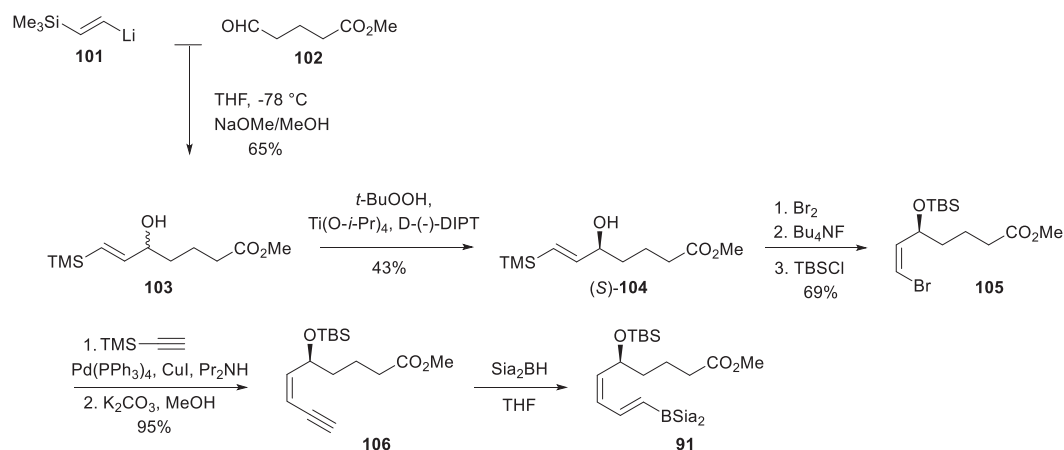
Racemic alcohol **97** was prepared by nucleophilic addition of TMS-acetylene anion to propanal followed by an *E*-selective reduction of the alkyne in 75% yield over the two steps. Next, Sharpless asymmetric epoxidation under kinetic resolution conditions<sup>211</sup> of **97** afforded a mixture of *anti*-epoxy alcohol **98** and (*S*)-alcohol **99** in excellent enantiopurity. After separation of (*S*)-**99** and **98**

by column chromatography and several additional transformations, both products were converted into aldehyde **100** via epoxide ring opening with  $\text{Et}_2\text{AlCN}$  and hydride reduction. The correct stereochemistry of aldehyde **100** from (*S*)-**99** was installed by a Mitsunobu inversion.<sup>212</sup> Finally, a Wittig reaction of aldehyde **100** with the ylide of **96** and subsequent desilylation furnished key fragment **90** (Scheme 1.29).



**Scheme 1.29** Construction of key fragment **90** for the Suzuki coupling reaction.<sup>169</sup>

The second coupling partner **91** was prepared in eight steps as outlined in Scheme 1.30.<sup>213</sup> An addition reaction of **101** with **102** afforded racemic alcohol **103** in 65% yield. Sharpless epoxidation under kinetic resolution conditions of racemic **103** resulted in alcohol (*S*)-**104** after separation from the epoxy-alcohol formed in the reaction. Then, bromination of **104** followed by Peterson elimination<sup>214</sup> using tetrabutylammonium fluoride (TBAF) and silylation of the secondary alcohol afforded *Z*-alkene **105**. A Sonogashira coupling reaction between **105** and TMS-acetylene followed by removal of the TMS-protecting group yielded intermediate **106**. Finally, hydroboration of the terminal alkyne in **106** using  $\text{Si}_2\text{BH}$  furnished borane reagent **91** *in situ* prior to the Suzuki coupling shown in Scheme 1.27.



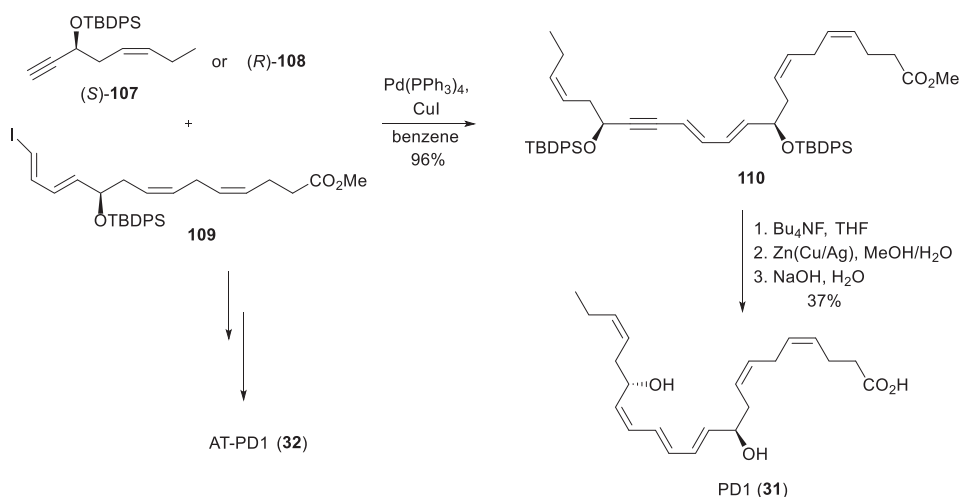
**Scheme 1.30** Construction of the key fragment **91** used in the Suzuki coupling reaction.<sup>169</sup>

The most recent total synthesis of RvE1 (**26**) was published by Anderson and co-workers early in 2020.<sup>215</sup> To unite three key fragments prepared, two Hiyama-Denmark<sup>216, 217</sup> cross-coupling reactions were utilized to control the stereochemistry of the *Z*-alkenes in the RvE1-polyene structure. Other key reactions employed in this synthesis included Sharpless asymmetric epoxidation under kinetic resolution conditions, Noyori asymmetric transfer hydrogenation (97%-99% *ee.*) and Takai olefination (*E/Z* = 5:1). The final compound was obtained over 12 linear steps (25 in total), but the yield is not mentioned by the authors. According to the experimental details published, RvE1 (**26**) was isolated in 2% yield (LLS).

Of note, in the presented schemes and strategies, selectivity and yields are specified whenever possible (i.e. if reported by the authors).

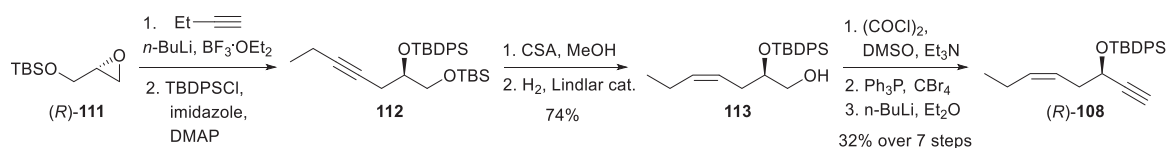
## 1.9 Literature syntheses of protectins

Several total syntheses of protectins have been reported by the same research groups that targeted RvE1 (**26**, Section 1.8). A selection of syntheses is presented in this section. The first total synthesis of PD1 (**31**) and AT-PD1 (**32**) was briefly announced in a biological journal by Petasis and collaborators in 2006.<sup>92</sup> Later, the syntheses were reported in detail, disclosing a successful Sonogashira coupling of acetylene (*S*)-**107** or the corresponding *R*-isomer **108** with iodide **109** (Scheme 1.31).<sup>111</sup> After *bis*-desilylation of **110**, reduction of the internal alkyne using the Boland conditions furnished the sensitive *E,E,Z*-triene in SPM **31** in 60% yield. In the final step, basic hydrolysis provided PD1 (**31**) over 16 steps in 4% yield (LLS). Analogously, by assembling (*R*)-**108** (depicted in Scheme 1.32) and key fragment **109**, AT-PD1 (**32**) was synthesized.



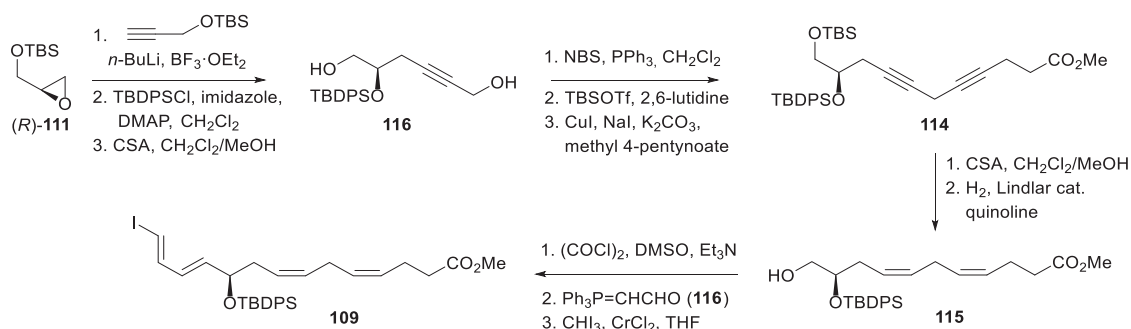
**Scheme 1.31** Final steps in the Petasis synthesis of PD1 (**31**) and AT-PD1 (**32**).<sup>111</sup>

Terminal acetylene (*S*)-**107** and (*R*)-**108** used in the above cross-coupling reaction were both prepared as outlined in Scheme 1.32.  $\text{BF}_3$ -mediated addition of the anion of 1-butyne to (*R*)-**111** followed by silylation of the resulting alcohol afforded intermediate **112**. Selective deprotection of the primary alcohol in **112** and *Z*-selective Lindlar hydrogenation of the alkyne afforded *Z*-alkene **113** in 74% yield over the two steps. Next, the primary alcohol was oxidized to the corresponding aldehyde that was converted into the Sonogashira coupling partner (*R*)-**108** via the Corey-Fuchs homologation reaction.<sup>218</sup> To obtain (*S*)-**107**, the enantiomer of (*R*)-**111** was used as starting material.



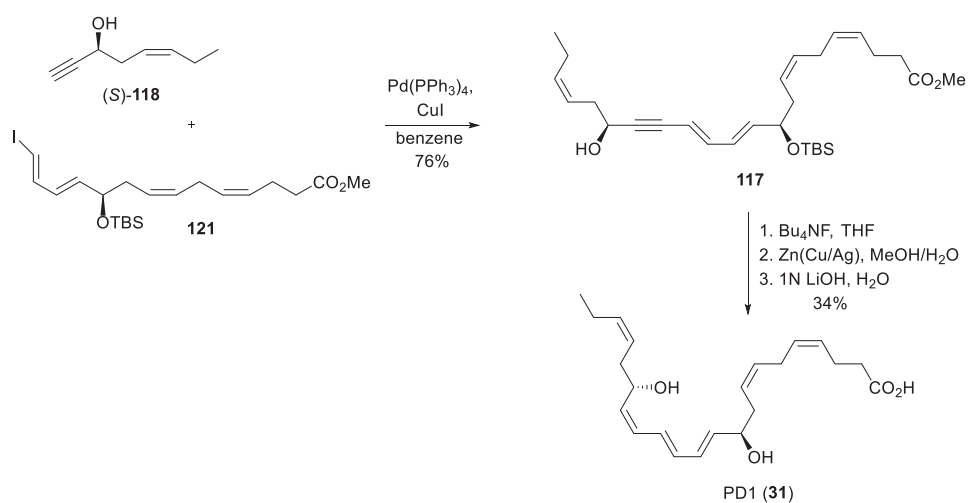
**Scheme 1.32** Preparation of the C<sub>15</sub>-C<sub>22</sub> fragment (*R*)-**108** used in the synthesis of AT-PD1 (**32**).<sup>111</sup>

Key fragment **109** was prepared in 11 steps as outlined in Scheme 1.33. The first three reactions were essentially the same as the first three steps in the construction of terminal acetylene (*R*)-**108** (Scheme 1.32). The next key transformations included a chemoselective Appel reaction,<sup>219</sup> Cu-mediated coupling with methyl 4-pentynoate to afford diyne **114**. Following selective deprotection of the primary alcohol, Lindlar hydrogenation of dialkyne **114** furnished the all *Z*-alkene **115** in 68% yield in the latter step. Swern oxidation<sup>204</sup> of **115** followed by a Wittig reaction<sup>159</sup> with ylide **116** and subsequent Takai olefination<sup>205</sup> then afforded intermediate **109**. The isomeric *Z*-iodo olefin was produced in small amounts in the Takai reaction and removed by column chromatography.



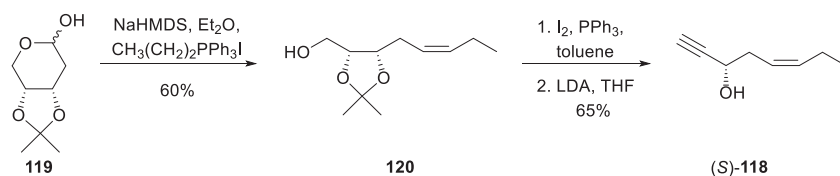
**Scheme 1.33** Construction of key fragment **109** for the Sonogashira cross-coupling reaction.<sup>111</sup>

In 2014, Spur and Rodriguez published a fourth synthesis of PD1 (**31**).<sup>220</sup> Analogous with the Petasis' synthesis discussed above (Scheme 1.31), a late stage Sonogashira reaction was applied to assemble the key fragments **121** and (*S*)-**118**, constructing the complete carbon chain of the target compound **31** (Scheme 1.34). Following desilylation of **117**, the Zn(Cu/Ag) Boland reagent was used to reduce the internal alkyne after unsuccessful attempts using Lindlar hydrogenation. However, the Boland protocol produced a mixture of 65:35 *Z/E*-isomers that was separated by column chromatography. In this synthesis, PD1 (**31**) was obtained over 12 linear steps and 2% overall yield.



Scheme 1.34 Final steps in Spur and Rodrigues' synthesis of PD1 (31).<sup>220</sup>

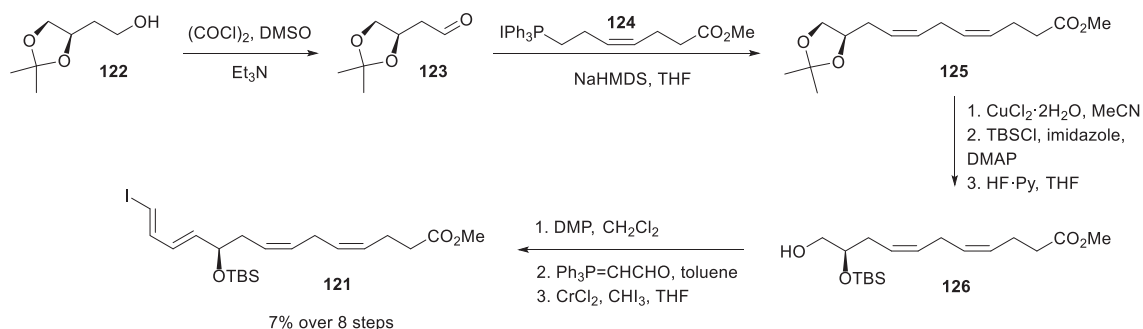
The C<sub>15</sub>-C<sub>22</sub> fragment (S)-118 was prepared from acetal-protected D-ribose 119 over three steps, which included a Wittig reaction to furnish 120, followed by an Appel reaction<sup>219</sup> and base induced *bis*-elimination of the resulting iodide to yield terminal acetylene 118 (Scheme 1.35).



Scheme 1.35 Preparation of fragment (S)-118 from D-ribose derivative 119.<sup>220</sup>

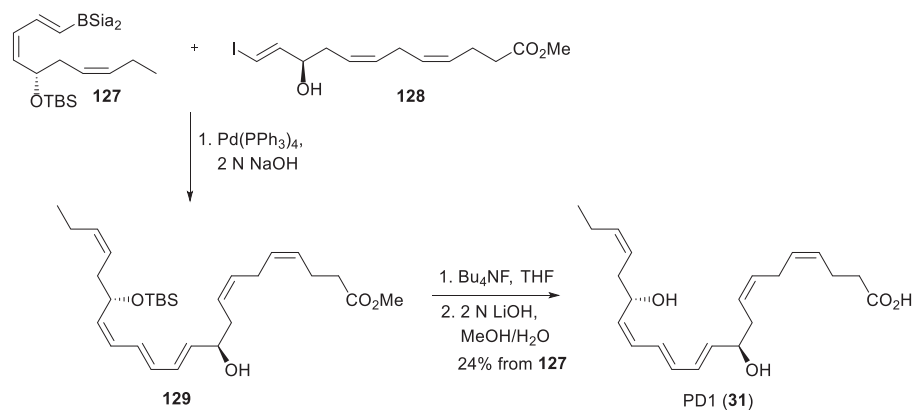
The *R*-configured stereocenter in coupling partner 121 was installed from chiral pool starting material 122 as outlined in Scheme 1.36. Aldehyde 123 was prepared using the Swern oxidation and subsequently subjected to a Wittig reaction with the ylide of 124 to form the skipped *Z*-diene 125. Cleavage of the acetal group in 125 followed by protecting group manipulations resulted in primary alcohol 126. This intermediate was then oxidized using the Dess-Martin reagent<sup>221</sup> followed by a Wittig homologation of the resulting aldehyde. Finally, a Takai reaction was applied to afford vinylic iodide 121 in 52% yield.





**Scheme 1.36** Construction of the C<sub>1</sub>-C<sub>14</sub> fragment **121** used in the synthesis of PD1 (**31**) by Spur and Rodriguez.<sup>220</sup>

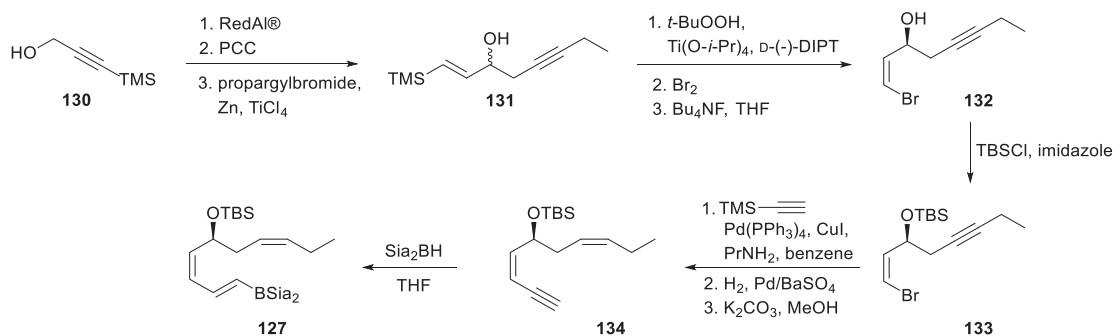
Ogawa and Kobayashi reported a total synthesis of PD1 (**31**) in 2011, which was based on the strategy developed for their synthesis of RvE1 (**26**) presented in the previous section.<sup>166</sup> Consequently, a late Suzuki cross-coupling<sup>172</sup> between key fragment **127** and **128** afforded the carbon-chain of PD1 (**31**, Scheme 1.37). Desilylation of **129** using TBAF followed by basic hydrolysis gave target compound **31** in 20 linear steps. However, the <sup>1</sup>H-NMR spectrum of the final compound, which is the only spectroscopical data published by the authors, was of such quality that neither characteristic signals nor coupling constants could be interpreted.



**Scheme 1.37** Synthesis of PD1 (**31**) by Ogawa and Kobayashi utilizing the Suzuki cross-coupling reaction.<sup>166</sup>

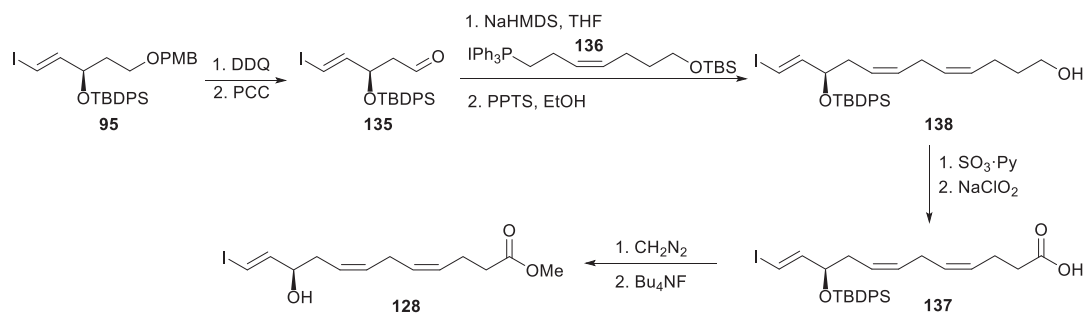
Fragment **127** was prepared in 11 steps from propargyl alcohol **130** as outlined in Scheme 1.38. The same methodology developed for the synthesis of **91** (Scheme 1.30) was applied to prepare **127**. Following reduction and oxidation of **130**, the resulting aldehyde was reacted with propargyl bromide, promoted by zinc and catalytic TiCl<sub>4</sub>, to afford racemic **131**. Sharpless asymmetric epoxidation under kinetic resolution conditions<sup>211</sup> followed by bromination and elimination installed the correct stereochemistry of **132**. Following TBS-protection of the secondary alcohol,

a Sonogashira cross-coupling between **133** and TMS-acetylene, followed by Lindlar hydrogenation and desilylation afforded intermediate **134** in 17% yield from **130**. Finally, hydroboration of the terminal acetylene **134** with  $\text{Si}_2\text{BH}$  provided borane reagent **127**.



**Scheme 1.38** Preparation of intermediate **127** used in the Suzuki cross-coupling reaction.<sup>166</sup>

Next, fragment **128** was prepared in eight steps from iodide **95**. The latter compound was prepared over six steps as outlined Section 1.8 (Scheme 1.28) in the synthesis of RvE1 (**26**). After selective deprotection and subsequent oxidation of **95**, the resulting aldehyde **135** was subjected to a *Z*-selective Wittig reaction with the ylide of **136**. Subsequent deprotection of the resulting primary silylether and oxidation afforded carboxylic acid **137**. Finally, methylation of the resulting acid using diazomethane and desilylation with TBAF provided methyl ester **128** intended for the Suzuki cross-coupling reaction (Scheme 1.39).



**Scheme 1.39** Assembly of the C<sub>1</sub>-C<sub>12</sub> fragment **128** used in Kobayashi and Ogawa's synthesis of PD1 (**31**).<sup>166</sup>

## 1.10 Aim of study

The main aim of this work was to apply different strategies to obtain anti-inflammatory and pro-resolving lipid mediators and analogues thereof. The partial objectives of this work are listed below:

- Obtain material of 22-OH-PD1<sub>n-3</sub> DPA (**139**) through stereoselective synthesis to assign its absolute stereochemistry and investigate its biosynthetic formation from PD1<sub>n-3</sub> DPA (**31**).
- Develop a stereoselective synthesis of 17*S*-3-oxa-PD1<sub>n-3</sub> DPA (**140**) and 17*R*-3-oxa-PD1<sub>n-3</sub> DPA (**141**), rendering these two synthetic analogues available for biological evaluations considering biosynthesis, metabolic resistance and pro-resolving properties relative to PD1<sub>n-3</sub> DPA (**31**).
- Develop an efficient, stereoselective and convergent synthesis of RvE1 (**26**).

## References

1. Fetterman, J. W. Jr.; Zdanowicz, M. M., *Am. J. Health Syst. Pharm.* **2009**, *66* (13), 1169.
2. Funk, C. D., *Science* **2001**, *294* (5548), 1871.
3. Serhan, C. N.; Chiang, N.; Van Dyke, T. E., *Nat. Rev. Immunol.* **2008**, *8* (5), 349.
4. Vance, J. E.; Vance, D. E., *Biochemistry Of Lipids, Lipoproteins And Membranes*. 5th ed.; Elsevier Amsterdam: Netherlands, 2008.
5. Rodríguez, M.; G Rebollar, P.; Mattioli, S.; Castellini, C., *Animals* **2019**, *9* (10), 806.
6. Calder, P. C.; Yaqoob, P., *Postgrad. Med. J.* **2009**, *121* (6), 148.
7. Calder, P. C., *Eur. J. Pharmacol.* **2011**, *668*, S50.
8. De Caterina, R., *N. Engl. J. Med.* **2011**, *364* (25), 2439.
9. Zárate, R.; El Jaber-Vazdekis, N.; Tejera, N.; Pérez, J. A.; Rodríguez, C., *Clin. Transl. Med.* **2017**, *6* (1), 25.
10. Qiu, X., *Prostaglandins Leukot. Essent. Fatty Acids* **2003**, *68* (2), 181.
11. Dewick, P. M., *Medicinal Natural Products: A Biosynthetic Approach*. 3rd ed.; John Willey and Sons: Chisester, 2009.
12. Burr, G. O.; Burr, M. M., *J. Biol. Chem.* **1929**, *82*, 345.
13. Burr, G. O.; Burr, M. M., *J. Biol. Chem.* **1930**, *86*, 587.
14. Spector, A. A.; Kim, H. Y., *J. Lipid. Res.* **2015**, *56* (1), 11.
15. Harper, C. R.; Jacobson, T. A., *Arch. Intern. Med.* **2001**, *161* (18), 2185.
16. Cleland, L. G.; James, M. J.; Proudman, S. M., *Drugs* **2003**, *63* (9), 845.
17. Nettleton, J. A.; Katz, R., *J. Am. Diet. Assoc.* **2005**, *105* (3), 428.
18. Dyall, S. C., *Front. Aging Neurosci.* **2015**, *7* (52), 52.
19. Chiang, N.; Serhan, C. N., *Mol. Asp. Med.* **2017**, *58*, 114.
20. Haeggström, J. Z.; Funk, C. D., *Chem. Rev.* **2011**, *111* (10), 5866.
21. Rouzer, C. A.; Marnett, L. J., *J. Lipid. Res.* **2009**, *50* Suppl (Suppl), S29.
22. Kuhn, H.; Banthiya, S.; van Leyen, K., *Biochim. Biophys. Acta* **2015**, *1851* (4), 308.
23. Mashima, R.; Okuyama, T., *Redox biol.* **2015**, *6*, 297.
24. Liavonchanka, A.; Feussner, I., *J. Plant. Physiol.* **2006**, *163* (3), 348.
25. Nelson, M. J.; Seitz, S. P., *Curr. Opin. Struct. Biol.* **1994**, *4* (6), 878.
26. Serhan, C. N.; Petasis, N. A., *Chem. Rev.* **2011**, *111* (10), 5922.
27. Ricciotti, E.; FitzGerald, G. A., *Arterioscler. Thromb. Vasc. Biol.* **2011**, *31* (5), 986.
28. Serhan, C. N., *Nature* **2014**, *510* (7503), 92.
29. Serhan, C. N.; Fredman, G.; Yang, R.; Karamnov, S.; Belayev, L. S.; Bazan, N. G.; Zhu, M.; Winkler, J. W.; Petasis, N. A., *Chem. Biol.* **2011**, *18* (8), 976.
30. Chiang, N.; Serhan, C. N., *Discov. Med.* **2004**, *4* (24), 470.
31. Ornelas, A.; Zacharias-Millward, N.; Menter, D. G.; Davis, J. S.; Lichtenberger, L.; Hawke, D.; Hawk, E.; Vilar, E.; Bhattacharya, P.; Millward, S., *Cancer Metastasis Rev.* **2017**, *36* (2), 289.
32. Baynes, J. D. M., In *Medical Biochemistry*, 4th ed.; Elsevier Mosby: Philadelphia, 2014; pp 182-191.
33. Schulz, H., *Biochim. Biophys. Acta* **1991**, *1081* (2), 109.
34. Newton, K.; Dixit, V. M., *Cold Spring Harb. Perspect. Biol.* **2012**, *4* (3), a006049.
35. Medzhitov, R., *Nature* **2008**, *454* (7203), 428.
36. Fullerton, J. N.; Gilroy, D. W., *Nat. Rev. Drug. Discov.* **2016**, *15* (8), 551.
37. Serhan, C. N., *Annu. Rev. Immunol.* **2007**, *25* (1), 101.

38. Tabas, I.; Glass, C. K., *Science* **2013**, 339 (6116), 166.
39. Serhan, C. N.; Savill, J., *Nat. Immunol.* **2005**, 6 (12), 1191.
40. Sugimoto, M. A.; Sousa, L. P.; Pinho, V.; Perretti, M.; Teixeira, M. M., *Front. Immunol.* **2016**, 7 (160), 160. PMID: 27199985.
41. Serhan, C. N., *J. Am. Phatol.* **2010**, 177 (4), 1576.
42. Libby, P., *Nutr. Rev.* **2007**, 65, S140.
43. Krishnamoorthy, N.; Burkett, P. R.; Dalli, J.; Abdalnour, R. E. E.; Colas, R.; Ramon, S.; Phipps, R. P.; Petasis, N. A.; Kuchroo, V. K.; Serhan, C. N.; Levy, B. D., *J. Immunol.* **2015**, 194 (3), 863.
44. Nathan, C.; Ding, A., *Cell* **2010**, 140 (6), 871.
45. Manabe, I., *Circ. J.* **2011**, 12 (75), 2739.
46. Gilroy, D.; De Maeyer, R., *Semin. Immunol.* **2015**, 27 (3), 161.
47. Dennis, E. A.; Norris, P. C., *Nat. Rev. Immunol.* **2015**, 15 (8), 511.
48. Gabbs, M.; Leng, S.; Devassy, J. G.; Monirujjaman, M.; Aukema, H. M., *Adv. Nutr.* **2015**, 6 (5), 513.
49. Bennett, M.; Gilroy, D. W., *Microbiol. Spectr.* **2016**, 4 (6). PMID: 27837747.
50. Wilson, D. B., *Postgrad. Med.* **1987**, 81 (4), 309.
51. Ruan, Y. C.; Zhou, W.; Chan, H. C., *Physiology* **2011**, 26 (3), 156.
52. Smith, W. L.; DeWitt, D. L.; Garavito, R. M., *Annu. Rev. Biochem.* **2000**, 69 (1), 145.
53. Marnett, L. J.; Rowlinson, S. W.; Goodwin, D. C.; Kalgutkar, A. S.; Lanzo, C. A., *J. Biol. Chem.* **1999**, 274 (33), 22903.
54. Rogge, C. E.; Ho, B.; Liu, W.; Kulmacz, R. J.; Tsai, A. L., *Biochemistry* **2006**, 45 (2), 523.
55. Harris, S. G.; Padilla, J.; Koumas, L.; Ray, D.; Phipps, R. P., *Trends. Immunol.* **2002**, 23 (3), 144.
56. Levy, B. D.; Clish, C. B.; Schmidt, B.; Gronert, K.; Serhan, C. N., *Nat. Immunol.* **2001**, 2 (7), 612.
57. Rådmark, O.; Werz, O.; Steinhilber, D.; Samuelsson, B., *Trends Biochem. Sci.* **2007**, 32 (7), 332.
58. Samuelsson, B.; Borgeat, P.; Hammarström, S.; Murphy, R. C., *Prostaglandins* **1979**, 17 (6), 785.
59. Samuelsson, B.; Dahlén, S. E.; Lindgren, J. A.; Rouzer, C. A.; Serhan, C. N., *Science* **1987**, 237 (4819), 1171.
60. Tager, A. M.; Luster, A. D., *Prostaglandins Leukot. Essent. Fatty Acids* **2003**, 69 (2), 123.
61. Kanaoka, Y.; Boyce, J. A., *J. Immunol.* **2004**, 173 (3), 1503.
62. Serhan, C. N., *Prostaglandins Leukot. Essent. Fatty Acids* **2005**, 73 (3), 141.
63. Serhan, C. N.; Hamberg, M.; Samuelsson, B., *Proc. Natl. Acad. Sci. U. S. A.* **1984**, 81 (17), 5335.
64. Serhan, C. N.; Hamberg, M.; Samuelsson, B., *Biochem. Biophys. Res. Commun.* **1984**, 118 (3), 943.
65. Petasis, N. A.; Akritopoulou-Zanze, I.; Fokin, V. V.; Bernasconi, G.; Keledjian, R.; Yang, R.; Uddin, J.; Nagulapalli, K. C.; Serhan, C. N., *Prostagandins Leukotr. Essent. Fatty Acids* **2005**, 73 (3), 301.
66. Chandrasekharan, J. A.; Sharma-Walia, N., *J. Inflamm. Res.* **2015**, 8, 181.
67. Serhan, C. N., *Prostaglandins* **1997**, 53 (2), 107.
68. Serhan, C. N.; Maddox, J. F.; Petasis, N. A.; Akritopoulou-Zanze, I.; Papayianni, A.; Brady, H. R.; Colgan, S. P.; Madara, J. L., *Biochemistry* **1995**, 34 (44), 14609.

69. Takano, T.; Clish, C. B.; Gronert, K.; Petasis, N.; Serhan, C. N., *J. Clin. Invest.* **1998**, *101* (4), 819.
70. Gaetano de, M.; McEvoy, C.; Andrews, D.; Cacace, A.; Hunter, J.; Brennan, E.; Godson, C., *Front. Pharmacol.* **2018**, *9*, 1488.
71. English, J. T.; Norris, P. C.; Hodges, R. R.; Dartt, D. A.; Serhan, C. N., *Prostagandins Leukotr. Essent. Fatty Acids* **2017**, *117*, 17.
72. Serhan, C.; Recchiuti, A., *Front. Immunol.* **2012**, *3* (298), 298.
73. Serhan, C. N.; Clish, C. B.; Brannon, J.; Colgan, S. P.; Chiang, N.; Gronert, K., *J. Exp. Med.* **2000**, *192* (8), 1197.
74. Serhan, C. N.; Hong, S.; Gronert, K.; Colgan, S. P.; Devchand, P. R.; Mirick, G.; Moussignac, R. L., *J. Exp. Med.* **2002**, *196* (8), 1025.
75. Vik, A.; Dalli, J.; Hansen, T. V., *Bioorg. Med. Chem. Lett.* **2017**, *27* (11), 2259.
76. Serhan, C. N.; Chiang, N., *Curr. Opin. Pharmacol.* **2013**, *13* (4), 632.
77. Serhan, C. N., *Mol. Asp. Med.* **2017**, *58*, 1.
78. Colas, R. A.; Shinohara, M.; Dalli, J.; Chiang, N.; Serhan, C. N., *Angew. Chem. Int.* **2014**, *307* (1), C39.
79. Serhan, C. N.; Clish, C. B.; Brannon, J.; Colgan, S. P.; Chiang, N.; Gronert, K., *J. Exp. Med.* **2000**, *192* (8), 1197.
80. Arita, M.; Bianchini, F.; Aliberti, J.; Sher, A.; Chiang, N.; Hong, S.; Yang, R.; Petasis, N. A.; Serhan, C. N., *J. Exp. Med.* **2005**, *201* (5), 713.
81. Serhan, C. N.; Levy, B. D., *J. Clin. Invest.* **2018**, *128* (7), 2657.
82. Isobe, Y.; Arita, M.; Iwamoto, R.; Urabe, D.; Todoroki, H.; Masuda, K.; Inoue, M.; Arai, H., *J. Biochem.* **2013**, *153* (4), 355.
83. Schwanke, R. C.; Marcon, R.; Bento, A. F.; Calixto, J. B., *Eur. J. Pharmacol.* **2016**, *785*, 156.
84. Isobe, Y.; Arita, M.; Matsueda, S.; Iwamoto, R.; Fujihara, T.; Nakanishi, H.; Taguchi, R.; Masuda, K.; Sasaki, K.; Urabe, D.; Inoue, M.; Arai, H., *J. Biol. Chem.* **2012**, *287* (13), 10525.
85. Oh, S. F.; Pillai, P. S.; Recchiuti, A.; Yang, R.; Serhan, C. N., *J. Clin. Invest.* **2011**, *121* (2), 569.
86. Balta, M. G.; Loos, B. G.; Nicu, E. A., *Front. Immunol.* **2017**, *8*, 1682.
87. Levy, B. D., *Prostagandins Leukotr. Essent. Fatty Acids* **2010**, *82* (4-6), 327.
88. Taubman, M. A.; Valverde, P.; Han, X.; Kawai, T., *J. Periodontol.* **2005**, *76* (11 Suppl), 2033.
89. Weylandt, K. H., *Eur. J. Pharmacol.* **2016**, *785*, 108.
90. Hong, S.; Gronert, K.; Devchand, P. R.; Moussignac, R. L.; Serhan, C. N.; Hong, S., *J. Biol. Chem.* **2003**, *278* (17), 14677.
91. Hansen, T. V.; Vik, A.; Serhan, C. N., *Front. Pharmacol.* **2019**, *9*, 1582.
92. Serhan, C. N.; Gotlinger, K.; Hong, S.; Lu, Y.; Siegelman, J.; Baer, T.; Yang, R.; Colgan, S. P.; Petasis, N. A., *J. Immunol.* **2006**, *176* (3), 1848.
93. Kenchegowda, S.; He, J.; Bazan, H. E., *Prostagandins Leukotr. Essent. Fatty Acids* **2013**, *88* (1), 27.
94. Katakura, M.; Hashimoto, M.; Inoue, T.; Al Mamun, A.; Tanabe, Y.; Iwamoto, R.; Arita, M.; Tsuchikura, S.; Shido, O., *Molecules* **2014**, *19* (3), 3247.
95. Xu, Z. Z.; Liu, X. J.; Berta, T.; Park, C. K.; Lü, N.; Serhan, C. N.; Ji, R.-R., *Ann. Neurol.* **2013**, *74* (3), 490.

96. Levy, B. D.; Kohli, P.; Gotlinger, K.; Haworth, O.; Hong, S.; Kazani, S.; Israel, E.; Haley, K. J.; Serhan, C. N., *J. Immunol.* **2007**, *178* (1), 496.
97. Serhan, C. N.; Dalli, J.; Colas, R. A.; Winkler, J. W.; Chiang, N., *Biochim. Biophys. Acta* **2015**, *1851* (4), 397.
98. Shinohara, M.; Mirakaj, V.; Serhan, C. N., *Front. Immunol.* **2012**, *3*, 81.
99. Dalli, J.; Colas, R. A.; Serhan, C. N., *Sci. Rep.* **2013**, *3*, 1940.
100. Tungen, J. E.; Primdahl, K. G.; Hansen, T. V., *J. Nat. Prod.* **2020**, *83* (7), 2255.
101. Aursnes, M.; Tungen, J. E.; Vik, A.; Colas, R.; Cheng, C. Y. C.; Dalli, J.; Serhan, C. N.; Hansen, T. V., *J. Nat. Prod.* **2014**, *77* (4), 910.
102. Tungen, J. E.; Gerstmann, L.; Vik, A.; De Matteis, R.; Colas, R. A.; Dalli, J.; Chiang, N.; Serhan, C. N.; Kalesse, M.; Hansen, T. V., *Chemistry* **2019**, *25* (6), 1476.
103. Tungen, J. E.; Aursnes, M.; Dalli, J.; Arnardottir, H.; Serhan, C. N.; Hansen, T. V., *Chem. Eur. J.* **2014**, *20* (45), 14575.
104. Primdahl, K. G.; Tungen, J. E.; De Souza, P. R. S.; Colas, R. A.; Dalli, J.; Hansen, T. V.; Vik, A., *Org. Biomol. Chem.* **2017**, *15* (40), 8606.
105. Frigerio, F.; Pasqualini, G.; Craparotta, I.; Marchini, S.; van Vliet, E. A.; Foerch, P.; Vandenplas, C.; Leclercq, K.; Aronica, E.; Porcu, L.; Pistorius, K.; Colas, R. A.; Hansen, T. V.; Perretti, M.; Kaminski, R. M.; Dalli, J.; Vezzani, A., *Brain* **2018**, *141* (11), 3130.
106. Dalli, J.; Chiang, N.; Serhan, C. N., *Proc. Natl. Acad. Sci. U. S. A.* **2014**, *111* (44), E4753.
107. Dalli, J.; Ramon, S.; Norris, P. C.; Colas, R. A.; Serhan, C. N., *FASEB J.* **2015**, *29* (5), 2120.
108. Ramon, S.; Dalli, J.; Sanger, J. M.; Winkler, J. W.; Aursnes, M.; Tungen, J. E.; Hansen, T. V.; Serhan, C. N., *J. Am. Phatol.* **2016**, *186* (4), 962.
109. Aursnes, M.; Tungen, J. E.; Colas, R. A.; Vlasakov, I.; Dalli, J.; Serhan, C. N.; Hansen, T. V., *J. Nat. Prod.* **2015**, *78* (12), 2924.
110. Pistorius, K.; Souza, P.; Matteis, R.; Austin-Williams, S.; Primdahl, K.; Vik, A.; Mazzacuva, F.; Colas, R.; Marques, R.; Hansen, T.; Dalli, J., *Cell Chem. Biol.* **2018**, *25* (6), 749.
111. Petasis, N. A.; Yang, R.; Winkler, J. W.; Zhu, M.; Uddin, J.; Bazan, N. G.; Serhan, C. N., *Tetrahedron Lett.* **2012**, *53* (14), 1695.
112. Feinmark, S. J.; Lindgren, J. Å.; Claesson, H. E.; Malmsten, C.; Samuelsson, B., *FEBS Lett.* **1981**, *136* (1), 141.
113. Tungen, J. E.; Aursnes, M.; Vik, A.; Ramon, S.; Colas, R. A.; Dalli, J.; Serhan, C. N.; Hansen, T. V., *J. Nat. Prod.* **2014**, *77* (10), 2241.
114. Shirley, M. A.; Murphy, R. C., *J. Biol. Chem.* **1990**, *265* (27), 16288.
115. Jedlitschky, G.; Huber, M.; Völkl, A.; Müller, M.; Leier, I.; Müller, J.; Lehmann, W. D.; Fahimi, H. D.; Keppler, D., *J. Biol. Chem.* **1991**, *266* (36), 24763.
116. Mayatepek, E.; Lehmann, W. D.; Fauler, J.; Tsikas, D.; Frölich, J. C.; Schutgens, R. B.; Wanders, R. J.; Keppler, D., *J. Clin. Invest.* **1993**, *91* (3), 881.
117. Balas, L.; Risé, P.; Gandrath, D.; Rovati, G.; Bolego, C.; Stellari, F.; Trenti, A.; Buccellati, C.; Durand, T.; Sala, A., *J. Med. Chem.* **2019**, *62* (21), 9961.
118. Arita, M.; Oh, S. F.; Chonan, T.; Hong, S.; Elangovan, S.; Sun, Y. P.; Uddin, J.; Petasis, N. A.; Serhan, C. N., *J. Biol. Chem.* **2006**, *281* (32), 22847.
119. Colas, R. A.; Dalli, J.; Chiang, N.; Vlasakov, I.; Sanger, J. M.; Riley, I. R.; Serhan, C. N., *J. Immunol.* **2016**, *197* (11), 4444.

120. Clish, C. B.; Levy, B. D.; Chiang, N.; Tai, H. H.; Serhan, C. N., *J. Biol. Chem.* **2000**, *275* (33), 25372.
121. Sun, Y. P.; Oh, S. F.; Uddin, J.; Yang, R.; Gotlinger, K.; Campbell, E.; Colgan, S. P.; Petasis, N. A.; Serhan, C. N., *J. Biol. Chem.* **2007**, *282* (13), 9323.
122. Rosenbaum, D. M.; Rasmussen, S. G. F.; Kobilka, B. K., *Nature* **2009**, *459* (7245), 356.
123. Capper, M. J.; Wacker, D., *Nature* **2018**, *558* (7711), 529.
124. Li, J.; Ning, Y.; Hedley, W.; Saunders, B.; Chen, Y.; Tindill, N.; Hannay, T.; Subramaniam, S., *Nature* **2002**, *420* (6916), 716.
125. (a) Dalli, J.; Serhan, C. N., *Br. J. Pharmacol.* **2019**, *176* (8), 1024. (b) Wire B (2009). Resolvix announces positive data from Phase 2 clinical trial of the reesolvin RX-10045 in patients with dry eye syndrome. Available at: <http://www.businesswire.com/news/home/20090824005320/en/Resolvix-AnnouncesPositive-Data-Phase-20090824005322-Clinical> (10.09.20).
126. Bang, S.; Xie, Y. K.; Zhang, Z. J.; Wang, Z.; Xu, Z. Z.; Ji, R.-R., *J. Clin. Invest.* **2018**, *128* (8), 3568.
127. Chiang, N.; Libreros, S.; Norris, P. C.; de la Rosa, X.; Serhan, C. N., *J. Clin. Invest.* **2019**, *129* (12), 5294.
128. Park, J.; Langmead, C. J.; Riddy, D. M., *ACS Pharmacol. Transl. Sci.* **2020**, *3* (1), 88.
129. Chiang, N.; de la Rosa, X.; Libreros, S.; Serhan, C. N., *J. Immunol.* **2017**, *198* (2), 842.
130. Sun, L.; Ye, R. D., *Acta Pharmacol. Sin.* **2012**, *33* (3), 342.
131. Fiore, S.; Maddox, J. F.; Perez, H. D.; Serhan, C. N., *J. Exp. Med.* **1994**, *180* (1), 253.
132. Pirault, J.; Bäck, M., *Front. Pharmacol.* **2018**, *9*, 1273.
133. Tao, X.; Lee, M. S.; Donnelly, C. R.; Ji, R.-R., *Neurotherapeutics* **2020**. PMID: 32696274.
134. Ohira, T.; Arita, M.; Omori, K.; Recchiuti, A.; Van Dyke, T. E.; Serhan, C. N., *J. Biol. Chem.* **2010**, *285* (5), 3451.
135. Sun, Y. P.; Tjonahen, E.; Keledjian, R.; Zhu, M.; Yang, R.; Recchiuti, A.; Pillai, P. S.; Petasis, N. A.; Serhan, C. N., *Prostaglandins Leukot. Essent. Fatty Acids* **2009**, *81* (5-6), 357.
136. Arita, M.; Ohira, T.; Sun, Y. P.; Elangovan, S.; Chiang, N.; Serhan, C. N., *J. Immunol.* **2007**, *178* (6), 3912.
137. Marcheselli, V. L.; Mukherjee, P. K.; Arita, M.; Hong, S.; Antony, R.; Sheets, K.; Winkler, J. W.; Petasis, N. A.; Serhan, C. N.; Bazan, N. G., *Prostaglandins Leukotr. Essent. Fatty Acids* **2010**, *82* (1), 27.
138. Marazziti, D.; Golini, E.; Gallo, A.; Lombardi, M. S.; Matteoni, R.; Tocchini-Valentini, G. P., *Genomics* **1997**, *45* (1), 68.
139. Leng, N.; Gu, G.; Simerly, R. B.; Spindel, E. R., *Brain Res. Mol. Brain. Res.* **1999**, *69* (1), 73.
140. McLean, L., Drug development. In *Rheumatology*, 6th ed.; Hochberg, M. C.; Silman, A. J.; Smolen, J. S.; Weinblatt, M. E.; Weisman, M. H., Elsevier Ltd.: Philadelphia, 2015; pp 395-400.
141. Hefti, F. F., *BMC Neurosci.* **2008**, *9 Suppl 3* (Suppl 3), S7.
142. Lombardino, J. G.; Lowe, J. A., *Nat. Rev. Drug. Discov.* **2004**, *3* (10), 853.
143. Hughes, J. P.; Rees, S.; Kalindjian, S. B.; Philpott, K. L., *Br. J. Pharmacol.* **2011**, *162* (6), 1239.
144. Mohs, R. C.; Greig, N. H., *Alzheimers Dement.* **2017**, *3* (4), 651.
145. Flier, J. S., *J. Clin. Invest.* **2019**, *129* (6), 2172.



146. Holladay, M. W.; Silverman, R. B., *The Organic Chemistry of Drug Design and Drug Action*. 3rd edition ed.; US: Academic Press: US, 2014.
147. Orr, S. K.; Colas, R. A.; Dalli, J.; Chiang, N.; Serhan, C. N., *Am. J. Physiol. Lung Cell Mol.* **2015**, *308* (9), L904.
148. Takano, T.; Fiore, S.; Maddox, J. F.; Brady, H. R.; Petasis, N. A.; Serhan, C. N., *J. Exp. Med.* **1997**, *185* (9), 1693.
149. Fukuda, H.; Muromoto, R.; Takakura, Y.; Ishimura, K.; Kanada, R.; Fushihara, D.; Tanabe, M.; Matsubara, K.; Hirao, T.; Hirashima, K.; Abe, H.; Arisawa, M.; Matsuda, T.; Shuto, S., *Org. Lett.* **2016**, *18* (24), 6224.
150. Duffy, C. D.; Guiry, P. J., *Med. Chem. Comm.* **2010**, *1* (4), 249.
151. Leonard, M. O.; Hannan, K.; Burne, M. J.; Lappin, D. W. P.; Doran, P.; Coleman, P.; Stenson, C.; Taylor, C. T.; Daniels, F.; Godson, C.; Petasis, N. A.; Rabb, H.; Brady, H. R., *J. Am. Soc. Nephrol.* **2002**, *13* (6), 1657.
152. Mitchell, S.; Thomas, G.; Harvey, K.; Cottell, D.; Reville, K.; Berlasconi, G.; Petasis, N. A.; Erwig, L.; Rees, A. J.; Savill, J.; Brady, H. R.; Godson, C., *J. Am. Soc. Nephrol.* **2002**, *13* (10), 2497.
153. Van Dyke, T. E.; Hasturk, H.; Kantarci, A.; Freire, M. O.; Nguyen, D.; Dalli, J.; Serhan, C. N., *J. Dent. Res.* **2015**, *94* (1), 148.
154. Safety and Preliminary Efficacy of Lipoxin Analog BLXA4-ME Oral Rinse for the Treatment of Gingivitis (BLXA4). Available at: <https://clinicaltrials.gov/ct2/show/NCT02342691?cond=NCT02342691&draw=2&rank=1> (09.07.2020).
155. Nicolaou, K. C., *Proc. Math. Phys. Eng. Sci.* **2014**, *470* (2163), 20130690.
156. Balas, L.; Guichardant, M.; Durand, T.; Lagarde, M., *Biochimie* **2014**, *99*, 1.
157. Dayaker, G.; Durand, T.; Balas, L., *Chem. Eur. J.* **2014**, *20* (10), 2879.
158. Balas, L.; Durand, T., *Prog. Lipid. Res.* **2016**, *61*, 1.
159. Wittig, G.; Schöllkopf, U., *Chem. Ber.* **1954**, *87* (9), 1318.
160. Maryanoff, B. E.; Reitz, A. B., *Chem. Rev.* **1989**, *89* (4), 863.
161. Clayden, J.; Greeves, N.; Warren, S., *Organic chemistry*. 2nd ed. ed.; Oxford University Press: Oxford, 2012.
162. Byrne, P. A.; Gilheany, D. G., *Chem. Soc. Rev.* **2013**, *42* (16), 6670.
163. Vedejs, E.; Marth, C. F.; Ruggeri, R., *J. Am. Chem. Soc.* **1988**, *110* (12), 3940.
164. Lars, L.; Thomas, W., *Pure Appl. Chem.* **2019**, *91* (1), 95.
165. Rodriguez, A. R.; Spur, B. W., *Tetrahedron Lett.* **2012**, *53* (32), 4169.
166. Ogawa, N.; Kobayashi, Y., *Tetrahedron Lett.* **2011**, *52* (23), 3001.
167. Nicolaou, K. C.; Veale, C. A.; Webber, S. E.; Katerinopoulos, H., *J. Am. Chem. Soc.* **1985**, *107* (25), 7515.
168. Li, J.; Leong, M. M.; Stewart, A.; Rizzacasa, M. A., *Beilstein J. Org. Chem.* **2013**, *9*, 2762.
169. Ogawa, N.; Kobayashi, Y., *Tetrahedron Letters* **2009**, *50* (44), 6079.
170. Heck, R. F.; Nolley, J. P., *J. Org. Chem.* **1972**, *37* (14), 2320.
171. King, A. O.; Okukado, N.; Negishi, E.-i., *J. Chem. Soc. Chem. Commun.* **1977**, (19), 683.
172. Miyaura, N.; Yamada, K.; Suzuki, A., *Tetrahedron Lett.* **1979**, *20* (36), 3437.
173. Sonogashira, K.; Tohda, Y.; Hagihara, N., *Tetrahedron Lett.* **1975**, *16* (50), 4467.
174. Nicolaou, K. C.; Bulger, P. G.; Sarlah, D., *Angew. Chem. Int.* **2005**, *44* (29), 4442.
175. The Nobel Price in Chemistry 2010. <https://www.nobelprize.org/prizes/chemistry/2010/summary/> (accessed 29.06.2020).

176. Ogawa, N.; Tojo, T.; Kobayashi, Y., *Tetrahedron Lett.* **2014**, *55* (16), 2738.
177. Tungen, J. E.; Aursnes, M.; Hansen, T. V., *Tetrahedron Lett.* **2015**, *56* (14), 1843.
178. Morita, M.; Wu, S.; Kobayashi, Y., *Org. Biomol. Chem.* **2019**, *17* (8), 2212.
179. Vaz, B.; Otero, L.; Álvarez, R.; de Lera, Á. R., *Chem. Eur. J.* **2013**, *19* (39), 13065.
180. Oger, C.; Balas, L.; Durand, T.; Galano, J. M., *Chem. Rev.* **2013**, *113* (3), 1313.
181. Lindlar, H., *Helv. Chim. Acta* **1952**, *35* (35), 446.
182. Lindlar, H.; Dubuis, R., *Org. Synth.* **1966**, *46*, 89.
183. Semmelhack, M. F.; Trost, B. M.; Fleming, I., *Comprehensive organic synthesis : selectivity, strategy & efficiency in modern organic chemistry*. Pergamon Press: Oxford, 1991; Vol. 4.
184. Brown, C. A.; Ahuja, V. K., *J. Chem. Soc. Chem. Commun.* **1973**, (15), 553.
185. Daeuble, J. F.; McGettigan, C.; Stryker, J. M., *Tetrahedron Lett.* **1990**, *31* (17), 2397.
186. Boland, W.; Schroer, N.; Sieler, C.; Feigel, M., *Helv. Chim. Acta* **1987**, *70* (4), 1025.
187. Mohamed, Y. M. A.; Hansen, T. V., *Tetrahedron* **2013**, *69* (19), 3872.
188. Wurtz, C. A., *Bull. Soc. Chim. Fr.* **1872**, *17*, 436.
189. Borodin, A., *Deut. Chem. Ges. Ber.* **1873**, *5*, 480.
190. Mandal, S.; Mandal, S.; Ghosh, S. K.; Ghosh, A.; Saha, R.; Banerjee, S.; Saha, B., *Synth. Commun.* **2016**, *46* (16), 1327.
191. Zimmerman, H. E.; Traxler, M. D., *J. Am. Chem. Soc.* **1957**, *79*, 1920.
192. Evans, D. A.; Takacs, J. M.; McGee, L. R.; Ennis, M. D.; Mathre, D. J.; Bartroli, J., *Pure Appl. Chem.* **1981**, *53* (6), 1109.
193. Teruaki, M.; Koichi, N.; Kazuo, B., *Chem. Lett.* **1973**, *2* (9), 1011.
194. Evans, D. A.; Bartroli, J.; Shih, T. L., *J. Am. Chem. Soc.* **1981**, *103* (8), 2127.
195. Evans, D. A.; Nelson, J. V.; Vogel, E.; Taber, T. R., *J. Am. Chem. Soc.* **1981**, *103* (11), 3099.
196. Do Van Thanh, N., *Tetrahedron* **2020**, *76* (4), 130618.
197. Crimmins, M. T.; King, B. W.; Tabet, E. A., *J. Am. Chem. Soc.* **1997**, *119* (33), 7883.
198. Crimmins, M. T.; Chaudhary, K., *Org. Lett.* **2000**, *2* (6), 775.
199. Evans, D. A.; Tedrow, J. S.; Shaw, J. T.; Downey, C. W., *J. Am. Chem. Soc.* **2002**, *124* (3), 392.
200. Nagao, Y.; Hagiwara, Y.; Kumagai, T.; Ochiai, M.; Inoue, T.; Hashimoto, K.; Fujita, E., *J. Org. Chem.* **1986**, *51* (12), 2391.
201. Zhang, Y.; Phillips, A. J.; Sammakia, T., *Org. Lett.* **2004**, *6* (1), 23.
202. Sugiyama, H.; Yokokawa, F.; Shioiri, T., *Org. Lett.* **2000**, *2* (14), 2149.
203. Petasis, N.A. Preparation of trihydroxy polyunsaturated eicosanoid derivatives for use as antiinflammatory agents. US20050228047A1, 2005.
204. Omura, K.; Swern, D., *Tetrahedron* **1978**, *34* (11), 1651.
205. Takai, K.; Nitta, K.; Utimoto, K., *J. Am. Chem. Soc.* **1986**, *108* (23), 7408.
206. Midland, M. M., *Chem. Rev.* **1989**, *89* (7), 1553.
207. Allard, M.; Barnes, K.; Chen, X.; Cheung, Y. Y.; Duffy, B.; Heap, C.; Inthavongsay, J.; Johnson, M.; Krishnamoorthy, R.; Manley, C.; Steffke, S.; Varughese, D.; Wang, R.; Wang, Y.; Schwartz, C. E., *Tetrahedron Lett.* **2011**, *52* (21), 2623.
208. Noyori, R.; Hashiguchi, S., *Acc. Chem. Res.* **1997**, *30* (2), 97.
209. Dale, J. A.; Dull, D. L.; Mosher, H. S., *J. Org. Chem.* **1969**, *34* (9), 2543.
210. Zhang, H. X.; Guibe, F.; Balavoine, G., *J. Org. Chem.* **1990**, *55* (6), 1857.

211. Martin, V. S.; Woodard, S. S.; Katsuki, T.; Yamada, Y.; Ikeda, M.; Sharpless, K. B., *J. Am. Chem. Soc.* **1981**, *103* (20), 6237.
212. Oyo, M.; Masaaki, Y., *Bull. Chem. Soc. Jpn.* **1967**, *40* (10), 2380.
213. Kobayashi, Y.; Shimazaki, T.; Taguchi, H.; Sato, F., *J. Org. Chem.* **1990**, *55* (19), 5324.
214. Peterson, D. J., *J. Org. Chem.* **1968**, *33* (2), 780.
215. Urbitsch, F.; Elbert, B. L.; Llaveria, J.; Streatfeild, P. E.; Anderson, E. A., *Org. Lett.* **2020**, *22* (4), 1510.
216. Nakao, Y.; Hiyama, T., *Chem. Soc. Rev.* **2011**, *40* (10), 4893.
217. Sore, H. F.; Galloway, W. R. J. D.; Spring, D. R., *Chem. Soc. Rev.* **2012**, *41* (5), 1845.
218. Corey, E. J.; Fuchs, P. L., *Tetrahedron Lett.* **1972**, *13* (36), 3769.
219. Appel, R., *Angew. Chem. Int.* **1975**, *14* (12), 801.
220. Rodriguez, A. R.; Spur, B. W., *Tetrahedron Lett.* **2014**, *55* (43), 6011.
221. Dess, D. B.; Martin, J. C., *J. Am. Chem. Soc.* **1991**, *113* (19), 7277.

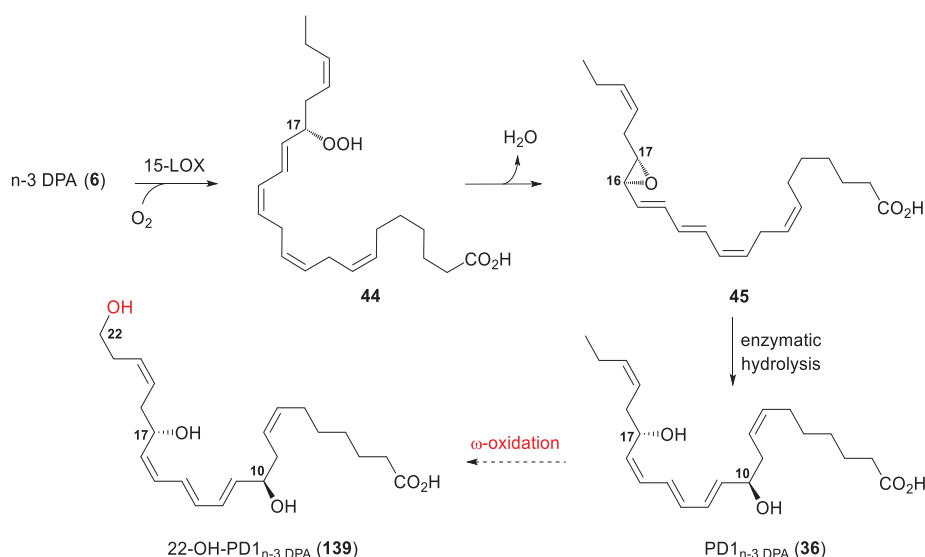
## Chapter 2 Results and discussion

### 2.1 Paper I: Synthesis, Structural Confirmation, and Biosynthesis of 22-OH-PD1<sub>n-3</sub> DPA

Several studies have established that PUFAs and their oxygenated products undergo oxidative metabolism by eicosanoid reductase and cytochrome P450 enzymes.<sup>1-4</sup> However, little information is available on  $\omega$ - and  $\beta$ -oxidative processes of SPMs. Such processes are known for all fatty acids<sup>5</sup> and PUFA-products, including the pro-inflammatory prostaglandins<sup>4</sup> and leukotrienes.<sup>3</sup>

In 2014, the LIPCHEM-group in collaboration with Professor Charles N. Serhan's group at Harvard Medical School, Brigham and Women's Hospital, showed that PD1 (**31**) was converted to the 22-OH-PD1 (**46**) metabolite,<sup>6</sup> by matching synthetic and authentic material of **31**. Further biological investigations demonstrated that 22-OH-PD1 (**46**) exhibited potent anti-inflammatory and pro-resolving bioactions.<sup>6</sup>

Recently, novel SPMs derived from n-3 DPA (**6**) were reported.<sup>7-9</sup> The exact structure and biosynthesis of PD1<sub>n-3</sub> DPA (**36**) was confirmed by matching biogenic material with synthetic standards (Scheme 2.1).<sup>7, 10, 11</sup> Due to the structural similarities with PD1 (**31**), further metabolism of **36** is likely to result in the formation of 22-OH-PD1<sub>n-3</sub> DPA (**139**). However, to investigate the biosynthetic conversion of PD1<sub>n-3</sub> DPA (**36**) into 22-OH-PD1<sub>n-3</sub> DPA (**139**), total synthesis of **139** was required. Hence, we wanted to prepare **139** through stereoselective synthesis, and utilize the synthetic material in biosynthetic investigations. This is the first total synthesis of the metabolite **139** reported.



**Scheme 2.1** Established biosynthesis of PD1<sub>n-3</sub> DPA (**36**) and proposed formation of 22-OH-PD1<sub>n-3</sub> DPA (**139**).

### 2.1.1 Synthetic strategy towards 22-OH-PD1<sub>n-3</sub> DPA

As emphasized in Section 1.7, the conjugated *E,E,Z*-triene moiety present in several SPMs, including 22-OH-PD1<sub>n-3</sub> DPA (**139**), is highly sensitive and may easily undergo isomerization when exposed to light, heat, and/or acidic conditions. The two chiral allylic alcohols present in **139** are likely prone to undergo dehydration, forming an extended conjugated system. It is therefore advantageous to install the *E,E,Z*-triene in a late stage of the synthesis under mild conditions to reduce the risk of unintended structural alterations through the synthesis. The synthetic strategy towards **139** was based on a convergent approach similar to those reported in the synthesis of PD1<sub>n-3</sub> DPA (**36**)<sup>11</sup> and 22-OH-PD1 (**46**) by the LIPCHEM group.<sup>6</sup> Furthermore, our group has prepared several SPMs by employing the Nagao acetate aldol reaction to construct related triene moieties from the key precursor **142**.<sup>11-15</sup> Based on the success in these syntheses, the retrosynthetic analysis outlined in Figure 2.1 was planned to afford 22-OH-PD1<sub>n-3</sub> DPA (**139**) in a stereoselective and convergent manner. Fragment **143** would be prepared as previously reported by our group.<sup>6, 11</sup>

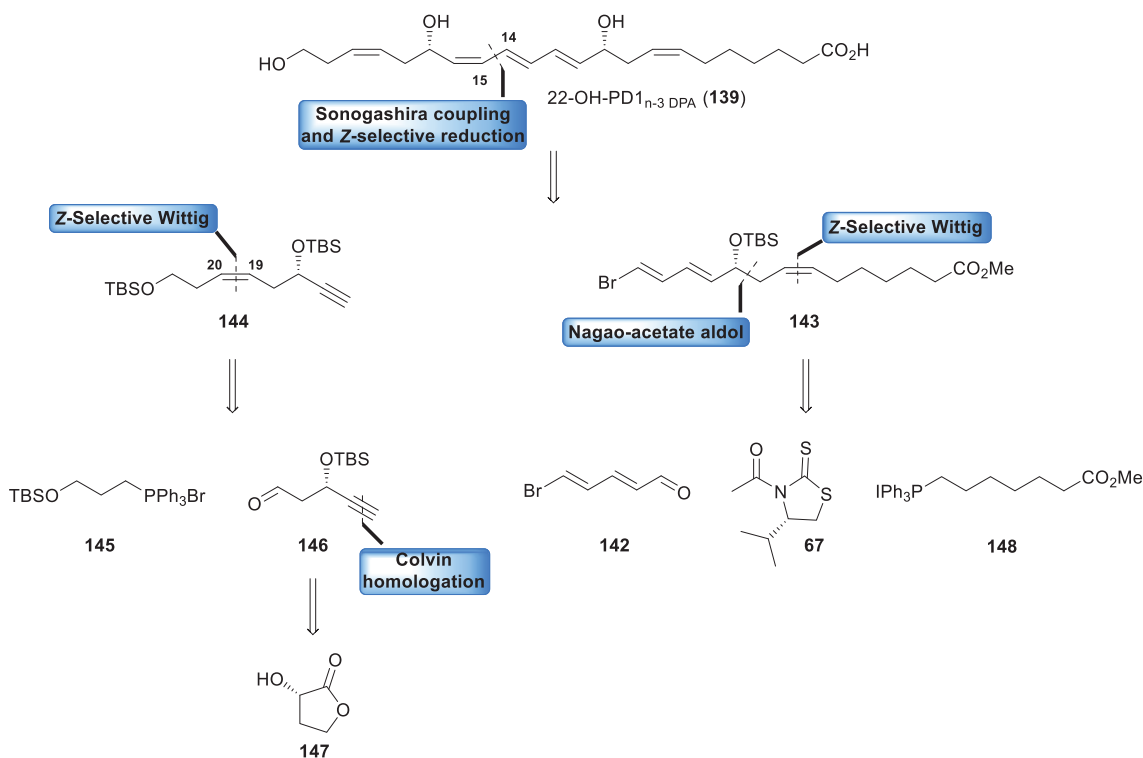
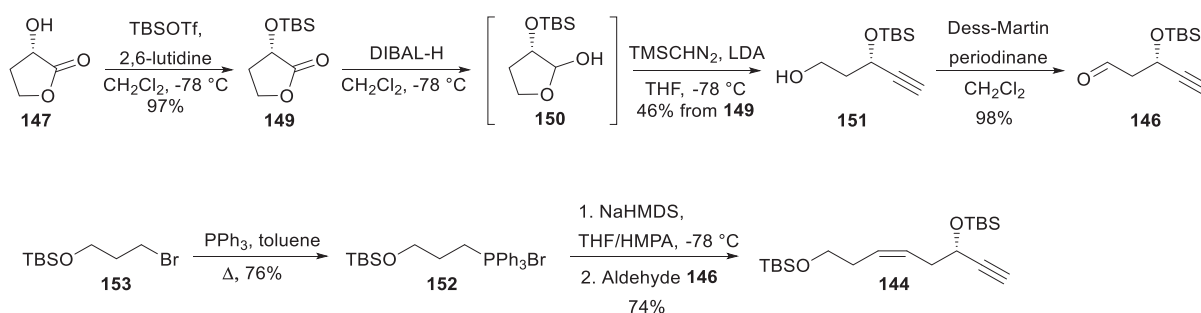


Figure 2.1 Retrosynthetic analysis of 22-OH-PD1<sub>n-3</sub> DPA (**139**).

First disconnecting the indicated C<sub>14</sub>-C<sub>15</sub> carbon bond (Figure 2.1), provided an opportunity to construct the C<sub>15</sub>-C<sub>16</sub> *cis*-olefin by a Sonogashira cross-coupling reaction between terminal alkyne **144** and vinyl halide **143** followed by a *Z*-selective reduction of the resulting internal alkyne. This would establish the *E,E,Z*-triene moiety at a late stage in the synthesis. Cleaving the indicated C<sub>19</sub>-C<sub>20</sub> *cis*-olefin in fragment **143** was performed with the intent of using a *Z*-selective Wittig reaction in the forward direction, leading back to Wittig-salt **145** and known aldehyde **146**.<sup>13</sup> This aldehyde could in turn be prepared from hydroxylactone **147** by employing a Colvin reaction in the forward synthetic direction, as earlier reported by our group.<sup>13</sup>

### 2.1.2 Total synthesis of 22-OH-PD1<sub>n-3</sub> DPA

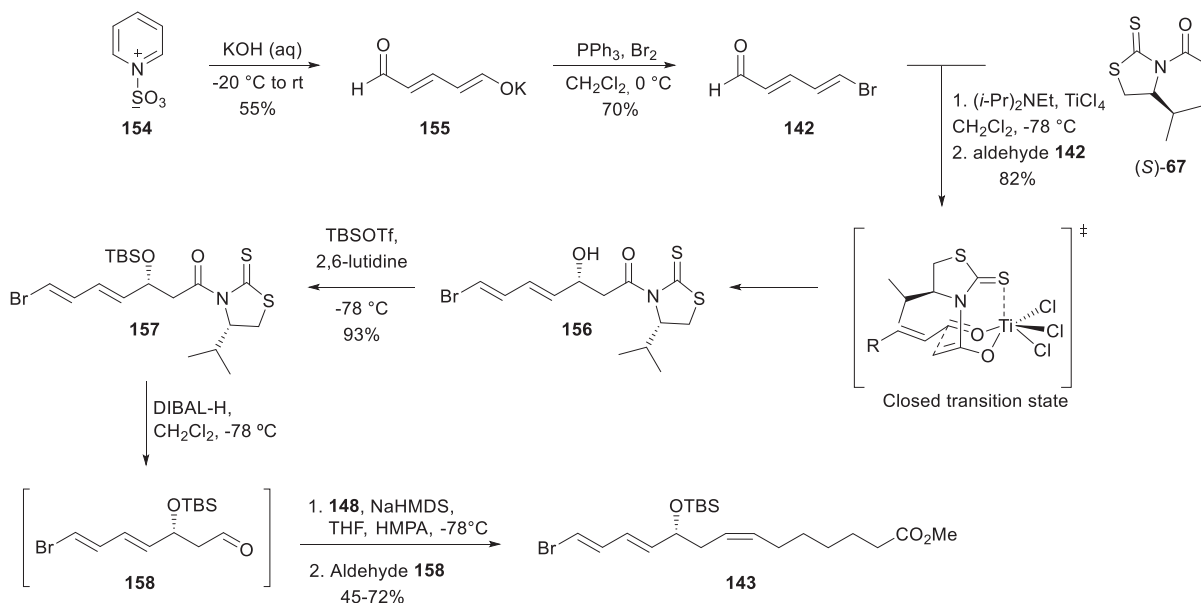
The first key fragment synthesized was the ω-end **144** as illustrated in Scheme 2.2. First, the aldehyde **146** was prepared over four steps as earlier reported.<sup>13</sup> Commercially available (*S*)-(-)-α-hydroxy-γ-butyrolactone (**147**) was protected using TBS-triflate, and the resulting TBS-lactone **149** was reduced to the corresponding lactol **150** with DIBAL-H. Following this, the crude lactol was subjected to a Colvin reaction to afford the terminal alkyne **151**. The primary alcohol in **151** was oxidized with the Dess-Martin reagent (DMP) to give aldehyde **146** in 44% yield from starting lactone **147**. Next, Wittig-salt **152** was prepared from commercially available (3-bromopropoxy)-*tert*-butyldimethylsilane (**153**) and treated with NaHMDS to form the corresponding ylide, which was reacted in a *Z*-selective Wittig reaction with aldehyde **146**. Following filtration of the crude product through a silica plug, only the desired *Z*-isomer **144** was detected by <sup>1</sup>H- and <sup>13</sup>C-NMR analysis. Overall, the ω-end **144** was prepared in five steps from starting lactone **147** in 33% yield.



Scheme 2.2 Synthesis of the ω-end **144**.

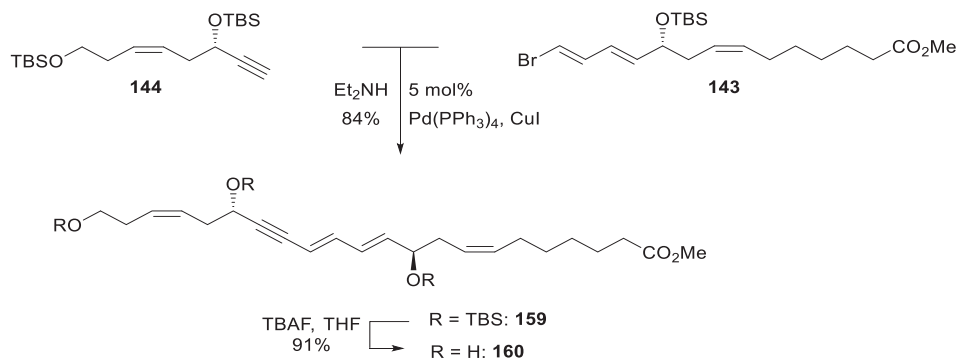
Next, the C<sub>1</sub>-C<sub>14</sub> fragment **143** was prepared as previously reported (Scheme 2.3).<sup>6,11</sup> Starting from the commercially available pyridinium salt **154**, treatment with aqueous base afforded potassium salt **155**, which was reacted with a PPh<sub>3</sub>/Br<sub>2</sub> complex prepared in dichloromethane. The resulting (*2E,4E*)-5-bromopenta-2,4-dienal **142** was subjected to a Nagao acetate aldol reaction<sup>16</sup> with

enantiopure (*S*)-**67**, using  $\text{TiCl}_4$  as the Lewis acid and  $(i\text{-Pr})_2\text{NEt}$  as the base. The reaction afforded intermediate **156** in good yield and selectivity up to a 15.3:1 ratio of the desired diastereomer (based on HPLC analysis). Next, the secondary alcohol in **156** was protected to give TBS-silyl ether **157**. The chiral auxiliary in **157** was removed by reductive cleavage using DIBAL-H to afford aldehyde **158**, which was immediately subjected to a *Z*-selective Wittig reaction with the pre-formed ylide of **148** to produce vinylic bromide **143** (Scheme 2.3). Following chromatographic purification of crude **143**, only the *Z*-isomer was observed by  $^1\text{H}$ - and  $^{13}\text{C}$ -NMR analysis. The yields in this reaction varied from modest to good. The difficulties encountered were likely due to the basic reaction conditions employed in the Wittig reaction. Under basic conditions, the aldehyde **158** is prone to deprotonation and elimination of the TBS-ether through the  $\text{E1}_{\text{cB}}$  mechanism, producing an all-conjugated system, and such product was identified according to  $^1\text{H}$ -NMR analysis. A similar observation was reported by Balas and co-workers in their synthesis of PD1 (**31**).<sup>17</sup> Furthermore, aldehyde **158** was highly unstable and readily decomposed when solvents were removed, forming a deep red color of the compound. It was therefore crucial to perform the following Wittig reaction rapidly.



Scheme 2.3 Preparation of vinylic bromide **143**.

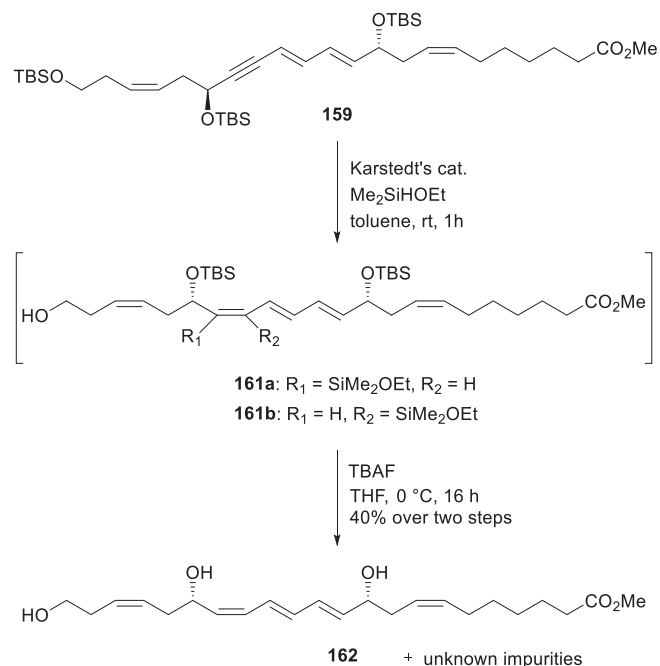
Next, the carbon skeleton of target compound **139** was constructed. Assembly of fragment **144** and **143** was achieved by employing a Sonogashira cross-coupling reaction, catalyzed by  $\text{Pd}(\text{PPh}_3)_4$  and  $\text{CuI}$  in diethylamine. The coupled product **159** was desilylated using 7.5 equivalents of TBAF, providing alkyne **160** in 76% yield over the two steps (Scheme 2.4).



**Scheme 2.4** Construction of the carbon-chain of 22-OH-PD1<sub>n-3</sub> DPA (**139**).

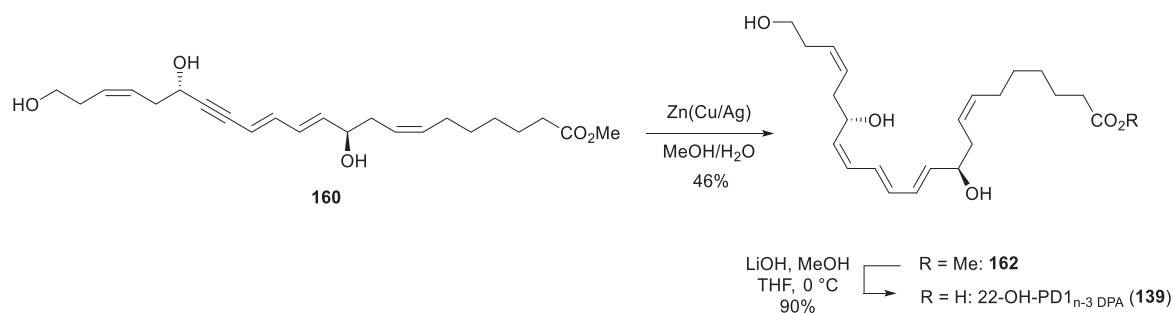
The Karstedt platinum-catalyzed alkyne hydrosilylation/protodesilylation protocol is an opportunity for *Z*-selective reduction of internal alkynes to produce *cis*-olefins.<sup>18</sup> This method was first attempted for partial hydrogenation of the internal alkyne in **159**. Using this procedure, the protodesilylation step could also remove the silyl ethers in **159** in one pot. Unfortunately, in the presence of the Karstedt's catalyst and excess dimethylethoxy silane, the resulting regioisomeric mixture of mono-*Z*-substituted alkene dimethylsilyl-ethoxy ethers **161a** and **161b** provided a mixture of the desired product **162** and inseparable impurities following treatment with TBAF. This was based on NMR and HPLC analyses of the purified product. In the <sup>13</sup>C-NMR spectrum recorded, several low intensity peaks were observed in the alkene region, and HPLC-UV of the isolated product indicated a purity of 85%. Several different combinations of eluent systems were also tested to achieve separation by thin layer chromatography (TLC) without success.





**Scheme 2.5** Z-selective reduction of the internal alkyne **159** utilizing the Karstedt protocol.<sup>18</sup>

As an alternative, the Boland protocol was applied,<sup>19</sup> which is a mild and selective reduction method for partial hydrogenation of internal alkynes. The freshly prepared Zn(Cu/Ag) reagent was stirred with alkyne **160** in aqueous methanol to provide methyl ester **162** without over-reduction and in high purity (96%, determined by NMR and HPLC analyses). However, dehydration of the two hydroxyl groups in **162** occurred during the reaction, as observed by TLC analysis and later by <sup>1</sup>H-NMR, where loss of the carbinol signals and additional signals in the olefin region was observed. Moreover, approximately 20% of the *E,E,E*-triene isomer of **162** was formed during the reaction (based on isolated material and NMR analyses), which altogether reflects the moderate yield of 46%. Fortunately, compound **162** could be isolated in high purity by means of column chromatography on silica gel. In the final step, basic hydrolysis of methyl ester **162** furnished 22-OH-PD1<sub>n-3</sub> DPA (**139**) in 90% yield and high chemical purity (94%, based on HPLC analysis).



**Scheme 2.6** Final steps in the total synthesis of 22-OH-PD1<sub>n-3</sub> DPA (**139**).

### 2.1.3 Matching experiments and biosynthetic investigations

The absolute configuration of the secondary alcohols in the n-3 DPA derived SPMs was not addressed in the original report.<sup>7</sup> Although it would be rational to expect it to be the same as for PD1<sub>n-3</sub> DPA (**36**), matching experiments between synthetic and authentic material of **139** was necessary. As previously mentioned, direct comparison of synthetic and biogenic material using an array of analytical and spectroscopic methods, including UV-Vis spectroscopy, LC-MS/MS, HPLC as well as biological experiments, were applied for this purpose.

In order to obtain evidence that our synthetic material was identical to authentic material of 22-OH-PD1<sub>n-3</sub> DPA (**139**) produced *in vivo*, LC-MS/MS-based lipid mediator profiling was employed to assess whether the physical properties of synthetic **139** matched with material isolated from human serum. These experiments were conducted during my 5-week sojourn in Professor Dalli's group at the William Harvey Research Institute in London. Figure 2.2, in panel A and B, shows the multiple reaction monitoring (MRM) chromatograms obtained from biologically generated **139** and our synthetic material, respectively. Both compounds displayed similar chromatographic behavior with an observed retention time ( $T_R$ ) of 10.4 minutes. Furthermore, when endogenous and synthetic material was co-injected, co-elution was observed as one single peak with a  $T_R$  at 10.4 minutes (Figure 2.2, C). The MS-MS spectra of 22-OH-PD1<sub>n-3</sub> DPA (**139**) obtained from human serum and synthetic material showed identical fragmentation patterns with the following fragments assigned  $m/z$  377, 359, 341, 323, 297, 245, 165, 139 (Figure 2.2, D-E). Altogether, these results meet the published identification criteria for the SPMs developed by the Serhan group,<sup>20</sup> including identical retention times, and at least six diagnostic ions in the MS-MS spectrum for each compound. Moreover, the UV chromophore and band shape of synthetic and authentic material were identical and found to be at ( $\lambda_{\text{max}}$  (MeOH)) 262, 271, 282 nm by UV-VIS analysis, which confirmed the integrity of the *E,E,Z*-triene moiety.<sup>21</sup> Based on the identical physical properties observed for our synthetic material and biologically produced **139**, the structure of **139** was established to be (7*Z*,10*R*,11*E*,13*E*,15*Z*,17*S*,19*Z*)-10,17,22-trihydroxydocosa-7,11,13,15,19-pentaenoic acid.

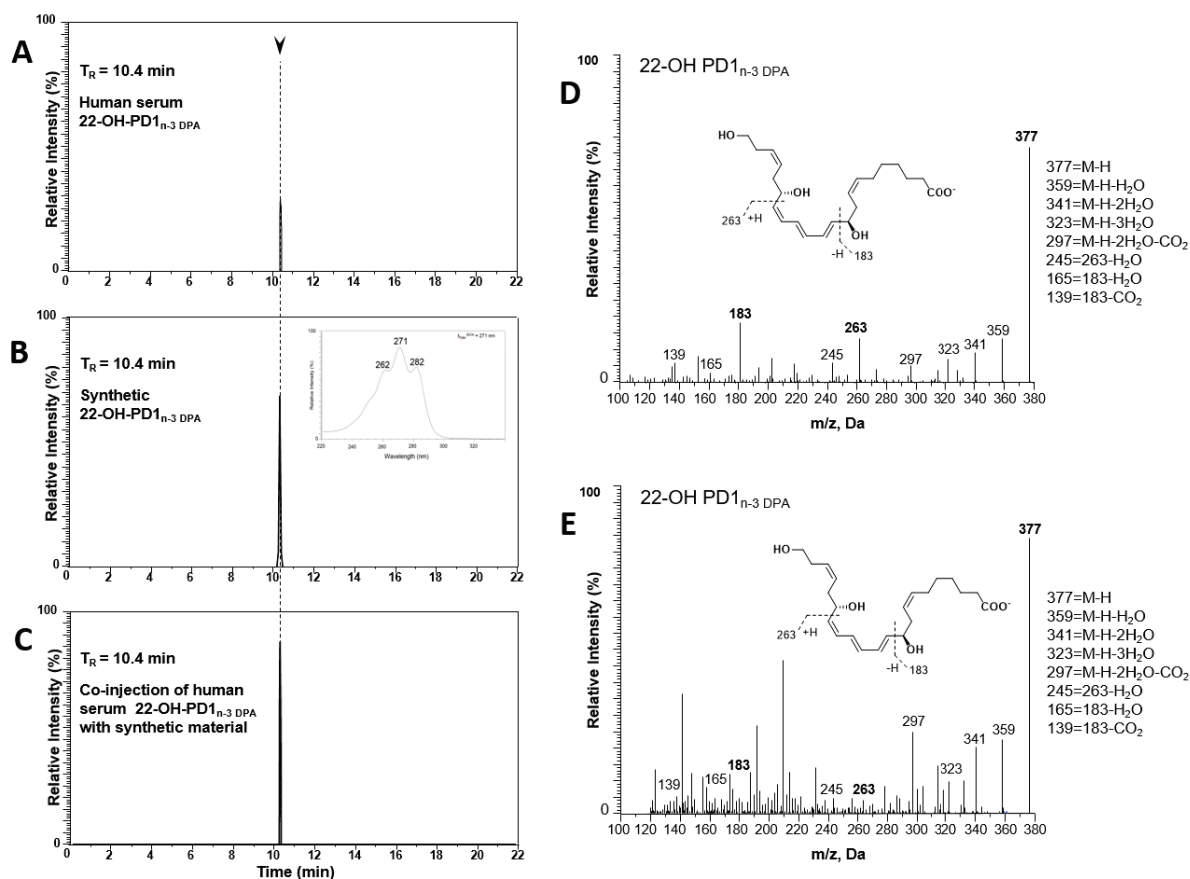


**Figure 2.2** MRM chromatograms of 22-OH-PD1<sub>n-3</sub> DPA (**139**) obtained from (A) human serum, (B) synthetic material (C) co-injection of A and B. MS-MS spectra employed for identification of **139** obtained from (D) synthetic material, (E) human serum.

Next, we wanted to investigate whether PD1<sub>n-3</sub> DPA (**36**) is a precursor in the biosynthesis of 22-OH-PD1<sub>n-3</sub> DPA (**139**). The former was obtained from earlier synthetic work.<sup>11</sup> For this purpose, human neutrophils were isolated from whole blood collected from healthy volunteers and incubated with and without synthetic PD1<sub>n-3</sub> DPA (**36**). The resulting products formed during these incubations were assessed using LC-MS/MS-based profiling. The peaks in panel A-C below (Figure 2.3) represents the relative abundance of 22-OH-PD1<sub>n-3</sub> DPA (**139**) at  $T_R = 10.4$  minutes resulting from the profiling. Panel A shows the MRM chromatogram obtained from neutrophils alone, whereas panel B shows the chromatogram obtained from neutrophils incubated with **36**. A noteworthy finding was that the levels of 22-OH-PD1<sub>n-3</sub> DPA (**139**) were markedly increased when the neutrophils were incubated with PD1<sub>n-3</sub> DPA (**36**) (Figure 2.3, B) compared to the levels obtained with neutrophils alone (Figure 2.3, A). Furthermore, the co-injection of samples from both incubations gave one sharp peak at  $T_R = 10.4$  minutes. Figure 2.3 (D-E) shows the MS-MS spectra employed for the identification of **139** in these experiments, which were essentially identical.

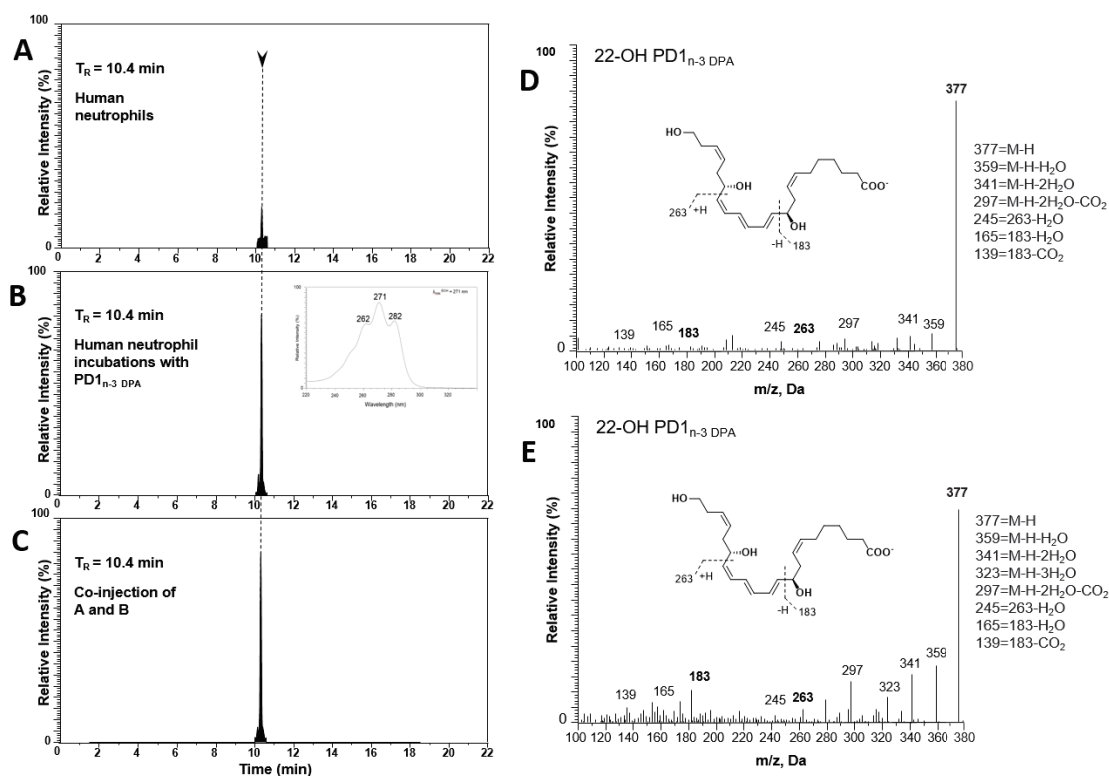


**Figure 2.3** MRM chromatograms of 22-OH-PD1<sub>n-3</sub> DPA (**139**) obtained from (A) human neutrophils, (B) human neutrophils incubated with PD1<sub>n-3</sub> DPA (**36**), (C) co-injection of A and B. MS-MS spectra employed for identification of **139** obtained from (D) human neutrophils (E) human neutrophils incubated with PD1<sub>n-3</sub> DPA (**36**).

To gain additional assurance that 22-OH-PD1<sub>n-3</sub> DPA (**139**) is formed directly from PD1<sub>n-3</sub> DPA (**36**), SPM **36** was incubated with human monocytes. As before, the data obtained from LC-MS/MS experiments demonstrated that 22-OH-PD1<sub>n-3</sub> DPA (**139**) was indeed formed from PD1<sub>n-3</sub> DPA (**36**), since identical retention times of the incubation product and synthetic material were observed. Moreover, the MS-MS-data of **139** in this experiment was in agreement with the data obtained from synthetic **139**.

### 2.1.3 Conclusion

22-OH-PD1<sub>n-3</sub> DPA (**139**) was stereoselectively synthesized in nine steps (LLS), and 10% overall yield from commercially available (*S*)-(-)- $\alpha$ -hydroxy- $\gamma$ -butyrolactone (**147**). Synthetic material matched authentic 22-OH-PD1<sub>n-3</sub> DPA (**139**), confirming the exact structure of **139** and that it is an  $\omega$ -oxidation metabolic product of the SPM PD1<sub>n-3</sub> DPA (**36**). In addition, it was demonstrated that 22-OH-PD1<sub>n-3</sub> DPA (**139**) is formed in human serum, human neutrophils and by human monocytes. The results reported herein contribute to new knowledge of the metabolism of the n-3 DPA

protectin class of specialized pro-resolving lipid mediators. Further investigations considering the anti-inflammatory and pro-resolving properties of 22-OH-PD1<sub>n-3</sub> DPA (**139**) will be assessed in future work.

## 2.2 Paper II: The synthetic protectin D1 analog 3-oxa-PD1<sub>n-3</sub> DPA reduces neuropathic pain and itching

PD1 (**31**), a congener of PD1<sub>n-3</sub> DPA (**36**), was recently reported to undergo rapid  $\beta$ -oxidation,<sup>22</sup> and several SPMs have proved to undergo enzymatic oxidation of the allylic alcohols to their respective ketones.<sup>2</sup> It has been demonstrated that PD1<sub>n-3</sub> DPA (**36**) possesses potent anti-inflammatory and pro-resolving bioactions.<sup>7, 10, 11</sup> However, the metabolism of PD1<sub>n-3</sub> DPA (**36**) has been less studied. For these reasons, we became interested in developing a synthetic route to access synthetic SPM analogues of **36** that are resistant to being metabolically inactivated while still retaining the desirable biological activities.

Hence, the  $\beta$ -methylene group in the C<sub>3</sub>-position of **36** was replaced with an oxygen to avoid  $\beta$ -oxidation (Figure 2.4) and inversion of the configuration at the C<sub>17</sub>-position was anticipated to inhibit enzymatic oxidation of the allylic alcohol into the corresponding ketone, leading to increased metabolic stability. These two structural alterations on SPM **36** resulted in the design of two SPM-analogues, termed 17*S*-3-oxa-protectin D1<sub>n-3</sub> DPA (17*S*-3-oxa-PD1<sub>n-3</sub> DPA, **140**) and 17*R*-3-oxa-protectin D1<sub>n-3</sub> DPA (17*R*-3-oxa-PD1<sub>n-3</sub> DPA, **141**), shown in Figure 2.4.

The core structure of native **36** was kept unaltered in order to mimic and retain the potent bioactions reported for this SPM. Investigation of the anti-inflammatory and pro-resolving properties of the analogues to be prepared would provide new knowledge of the structure-activity relationship of naturally produced **36**, including the importance of the C<sub>17</sub> stereocenter to retain biological activity and the effect of introducing an oxygen in 3-position.

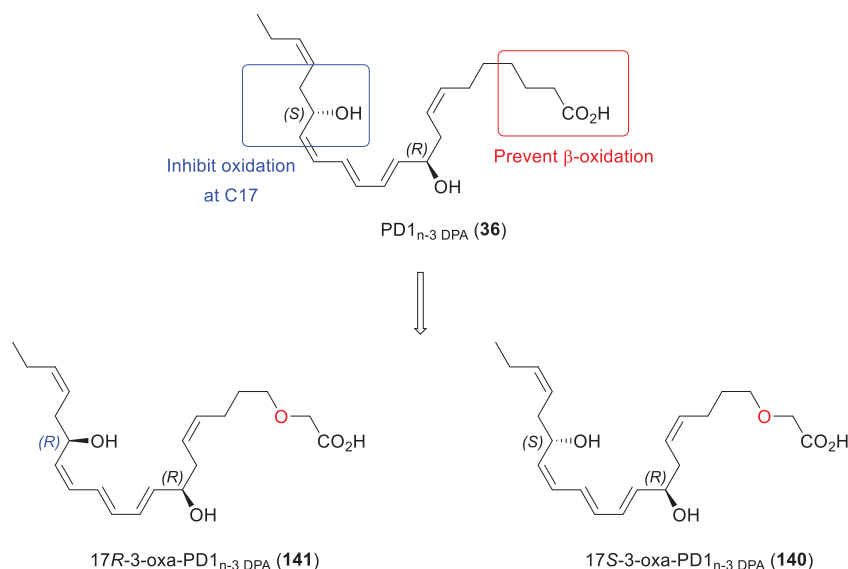


**Figure 2.4** Structural modifications made on PD1<sub>n-3</sub> DPA (**36**) into analogues **140** and **141**.

## 2.2.1 Retrosynthetic analysis and strategy

17*S*-3-oxa-PD<sub>1n-3</sub> DPA (**140**) shares many structural similarities with both PD<sub>1n-3</sub> DPA (**36**) and the 22-OH metabolite **139**. Consequently, a similar retrosynthetic analysis as presented for 22-OH-PD<sub>1n-3</sub> DPA (Section 2.1) was applied in this strategy by altering the Wittig salt resulting in the  $\omega$ -end (*S*)-**163**, and utilizing the same middle fragment **158** (Figure 2.5). Thus, a disconnection of the C<sub>14</sub>-C<sub>15</sub> carbon bond in target compound **140** was made with the intention of employing a Sonogashira cross-coupling reaction and a *Z*-selective hydrogenation in the forward synthesis, which furnished the two key fragments (*S*)-**163** and **164**. Disconnecting the indicated C<sub>7</sub>-C<sub>8</sub> *cis*-olefin in fragment **164** was performed with the intent of using a *Z*-selective Wittig reaction between the aldehyde **158** and the ylide of Wittig-salt **165**. Recognizing that the C<sub>2</sub>-oxygen bond in **164** could be formed by O-alkylation in the forward synthesis provided the alkylating  $\alpha$ -halo ester **166** as a precursor. Cleavage of the C<sub>19</sub>-C<sub>20</sub> alkene in  $\omega$ -end (*S*)-**163** led back to the known aldehyde (*S*)-**146** and phosphonium salt **167** corresponding to a Wittig reaction in the forward direction.

In analog **141**, the C<sub>17</sub> carbinol is *R*-configured. Thus, by changing the chiral pool starting material (*S*)-**147** into the corresponding commercially available *R*-configured enantiomer **168**, the same synthetic strategy presented in Figure 2.5 could be applied for the total synthesis of 17*R*-3-oxa-PD<sub>1n-3</sub> DPA (**141**).

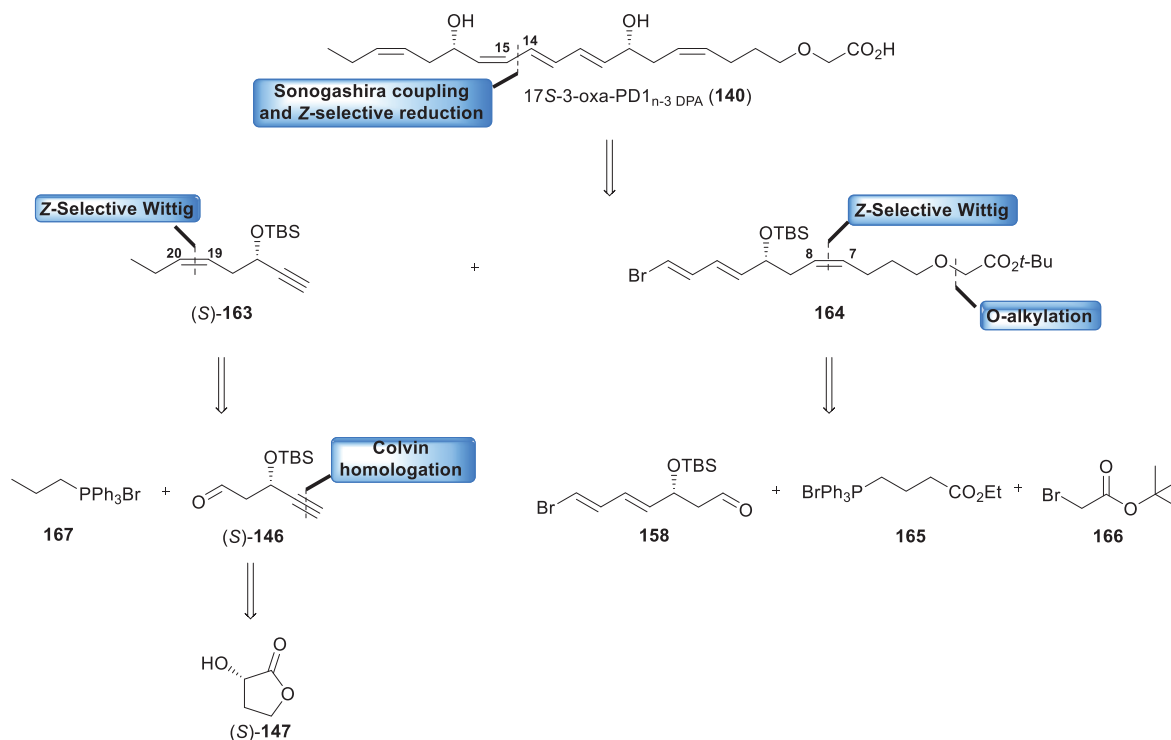
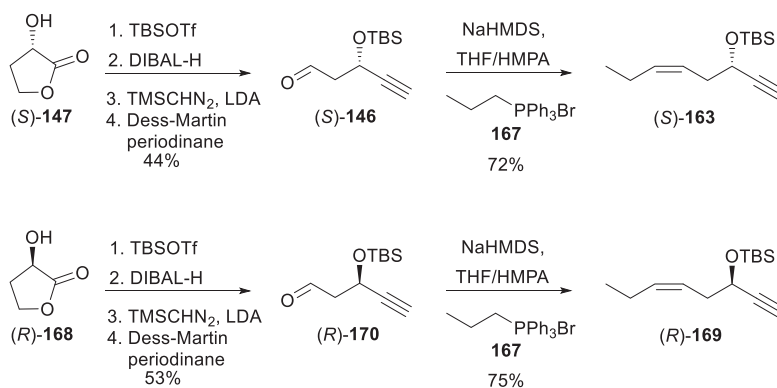


Figure 2.5 Retrosynthetic analysis of 17*S*-3-oxa-PD<sub>1n-3</sub> DPA (**140**).

### 2.2.2 Total synthesis of 3-oxa-PD1<sub>n-3</sub> DPA and the 17*R*-epimer

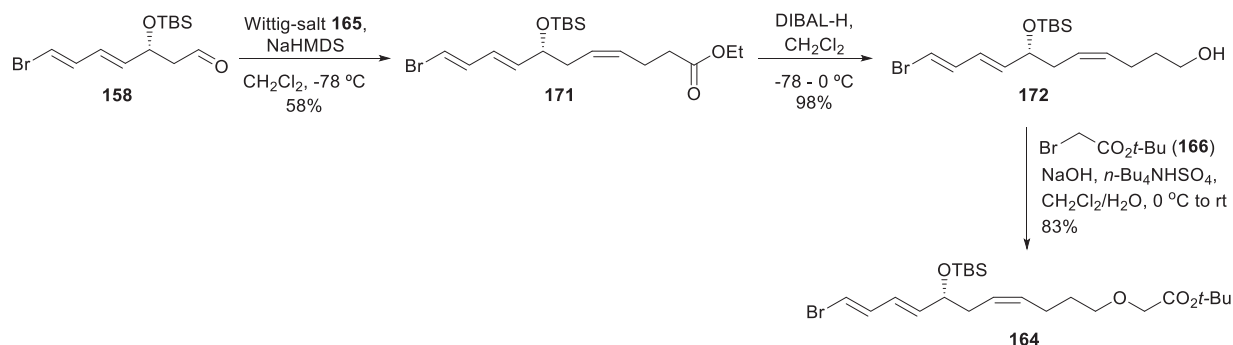
The syntheses towards analog **140** and **141** started with the preparation of the  $\omega$ -fragment (*S*)-**163** and (*R*)-**169** (Scheme 2.7). The former was prepared as previously reported by our group,<sup>23</sup> whereas fragment (*R*)-**169** was synthesized using the same procedures starting from (*R*)-**168**. Aldehyde (*S*)-**146** and (*R*)-**170** were obtained over four synthetic steps as previously described (Section 2.1.2). In brief, the starting lactones were TBS-protected, reduced to the corresponding lactols and subjected to a Colvin reaction with TMS-diazomethane. The resulting alcohols were oxidized to afford aldehyde (*S*)-**146** and (*R*)-**170**. Both aldehydes were separately reacted in a *Z*-selective Wittig reaction with the pre-formed ylide of Wittig-salt **167** to give the key  $\omega$ -end fragments (*S*)-**163** and (*R*)-**169**, respectively. Both final products were obtained as pure *Z*-alkenes following purification by column chromatography (Scheme 2.7).



Scheme 2.7 Preparation of the  $\omega$ -fragments (*S*)-**163** and (*R*)-**169**.

Next, the 3-oxa group was introduced into key fragment **164** as outlined in Scheme 2.8. Aldehyde **158** was prepared over five steps from commercially available pyridinium-1-sulfonate **154** as previously presented (Section 2.1). Then, following treatment of commercial Wittig-salt **165** with NaHMDS, dropwise addition of aldehyde **158** gave ethyl ester **171** as one single isomer in 58% yield. The ester was reduced using 2.5 equivalents of DIBAL-H, and the resulting alcohol **172** was reacted with *tert*-butyl bromoacetate **166** under basic phase transfer conditions to afford *tert*-butyl ester **164**.

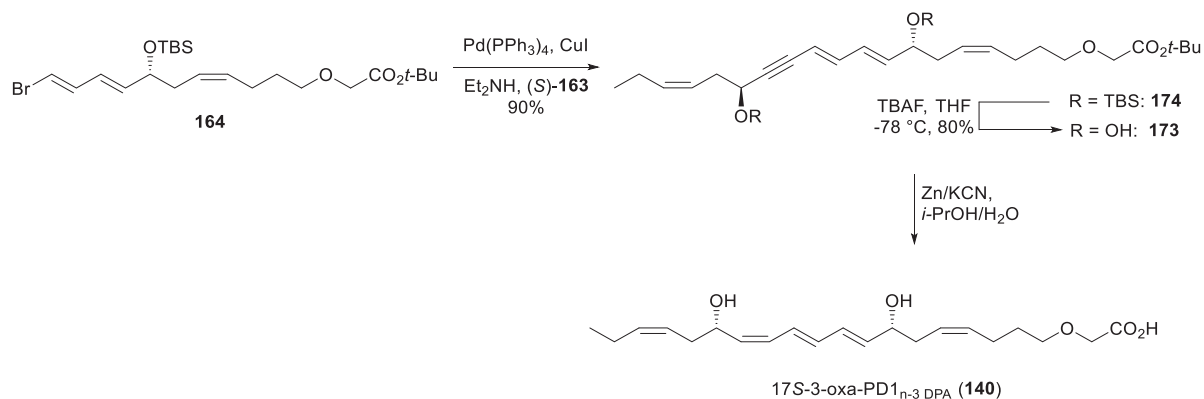




**Scheme 2.8** Synthesis of key fragment **164**.

With the two fragments (*S*)-**163** and **164** in hand, the remaining steps towards the synthesis of analog **140** were performed as outlined in Scheme 2.9. Again, by utilizing a Sonogashira coupling reaction, the vinyl bromide **164** was reacted with (*S*)-**163** in the presence of Pd(PPh<sub>3</sub>)<sub>4</sub> and CuI in diethylamine. This step provided the entire carbon-chain of target compound **140**. Removal of the two TBS-groups was achieved with TBAF in THF to afford diol **173** in 80% yield. Next, a protocol reported by Näf and co-workers<sup>24</sup> was applied to stereoselectively reduce the conjugated acetylene in **173** into a *Z*-alkene. The authors of this paper obtained pure *Z*-alkenes in high yields from the reduction of conjugated dienes using activated zinc at ambient temperature. For this purpose, compound **173** was stirred at ambient temperature in the presence of a large excess zinc powder activated by potassium cyanide in 50% aqueous *iso*-propanol. The reaction was monitored by TLC-analysis, which indicated that both of the allylic alcohols in **173** remained intact as no spots with a marked increased retardation factor relative to the starting material were observed.

Unintentionally, the reaction afforded both the *Z*-alkene and the carboxylic acid functionality in **140** in one pot. A reasonable explanation to this observation could be a result of the excess zinc metal acting as a Lewis acid, and dissociation of the *tert*-butyl alkyl group followed by protonation of the resulting carboxylate. The crude acid **140** was purified by chromatographic separation and obtained in high purity (>98%), as determined by HPLC prior to evaporation of the solvent. Unfortunately, despite careful handling of compound **140**, including protection from light and oxygen to the best of our ability, the NMR-recordings obtained showed that the compound was not isolated in pure form after being concentrated. This was determined from the <sup>13</sup>C-NMR spectrum of target acid **140** shown in Figure 2.6. In this spectrum, the four low intensity signals from approximately 87.0-88.5 ppm closely resemble the four signals at 68.6-73.1 ppm, and several low intensity signals can be observed in the alkene region, which might be due to the presence of an isomeric mixture of compound **140**. Additionally, HPLC analysis of the isolated compound after concentration indicated a purity of 86%.



**Scheme 2.9** Final steps in the synthesis of 17S-3-oxa-PD1<sub>n-3</sub> DPA (**140**).

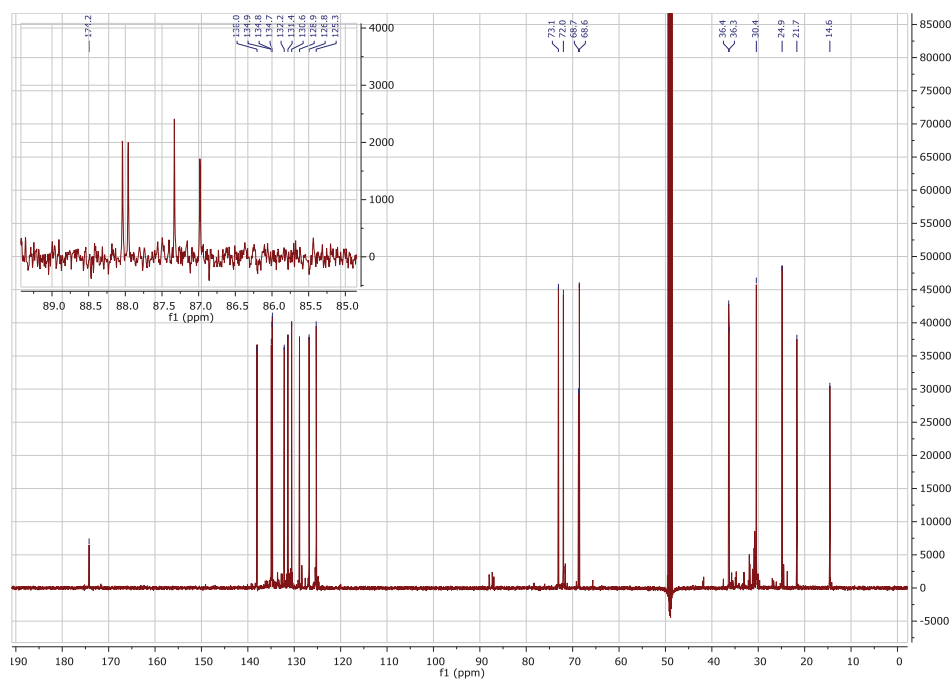
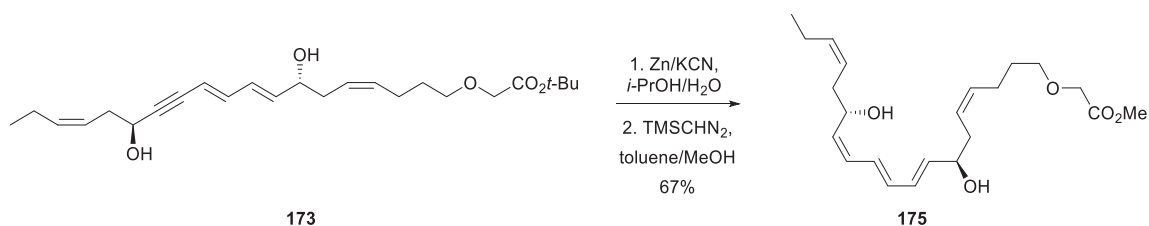


**Figure 2.6** <sup>13</sup>C-NMR spectrum of isolated material obtained from the Zn/KCN reduction of alkyne **173**.

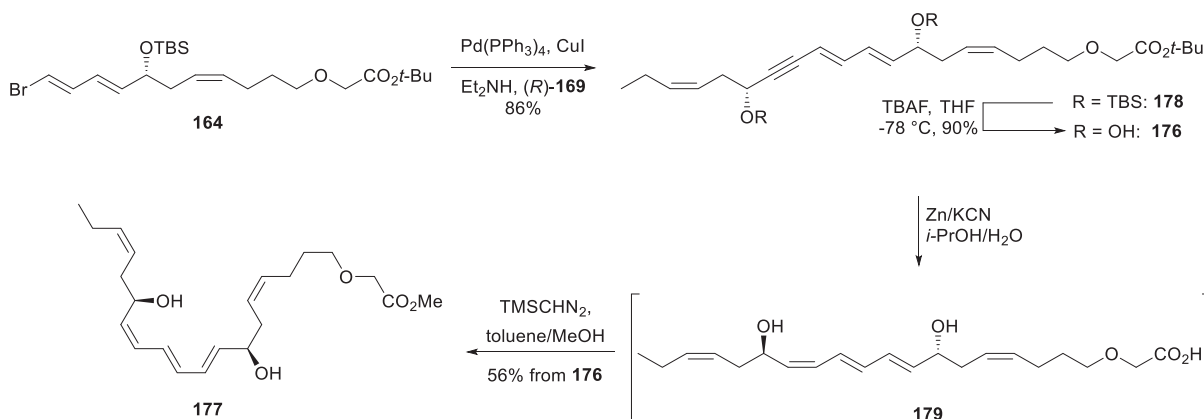
Introducing an oxygen in 3-position of target acid **140** enhanced the acidity of the carboxylic acid, which might be the cause of the reduced stability of this compound. It was, however, possible to obtain **140** in excellent chemical purity (98%) based on HPLC analysis when the compound was not evaporated to dryness. The <sup>1</sup>H-NMR spectra obtained showed residual hexane solvent peaks, in addition to an observed singlet at 1.40 ppm, which is likely from residual *tert*-butanol formed under the reaction conditions.

Intrigued by the seemingly high *Z*-selectivity in the reduction of the internal alkyne using the protocol reported by Näf *et. al.*,<sup>24</sup> we subjected alkyne **173** to the same reaction, but the resulting crude acid **140** was subsequently methylated using trimethylsilyldiazomethane to avoid potential isomerization and/or instability issues as the free acid (Scheme 2.10). Following purification and evaporation of solvents, the methyl ester **175** was isolated as one isomer in excellent purity (>98%, determined by HPLC analysis) and in 67% yield over the two steps.



**Scheme 2.10** Final steps in the synthesis of 17*S*-3-oxa-PD1<sub>n-3</sub> DPA methyl ester **175**.

The methyl ester of 17*R*-3-oxa-PD1<sub>n-3</sub> DPA (**177**) was synthesized equivalent to methyl ester **175** (Scheme 2.11). The terminal alkyne (*R*)-**169** was reacted in a Sonogashira reaction with vinyl bromide **164**, followed by deprotection of the silyl ethers with TBAF to afford diol **176**. Reduction of the internal alkyne in **176** following the Näf protocol<sup>24</sup> and subsequent methylation of the resulting acid, provided methyl ester **177**. After chromatographic purification on silica gel, the methyl ester **177** was isolated in 56% yield over the two steps in high purity (>97%, based on HPLC analysis).



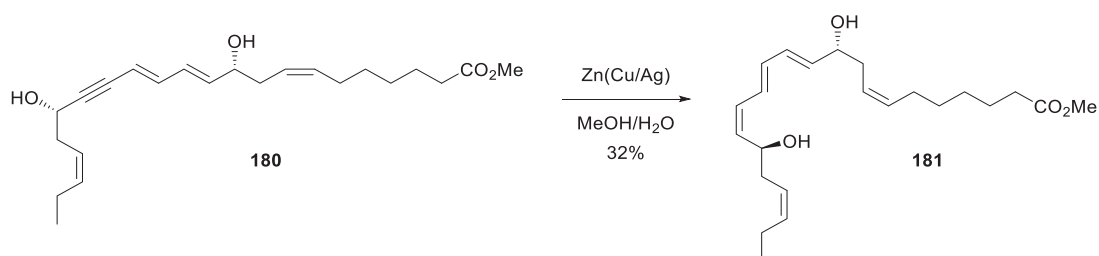
**Scheme 2.11** Synthesis of 17*R*-3-oxa-PD1<sub>n-3</sub> DPA methyl ester **177**.

As for other SPMs possessing similar instability challenges as free acids, both target compounds **140** and **141** were stored as their corresponding methyl esters that can be hydrolyzed just prior to conducting biological experiments.<sup>10</sup> Alternatively, both of these compounds may be subjected to biological studies as the methyl esters, which can be enzymatically transformed into the desired acids in the test system. For example, in the case of pro-drug approaches, pharmacologically active compounds are commonly delivered through esterase bioconversion to overcome difficulties with chemical instability.<sup>25, 26</sup> This fact may be adapted to our biological investigations.

#### 2.2.4 Total synthesis of PD1<sub>n-3</sub> DPA

A key part of the biological investigations to be done was to compare the metabolic resistance of analog **140** and **141** relative to native PD1<sub>n-3</sub> DPA (**36**). It was therefore necessary to synthesize PD1<sub>n-3</sub> DPA (**36**) as this SPM currently is not commercially available. Our group has previously reported a synthesis of PD1<sub>n-3</sub> DPA (**36**).<sup>11</sup> A modified procedure was utilized to resynthesize SPM **36**.

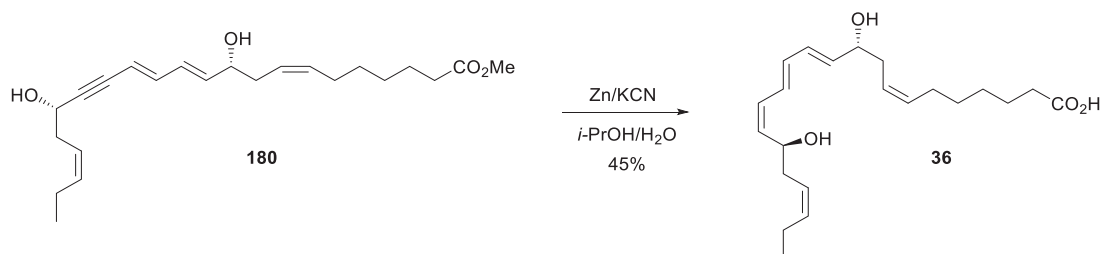
Alkyne **180** was obtained as previously presented (Scheme 2.4), using the  $\omega$ -end (*S*)-**163** in the Sonogashira coupling. In addition, instead of applying the Lindlar reduction as previously reported,<sup>11</sup> the internal alkyne in **180** was stereoselectively reduced into the *Z*-alkene using the methods reported by Boland<sup>19</sup> and Näf.<sup>24</sup> When alkyne **180** was stirred with the freshly prepared Zn(Cu/Ag) reagent in methanol and water, methyl ester **181** was formed in high purity (>99%, determined by HPLC) after purification by column chromatography (Scheme 2.12). However, the yield of the desired methyl ester **181** was modest following purification (32%), which was likely due to dehydration of one or both of the allylic alcohols based on TLC analysis, although the observed by-products were not isolated and characterized.



Scheme 2.12 Reduction of acetylene **180** employing the Boland<sup>19</sup> protocol.

When alkyne **180** was subjected to a mixture with excess zinc powder and potassium cyanide in aqueous isopropanol, the internal alkyne was semi-reduced and the methyl ester was also

hydrolyzed into the carboxylic acid **36** (Scheme 2.13). Thus, the final target compound was produced in one pot and 45% yield over the two steps in high chemical purity (>99%) following purification by C-18 reversed phase chromatography, as determined by HPLC analysis.



**Scheme 2.13** Final steps in the synthesis of PD1<sub>n-3</sub> DPA (**36**) utilizing the Naf<sup>24</sup> protocol.

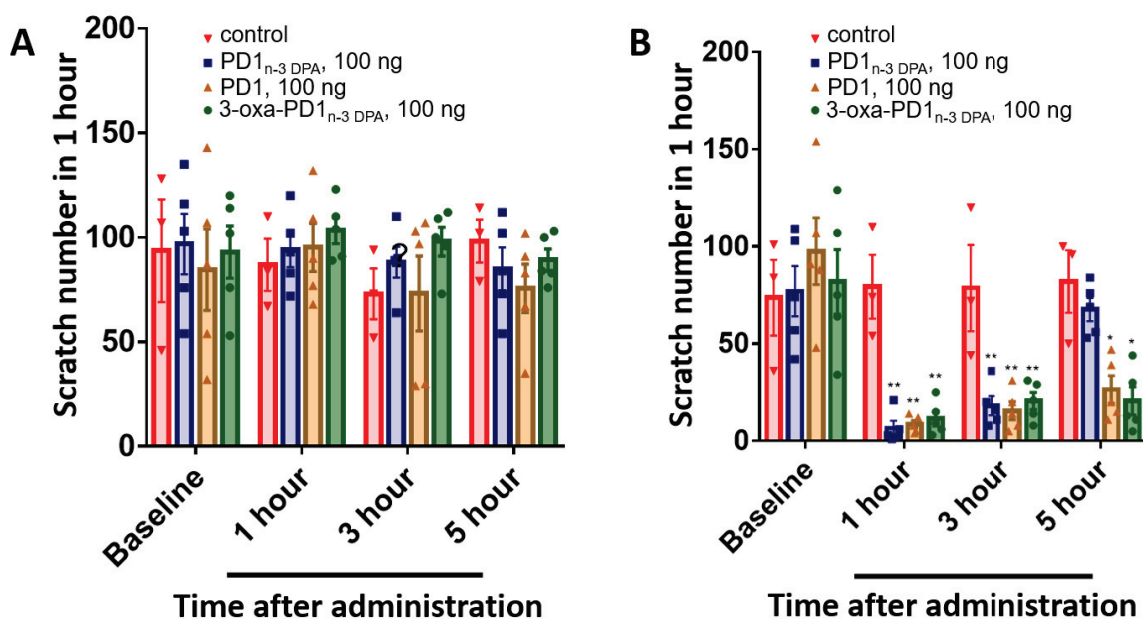
The findings made in the above reaction were unexpected, as the ester methyl group is not eliminated to form a stabilized carbocation intermediate, as opposed to the *tert*-butyl group (see Section 2.2.2). A plausible explanation for this observation may be that it is due to the presence of potassium cyanide, which in an equilibrium with water produces basic conditions, resulting in hydrolysis of the methyl ester to give PD1<sub>n-3</sub> DPA (**36**). Alternatively, the cyanide ion may act as a nucleophile by attacking the ester methyl group in **180** in a S<sub>N</sub>2-type substitution, resulting in cleavage of the ester O-methyl bond mediated by zinc as a Lewis acid followed by protonation of the resulting carboxylate, which is reminiscent of the Krapcho reaction.<sup>27, 28</sup>

### 2.2.5 Biological evaluations

Professor Ru-Rong Ji and his group at Duke University Medical Center in North Carolina, USA, were provided samples of synthetic PD1<sub>n-3</sub> DPA (**36**) and 17*S*-3-oxa-PD1<sub>n-3</sub> DPA (**140**) to perform biological investigations. The work performed by this research group aims at elucidating the underlying molecular and cellular mechanisms that result in neuropathic pain, and how distinct SPMs control pain by regulating inflammation and alleviating pain via specific receptors. In 2018, the Ji-group identified the GPR-37 receptor as a contributor involved in the resolution of inflammatory pain, mediated by PD1 (**31**).<sup>29</sup>

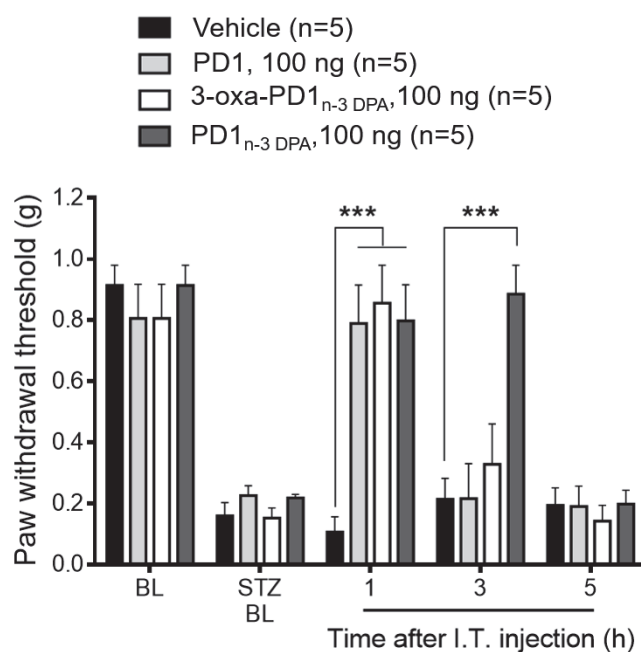
In the first study conducted, mice were induced with cutaneous T-cell lymphoma (CTCL, causing itch) and then treated with 100 ng of PD1 (**31**), PD1<sub>n-3</sub> DPA (**36**) and 17*S*-3-oxa-PD1<sub>n-3</sub> DPA (**140**) to investigate the effect on relieving the unpleasant sensation provoking the desire to scratch, caused by the cancer. Two distinct injection methods were applied to deliver the compounds.

Figure 2.7A shows the results obtained following intraperitoneal injection (IP, in the body cavity) of each compound, resulting in no effect on the scratch numbers over five hours. However, when PD1 (**31**), PD1<sub>n-3</sub> DPA (**36**) and 17*S*-3-oxa-PD1<sub>n-3</sub> DPA (**140**) were delivered via intrathecal injection (IT, into the spinal canal); a significant reduction in the scratch numbers was observed (Figure 2.7B). The effect from each of the compounds using this model mainly remained three hours following injection. For PD1 (**31**) and synthetic analog **140**, a significant lowered scratch number compared to the control was also observed after five hours. However, PD1<sub>n-3</sub> DPA (**36**) gave a different outcome, as no significant relief from itching was observed after five hours.



**Figure 2.7** Evaluations of the reduction in scratch number mediated by 100 ng of each of PD1 (**31**), PD1<sub>n-3</sub> DPA (**36**) and 17*S*-3-oxa-PD1<sub>n-3</sub> DPA (**140**) showing (A) no relief from itching after IP injection and (B) significant reduction of itching following IT injection. n = 5 mice per treatment.

In the second study, mice suffering from diabetes were used as a model for diabetic neuropathic pain. This model was established by IP injection of streptozocin (STZ, 75 mg/kg) to the mice. Figure 2.8 shows the effects of PD1 (**31**), PD1<sub>n-3</sub> DPA (**36**) and 17*S*-3-oxa-PD1<sub>n-3</sub> DPA (**140**) following IT injection with 100 ng of each compound. In this experiment, all compounds significantly protected the mice from the evoked and ongoing unpleasantness induced over the first hour. However, the protection gained from 100 ng each of PD1 (**31**) and 17*S*-3-oxa-PD1<sub>n-3</sub> DPA (**140**) was lost after three hours. PD1<sub>n-3</sub> DPA (**36**) on the other hand, proved to exert significant protection after three hours, but this effect disappeared after an additional two hours. These initial results merit further biological evaluations that will be performed in the near future.



**Figure 2.8** Evaluations of pain threshold using a mice paw withdrawal model mediated by 100 ng of each of PD1 (**31**), PD1<sub>n-3</sub> DPA (**36**) and 17S-3-oxa-PD1<sub>n-3</sub> DPA (**140**). Compounds were delivered by IT injection. n = 5 mice per treatment.

Due to the newly identified strain of severe acute respiratory syndrome coronavirus 2 (SARS-CoV-2) resulting in a worldwide pandemic,<sup>30</sup> the remaining biological investigations in this project were delayed and are currently ongoing with our collaborators at the Oslo University Hospital.

To increase our understanding of protectin metabolism, the experiments being conducted include time-course incubation studies of known quantities of synthetic PD1<sub>n-3</sub> DPA (**36**), 17S-3-oxa-PD1<sub>n-3</sub> DPA (**140**), and 17R-3-oxa-PD1<sub>n-3</sub> DPA (**141**) with human hepatoma cell lines (HepG2). These cells will be used as a model for potential hepatic metabolism in humans to investigate hepatic biotransformation of compound **36** relative to analogue **140** and **141** into possible metabolites. Analysis of cell media after incubation in the presence or absence of our synthetic compounds will be performed, and the resulting metabolites will be determined by means of reversed phase HPLC-UV (RP-HPLC-UV) and LC-MS/MS based profiling.

Furthermore, investigation of the anti-inflammatory and pro-resolving properties of the synthetic analogues are currently ongoing and conducted by the research group led by Professor Jesmond Dalli at Queen Mary University of London.

Overall, the results obtained from these experiments will enable comparison the three compounds PD1<sub>n-3</sub> DPA (**36**), 17S-3-oxa-PD1<sub>n-3</sub> DPA (**140**) and 17R-3-oxa-PD1<sub>n-3</sub> DPA (**141**) with respect to the observed biological activity and enzymatic metabolism, and thus provide a basis to judge structure-activity relationships. This in turn will give new information on SPM biology that may contribute to development of anti-inflammatory immunoresolvents in the future.

## 2.2.6 Conclusion

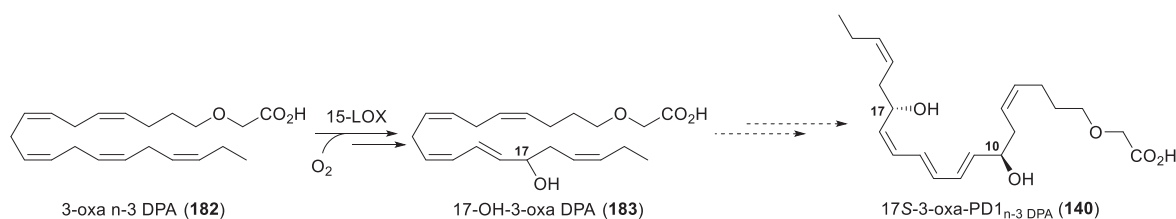
Stereoselective synthesis of the methyl esters of 17*S*-3-oxa-PD1<sub>n-3</sub> DPA **174** and 17*R*-3-oxa-PD1<sub>n-3</sub> DPA **177** were achieved over 12 synthetic steps (LLS) in each synthetic route with an overall yield of 15% and 17%, respectively. PD1<sub>n-3</sub> DPA (**36**) was synthesized over 10 linear steps in 7% overall yield (LLS). The stereoselective reduction of alkyne **173** was achieved using the protocol developed by Näf and co-workers,<sup>24</sup> which also provided a procedure to produce carboxylic acids from esters under mild conditions. The synthetic analog 17*S*-3-oxa-PD1<sub>n-3</sub> DPA (**140**) showed equal potency as PD1 (**31**) and PD1<sub>n-3</sub> DPA (**36**) in reducing neuropathic pain and itching following IT injection in animal models, and thus retained the potent bioactions to SPM **36**. These results contribute to new knowledge on the structure-function of the growing numbers of specialized pro-resolving lipid mediators. Further biological evaluations are currently ongoing and will be reported in due course.



## 2.3 Biosynthetic studies of 3-oxa-PD1<sub>n-3</sub> DPA

The host protective and pro-resolving protectins PD1 (**31**) and PD1<sub>n-3</sub> DPA (**36**) are biosynthesized from DHA (**5**) and n-3 DPA (**6**) via equivalent pathways, respectively.<sup>7, 31, 32</sup> The biosynthetic formation of PD1<sub>n-3</sub> DPA was established in 2017 (Scheme 2.1).<sup>10</sup>

Very recently, an analog of PUFA **6**, namely 3-oxa n-3 DPA (**182**) was prepared and subjected to incubation studies with various oxygenase enzymes.<sup>33</sup> In this study, synthetic **182**, like n-3 DPA (**6**), was a substrate for 15-LOX yielding mono-hydroxylated 17-OH-3-oxa DPA (**183**, Scheme 2.14). The product **183** was identified by means of RP-HPLC-UV and LC-MS/MS based profiling. Hence, without synthetic standards available for matching studies, the absolute configuration of **183** could not be determined. Since the 15-LOX enzyme is involved in the biosynthesis of the protectins to produce predominantly *S*-configured products in the 17-position of a C<sub>22</sub>-PUFA,<sup>34</sup> we wanted to investigate if intermediate **183** could be biologically converted into 17*S*-3-oxa-PD1<sub>n-3</sub> DPA (**140**), and thus is an intermediate in the bioconversion of 3-oxa n-3 DPA (**182**) into **140** (Scheme 2.14).



**Scheme 2.14** Biosynthetic investigations of 17*S*-3-oxa-PD1<sub>n-3</sub> DPA (**140**) using 3-oxa n-3 DPA (**182**) as substrate.

### 2.3.1 Initial biosynthetic studies using 3-oxa n-3 DPA

In order to obtain sufficient biologically produced material of 17*S*-3-oxa-PD1<sub>n-3</sub> DPA (**140**) to be utilized in the novel biosynthetic investigations outlined above, incubation studies with synthetic 3-oxa n-3 DPA (**182**) were performed. In three parallels, 3-oxa n-3 DPA (**182**, 167 μg) was incubated with soybean 15-LOX (borate buffer, 4 °C, pH 9.0, 167 μg/mL).

The resulting product was dissolved in methanol and subjected to UV-Vis and HRMS analyses: UV (MeOH) λ<sub>max</sub> = 233-235 nm; HRMS (ESI): calculated for C<sub>21</sub>H<sub>31</sub>NaO<sub>4</sub> [*M*+Na]<sup>+</sup>: 347.2228, found: 347.2227 (Figure 2.9). Based on the UV chromophore observed, which is characteristic for the formation of an *E,Z*-conjugated double bond system, and the HRMS data obtained, the resulting product was determined to be **183**.

Overlaid Spectra:

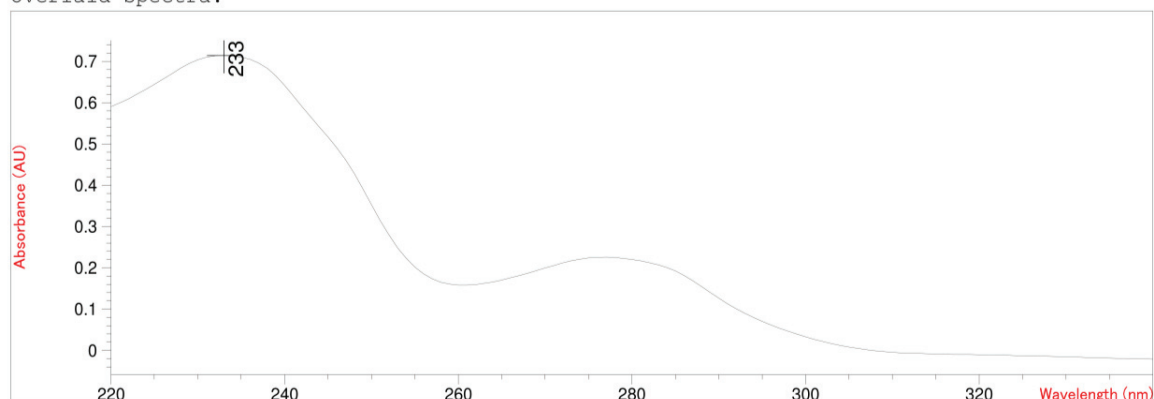


**Figure 2.9** UV-Vis chromatogram of 17-OH-3-oxa DPA (**183**) obtained from incubation studies with 3-oxa n-3 DPA (**182**) and 15-LOX.

Further investigations in this project were also halted due to the SARS-CoV-2 situation. In future studies, completion of this project includes investigating if the above product can serve as a substrate in the bioconversion into 17*S*-3-oxa-PD1<sub>n-3</sub> DPA (**140**). In this experiment, human neutrophils would be isolated from peripheral blood of healthy donors and incubated with intermediate **183** produced by 15-LOX. The products formed during this incubation would then be profiled using LC-MS/MS based lipid mediator lipidomics. Then, if identified in the latter analytical method, the biologically generated material of analog **140** would be subjected to matching studies with our chemically synthesized material of 17*S*-3-oxa-PD1<sub>n-3</sub> DPA (**140**) to confirm the absolute configuration. From these studies, we envision to establish if substitution of the  $\beta$ -methylene group in PUFA **6** with oxygen would result in the biological generation of analog **140** that is resistant to enzymatic oxidative metabolism and thereby potentially display prolonged biological activity.

## 2.4 Paper III: Stereoselective synthesis of the specialized pro-resolving and anti-inflammatory mediator resolvin E1

Resolvin E1 (**26**) is a potent anti-inflammatory and pro-resolving mediator derived from EPA (**4**). This SPM has proved to exert several interesting biological activities and thus has entered clinical trial development programs.<sup>35</sup> Moreover, RvE1 (**26**) has recently been directly correlated with the resolution of inflammatory periodontal disease.<sup>36</sup> To the author's knowledge, there is currently no effective drug treatment available against this chronic condition.<sup>37</sup> In collaborative efforts with the Institute of Oral Biology at University of Oslo, Norway, we became interested in developing a stereoselective synthesis of SPM **26** to access multi milligram amounts of this compound that could be subjected to biological evaluations by our collaborators against periodontitis.

### 2.4.1 Retrosynthetic analysis of resolvin E1

The structure of RvE1 (**26**) contains the same sensitive *E,E,Z*-triene moiety as 22-OH-PD1<sub>n-3</sub> DPA (**139**) and other SPMs, connecting two of the secondary allylic alcohols. Accordingly, the same approach using key fragment **158** was adapted in this strategy to ensure a highly stereoselective construction of the secondary alcohol at C<sub>12</sub> in RvE1 (**26**). The retrosynthetic analysis of target compound **26** is outlined in Figure 2.10. Disconnecting the C<sub>7</sub>-C<sub>8</sub> carbon bond, corresponding to a Sonogashira reaction and a *Z*-selective reduction, led back to the  $\alpha$ -end **184**. This fragment could in turn be prepared from chiral pool starting material **147** and ylide **185** analogous to the way previously described (Section 2.2), using a Colvin and a Wittig reaction in the forward synthetic direction. Disconnecting the indicated C<sub>14</sub>-C<sub>15</sub> olefin in **26** with a *Z*-selective Wittig reaction in mind, furnished key fragment **186** and **158**. Cleavage of the *E*-alkene in  $\omega$ -end **186** led back to an aldehyde and ylide **185**, where the former could be prepared from chiral pool starting material **187**.

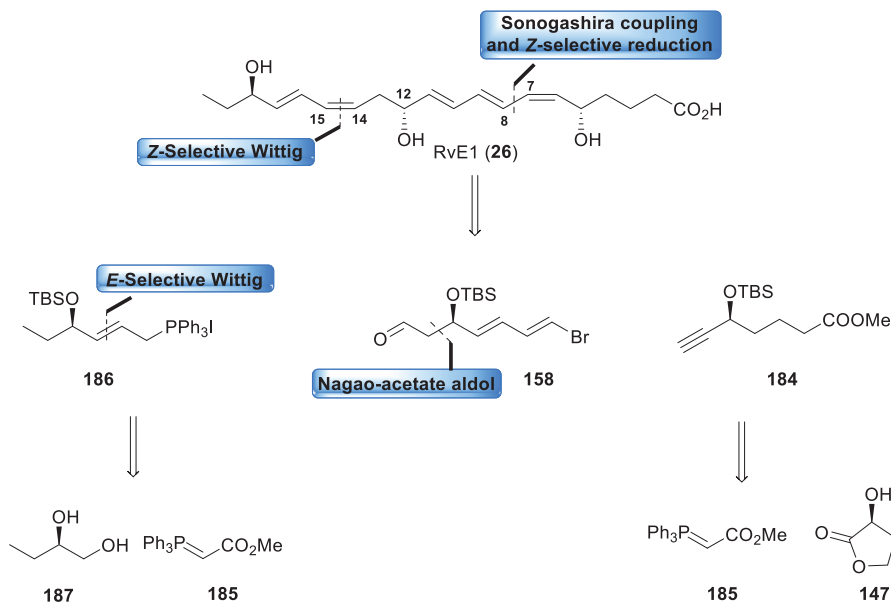
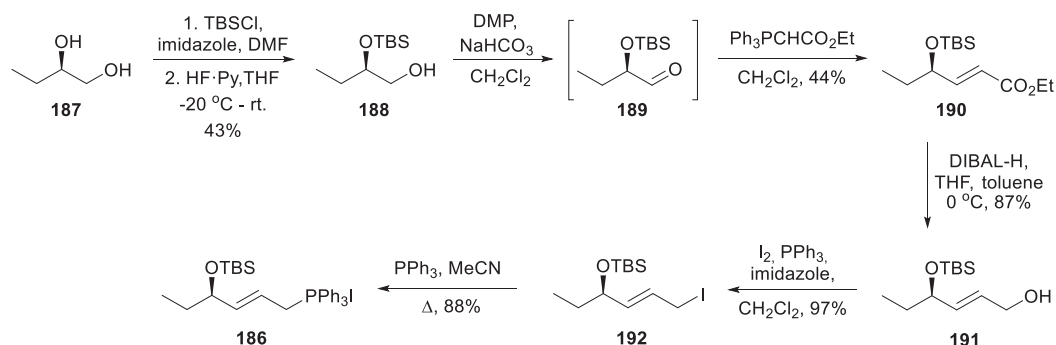


Figure 2.10 Retrosynthetic analysis of RvE1 (26).

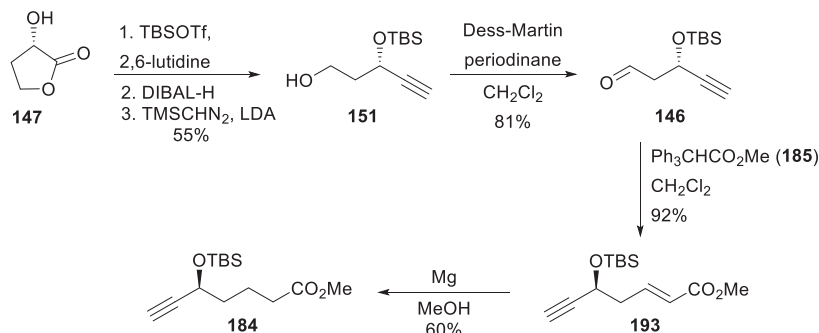
## 2.4.2 Total synthesis of resolvin E1

The synthesis towards RvE1 (26) commenced with the preparation of Wittig-salt **186** from commercial (*R*)-butane-1,2-diol (**187**) as outlined in Scheme 2.15. First, starting compound **187** was *bis*-protected using TBSCl, followed by regioselective deprotection of the primary silyl ether under fluoride conditions to afford alcohol **188**. Next, alcohol **188** was oxidized with DMP to afford aldehyde **189** that was immediately subjected to an *E*-selective Wittig-reaction to produce ethyl ester **190**. Only the desired *E*-isomer was isolated from the reaction. The ester functionality in **190** was then reduced using 2.5 equivalents of DIBAL-H to afford alcohol **191**, which was reacted in an Appel reaction to yield the corresponding iodide. Iodide **192** was finally converted to key fragment **186** following treatment with triphenylphosphine in acetonitrile under reflux.



Scheme 2.15 Synthesis of  $\omega$ -end **186**.

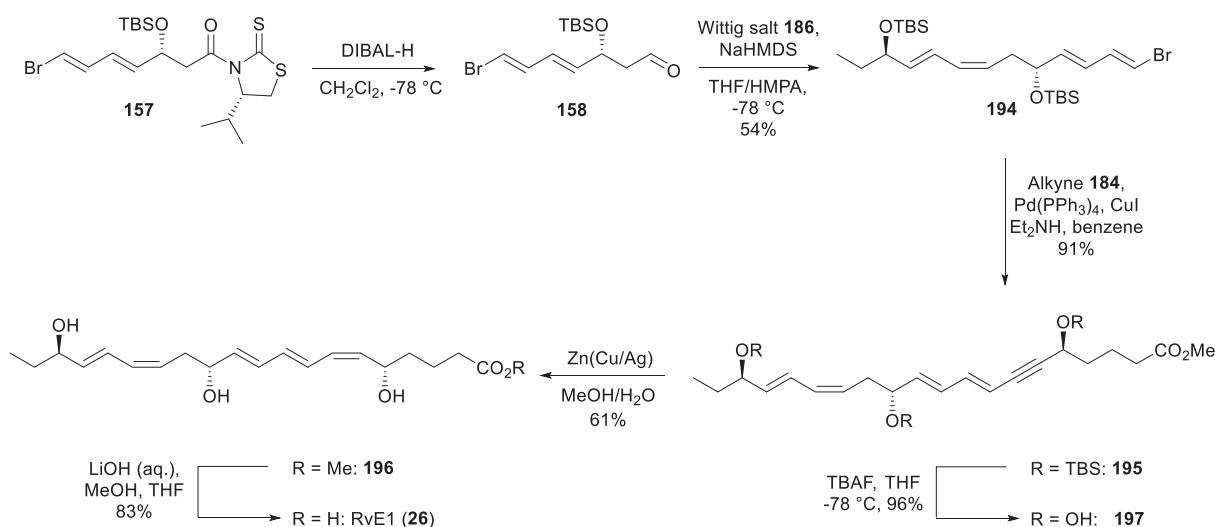
Terminal alkyne **184** was synthesized over six steps as previously reported (Scheme 2.16).<sup>13</sup> First, aldehyde **146** was prepared from (*S*)-(-)- $\alpha$ -hydroxy- $\gamma$ -butyrolactone (**147**) as before (Section 2.2). Aldehyde **146** was then subjected to an *E*-selective Wittig reaction with ylide **185** to form the unsaturated ester **193**. A chemoselective reduction of the conjugated alkene in **193** using magnesium turnings in methanol<sup>38</sup> afforded the methyl ester **184** in 25% yield from lactone **147**.



Scheme 2.16 Synthesis of the  $\alpha$ -end **184**.

Following preparation of the two key fragments, the  $\alpha$ -end **184** and the RvE1  $\omega$ -end **186**, the remaining steps in the synthesis of RvE1 (**26**) are outlined in Scheme 2.17. In a *Z*-selective Wittig reaction, aldehyde **158** was dropwise added to the pre-formed ylide of phosphonium salt **186** at -78 °C. The desired vinylic bromide **194** was formed in a 3.5:1 (*Z*:*E*) ratio, and isolated as one diastereomer in 54% yield from thiazolidinethione **157** after chromatographic purification. The moderate selectivity in this step may be explained by the nature of the ylide formed from **186**, which is semistabilized by the conjugated alkene. Approximately 20% of the undesired all *E*-alkene of **194** was isolated and characterized by <sup>1</sup>H-NMR analysis from the reaction. Furthermore, temperature control was important to prevent elimination of the silylether in Wittig-salt **186** after

treatment with NaHMDS. The Sonogashira reaction between  $\alpha$ -end **184** and vinylic bromide **194** under classical conditions gave the internal alkyne **195** in 91% yield. Desilylation of the three protecting groups with TBAF followed by a *Z*-selective Boland reduction provided methyl ester **196** in 59% yield over the two steps. Again, although to a smaller extent, dehydration of the alcohols was observed under the Boland conditions. Finally, a mild basic hydrolysis afforded RvE1 (**26**) in 83% yield and high chemical purity (94%, based on HPLC) following chromatographic purification. The target compound **26** was demanding to handle and readily decomposed when solvents were evaporated and upon contact with air. The final acid **26** was therefore converted back to the methyl ester using trimethylsilyldiazomethane and stored at  $-80\text{ }^{\circ}\text{C}$ .

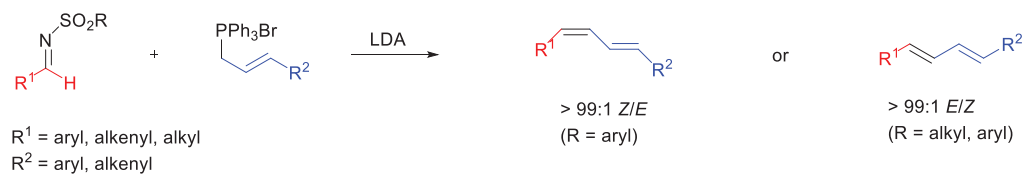


**Scheme 2.17** Assembly of the three key fragments **158**, **186** and **184** in the final steps in the synthesis of RvE1 (**26**).

The total synthesis of RvE1 (**26**) was achieved in 12 steps (LLS) with an overall yield of 3% and is thus one of the shortest synthetic routes to obtain SPM **26** compared to those published to date (Section 1.8). Nonetheless, the above strategy suffers from moderate yield, and a moderate selectivity in the *Z*-selective Wittig reaction between aldehyde **158** and the semistabilized ylide of phosphonium salt **186** (Scheme 2.17). For comparison, the mean yield in each synthetic step (LLS) in Schwartz's synthesis of RvE1 was 78% and ours 75%, thus both of these strategies are equally efficient and both syntheses has a total number of 23 steps.

Converting the aldehyde **158** into an *N*-sulfonyl imine prior to the Wittig reaction above (Scheme 2.17) could potentially improve our synthesis in terms of selectivity and yield. In 2010, Tian and co-workers reported a protocol that allow for highly stereoselective olefination of semistabilized triphenylphosphonium ylides with *N*-Sulfonyl imines.<sup>39</sup> In these protocols, the aldehydes were replaced with corresponding *N*-sulfonyl imines and subjected to Wittig reactions with

semistabilized ylides, resulting in *Z* or *E* alkenes with excellent selectivity and yields depending on the imine sulfonyl substituents (Scheme 2.18). Furthermore, the *N*-sulfonyl imines can be readily prepared through the condensation reaction of the aldehyde with various primary sulfonamides.<sup>39</sup>



**Scheme 2.18** Stereoselective olefination of semistabilized triphenylphosphonium ylides.<sup>39</sup>

### 2.4.3 Matching experiments

In order to confirm that our synthetically produced material was identical to authentic RvE1 (**26**), matching experiments using HPLC-UV were performed. Figure 2.11 shows the HPLC chromatograms obtained from the experiments of synthetic RvE1 (**26**) in panel A, authentic RvE1 (**26**) in panel B and the co-injection of both synthetic and authentic material in panel C. As demonstrated in the chromatograms, synthetic and authentic material display identical retention times and co-elutes upon co-injection (panel C), which confirms that the correct isomer of **26** has been prepared.

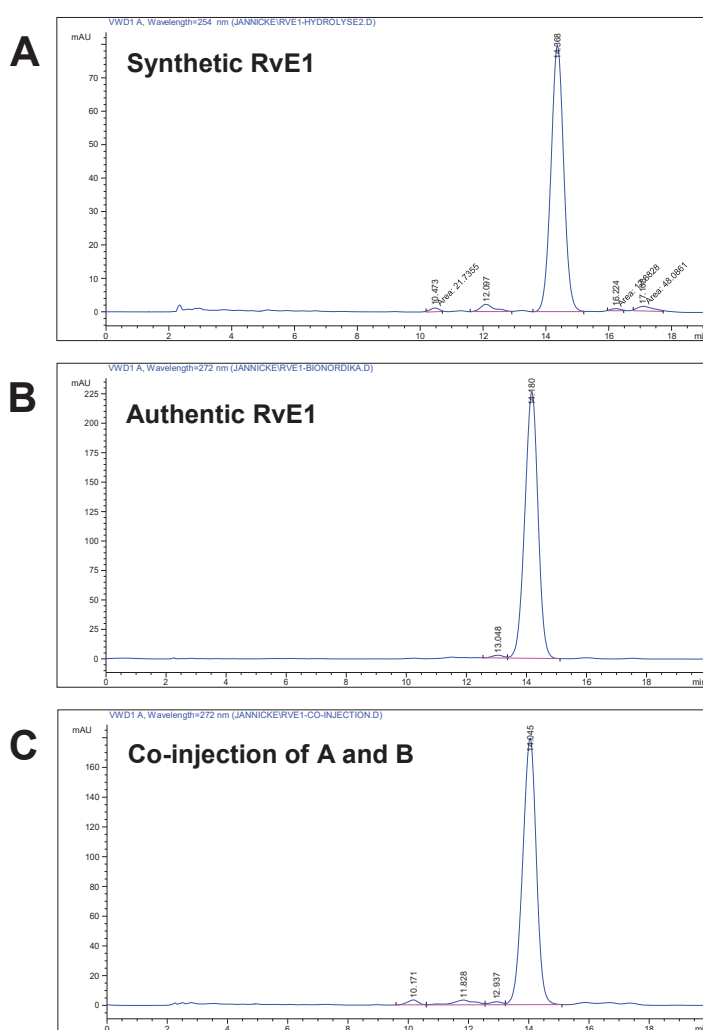


**Figure 2.11** Chromatograms obtained from matching experiments with synthetic and authentic RvE1 (**26**).



#### 2.4.4 Conclusion

The potent SPM resolvin E1 (**26**) was stereoselectively synthesized in 3% yield over 12 steps (LLS). The RvE1-methyl ester **196** and final acid **26** were isolated in high chemical purity (97% and 94%, respectively), which is a prerequisite for further biological evaluations. The synthesized material displayed identical chromatographic and spectroscopic properties as authentic RvE1 (**26**), demonstrating that the desired stereoisomer was synthesized. Finally, our collaborative efforts regarding biological investigations of RvE1 (**26**) will be reported in due course.

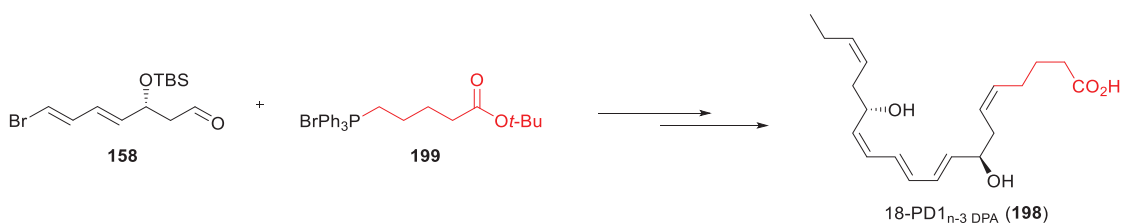
## Chapter 3 Summary and future outlook

This thesis describes the synthesis of 22-OH-PD1<sub>n-3</sub> DPA (**139**), PD1<sub>n-3</sub> DPA (**36**) and RvE1 (**26**). 22-OH-PD1<sub>n-3</sub> DPA (**139**) is the first metabolite of PD1<sub>n-3</sub> DPA (**36**) to be isolated and synthesized. All of the listed compounds were provided in multi milligram quantities that are available for biological evaluations. The authenticities of synthetic products were confirmed by matching experiments with endogenously produced materials, resulting in confirmed structural assignment and stereochemistry of 22-OH-PD1<sub>n-3</sub> DPA (**139**) and RvE1 (**26**).

Modifications of two target areas on the structure of PD1<sub>n-3</sub> DPA (**36**) resulted in the design and synthesis of two novel analogues – 17*S*-3-oxa-PD1<sub>n-3</sub> DPA (**140**) and the methyl ester of 17*R*-3-oxa-PD1<sub>n-3</sub> DPA (**141**), with the aim of increasing the metabolic stability, resulting in retained and prolonged biological activity compared to SPM **36**. Biological studies showed that the synthetic analog 17*S*-3-oxa-PD1<sub>n-3</sub> DPA (**140**) was equally potent as both PD1 (**31**) and PD1<sub>n-3</sub> DPA (**36**) in reducing neuropathic pain and itching following IT injection using animal models. The preliminary results presented herein are encouraging and will be published in due time.

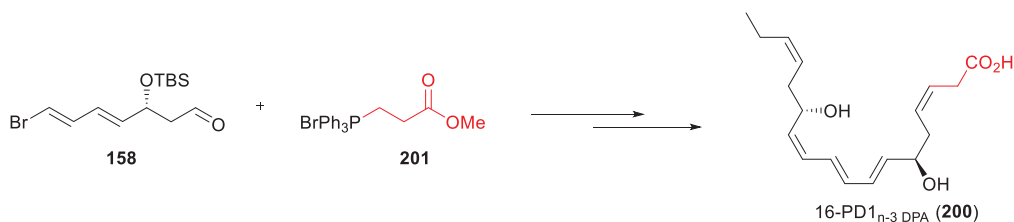
Several experiments have been left for the future to be completed. Synthetic samples of the above-mentioned analogues have been sent to our collaborator Professor Jesmond Dalli and his team at Queen Mary University of London. The biological investigations performed by this research group are currently ongoing and aim at providing information of the structure-activity relationship of our synthetic analogues relative to PD1<sub>n-3</sub> DPA (**36**) in terms of anti-inflammatory and pro-resolving properties. Additionally, synthetic samples of 17*S*-3-oxa-PD1<sub>n-3</sub> DPA (**140**), the methyl ester of 17*R*-3-oxa-PD1<sub>n-3</sub> DPA (**141**) and PD1<sub>n-3</sub> DPA (**36**) have been provided to the Oslo University Hospital in order to evaluate the impact of our structural modifications on PD1<sub>n-3</sub> DPA (**36**) with respect to enzymatic oxidative metabolism. The product profile resulting from this experiment will be determined by means of LC-MS/MS based lipid mediator profiling.

To ascertain the structure and stereochemistry of the presumed metabolites formed as a result of protectin metabolism, matching studies with synthetic standards are necessary. The metabolite resulting from one round of  $\beta$ -oxidation of PD1<sub>n-3</sub> DPA (**36**) is depicted in Scheme 3.1, namely 18-PD1<sub>n-3</sub> DPA (**198**). This compound may be prepared using the same protocols utilized in the synthesis of SPM **36**, after exchanging Wittig-salt **148** with Wittig-salt **199**, where the latter is two carbons shortened in chain-length.



**Scheme 3.1** Proposed synthesis of 18-PD<sub>1n-3</sub> DPA (**198**) utilizing Wittig-salt **199**.

Essentially equivalent, the same procedures may be followed to produce 16-PD<sub>1n-3</sub> DPA (**200**), by exchanging the  $\alpha$ -end with phosphonium salt **201** (Scheme 3.2.). Compound **200** would then correspond to the metabolite of PD<sub>1n-3</sub> DPA (**36**) formed after two rounds of  $\beta$ -oxidation.



**Scheme 3.2** Proposed synthesis of 16-PD<sub>1n-3</sub> DPA (**200**) utilizing Wittig-salt **201**.

Unfortunately, biosynthetic studies of 17*S*-3-oxa-PD<sub>1n-3</sub> DPA (**140**) were not conducted at this time. To confirm the structure and stereochemistry of the intermediate 17-OH-3-oxa PD<sub>1n-3</sub> DPA (**183**) and its conversion from 3-oxa n-3 DPA (**182**) catalyzed by 15-LOX, total synthesis and matching experiments are necessary. For this purpose, a proposed retrosynthesis to access 17*S*-OH-3-oxa PD<sub>1n-3</sub> DPA (**202**) is outlined in Figure 3.1, which is based on the chemistry presented in Chapter 2. For instance, disconnecting the C<sub>7</sub>-C<sub>8</sub> and C<sub>14</sub>-C<sub>15</sub> carbon bonds in **202** leads back to  $\alpha$ -end **203**,  $\omega$ -end **204** and the commercially available alkynes **205** and **206**.

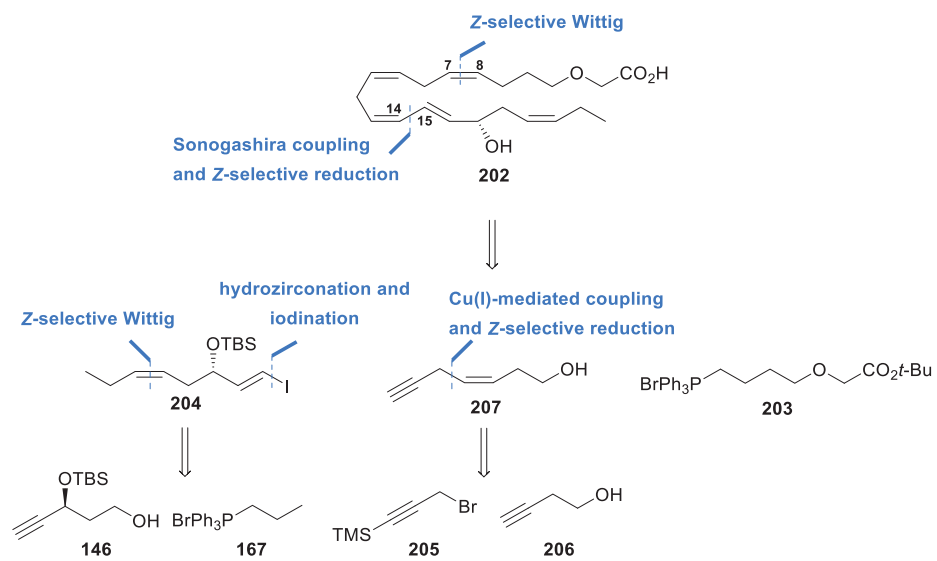


**Figure 3.1** Retrosynthetic analysis of 17*S*-OH-3-oxa DPA (**202**).

## Chapter 4 Conclusions

It is well recognized that chronic inflammation is an underlying cause of many common diseases. Following the discovery of the lipoxins as anti-inflammatory eicosanoids, immense efforts have been devoted to increasing our understanding of the inflammatory process. Revealing that resolution of inflammation is an active and highly regulated process orchestrated by locally produced signaling molecules has led to years of bioactive lipid research. Among these signals, essential-fatty acid derived resolvins, protectins and maresins have been identified as potent regulators of immune responses, including leukocyte trafficking, clearance, and pain. Discovery of the SPMs and an increased understanding of the mechanisms that control the resolution of ongoing inflammation has opened up new research areas aiming at treating inflammatory related diseases. Accordingly, the SPMs have great potential as novel lead compounds in medicinal chemistry programs towards the development of new therapeutics and treatment opportunities with a lower burden of side-effects. However, determining the detailed metabolic pathways for the SPMs, establish the exact structure for each individual SPM and performing structure-activity relationship studies are essential to gain new information of SPM biology that can contribute to such efforts.

In this thesis, the total synthesis of three SPMs and two SPM-analogues have been reported, namely 22-OH-PD1<sub>n-3</sub> DPA (**139**), PD1<sub>n-3</sub> DPA (**36**), RvE1 (**26**), 17*S*-3-oxa-PD1<sub>n-3</sub> DPA (**140**) and 17*R*-3-oxa-PD1<sub>n-3</sub> DPA (**141**). The structure of naturally produced 22-OH-PD1<sub>n-3</sub> DPA (**139**) has been established together with its bioconversion from PD1<sub>n-3</sub> DPA (**36**). The synthetic analog 17*S*-3-oxa-PD1<sub>n-3</sub> DPA (**140**) demonstrated to reduce neuropathic pain and itching with comparable potency to PD1 (**31**) and PD1<sub>n-3</sub> DPA (**36**) *in vivo*. All of the synthesized compounds have been or are currently in biological evaluation programs as a result of successful national and international collaborations.

## References

1. Divanovic, S.; Dalli, J.; Jorge-Nebert, L. F.; Flick, L. M.; Gálvez-Peralta, M.; Boespflug, N. D.; Stankiewicz, T. E.; Fitzgerald, J. M.; Somarathna, M.; Karp, C. L.; Serhan, C. N.; Nebert, D. W., *J. Immunol.* **2013**, *191* (6), 3347.
2. Serhan, C. N.; Petasis, N. A., *Chem. Rev.* **2011**, *111* (10), 5922.
3. Sumimoto, H.; Minakami, S., *J. Biol. Chem.* **1990**, *265* (8), 4348.
4. Hardwick, J. P., *Biochem. Pharmacol.* **2008**, *75* (12), 2263.
5. Lopaschuk, G. D.; Ussher, J. R.; Folmes, C. D. L.; Jaswal, J. S.; Stanley, W. C., *Phys. Rev.* **2010**, *90* (1), 207.
6. Tungen, J. E.; Aursnes, M.; Vik, A.; Ramon, S.; Colas, R. A.; Dalli, J.; Serhan, C. N.; Hansen, T. V., *J. Nat. Prod.* **2014**, *77* (10), 2241.
7. Dalli, J.; Colas, R. A.; Serhan, C. N., *Sci. Rep.* **2013**, *3* (1), 1940.
8. Dalli, J.; Chiang, N.; Serhan, C. N., *Nat. Med.* **2015**, *21* (9), 1071.
9. Vik, A.; Dalli, J.; Hansen, T. V., *Bioorg. Med. Chem. Lett.* **2017**, *27* (11), 2259.
10. Primdahl, K. G.; Tungen, J. E.; De Souza, P. R. S.; Colas, R. A.; Dalli, J.; Hansen, T. V.; Vik, A., *Org. Biomol. Chem.* **2017**, *15* (40), 8606.
11. Aursnes, M.; Tungen, J. E.; Vik, A.; Colas, R.; Cheng, C. Y. C.; Dalli, J.; Serhan, C. N.; Hansen, T. V., *J. Nat. Prod.* **2014**, *77* (4), 910.
12. Aursnes, M.; Tungen, J. E.; Vik, A.; Dalli, J.; Hansen, T. V., *Org. Biomol. Chem.* **2014**, *12* (3), 432.
13. Primdahl, K. G.; Tungen, J. E.; Aursnes, M.; Hansen, T. V.; Vik, A., *Org. Biomol. Chem.* **2015**, *13* (19), 5412.
14. Tungen, J. E.; Aursnes, M.; Hansen, T. V., *Tetrahedron Lett.* **2015**, *56* (14), 1843.
15. Tungen, J. E.; Aursnes, M.; Dalli, J.; Arnardottir, H.; Serhan, C. N.; Hansen, T. V., *Chem. Eur. J.* **2014**, *20* (45), 14575.
16. Nagao, Y.; Hagiwara, Y.; Kumagai, T.; Ochiai, M.; Inoue, T.; Hashimoto, K.; Fujita, E., *J. Org. Chem.* **1986**, *51* (12), 2391.
17. Dayaker, G.; Durand, T.; Balas, L., *J. Org. Chem.* **2014**, *79* (6), 2657.
18. Rooke, D. A.; Ferreira, E. M., *Angew. Chem. Int.* **2012**, *51* (13), 3225.
19. Boland, W.; Schroer, N.; Sieler, C.; Feigel, M., *Helv. Chim. Acta* **1987**, *70* (4), 1025.
20. Colas, R. A.; Shinohara, M.; Dalli, J.; Chiang, N.; Serhan, C. N., *Am. J. Physiol. Cell Physiol.* **2014**, *307* (1), C39.
21. Serhan, C.; Recchiuti, A., *Front. Immunol.* **2012**, *3* (298), PMID: **23093949**.
22. Balas, L.; Risé, P.; Gandrath, D.; Rovati, G.; Bolego, C.; Stellari, F.; Trenti, A.; Buccellati, C.; Durand, T.; Sala, A., *J. Med. Chem.* **2019**, *62* (21), 9961.
23. Tungen, J. E.; Gerstmann, L.; Vik, A.; De Matteis, R.; Colas, R. A.; Dalli, J.; Chiang, N.; Serhan, C. N.; Kalesse, M.; Hansen, T. V., *Chem. Eur. J.* **2019**, *25* (6), 1476.
24. Näf, F.; Decorzant, R.; Thommen, W.; Willhalm, B.; Ohloff, G., *Helv. Chim. Acta* **1975**, *58* (4), 1016.

25. Rautio, J.; Kumpulainen, H.; Heimbach, T.; Oliyai, R.; Oh, D.; Järvinen, T.; Savolainen, J., *Nat. Rev. Drug. Discov.* **2008**, *7* (3), 255.
26. Perez, C.; Daniel, K. B.; Cohen, S. M., *Chem. Med. Chem.* **2013**, *8* (10), 1662.
27. Krapcho, A. P.; Weimaster, J. F.; Eldridge, J. M.; Jahngen, E. G. E.; Lovey, A. J.; Stephens, W. P., *J. Org. Chem.* **1978**, *43* (1), 138.
28. Krapcho, A. P.; Gadamasetti, G., *J. Org. Chem.* **1987**, *52* (9), 1880.
29. Bang, S.; Xie, Y.-K.; Zhang, Z.-J.; Wang, Z.; Xu, Z.-Z.; Ji, R.-R., *J. Clin. Invest.* **2018**, *128* (8), 3568.
30. Gorbalenya, A. E.; Baker, S. C.; Baric, R. S.; de Groot, R. J.; Drosten, C.; Gulyaeva, A. A.; Haagmans, B. L.; Lauber, C.; Leontovich, A. M.; Neuman, B. W.; Penzar, D.; Perlman, S.; Poon, L. L. M.; Samborskiy, D. V.; Sidorov, I. A.; Sola, I.; Ziebuhr, J.; Coronaviridae *Nat. Microbiol.* **2020**, *5* (4), 536.
31. Serhan, C. N.; Gotlinger, K.; Hong, S.; Lu, Y.; Siegelman, J.; Baer, T.; Yang, R.; Colgan, S. P.; Petasis, N. A., *J. Immunol.* **2006**, *176* (3), 1848.
32. Hansen, T. V.; Dalli, J.; Serhan, C. N., *Prostag. Oth. Lipid M.* **2017**, *133*, 103.
33. Pangopoulos, M. K.; Nolsøe, J. M. N.; Antonsen, S. G.; Colas, R. A.; Dalli, J.; Aursnes, M.; Stenstrøm, Y.; Hansen, T. V., *Bioorg. Chem.* **2020**, *96*, 103653.
34. Serhan, C. N., *Am. J. Pathol.* **2010**, *177* (4), 1576.
35. Dalli, J.; Serhan, C. N., *Br. J. Pharmacol.* **2019**, *176* (8), 1024.
36. Balta, M. G.; Loos, B. G.; Nicu, E. A., *Front. Immunol.* **2017**, *8* (1682).
37. Van Dyke, T. E., *J. Clin. Periodontol.* **2011**, *38* (s11), 119.
38. Youn, I. K.; Yon, G. H.; Pak, C. S., *Tetrahedron lett.* **1986**, *27* (21), 2409.
39. Dong, D. J.; Li, H. H.; Tian, S. K., *J. Am. Chem. Soc.* **2010**, *132* (14), 5018.

## Chapter 5 Experimental procedures

In this section, unpublished experimental procedures concerning the total synthesis of PD1<sub>n-3</sub> DPA (**36**), 17*R*-3-oxa-PD1<sub>n-3</sub> DPA (**141**) and incubation studies with 3-oxa n-3 DPA (**182**) are presented with characterization data.

### General Information

Unless otherwise stated, all commercially available reagents and solvents were used in the form in which they were supplied without any further purification. The stated yields are based on isolated material. All reactions were performed under an argon atmosphere using Schlenk techniques. Reaction flasks were covered with aluminum foil during reactions and storage to minimize exposure to light. Thin layer chromatography was performed on silica gel 60 F<sub>254</sub> aluminum-backed plates fabricated by Merck. Flash column chromatography was performed on silica gel 60 (40-63 μm) produced by Merck. NMR spectra were recorded on a Bruker AVI600, Bruker AVII400 or a Bruker DPX300 spectrometer at 600 MHz, 400 MHz or 300 MHz respectively for <sup>1</sup>H NMR and at 150 MHz, 100 MHz or 75 MHz respectively for <sup>13</sup>C NMR. Coupling constants (*J*) are reported in hertz and chemical shifts are reported in parts per million (δ) relative to the central residual protium solvent resonance in <sup>1</sup>H NMR (CDCl<sub>3</sub> = δ 7.26, DMSO-*d*<sub>6</sub> = δ 2.50 and MeOD = δ 3.31) and the central carbon solvent resonance in <sup>13</sup>C NMR (CDCl<sub>3</sub> = δ 77.00 ppm, DMSO-*d*<sub>6</sub> = δ 39.43 and MeOD = δ 49.00). Optical rotations were measured using a 0.7 mL cell with a 1.0 dm path length on an Anton Paar MCP 100 polarimeter. Mass spectra were recorded at 70 eV on a Micromass Prospec Q or Micromass QTOF 2 W spectrometer using ESI as the method of ionization. High-resolution mass spectra were recorded at 70 eV on a Micromass Prospec Q or Micromass QTOF 2W spectrometer using ESI as the method of ionization. HPLC-analyses were performed using a C18 stationary phase (Eclipse XDB-C18, 4.6 × 250 mm, particle size 5 μm, from Agilent Technologies), applying the conditions stated. The UV/Vis spectra were recorded using an Agilent Technologies Cary 8485 UV-VIS spectrophotometer using quartz cuvettes.



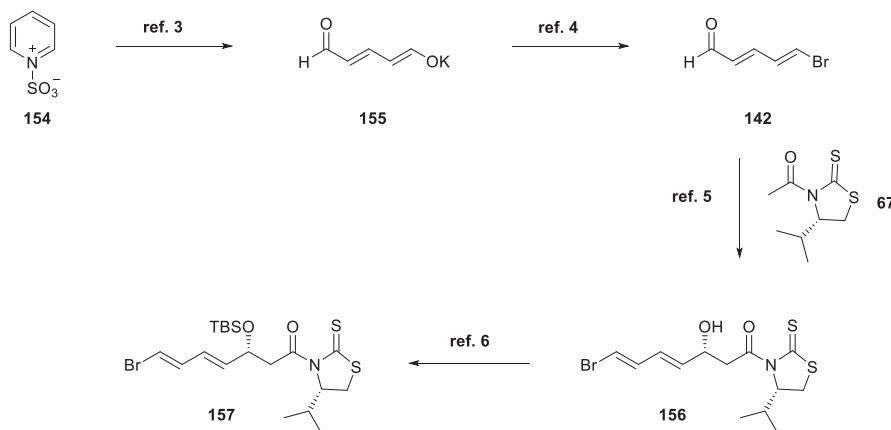
## Total synthesis of protectin D1<sub>n-3</sub> DPA (**36**)

### Synthesis of (*S,Z*)-*tert*-butyldimethyl(oct-5-en-1-yn-3-yloxy)silane (**163**)



Omega fragment **163**, was prepared from commercially available (*S*)-(-)- $\alpha$ -hydroxy- $\gamma$ -butyrolactone (**147**) as previously reported.<sup>1,2</sup> Yield: 32 % over the five steps. All spectroscopic and physical data were in agreement with those reported in the literature.<sup>2</sup> <sup>1</sup>H NMR (400 MHz, CDCl<sub>3</sub>)  $\delta$  5.64 – 5.32 (m, 2H), 4.34 (td,  $J$  = 6.6, 2.1 Hz, 1H), 2.44 (t,  $J$  = 7.0 Hz, 2H), 2.38 (d,  $J$  = 2.1 Hz, 1H), 2.07 (p,  $J$  = 7.5 Hz, 2H), 0.97 (t,  $J$  = 7.5 Hz, 3H), 0.91 (s, 9H), 0.13 (s, 3H), 0.11 (s, 3H); <sup>13</sup>C NMR (100 MHz, CDCl<sub>3</sub>)  $\delta$  134.6, 123.9, 85.6, 72.2, 63.0, 36.7, 26.0, 21.0, 18.4, 14.4, -4.5, -4.9;  $[\alpha]_D^{25}$  = -24.1 ( $c$  = 1.0, MeOH); TLC (hexane, KMnO<sub>4</sub>-stain)  $R_f$  = 0.25.

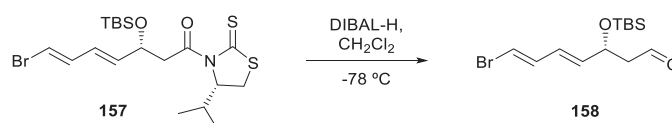
### (*R,4E,6E*)-7-bromo-3-((*tert*-butyldimethylsilyl)oxy)-1-((*R*)-4-isopropyl-2-thioxothiazolidin-3-yl)hepta-4,6-dien-1-one (**157**)



Thiazolidinethione **157** was prepared in four steps from commercially available pyridinium-1-sulfonate **154** as previously reported in the literature.<sup>3-6</sup> Yield: 38% over the four steps. All spectroscopic and physical data were in agreement with those reported in the literature.<sup>6</sup>  $[\alpha]_D^{20}$  = +265 ( $c$  = 0.40, CHCl<sub>3</sub>); <sup>1</sup>H NMR (400 MHz, CDCl<sub>3</sub>)  $\delta$  6.69 (dd,  $J$  = 13.5, 10.9 Hz, 1H), 6.31 (d,  $J$  = 13.5 Hz, 1H), 6.15 (dd,  $J$  = 15.3, 10.9 Hz, 1H), 5.79 (dd,  $J$  = 15.4, 6.3 Hz, 1H), 5.08 – 4.98 (m,

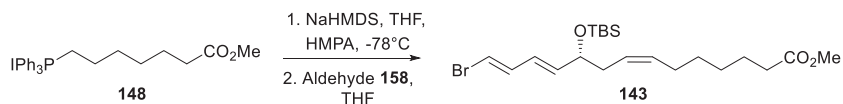
1H), 4.79 – 4.69 (m, 1H), 3.64 (dd,  $J = 16.6, 7.9$  Hz, 1H), 3.47 (dd,  $J = 11.5, 7.8$  Hz, 1H), 3.21 (dd,  $J = 16.6, 4.5$  Hz, 1H), 3.03 (dd,  $J = 11.4, 1.1$  Hz, 1H), 2.43 – 2.29 (m,  $J = 6.9$  Hz, 1H), 1.05 (d,  $J = 6.8$  Hz, 3H), 0.97 (d,  $J = 7.0$  Hz, 3H), 0.86 (s, 9H), 0.05 (s, 3H), 0.03 (s, 3H);  $^{13}\text{C}$  NMR (101 MHz,  $\text{CDCl}_3$ )  $\delta$  203.0, 171.0, 136.9, 127.5, 109.1, 71.8, 69.9, 46.3, 31.0, 30.9, 26.0 (3C), 19.3, 18.2, 18.0, -4.2, -4.8; TLC (hexane/EtOAc 7:3,  $\text{KMnO}_4$ -stain)  $R_f = 0.56$ .

**(*R,4E,6E*)-7-bromo-3-((*tert*-butyldimethylsilyl)oxy)hepta-4,6-dienal (**158**)**



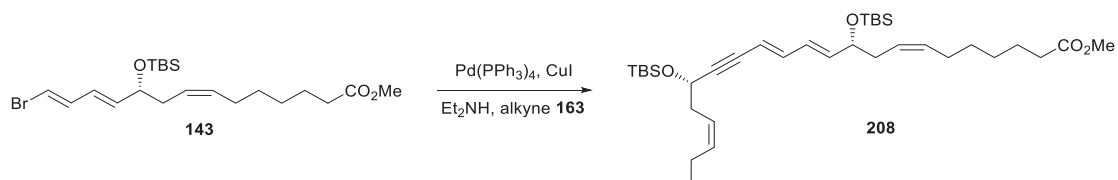
Aldehyde **158** was prepared according to the procedure reported by Olivo *et. al.*<sup>7</sup> The protected thiazolidinethione **157** (1.72 g, 3.59 mmol, 1.00 equiv.) was dissolved in  $\text{CH}_2\text{Cl}_2$  (69 mL) followed by dropwise addition of DIBAL-H (1.0 M in  $\text{CH}_2\text{Cl}_2$ , 4.60 mmol, 1.30 equiv.) at  $-78$  °C. After three h., additional DIBAL-H was added (1.0 M in  $\text{CH}_2\text{Cl}_2$ , 1.30 mmol, 0.362 equiv.). The mixture was allowed to stir for 30 min and then quenched with sat. aq.  $\text{NaHCO}_3$  (60 mL). The cooling bath was removed and solid Na-K tartrate (~ 1.50 g, Rochelle salt) was added and stirring was continued for another 45 min. The layers were separated and the aq. layer was extracted with  $\text{Et}_2\text{O}$  ( $3 \times 50$  mL). The combined organic layers were dried ( $\text{Na}_2\text{SO}_4$ ) and concentrated *in vacuo*, but not to dryness. The residue was purified by column chromatography on silica gel (hexane/EtOAc 95:5), and the solvent evaporated to give the title compound **158** as a yellow oil. Yield: 1.03 g (89%). All spectroscopic and physical data were in agreement with those reported in the literature.<sup>7</sup>  $[\alpha]_D^{20} = +32.0$  ( $c = 0.20$ ,  $\text{CHCl}_3$ );  $^1\text{H}$  NMR (400 MHz,  $\text{CDCl}_3$ )  $\delta$  9.75 (t,  $J = 2.3$  Hz, 1H), 6.69 (dd,  $J = 13.5, 10.9$  Hz, 1H), 6.33 (d,  $J = 13.5$  Hz, 1H), 6.23 – 6.09 (m, 1H), 5.76 (dd,  $J = 15.2, 5.9$  Hz, 1H), 4.71 – 4.64 (m, 1H), 2.63 (ddd,  $J = 15.9, 6.7, 2.5$  Hz, 1H), 2.53 (ddd,  $J = 15.9, 5.1, 2.1$  Hz, 1H), 0.88 (s, 9H), 0.06 (s, 3H), 0.04 (s, 3H);  $^{13}\text{C}$  NMR (101 MHz,  $\text{CDCl}_3$ )  $\delta$  201.2, 136.6, 136.1, 127.6, 109.6, 68.5, 51.4, 25.9, 14.3, -4.2, -4.9; TLC (hexane/EtOAc 95:5,  $\text{KMnO}_4$ -stain)  $R_f = 0.24$ .

**Methyl (*R*,*7Z*,*11E*,*13E*)-14-bromo-10-((*tert*-butyldimethylsilyl)oxy)tetradeca-7,11,13-trienoate (**143**)**



To the commercially available Wittig salt **148** (670 mg, 1.26 mmol, 1.00 equiv.) in THF (16 mL) and HMPA (1.7 mL) was added NaHMDS (0.6 M in THF, 2.1 mL, 1.00 equiv.) at -78 °C. Over 1h, this solution was warmed to rt and then re-cooled to -78 °C followed by dropwise addition of aldehyde **x** (402 mg, 1.26 mmol, 1.00 eq.) in THF (5 mL). The solution was allowed to slowly warm up to room temperature in a dry ice/acetone bath for 24 h before it was quenched with phosphate buffer (12 mL, pH = 7.2). Et<sub>2</sub>O (15 mL) was added and the phases were separated. The aqueous phase was extracted with Et<sub>2</sub>O (2 × 15 mL) and the combined organic layers were dried (Na<sub>2</sub>SO<sub>4</sub>), before concentrated *in vacuo*. The crude product was purified by column chromatography on silica gel (hexane/EtOAc 95:5) to afford the title compound **143** as a clear oil. Yield: 386 mg (69%). All spectroscopic and physical data were in full agreement with those reported in the literature.<sup>8</sup> [ $\alpha$ ]<sub>D</sub><sup>20</sup> = -18.0 (c = 0.090, MeOH); <sup>1</sup>H NMR (400 MHz, CDCl<sub>3</sub>)  $\delta$  6.68 (dd, *J* = 13.4, 10.9 Hz, 1H), 6.27 (d, *J* = 13.5 Hz, 1H), 6.09 (dd, *J* = 15.2, 10.9 Hz, 1H), 5.71 (dd, *J* = 15.3, 9.6 Hz, 1H), 5.48–5.29 (m, 2H), 4.17–4.11 (m, 1H), 3.67 (s, 3H), 2.34–2.16 (m, 4H), 2.00 (q, *J* = 6.8 Hz, 2H), 1.62 (p, *J* = 7.5 Hz, 2H), 1.4–1.26 (m, 4H), 0.89 (s, 9H), 0.04 (s, 3H), 0.02 (s, 3H); <sup>13</sup>C NMR (101 MHz, CDCl<sub>3</sub>)  $\delta$  174.4, 138.1, 137.2, 131.9, 126.6, 125.2, 108.2, 72.7, 51.6, 36.3, 34.2, 29.4, 29.0, 27.4, 26.0 (3C), 25.0, 18.4, -4.4, -4.6; TLC (hexane/EtOAc 95:5, KMnO<sub>4</sub>-stain) R<sub>f</sub> = 0.33.

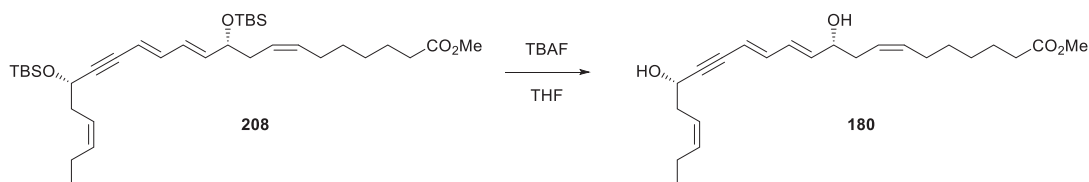
**Methyl (*7Z*,*10R*,*11E*,*13E*,*17S*,*19Z*)-10,17-bis((*tert*-butyldimethylsilyl)oxy)docosa-7,11,13,19-tetraen-15-ynoate (**208**)**



To a solution of vinyl bromide **143** (182 mg, 0.409 mmol, 1.00 eq.) in Et<sub>2</sub>NH (0.8 mL) and benzene (0.3 mL) was added Pd(PPh<sub>3</sub>)<sub>4</sub> (16.0 mg, 0.0140 mmol, 3.00 mol%), and the reaction was stirred

for 45 min in the dark. CuI (4.00 mg, 0.0210 mmol, 5.00 mol%) dissolved in a minimum amount of Et<sub>2</sub>NH was added, followed by dropwise addition of alkyne **163** (104 mg, 0.436 mmol, 1.07 eq.) in Et<sub>2</sub>NH (0.8 mL). After 20 hours of stirring at ambient temperature, the reaction was quenched with sat. aq. NH<sub>4</sub>Cl (10 mL). Et<sub>2</sub>O (15 mL) was added, and the phases were separated. The aq. phase was extracted with Et<sub>2</sub>O (2 × 15 mL), and the combined organic layers were dried (Na<sub>2</sub>SO<sub>4</sub>), before being concentrated *in vacuo*. The crude product was purified by column chromatography on silica gel (hexane/EtOAc, 95:5) to afford the title compound **208** as a pale yellow oil. Yield: 225 mg (91%). All spectroscopic and physical data were in full agreement with those reported in the literature.<sup>8</sup>  $[\alpha]_D^{20} = -21.0$  (c = 0.080, MeOH); <sup>1</sup>H NMR (400 MHz, CDCl<sub>3</sub>) δ 6.51 (dd, *J* = 15.5, 10.9 Hz, 1H), 6.18 (ddd, *J* = 14.2, 10.3, 1.0 Hz, 1H), 5.75 (dd, *J* = 15.2, 5.9 Hz, 1H), 5.62–5.31 (m, 5H), 4.47 (td, *J* = 6.6, 1.8 Hz, 1H), 4.21–4.12 (m, 1H), 3.66 (t, 3H), 2.44 (t, *J* = 7.9 Hz, 2H), 2.30 (t, *J* = 7.6 Hz, 2H), 2.28–2.15 (m, 2H), 2.11–1.94 (m, 4H), 1.63 (q, *J* = 7.4 Hz, 2H), 1.40–1.25 (m, 4H), 0.96 (t, *J* = 7.5 Hz, 3H), 0.91 (s, 9H), 0.89 (s, 9H), 0.12 (d, *J* = 8.3 Hz, 6H), 0.03 (d, *J* = 8.3 Hz, 6H); <sup>13</sup>C NMR (101 MHz, CDCl<sub>3</sub>) δ 174.3, 141.2, 139.3, 134.4, 131.9, 128.6, 125.4, 124.1, 110.7, 93.4, 83.6, 72.9, 63.7, 51.6, 36.8, 36.4, 34.2, 29.4, 29.0, 27.4, 26.0 (3C), 26.0 (3C), 25.0, 20.9, 18.5, 18.4, 14.4, -4.3 (2C), -4.6, -4.8; TLC (hexane/EtOAc, 9:1, CAM-stain) R<sub>f</sub> = 0.63.

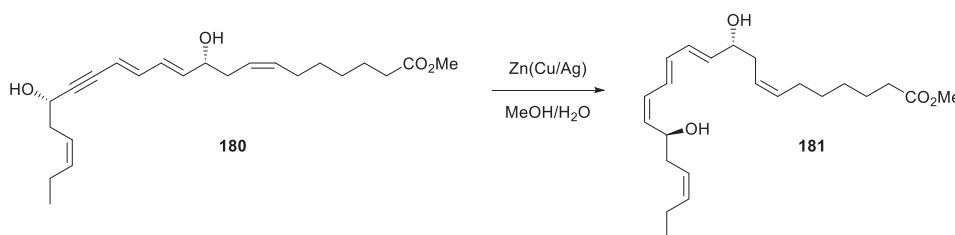
**Methyl (7Z,10R,11E,13E,17S,19Z)-10,17-dihydrodocosa-7,11,13,19-tetraen-15-ynoate (180)**



TBAF (1.0 M in THF, 0.9 mL, 0.900 mmol, 4.95 eq.) was added to a solution of TBS-protected alcohol **208** (110 mg, 0.182 mmol, 1.00 equiv) in THF (2.0 mL) at -78 °C. The reaction was stirred for 21 h before it was quenched with phosphate buffer (pH = 7.2, 3.5 mL). Brine (15 mL) and EtOAc (15 mL) were added, and the phases were separated. The aq. phase was extracted with EtOAc (2 × 15 mL) and the combined organic layers were dried (Na<sub>2</sub>SO<sub>4</sub>) before the solvent was evaporated. The crude product was purified by column chromatography on silica gel (hexanes/EtOAc, 7:3) to afford the title compound **180** as a pale yellow oil. Yield: 58 mg (87%). All spectroscopic and physical data were in full agreement with those reported in the literature.<sup>8</sup>  $[\alpha]_D^{20} = -16.0$  (c = 0.060, MeOH); <sup>1</sup>H NMR (400 MHz, CDCl<sub>3</sub>) δ 6.55 (dd, *J* = 15.6, 11.0 Hz, 1H), 6.27 (dd, *J* = 14.9, 11.6 Hz, 1H), 5.81 (dd, *J* = 15.2, 6.1 Hz, 1H), 5.67–5.49 (m, 3H), 5.48–5.31 (m, 2H), 4.52 (td, *J* = 6.4, 1.9 Hz, 1H), 4.25–4.16 (m, 1H), 3.68 (t, 3H), 2.49 (t, *J* = 6.9 Hz, 2H),

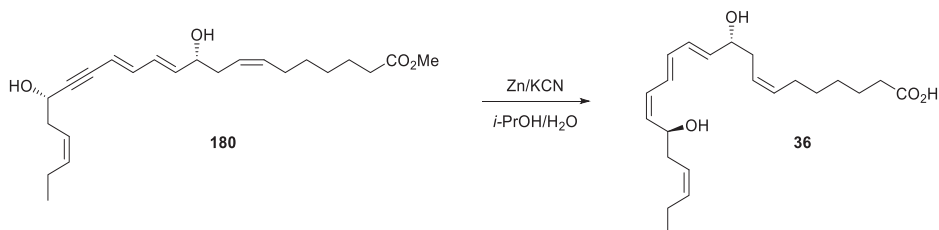
2.35–2.26 (m, 4H), 2.14–1.99 (m, 4H), 1.98 (d,  $J = 5.4$  Hz, 1H), 1.71 (s, 1H); 1.62 (p,  $J = 7.5$  Hz, 2H), 1.43–1.27 (m, 4H), 0.97 (t,  $J = 7.5$  Hz, 3H);  $^{13}\text{C}$  NMR (101 MHz,  $\text{CDCl}_3$ )  $\delta$  174.4, 141.5, 138.4, 136.1, 133.8, 129.4, 124.3, 122.9, 110.9, 92.6, 84.1, 71.7, 62.7, 51.7, 35.8, 35.5, 34.2, 29.3, 28.9, 27.4, 25.0, 21.0, 14.4; TLC (hexane/EtOAc, 7:3,  $\text{KMnO}_4$ -stain)  $R_f = 0.26$ .

**Methyl (7Z,10R,11E,13E,15Z,17S,19Z)-10,17-dihydrodocosa-7,11,13,15,19-pentaenoate (181)**



The  $\text{Zn}(\text{Cu}/\text{Ag})$  reagent was prepared as described by Boland *et al.*<sup>9</sup> Zinc dust (1.80 g) in degassed  $\text{H}_2\text{O}$  (10.8 mL, pH = 7.0) was stirred under argon for 15 min before  $\text{Cu}(\text{OAc})_2$  (180 mg) was added and stirred for an additional 15 min.  $\text{AgNO}_3$  (180 mg) was then added and the reaction mixture was stirred for 30 minutes. The mixture was filtered and washed successively with  $\text{H}_2\text{O}$ , MeOH, acetone and  $\text{Et}_2\text{O}$  before it was transferred to a flask containing alkyne **180** (25.0 mg, 0.067 mmol) in MeOH/ $\text{H}_2\text{O}$  (1:1, 7.4 mL). The mixture was stirred at rt and monitored by TLC analysis. After 5 h, the reaction was judged complete and the reaction mixture was filtered through a pad of Celite<sup>®</sup> with  $\text{Et}_2\text{O}$ . Water was added to the filtrate, and the layers were separated. The aq. layer was extracted with  $\text{Et}_2\text{O}$  ( $3 \times 10$  mL). The combined organic layers were washed with brine and dried ( $\text{Na}_2\text{SO}_4$ ). The solvent was evaporated and the crude product was purified by column chromatography on silica gel (10–30% hexane in EtOAc with drops of MeOH) to afford the methyl ester **181** as a pale yellow oil. Yield: 8.0 mg (32%). All spectroscopic and physical data were in full agreement with those reported in the literature.<sup>8</sup>  $[\alpha]_D^{20} = -19.0$  ( $c = 0.100$ , MeOH); UV (MeOH)  $\lambda_{\text{max}}$  262, 271, 282 nm;  $^1\text{H}$  NMR (400 MHz, MeOH- $d_4$ )  $\delta$  6.52 (dd,  $J = 14.2, 11.3$  Hz, 1H), 6.32–6.18 (m, 2H), 6.07 (t,  $J = 11.0$  Hz, 1H), 5.74 (dd,  $J = 14.4, 6.6$  Hz, 1H), 5.51–5.29 (m, 5H), 4.45 (dt,  $J = 8.9, 6.8$  Hz, 1H), 4.12 (q,  $J = 6.7$  Hz, 1H), 3.65 (s, 3H), 2.41–2.16 (m, 5H), 2.11–1.99 (m, 4H), 1.61 (p,  $J = 7.4$  Hz, 2H), 1.42–1.21 (m, 5H), 0.97 (t, 3H);  $^{13}\text{C}$  NMR (101 MHz, MeOH- $d_4$ )  $\delta$  176.0, 138.0, 134.9, 134.4, 134.7, 132.8, 131.3, 130.5, 128.9, 126.2, 125.3, 73.1, 68.6, 52.0, 36.4, 36.4, 34.8, 30.3, 29.8, 28.2, 25.9, 21.7, 14.6; TLC (hexane/EtOAc, 7:3,  $\text{KMnO}_4$ -stain)  $R_f = 0.20$ . The purity (>99%) was determined by HPLC analysis (Eclipse XDB-C18, MeOH/ $\text{H}_2\text{O}$ , 80:20, 1.0 mL/min);  $t_r = 10.5$  min. HRMS (ESI): calculated for  $\text{C}_{23}\text{H}_{36}\text{NaO}_4$   $[M+\text{Na}]^+$ : 399.2506, found: 399.2505.

**(7Z,10R,11E,13E,15Z,17S,19Z)-10,17-dihydrodocosa-7,11,13,15,19-pentaenoic acid  
Protectin D1<sub>n-3</sub> DPA (36)**



Compound **36** was prepared as described by Näf *et. al.*<sup>10</sup> A mixture of alkyne **180** (15.0 mg, 43.3  $\mu\text{mol}$ , 1.00 eq.), zinc powder (566 mg, 8.65 mmol, 200 eq.) and potassium cyanide (40 mg, 0.610 mmol, 14.0 eq.) was added to a solution of *i*-PrOH/H<sub>2</sub>O (3.0 mL 1:1, pH = 7.0), and stirred at ambient temperature under protection of argon in the dark. After stirring for 20 h, the reaction mixture was filtered through a pad of Celite<sup>®</sup> and the pad washed with EtOAc (10 mL). Sat. aq. NH<sub>4</sub>Cl (10 mL) was added to the filtrate and the phases were separated. The aq. phase was extracted with EtOAc (3  $\times$  6.0 mL), and the combined organic layer was dried (Na<sub>2</sub>SO<sub>4</sub>), filtrated, and the solvent evaporated. The crude acid was purified using Biotage<sup>®</sup> Select purification system (Biotage<sup>®</sup> Sfär-C-18, 40-50% MeOH/3.3mM AcOH, 6.0 mL/min). Following purification, the MeOH was evaporated and the aq. phase added sat. aq. NaH<sub>2</sub>PO<sub>4</sub> (3.0 mL), and was then extracted with EtOAc (3  $\times$  5.0 mL). The combined organic layer was dried (Na<sub>2</sub>SO<sub>4</sub>), filtered, and concentrated *in vacuo* to give the title compound **36** as a clear oil. Yield: 7.0 mg (45%). All spectroscopic and physical data were in full agreement with those reported in the literature.<sup>8</sup>  $[\alpha]_D^{20} = -28.0$  (c = 0.10, MeOH); UV (MeOH)  $\lambda_{\text{max}}$  262, 271, 282 nm; <sup>1</sup>H NMR (400 MHz, MeOH-*d*<sub>4</sub>)  $\delta$  6.52 (dd, *J* = 13.7, 11.1 Hz, 1H), 6.31–6.20 (m, 2H), 6.08 (t, *J* = 11.0 Hz, 1H), 5.74 (dd, *J* = 14.5, 6.6 Hz, 1H), 5.50–5.30 (m, 5H), 4.56 (dt, *J* = 8.6, 6.3 Hz, 1H), 4.15–4.09 (m, 1H), 2.40–2.17 (m, 6H), 2.10–2.02 (m, 4H), 1.60 (p, *J* = 7.4 Hz, 2H), 1.42–1.30 (m, 4H), 0.97 (t, *J* = 7.5 Hz, 3H); <sup>13</sup>C NMR (101 MHz, MeOH-*d*<sub>4</sub>)  $\delta$  178.2, 138.0, 134.9, 134.8, 134.7, 132.9, 131.3, 130.6, 128.9, 126.2, 125.3, 73.1, 68.6, 36.4, 36.4, 35.4, 30.4, 29.9, 28.3, 26.2, 21.7, 14.6; TLC (Et<sub>2</sub>O with a drop of AcOH, CAM-stain)  $R_f$  = 0.34. ). The purity (>99%) was determined by HPLC analysis (Eclipse XDB-C18, MeOH/H<sub>2</sub>O/10 mM HCOOH, 75:20:5, 1.0 mL/min);  $t_r$  = 11.6 min. HRMS (ESI): calculated for C<sub>22</sub>H<sub>34</sub>NaO<sub>4</sub> [*M*+Na]<sup>+</sup>: 385.2349, found: 385.2349.

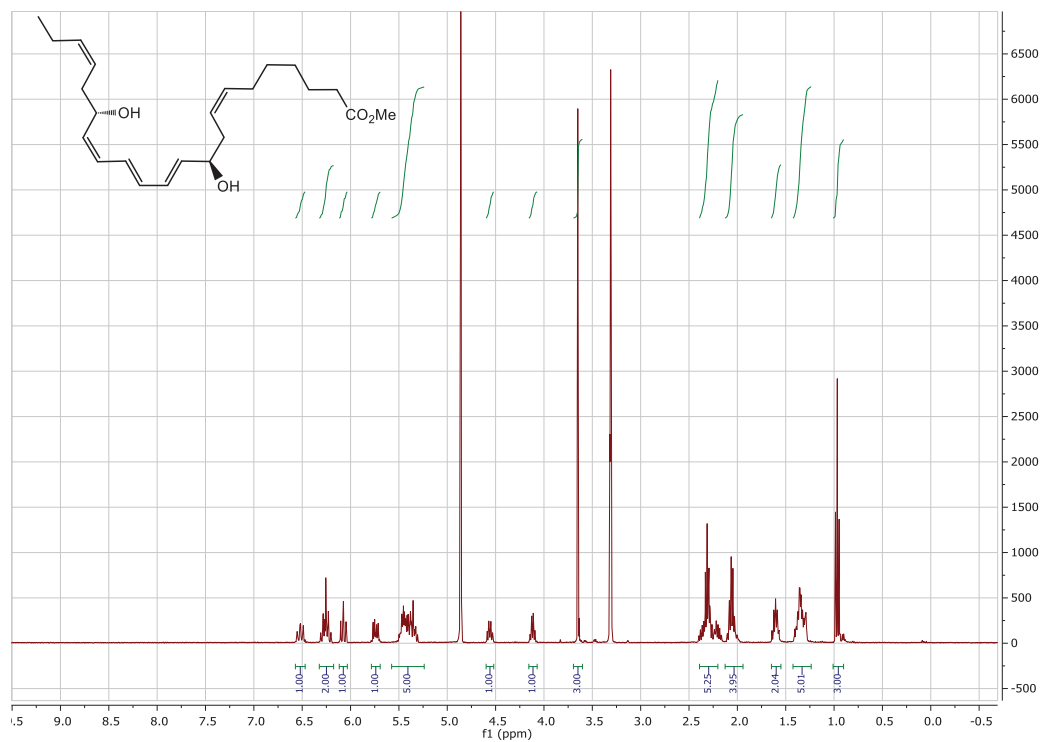


Figure 5.1 <sup>1</sup>H-NMR spectrum of PD1<sub>n-3</sub> DPA methyl ester (181).

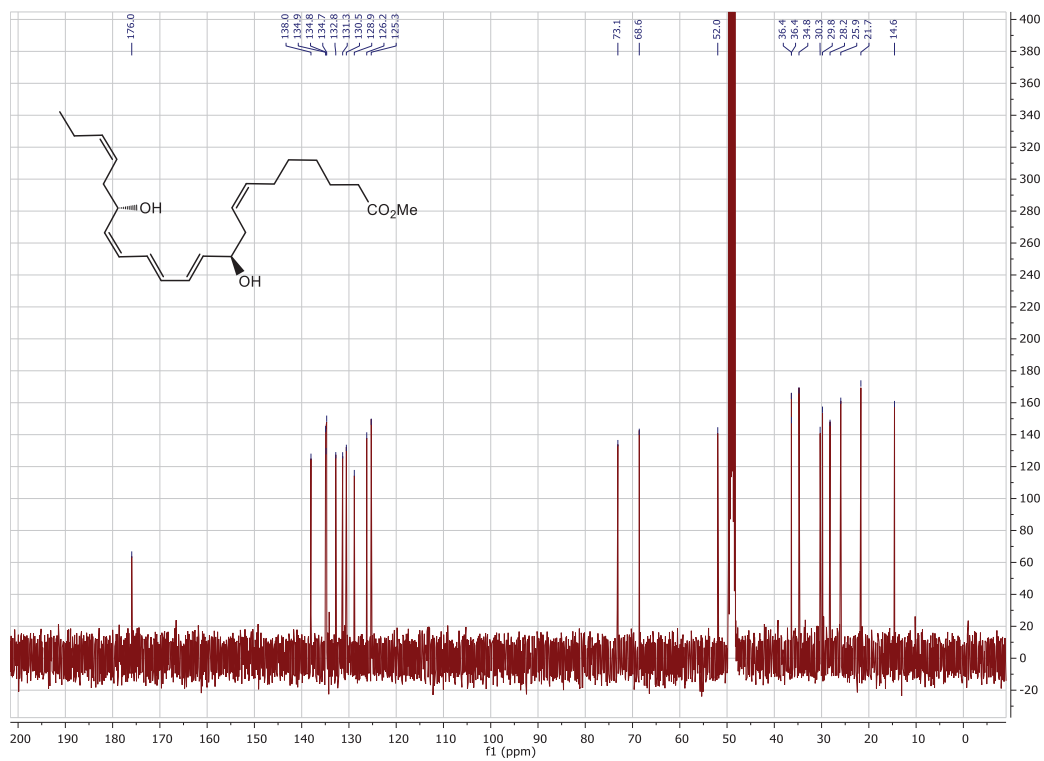
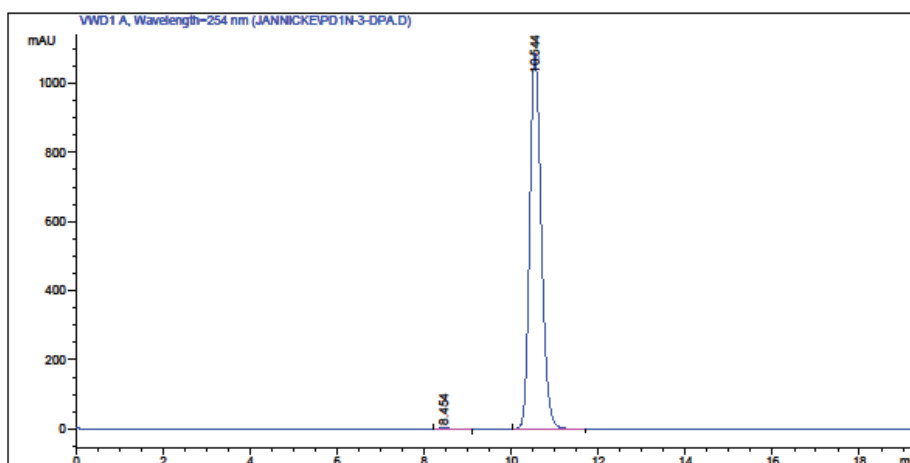


Figure 5.2 <sup>13</sup>C-NMR spectrum of PD1<sub>n-3</sub> DPA methyl ester (181).

Data File C:\CHEM32\1\DATA\JANNICKE\PD1n-3-DPA.D  
Sample Name: PD1n-3-DPA

```
=====
Acq. Operator   : Jannicke
Acq. Instrument : Instrument 1          Location : Vial 1
Injection Date  : 17.02.2020 16:42:32
                                           Inj Volume : 10 µl
Method          : C:\CHEM32\1\METHODS\C18 ISOKRATISK.M
Last changed    : 17.02.2020 16:39:01 by Jannicke
                  (modified after loading)
Sample Info     : PD1n-3 DFA methyl ester MeOH/H2O 8:2, 1.0 mL/min
=====
```



=====  
Area Percent Report  
=====

Sorted By : Signal  
Multiplier : 1.0000  
Dilution : 1.0000  
Use Multiplier & Dilution Factor with ISTDs

Signal 1: VWD1 A, Wavelength=254 nm

Peak #	RetTime [min]	Type	Width [min]	Area mAU *s	Height [mAU]	Area %
1	8.454	VB	0.2899	54.41904	2.70633	0.2716
2	10.544	BB	0.2844	1.99852e4	1086.78198	99.7284

Totals : 2.00396e4 1089.48831

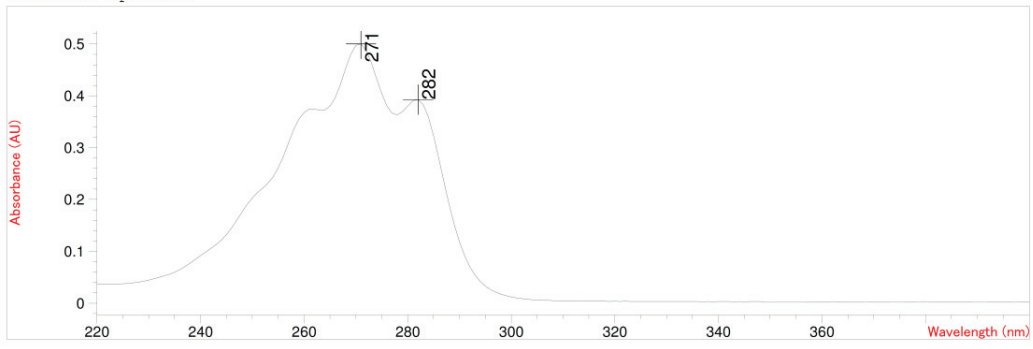
=====  
\*\*\* End of Report \*\*\*

Figure 5.3 HPLC chromatogram of PD1<sub>n</sub>-3 DPA methyl ester (181).



Method file : <method not saved>  
 Information : Default Method  
 Data File : <data not saved>

Overlaid Spectra:



#	Name	Peaks (nm)	Abs (AU)	#	Name	Peaks (nm)	Abs (AU)
1		271.0	0.50025	1		***	***
1		282.0	0.39285				

Figure 5.4 UV-Vis chromatogram of PD1<sub>n-3</sub> DPA methyl ester (181).

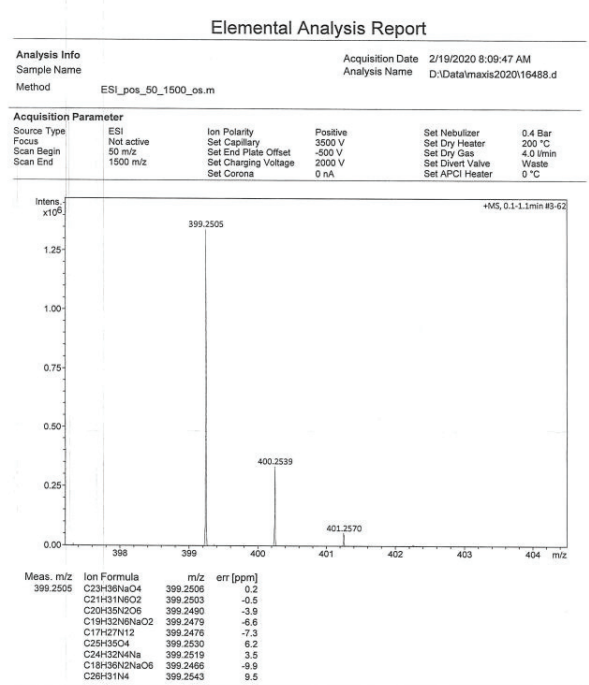


Figure 5.5 HRMS spectrum of PD1<sub>n-3</sub> DPA methyl ester (181).

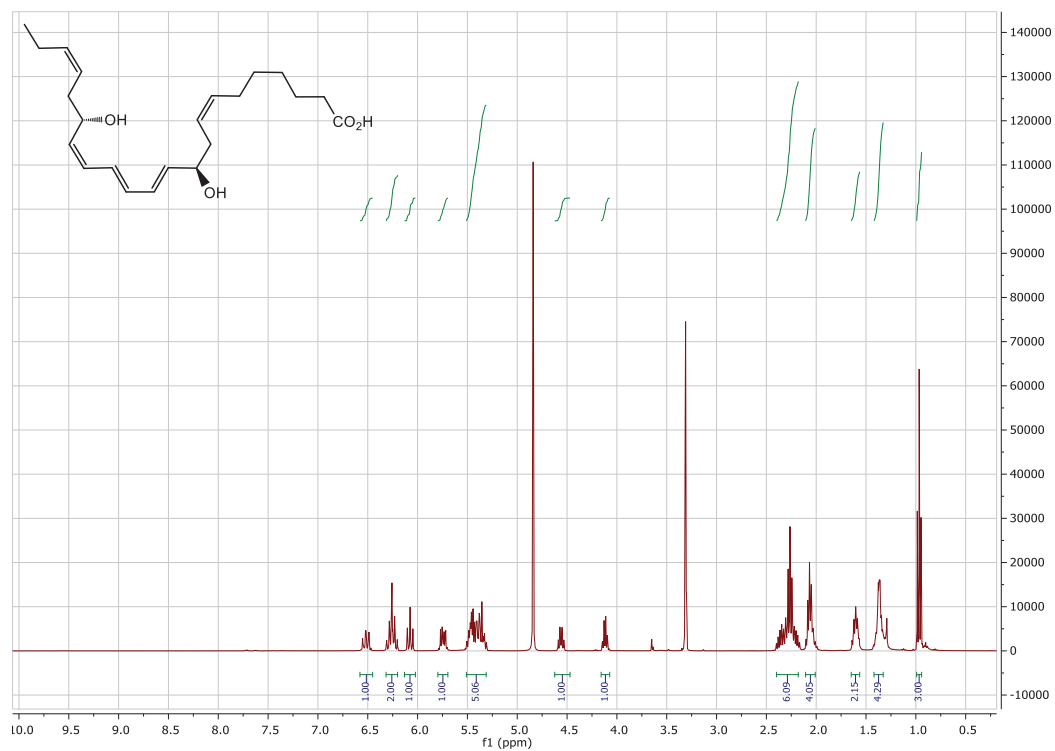


Figure 5.6 <sup>1</sup>H-NMR spectrum of PD1<sub>n-3</sub> DPA (36).

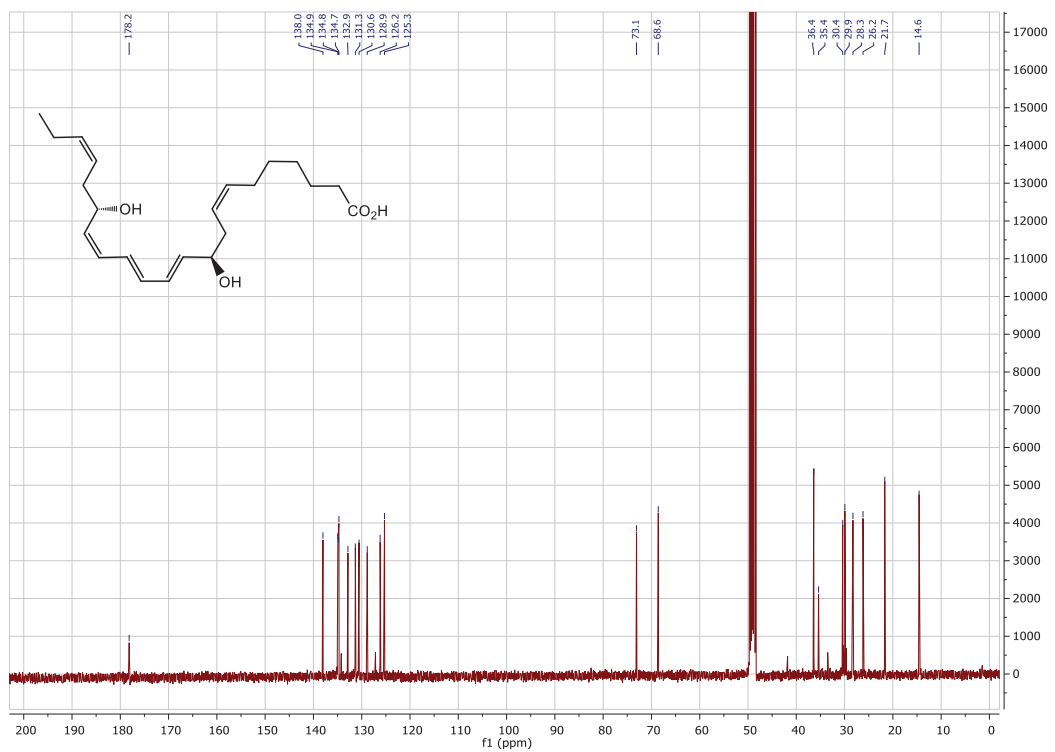
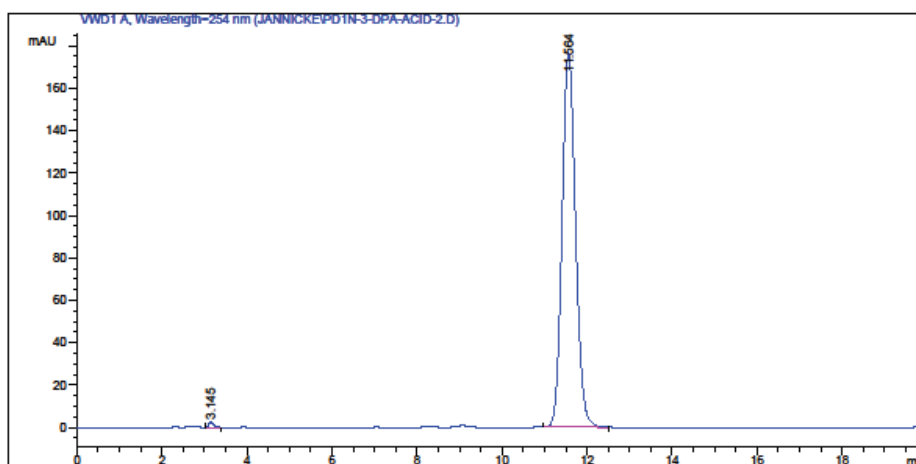


Figure 5.7 <sup>13</sup>C-NMR spectrum of PD1<sub>n-3</sub> DPA (36).

Data File C:\CHEM32\1\DATA\JANNICKE\PD1n-3-DPA-ACID-2.D  
Sample Name: PD1n-3-dpa-Acid-2

=====  
Acq. Operator : Jannicke  
Acq. Instrument : Instrument 1 Location : Vial 1  
Injection Date : 28.02.2020 11:11:23 Inj Volume : 10 µl  
Method : C:\CHEM32\1\METHODS\C18 ISOKRATISK.M  
Last changed : 28.02.2020 11:18:16 by Jannicke  
(modified after loading)  
Sample Info : PD1n-3 DPA final product  
MeOH/H2O/10mM formic acid 75:20:5



=====  
Area Percent Report  
=====

Sorted By : Signal  
Multiplier : 1.0000  
Dilution : 1.0000  
Use Multiplier & Dilution Factor with ISTDs

Signal 1: VWD1 A, Wavelength=254 nm

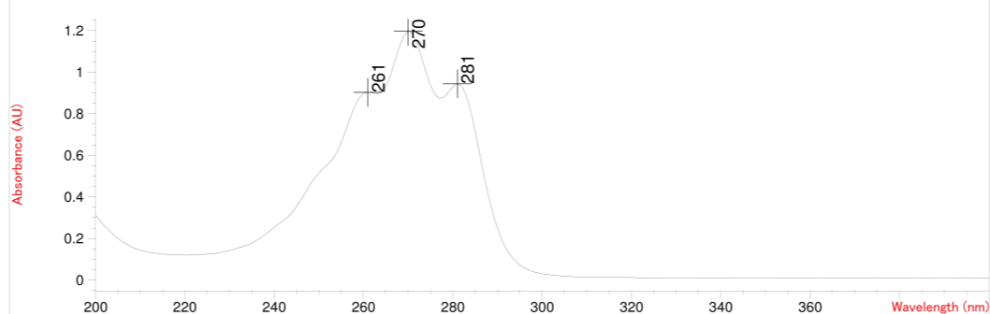
Peak #	RetTime [min]	Type	Width [min]	Area mAU	Area %	Height [mAU]	Area #
1	3.145	VB	0.1072	17.82408	0.4587	2.47783	
2	11.564	BB	0.3385	3868.19409	99.5413	176.65689	
Totals :				3886.01817		179.13472	

=====  
\*\*\* End of Report \*\*\*

Figure 5.8 HPLC chromatogram of PD1<sub>n</sub>-3 DPA (36).

Method file : <method not saved>  
 Information : Default Method  
 Data File : <data not saved>

Overlaid Spectra:



#	Name	Peaks (nm)	Abs (AU)	#	Name	Peaks (nm)	Abs (AU)
1		270.0	1.19730	1		261.0	0.90333
1		281.0	0.94471				

Figure 5.9 UV-Vis chromatogram of PD1<sub>n-3</sub> DPA (36).

## Elemental Analysis Report

Analysis Info		Acquisition Date		2/20/2020 10:48:50 AM	
Sample Name		Analysis Name	D:\Data\maxis2020\16506.d		
Method	ESI_pos_50_1500_os.m				
Acquisition Parameter					
Source Type	ESI	Ion Polarity	Positive	Set Nebulizer	0.4 Bar
Focus	Not active	Set Capillary	3500 V	Set Dry Heater	200 °C
Scan Begin	50 m/z	Set End Plate Offset	-300 V	Set Dry Gas	4.0 l/min
Scan End	1500 m/z	Set Charging Voltage	2000 V	Set Divert Valve	Waste
		Set Corona	0 nA	Set APCI Heater	0 °C

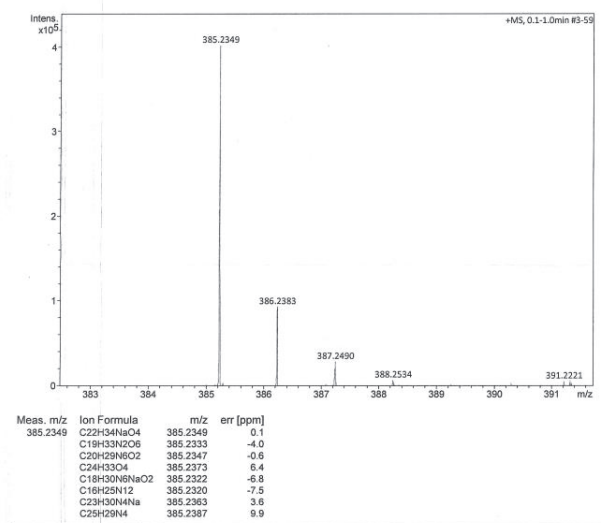


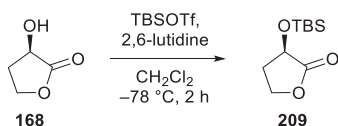
Figure 5.10 HRMS spectrum of PD1<sub>n-3</sub> DPA (36).

## References

1. Tungen, J. E.; Aursnes, M.; Dalli, J.; Arnardottir, H.; Serhan, C. N.; Hansen, T. V., *Chem. Eur. J.* **2014**, *20* (45), 14575.
2. Tungen, J. E.; Gerstmann, L.; Vik, A.; De Matteis, R.; Colas, R. A.; Dalli, J.; Chiang, N.; Serhan, C. N.; Kalesse, M.; Hansen, T.V, *Chemistry* **2019**, *25* (6), 1476.
3. Becher, J., *Org. Synth.* **1979**, *59*, 79.
4. Soullez, D.; Plé, G.; Duhamel, L., *J. Chem. Soc., Perkin Transactions I.* **1997**, (11), 1639.
5. Romero-Ortega, M.; Colby, D. A.; Olivo, H. F., *Tetrahedron Lett.* **2002**, *43*, 6439.
6. Corey, E. J.; Cho, H.; Rucker, C.; Hua, D. H., *Tetrahedron Lett.* **1981**, *22*, 3455.
7. Tello-Aburto, R.; Ochoa-Teran, A.; Olivo, H. F., *Tetrahedron Lett.* **2006**, *47*, 5915.
8. Aursnes, M.; Tungen, J. E.; Vik, A.; Colas, R.; Cheng, C. Y.; Dalli, J.; Serhan, C.N.; Hansen, T.V., *J. Nat. Prod.* **2014**, *77* (4), 910.
9. Boland, W.; Schroer, C. N.; Sieler, C. M.; Feigel, M. *Helv. Chim. Acta* **1987**, *70*, 1025.
10. Näf, F.; Decorzant, R.; Thommen, W.; Willhalm, B.; Ohloff, G. *Helv. Chim. Acta* **1975**, *58* (4), 1016.

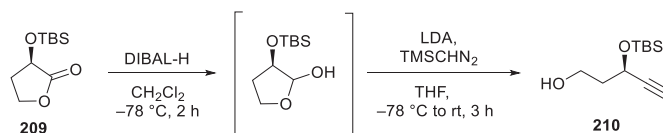
## Total synthesis of 17*R*-3-oxa PD1n-3 DPA (141)

### (*R*)-3-((*tert*-butyldimethylsilyl)oxy)dihydrofuran-2(3*H*)-one (209)



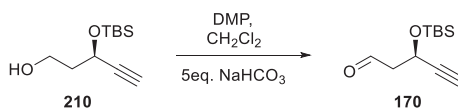
(*R*)-(+)- $\alpha$ -hydroxy- $\gamma$ -butyrolactone **168** (1.52 g, 14.9 mmol, 1.00 eq.) was dissolved in CH<sub>2</sub>Cl<sub>2</sub> (150 mL) under argon. The solution was cooled to -78 °C and added 2,6-lutidine (4.79 g, 44.7 mmol, 3.00 eq.) after stirring for ten minutes. Following an additional ten minutes, TBSOTf (4.25 g, 19.1 mmol, 1.28 eq.) was added dropwise. The reaction mixture was stirred at -78 °C until judged complete after 3 hours. Sat. aq. NH<sub>4</sub>Cl (100 mL) was added and the layers separated. The aq. layer was extracted with CH<sub>2</sub>Cl<sub>2</sub> (3  $\times$  50 mL) and the combined organic extract was dried (Na<sub>2</sub>SO<sub>4</sub>), filtered, and the solvent removed *in vacuo*. The residue was purified by column chromatography on silica gel (hexane/EtOAc, 9:1) to afford the title compound **209** as a clear oil. Yield: 2.98 g (93%); All spectroscopic and physical data were in agreement with those reported in the literature.<sup>1</sup>  $[\alpha]_D^{20} = +34.4$  (c = 1.1, CHCl<sub>3</sub>); <sup>1</sup>H NMR (400 MHz, CDCl<sub>3</sub>)  $\delta$  4.44 – 4.35 (m, 2H), 4.19 (td, *J* = 9.2, 6.4 Hz, 1H), 2.50 – 2.42 (m, 1H), 2.28 – 2.16 (m, 1H), 0.91 (s, 9H), 0.17 (s, 3H), 0.15 (s, 3H); <sup>13</sup>C NMR (101 MHz, CDCl<sub>3</sub>)  $\delta$  176.0, 68.4, 64.9, 32.5, 25.8(3C), 18.4, -4.5, -5.1; TLC (hexane/EtOAc, 9:1) *R<sub>f</sub>* = 0.24. HRMS (ESI): calculated for C<sub>10</sub>H<sub>20</sub>NaO<sub>3</sub>Si [*M*+Na]<sup>+</sup>: 239.1075, found: 239.1074.

**(R)-3-((tert-butyldimethylsilyloxy)pent-4-yn-1-ol (210)**



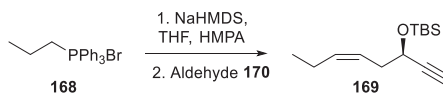
To a solution of TBS-lactone **209** (959 mg, 4.43 mmol, 1.00 eq.) in CH<sub>2</sub>Cl<sub>2</sub> (50 mL) it was added DIBAL-H (1.0 M in CH<sub>2</sub>Cl<sub>2</sub>, 6.2 mL, 6.2 mmol, 1.40 eq.) at -78 °C. The reaction mixture was stirred for 2 h at this temperature and then quenched by addition of MeOH (30 mL). The solution was poured into a sat. aq. solution of Rochelle salt (potassium sodium tartrate) (50 mL) and vigorously stirred for 3 h at rt. The layers were separated and the aq. layer was extracted with CH<sub>2</sub>Cl<sub>2</sub> (3 × 50 mL). The combined organic layers were washed with brine (100 mL), dried (Na<sub>2</sub>SO<sub>4</sub>), filtered, and the solvent removed *in vacuo* to yield the crude lactol. TLC (hexane/EtOAc 8:2, KMnO<sub>4</sub> stain) R<sub>f</sub> = 0.25. Next, TMSCHN<sub>2</sub> (2.0 M in Et<sub>2</sub>O, 2.7 mL, 5.32 mmol, 1.20 eq.) was added to a solution of LDA (1.0 M in hexane/THF, 10.6 mL, 10.6 mmol, 2.40 eq.) in THF (11 mL) at -78 °C, and the reaction mixture was stirred for 30 min at this temperature. The crude lactol in THF (13.8 mL) was carefully added and stirring was continued for 2 h. The reaction was warmed to rt, stirred for 30 min. and then quenched by careful addition of a sat. aq. solution of NH<sub>4</sub>Cl (30 mL). The layers were separated and the aq. layer was extracted with Et<sub>2</sub>O (3 × 30 mL). The combined organic extracts were washed with brine (40 mL), dried (Na<sub>2</sub>SO<sub>4</sub>), filtered, and the solvent removed *in vacuo*. Alcohol **210** was obtained after purification by column chromatography on silica gel (5-10% hexane/EtOAc) as a pale yellow oil. Yield: 643 mg (68% over the two steps). [α]<sub>D</sub><sup>20</sup> = +64.0 (c = 1.2, CHCl<sub>3</sub>); <sup>1</sup>H NMR (400 MHz, CDCl<sub>3</sub>) δ 4.64 (ddd, *J* = 6.3, 5.0, 2.1 Hz, 1H), 3.95 (ddd, *J* = 11.5, 7.8, 3.9 Hz, 1H), 3.79 (ddd, *J* = 11.1, 6.2, 4.2 Hz, 1H), 2.45 (d, *J* = 2.1 Hz, 1H), 2.11 (bs, 1H), 2.04 – 1.87 (m, 2H), 0.91 (s, 9H), 0.17 (s, 3H), 0.14 (s, 3H); <sup>13</sup>C NMR (101 MHz, CDCl<sub>3</sub>) δ 84.7, 73.3, 62.0, 60.1, 40.1, 25.9 (3C), 18.2, -4.5, -5.1; TLC (hexane/EtOAc 8:2, KMnO<sub>4</sub> stain) R<sub>f</sub> = 0.35; HRMS (ESI): calculated for C<sub>11</sub>H<sub>22</sub>NaO<sub>2</sub>Si [M+Na]<sup>+</sup>: 237.1281, found: 237.1281.

**(R)-3-((tert-butyldimethylsilyloxy)pent-4-ynal (170)**



Alcohol **210** (616 mg, 2.87 mmol, 1.00 eq.) dissolved in dry CH<sub>2</sub>Cl<sub>2</sub> (25 mL) was added Dess-Martin periodinane (1.54 g, 3.63 mmol, 1.26 eq.) and NaHCO<sub>3</sub> (s) (1.22 g, 14.0 mmol, 4.87 eq.). After stirring for 4 hours, hexane was added and the resulting precipitate was removed through a pad of Celite<sup>®</sup>. The mixture was transferred to a separatory funnel and washed with sat. aq. Na<sub>2</sub>S<sub>2</sub>O<sub>3</sub> (16 mL). The layers were separated and the aq. layer was extracted with Et<sub>2</sub>O (3 × 10 mL). The combined organic extracts were washed with brine (10 mL) dried (Na<sub>2</sub>SO<sub>4</sub>) and concentrated *in vacuo*. The crude product was passed through a silica plug with hexane/EtOAc 8:2 as eluent to afford the title compound **170** as a colorless oil. Yield: 565 mg (83%).  $[\alpha]_D^{25} = +17.0$  (c = 0.10); <sup>1</sup>H NMR (400 MHz, CDCl<sub>3</sub>) δ 9.82 (t, *J* = 2.1 Hz, 1H), 4.86 (ddd, *J* = 6.9, 4.9, 2.2 Hz, 1H), 2.80 (ddd, *J* = 16.4, 6.8, 2.2 Hz, 1H), 2.70 (ddd, *J* = 16.4, 4.9, 2.0 Hz, 1H), 2.49 (d, *J* = 2.1 Hz, 1H), 0.88 (s, 9H), 0.17 (s, 3H), 0.13 (s, 3H); <sup>13</sup>C NMR (101 MHz, CDCl<sub>3</sub>) δ 200.2, 83.9, 73.9, 58.2, 51.5, 25.8 (3C), 18.2, -4.5, -5.1; TLC (hexane/EtOAc 95:5, KMnO<sub>4</sub> stain) R<sub>f</sub> = 0.35; HRMS (ESI): calculated for C<sub>11</sub>H<sub>20</sub>NaO<sub>2</sub>Si [*M*+Na]<sup>+</sup>: 235.1125, found: 235.1125.

**(R,Z)-tert-butyldimethyl(oct-5-en-1-yn-3-yloxy)silane (169)**

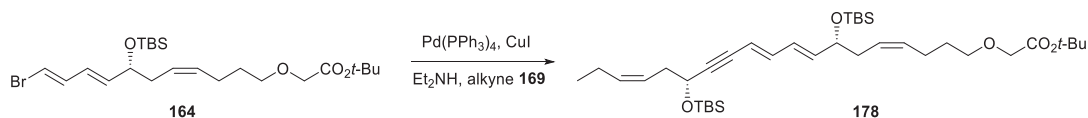


To a solution of propyltriphenylphosphonium bromide **168** (903 mg, 2.34 mmol, 1.08 eq.) in THF (40 mL) it was added hexamethylphosphoramide (HMPA) (3.0 mL) and NaHMDS (0.6 M in toluene, 3.6 mL, 2.16 mmol, 1.00 eq.) at -78 °C. The reaction mixture was warmed to rt, stirred for 10 min, and then re-cooled to -78 °C. Aldehyde **170** (490 mg, 2.31 mmol 0.95 eq.) in THF (7.0 mL) was added dropwise, and the reaction was allowed to warm to rt overnight and stirred for



20 h. The reaction was quenched by addition of a phosphate buffer solution (pH = 7.0, 25 mL). The phases were separated and the aq. layer was extracted with Et<sub>2</sub>O (3 × 10 mL). The combined organic layers were washed with brine (20 mL), dried (MgSO<sub>4</sub>), filtered, and the solvent removed *in vacuo*. Alkene **169** was obtained after purification by column chromatography (hexane - 1% EtOAc in hexane) as a yellow oil. Yield: 384 mg (75%).  $[\alpha]_D^{25} = +25.0$  (c = 0.30, CHCl<sub>3</sub>); <sup>1</sup>H NMR (400 MHz, CDCl<sub>3</sub>) δ 5.58 – 5.36 (m, 2H), 4.34 (td, *J* = 6.6, 2.1 Hz, 1H), 2.44 (t, *J* = 6.8 Hz, 2H), 2.38 (d, *J* = 2.1 Hz, 1H), 2.07 (p, *J* = 7.4 Hz, 2H), 0.97 (t, *J* = 7.5 Hz, 3H), 0.91 (s, 9H), 0.13 (s, 3H), 0.11 (s, 3H); <sup>13</sup>C NMR (101 MHz, CDCl<sub>3</sub>) δ 134.6, 123.8, 85.6, 72.2, 63.0, 36.7, 25.9, 21.0, 18.4, 14.3, -4.6, -4.9; TLC (hexane, KMnO<sub>4</sub> stain) R<sub>f</sub> = 0.25; HRMS (ESI): calculated for C<sub>14</sub>H<sub>26</sub>NaOSi [*M*+Na]<sup>+</sup>: 261.1645, found: 261.1645.

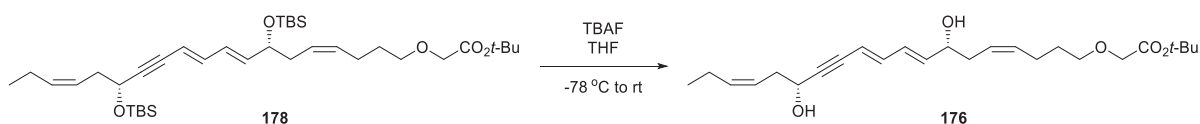
***tert*-butyl 2-(((4*Z*,7*R*,8*E*,10*E*,14*R*,16*Z*)-7,14-bis((*tert*-butyldimethylsilyl)oxy)nonadeca-4,8,10,16-tetraen-12-yn-1-yl)oxy)acetate (**178**)**



Vinyl bromide **164** (151 mg, 0.308 mmol, 1.00 eq.) was added Pd(PPh<sub>3</sub>)<sub>4</sub> (11.0 mg, 9.52 μmol, 3.00 mol%) and the flask evacuated and filled with argon. Et<sub>2</sub>NH (0.60 mL) and benzene (0.25 mL) were added, and the reaction was stirred for 45 min in the dark. CuI (3.00 mg, 0.0158 mmol, 5 mol%) dissolved in a minimal amount of Et<sub>2</sub>NH was added, followed by dropwise addition of alkyne **169** (95.0 mg, 0.398 mmol, 1.30 eq.) in Et<sub>2</sub>NH (1.0 mL). After 26 h of stirring at ambient temperature, the reaction was quenched with sat. aq. NH<sub>4</sub>Cl (10 mL). Et<sub>2</sub>O (10 mL) was added, and the phases were separated. The aq. phase was extracted with Et<sub>2</sub>O (2 × 10 mL), and the combined organic layers were dried (Na<sub>2</sub>SO<sub>4</sub>), filtered, and concentrated *in vacuo*. The crude product was purified by column chromatography on silica (hexane/EtOAc, 98:2) to afford the title compound **178** as a clear oil. Yield: 172 mg (86%).  $[\alpha]_D^{20} = +9.14$  (c = 1.3, CHCl<sub>3</sub>); <sup>1</sup>H NMR (400 MHz, CDCl<sub>3</sub>) δ 6.50 (dd, *J* = 15.5, 10.9 Hz, 1H), 6.18 (dd, *J* = 15.2, 10.9 Hz, 1H), 5.75 (dd, *J* = 15.2, 6.0 Hz, 1H), 5.61 – 5.33 (m, 5H), 4.46 (td, *J* = 6.5, 1.5 Hz, 1H), 4.17 (q, *J* = 6.0 Hz, 1H),

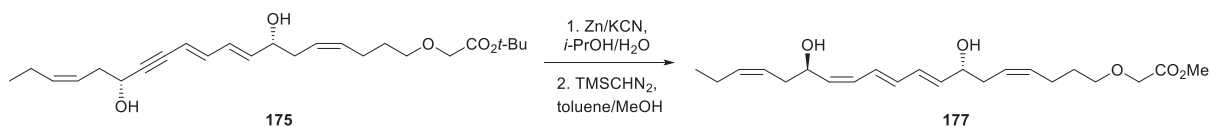
3.93 (s, 2H), 3.50 (t,  $J = 6.6$  Hz, 2H), 2.43 (t,  $J = 6.8$  Hz, 2H), 2.33 – 2.17 (m, 2H), 2.15 – 2.00 (m, 4H), 1.66 (p,  $J = 6.7$  Hz, 2H), 1.48 (s, 9H), 0.96 (t,  $J = 7.5$ , 3H), 0.9 (s, 9H), 0.88 (s, 9H), 0.13 (s, 3H), 0.11 (s, 3H), 0.04 (s, 3H), 0.02 (s, 3H);  $^{13}\text{C}$  NMR (101 MHz,  $\text{CDCl}_3$ )  $\delta$  169.2, 141.2, 139.3, 134.4, 131.2, 128.7, 125.9, 124.1, 110.7, 93.4, 83.5, 81.6, 72.9, 71.2, 69.0, 63.7, 36.8, 36.3, 29.6, 28.3(3C), 26.0(3C), 26.0(3C), 24.1, 20.9, 18.5, 18.4, 14.4, -4.3(2C), -4.6, -4.8; TLC (hexane/EtOAc 95:5, visualized by UV and  $\text{KMnO}_4$ -stain)  $R_f = 0.34$ ; HRMS (ESI): calculated for  $\text{C}_{37}\text{H}_{66}\text{NaO}_5\text{Si}_2$  [ $M+\text{Na}$ ] $^+$ : 669.4341, found: 669.4340.

***tert*-butyl 2-(((4*Z*,7*R*,8*E*,10*E*,14*R*,16*Z*)-7,14-dihydroxynonadeca-4,8,10,16-tetraen-12-yn-1-yl)oxy)acetate (**176**)**



TBAF (1.0 M in THF, 1.3 mL, 1.30 mmol, 5.26 eq.) was added to a solution of silyl ether **178** (160 mg, 0.247 mmol, 1.00 eq.) in THF (2.5 mL) at  $-78$  °C. The reaction was stirred for 21 h before it was quenched with phosphate buffer (pH = 7.0, 4.0 mL). Brine (15 mL) and EtOAc (15 mL) were added, and the phases were separated. The aq. phase was extracted with EtOAc ( $2 \times 10$  mL), and the combined organic layer was dried ( $\text{Na}_2\text{SO}_4$ ) before being concentrated *in vacuo*. The crude product was purified by column chromatography on silica gel (hexane/EtOAc, 7:3) to afford diol **176** as a clear oil. Yield: 93 mg (90%).  $[\alpha]_D^{20} = -30.0$  ( $c = 0.39$ , MeOH);  $^1\text{H}$  NMR (400 MHz, MeOD)  $\delta$  6.54 (dd,  $J = 15.5, 10.8$  Hz, 1H), 6.28 (dd,  $J = 15.3, 10.9$  Hz, 1H), 5.82 (dd,  $J = 15.2, 6.3$  Hz, 1H), 5.66 (d,  $J = 15.6$  Hz, 1H), 5.57 – 5.33 (m, 4H), 4.40 (td,  $J = 6.8, 1.67$  Hz, 1H), 4.13 (q,  $J = 6.5$  Hz, 1H), 3.96 (s, 2H), 3.50 (t,  $J = 6.3$  Hz, 2H), 2.49 – 2.38 (m, 2H), 2.35 – 2.26 (m, 2H), 2.19 – 2.00 (m, 4H), 1.68 – 1.59 (m, 2H), 1.48 (s, 9H), 0.98 (t,  $J = 7.5$  Hz, 3H);  $^{13}\text{C}$  NMR (101 MHz, MeOD)  $\delta$  171.7, 142.5, 139.9, 135.3, 132.3, 130.3, 126.7, 124.7, 111.7, 93.8, 84.3, 82.7, 72.8, 72.0, 69.6, 63.3, 36.9, 36.2, 30.5, 28.4(3C), 24.9, 21.7, 14.6; TLC (hexane/EtOAc 7:3, visualized by UV and  $\text{KMnO}_4$ -stain)  $R_f = 0.25$ ; HRMS (ESI): calculated for  $\text{C}_{25}\text{H}_{38}\text{NaO}_5$  [ $M+\text{Na}$ ] $^+$ : 441.2611, found: 441.2611.

**Methyl 2-(((4Z,7R,8E,10E,12Z,14R,16Z)-7,14-dihydroxynonadeca-4,8,10,12,16-pentaen-1-yl)oxy)acetate (177)**



Compound **177** was prepared by following the protocol reported by Näf and coworkers.<sup>2</sup> A mixture of alkyne **175** (35.0 mg, 83.6  $\mu$ mol, 1.00 eq.), zinc powder (1.19 g, 18.2 mmol, 218 eq.) and potassium cyanide (77.0 mg, 1.18 mmol, 14.1 eq.) was added a solution of *i*-PrOH/H<sub>2</sub>O (3.8 mL 1:1, pH = 7.0), and stirred at ambient temperature under protection of argon in the dark. After stirring for 26 h, the reaction mixture was filtered through a pad of Celite<sup>®</sup> and the pad washed with EtOAc (8.0 mL). Sat. aq. NH<sub>4</sub>Cl (8.0 mL) was added to the filtrate and the phases were separated. The aq. phase was extracted with EtOAc (3  $\times$  6.0 mL), and the combined organic layer evaporated, but not to dryness. The crude product was immediately added to a solvent mixture of toluene/MeOH (3:2, 1.5 mL). Next, TMS-diazomethane (2.0 M in Et<sub>2</sub>O, 0.10 mL, 1.30 eq.) was dropwise added under rapid stirring until the yellow color persisted. After strring for 45 min, the reaction was quenched with sat. aq. NH<sub>4</sub>Cl (8.0 mL). The layers were separated and the aq. phase extracted with Et<sub>2</sub>O (3  $\times$  5.0 mL). The combined organic layer was evaporated, and the residue was purified by column chromatography on silica gel (hexane/EtOAc, 4:6 and drops of MeOH) to afford methyl ester **177** as a clear oil. Yield: 18 mg (56% over the two steps);  $[\alpha]_D^{20} = -12.3$  ( $c = 0.065$ , MeOH); <sup>1</sup>H NMR (600 MHz, MeOD)  $\delta$  6.52 (dd,  $J = 13.5, 11.5$  Hz, 1H), 6.31 – 6.20 (m, 2H), 6.07 (t,  $J = 11.4$  Hz, 1H), 5.75 (dd,  $J = 14.5, 6.5$  Hz, 1H), 5.51 – 5.29 (m, 5H), 4.58 – 4.52 (m, 1H), 4.13 (q,  $J = 6.5$  Hz, 1H), 4.09 (s, 2H), 3.73 (s, 3H), 3.52 (t,  $J = 6.4$  Hz, 2H), 2.40 – 2.25 (m, 3H), 2.23 – 2.17 (m, 1H), 2.17 – 2.12 (m, 2H), 2.06 (pd,  $J = 7.5, 1.6$  Hz, 2H), 1.65 (p,  $J = 6.5$  Hz, 2H), 0.97 (t,  $J = 7.5$  Hz, 3H); <sup>13</sup>C NMR (151 MHz, MeOD)  $\delta$  172.8, 138.0, 134.9, 134.8, 134.7, 132.1, 131.4, 130.5, 128.9, 126.8, 125.3, 73.1, 72.1, 68.8, 68.6, 52.2, 36.4, 36.3, 30.4, 24.8, 21.7, 14.6; TLC (hexane/EtOAc 4:6, visualized by UV and KMnO<sub>4</sub>-stain)  $R_f = 0.40$ ; HRMS (ESI): calculated for C<sub>22</sub>H<sub>34</sub>NaO<sub>5</sub> [ $M+Na$ ]<sup>+</sup>: 401.2298, found: 401.2298; UV-VIS:  $\lambda_{max}$  (MeOH) = 261, 271, 282 nm. The purity (>97%) was determined by HPLC analysis (Eclipse XDB-C18, MeOH/H<sub>2</sub>O, 65:35, 1.0 mL/min);  $t_r = 18.6$ .

## References

1. Mohapatra, D. K.; Umamaheshwar, G.; Rao, M. M.; Umadevi, D.; Yadav, J. S., *R. Soc. Chem.* **2014**, *4* (16), 8335.
2. Näf, F.; Decorzant, R.; Thommen, W.; Willhalm, B.; Ohloff, G. *Helv. Chim. Acta* **1975**, *58*, 1016.

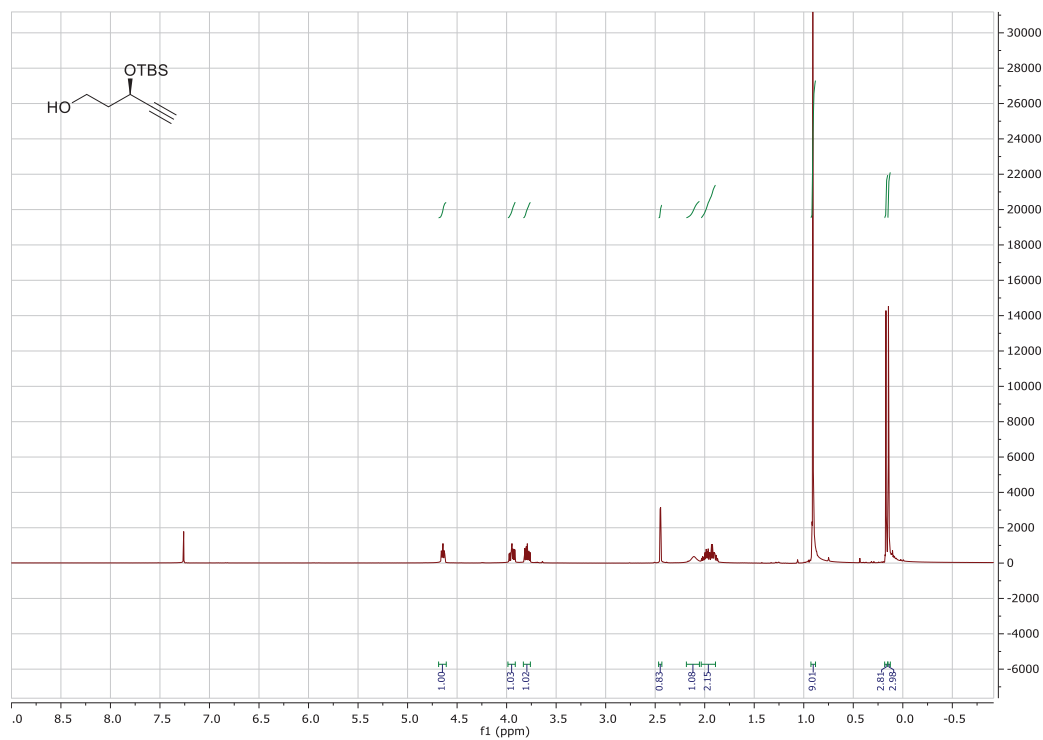


Figure 5.11 <sup>1</sup>H-NMR spectrum of compound 210.

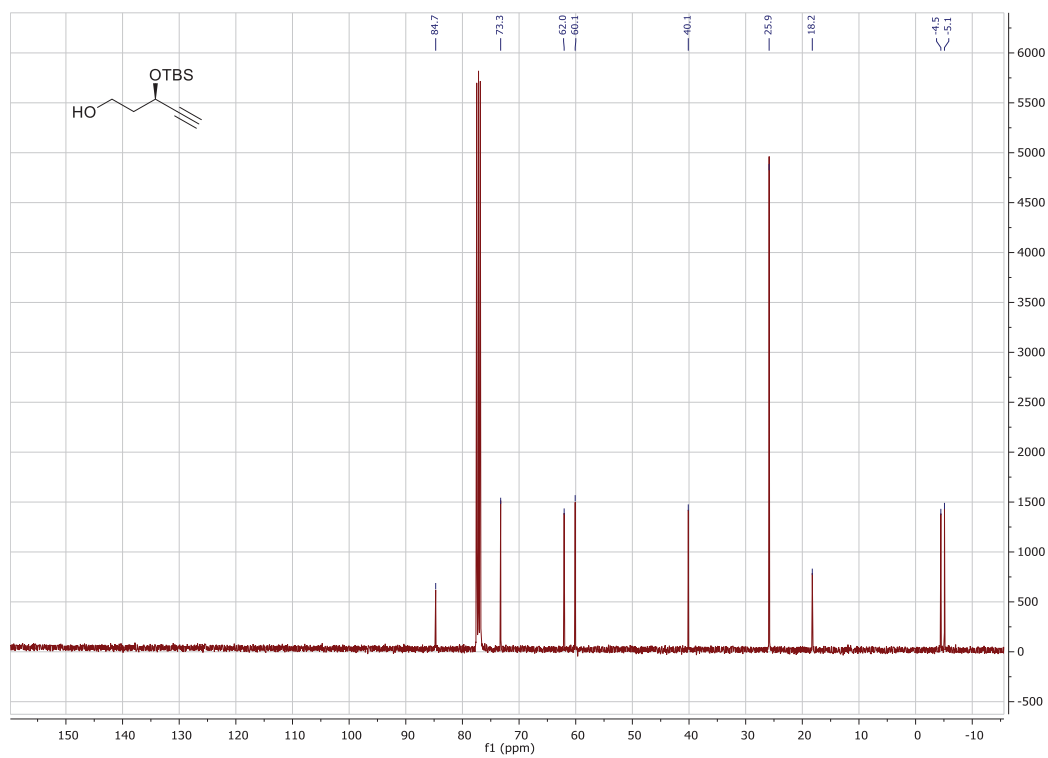
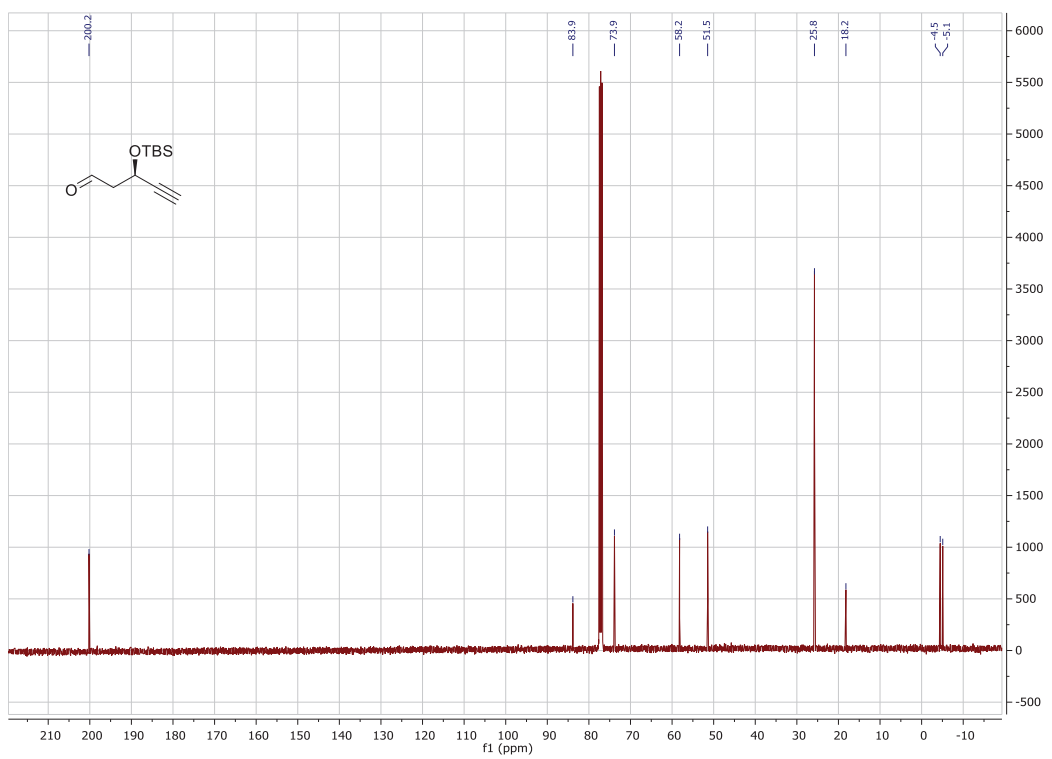
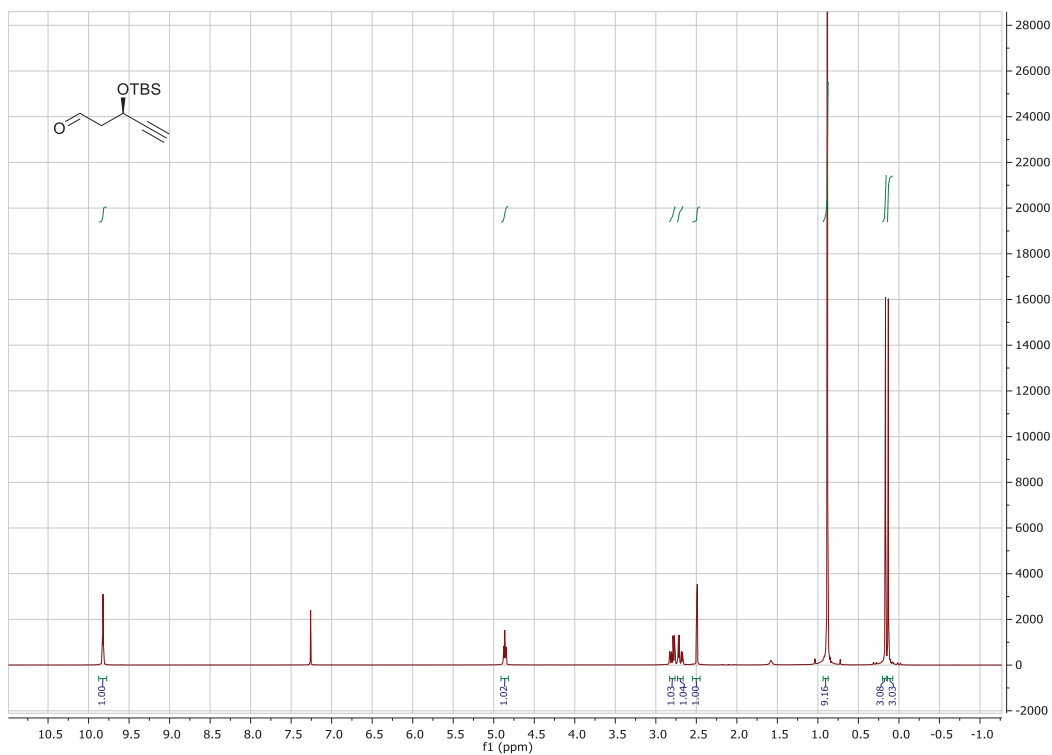


Figure 5.12 <sup>13</sup>C-NMR spectrum of compound 210.



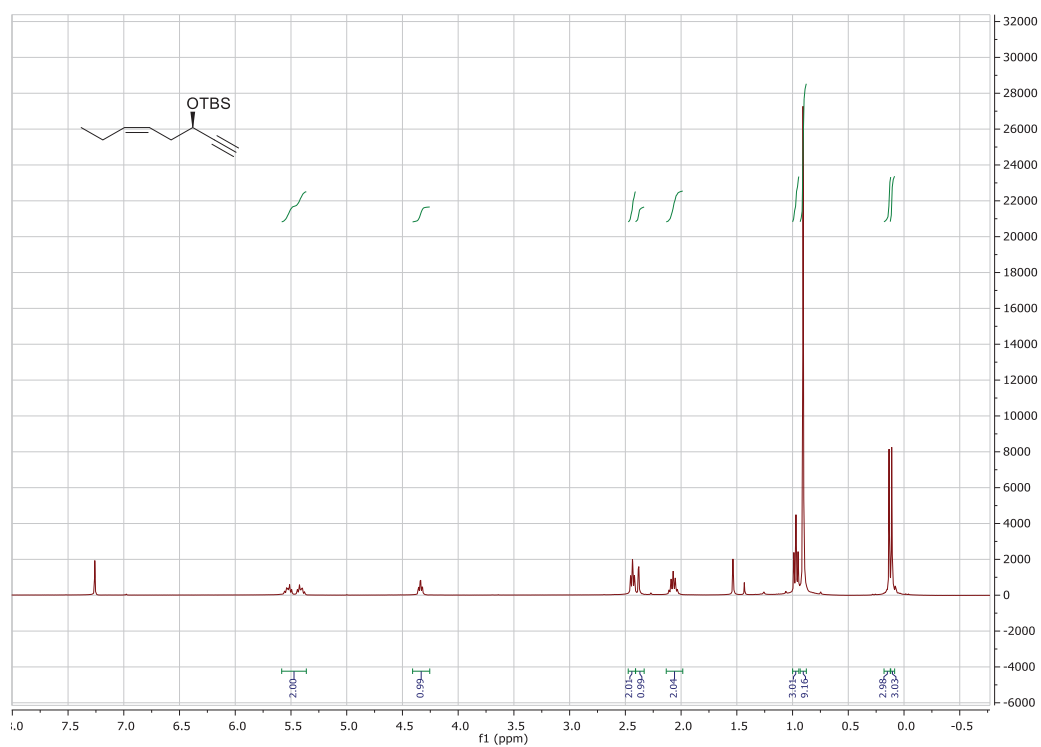


Figure 5.15 <sup>1</sup>H-NMR spectrum of compound 169.

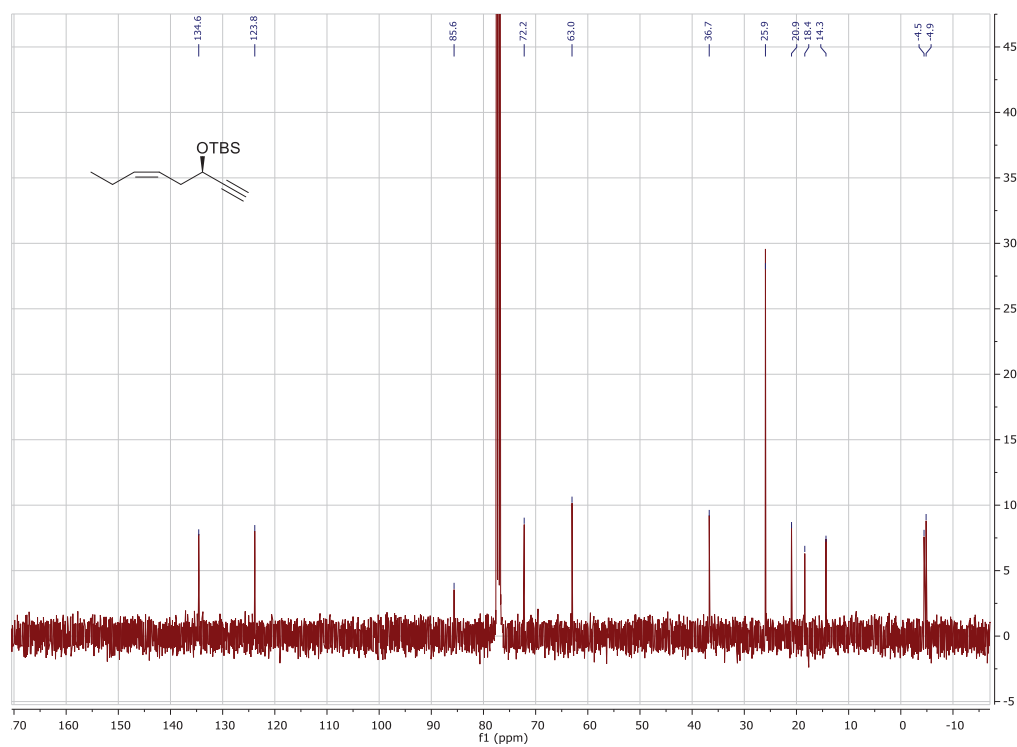


Figure 5.16 <sup>13</sup>C-NMR spectrum of compound 169.

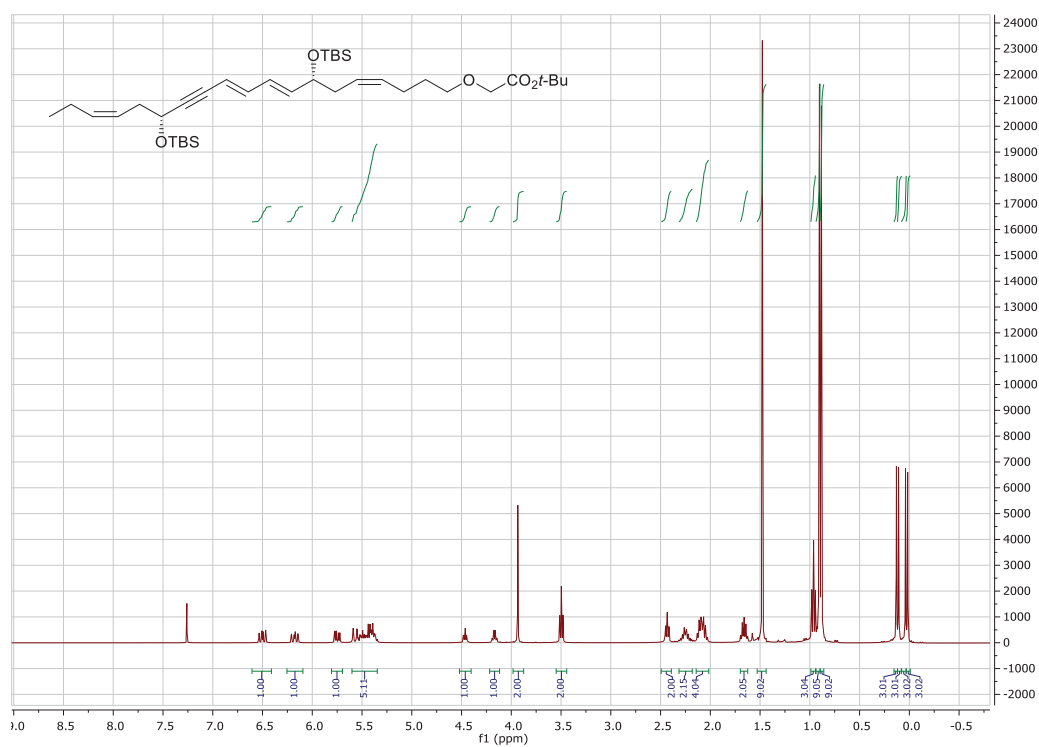


Figure 5.17 <sup>1</sup>H-NMR spectrum of compound 178.

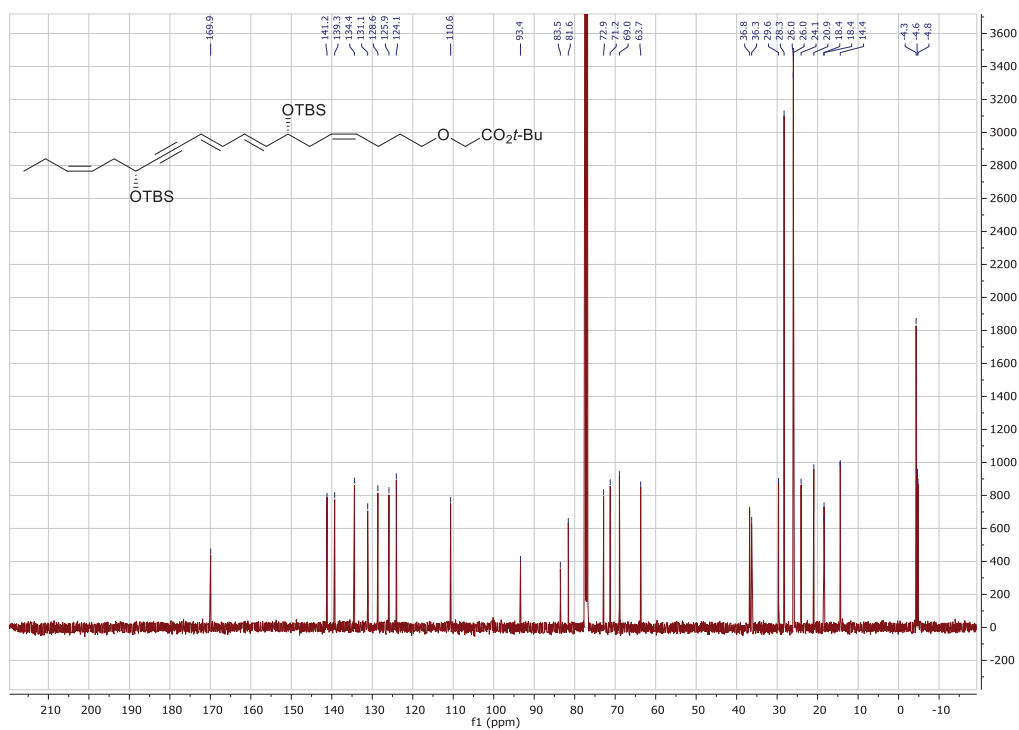


Figure 5.18 <sup>13</sup>C-NMR spectrum of compound 178.



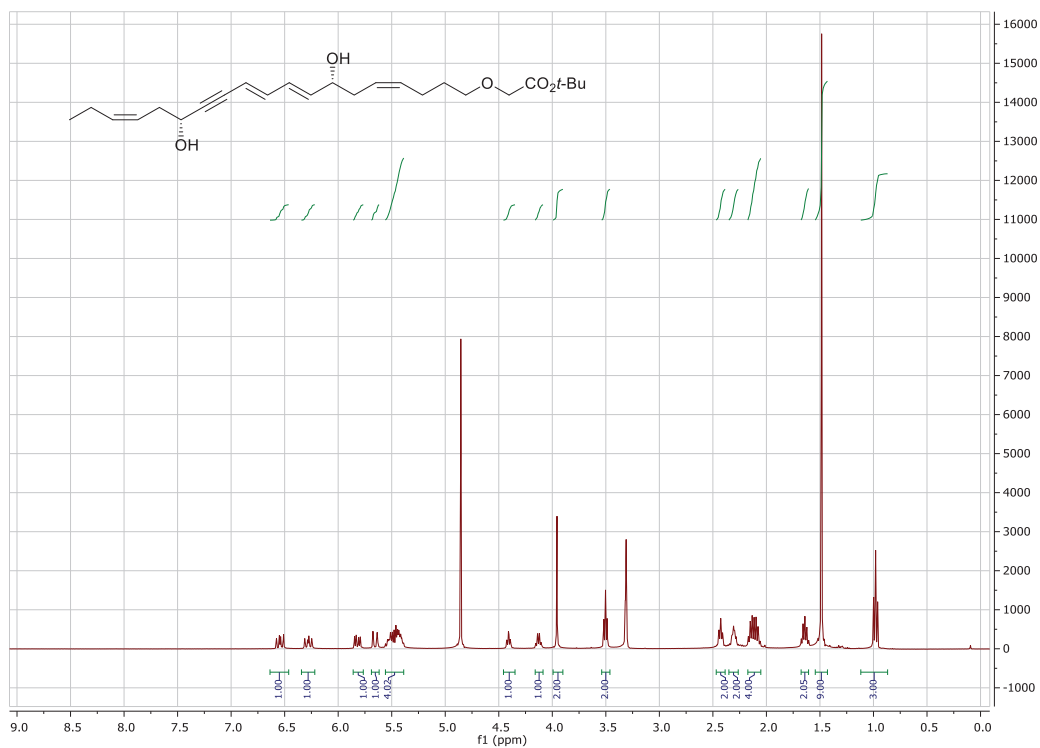


Figure 5.19 <sup>1</sup>H-NMR spectrum of compound 176.

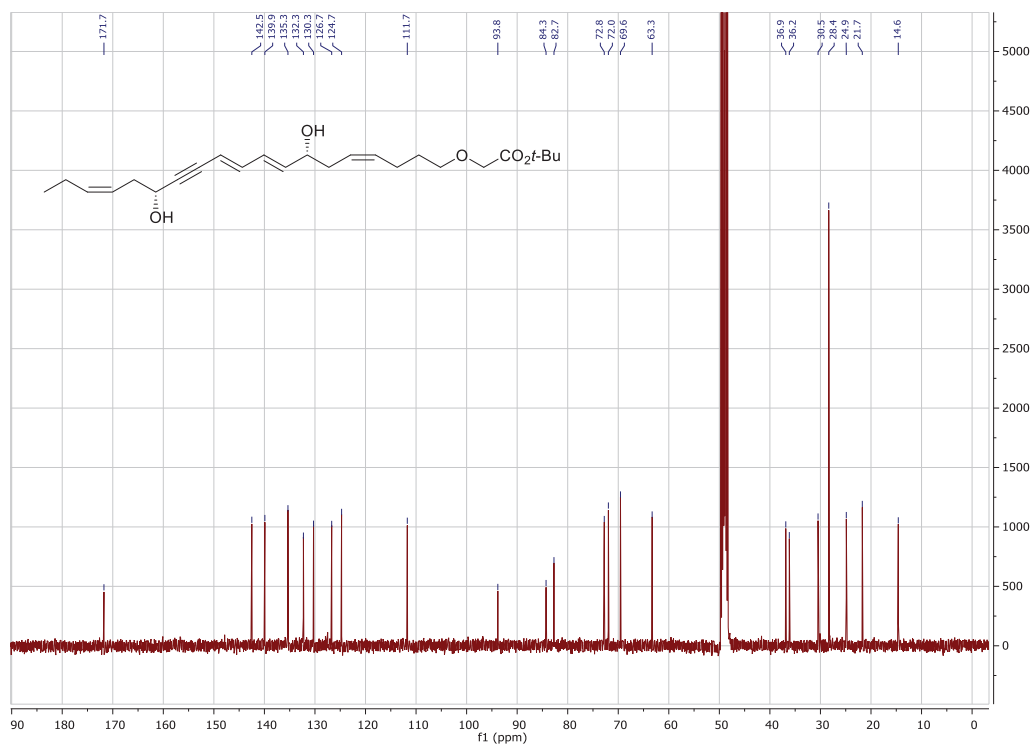


Figure 5.20 <sup>13</sup>C-NMR spectrum of compound 176.

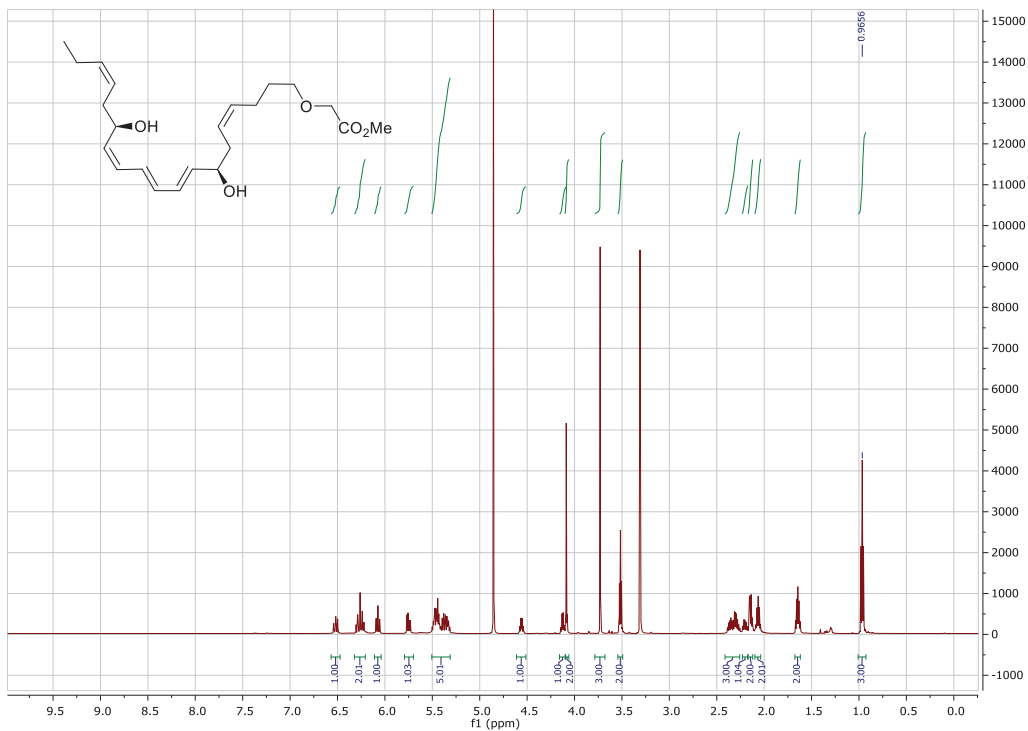


Figure 5.21 <sup>1</sup>H-NMR spectrum of compound 177.

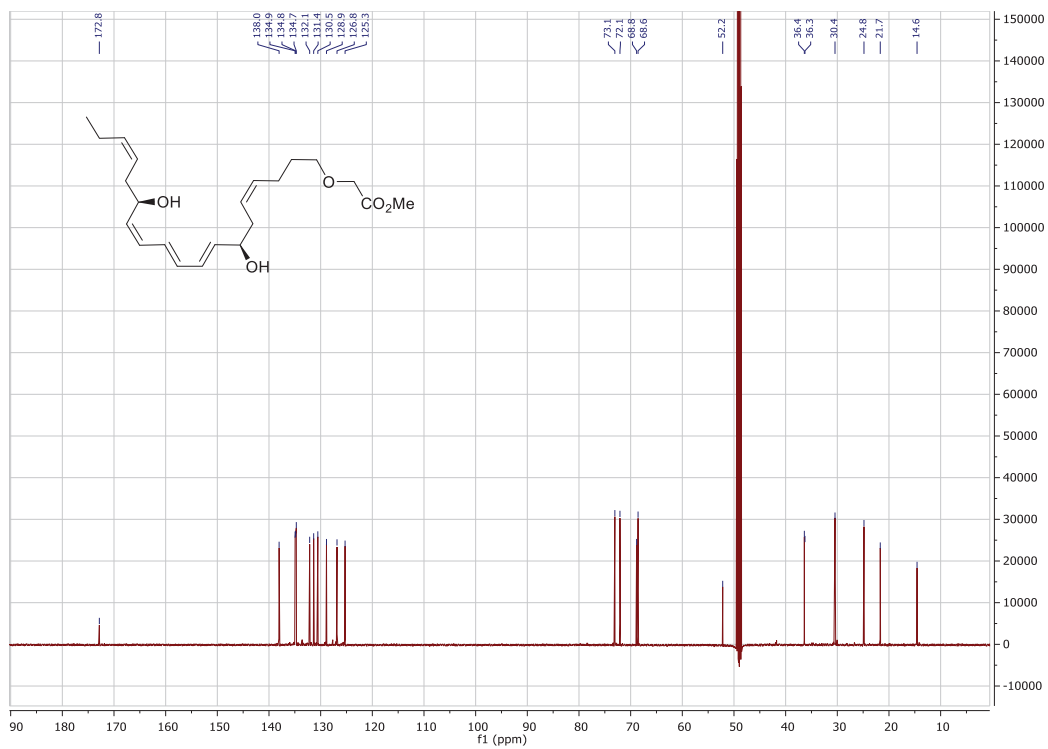


Figure 5.22 <sup>13</sup>C-NMR spectrum of compound 177.

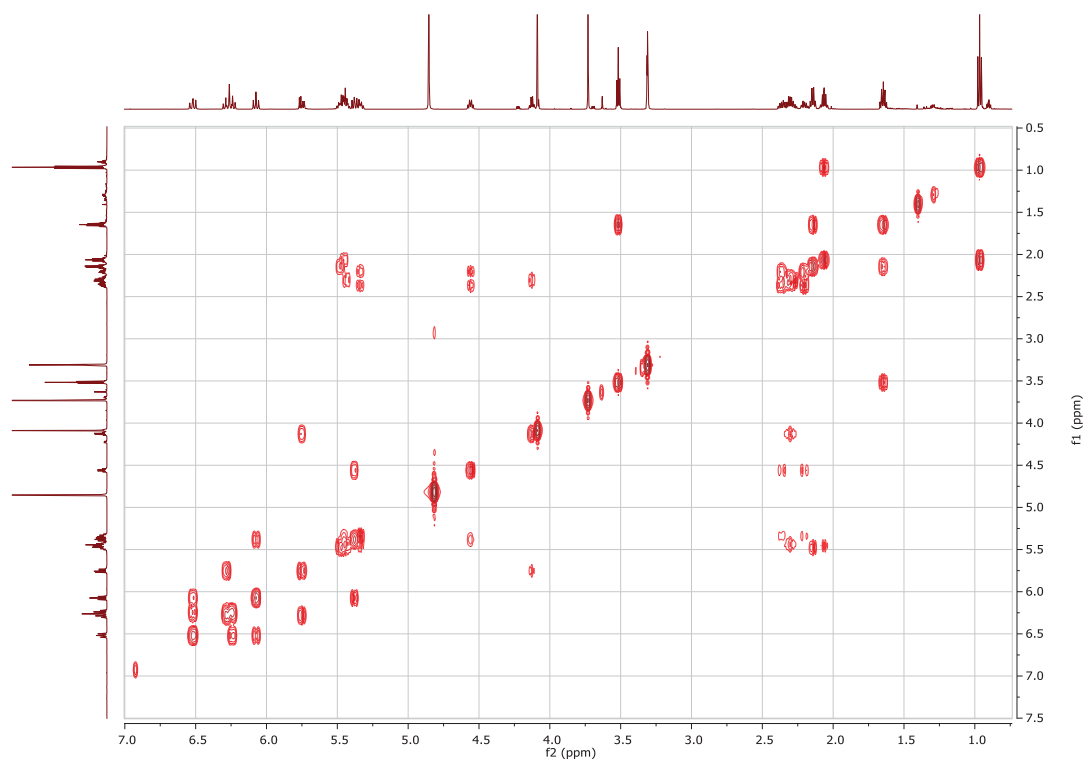


Figure 5.23 COSY spectrum of compound 177.

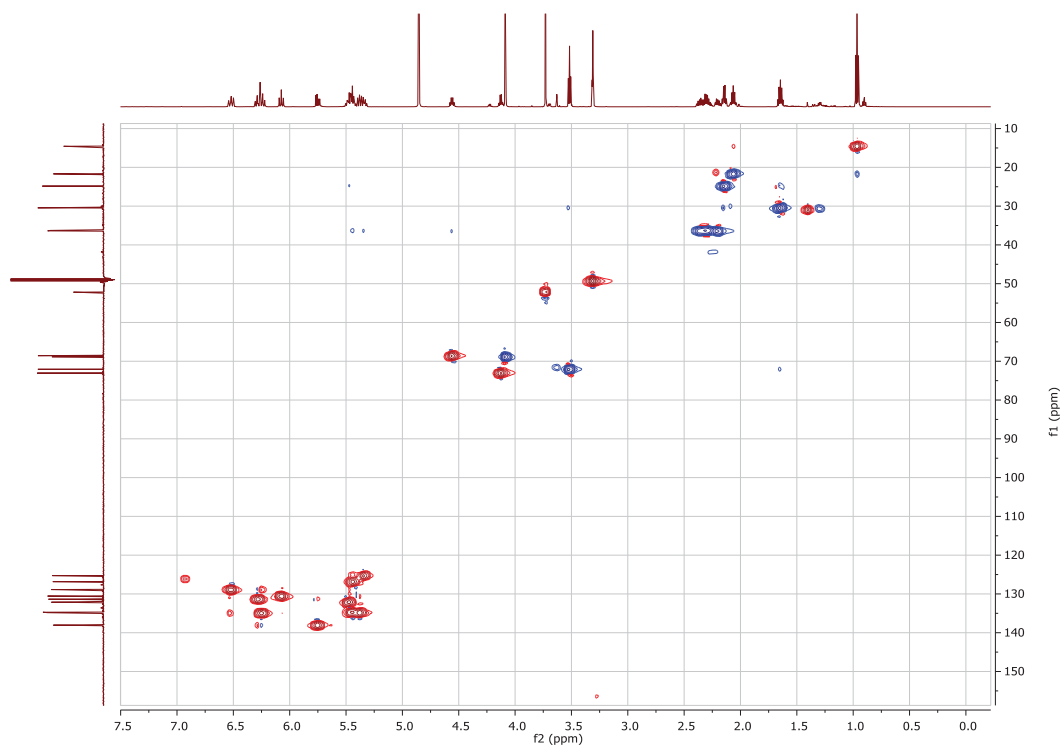
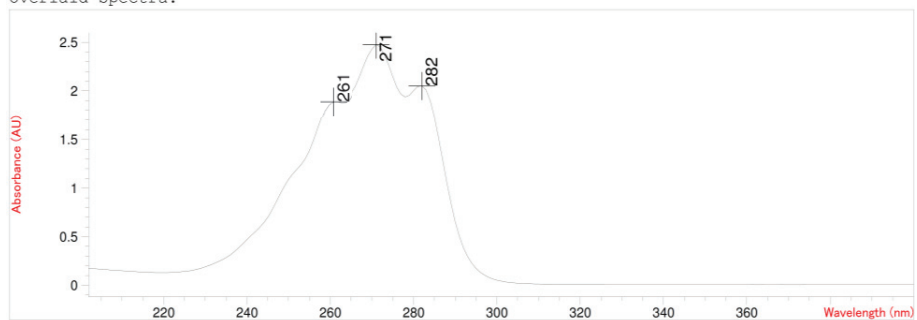


Figure 5.24 HSQC spectrum of compound 177.



Method file : <method not saved>  
 Information : Default Method  
 Data File : <data not saved>

Overlaid Spectra:



#	Name	Peaks (nm)	Abs (AU)	#	Name	Peaks (nm)	Abs (AU)
1		271.0	2.47600	1		***	***
1		282.0	2.05050	1		***	***

**Figure 5.26** UV-Vis chromatogram of 17R-3-oxa-PD1<sub>n-3</sub> DPA methyl ester (177).

## Incubation studies with 3-oxa n-3 DPA (182)

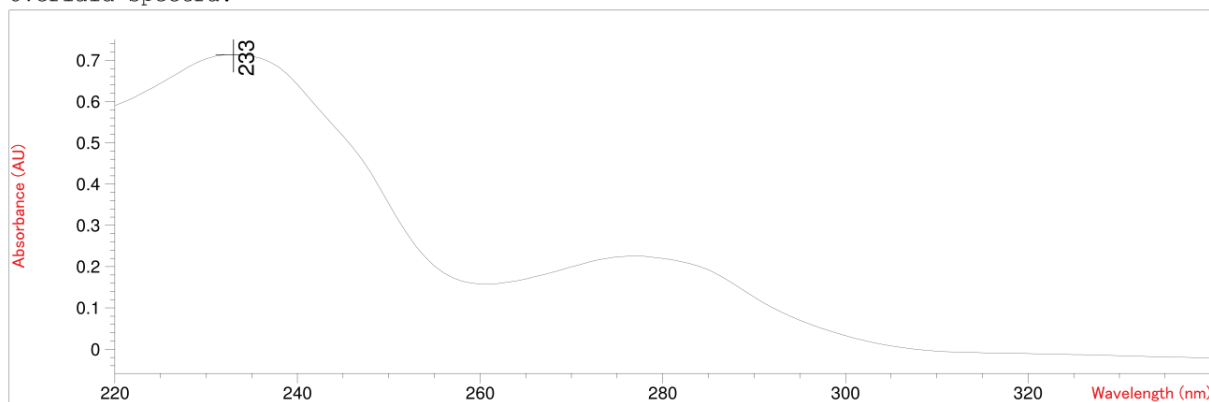
In three parallels, 3-oxa n-3 DPA (**182**, 167  $\mu\text{g}$ ) was incubated with soybean 15-LOX (borate buffer, 4  $^{\circ}\text{C}$ , pH 9.0, 167  $\mu\text{g}/\text{mL}$ ). After 45 minutes, the reaction was quenched using 2 volumes of ice cold methanol with sodium borohydride (0.01 M), and the solution was acidified with 2.5% aq. acetic acid to pH 2-3. The aq. phase was extracted with  $\text{Et}_2\text{O}$  ( $10 \times 3.0 \text{ mL}$ ), and the combined etheric layers washed with water ( $5 \times 5.0 \text{ mL}$ ), dried ( $\text{Na}_2\text{SO}_4$ ), filtered, and the solvent evaporated. The product was dissolved in methanol and subjected to UV-Vis and HRMS analyses. UV (MeOH)  $\lambda_{\text{max}}$  233-237 nm; HRMS (ESI): calculated for  $\text{C}_{21}\text{H}_{31}\text{NaO}_4$   $[M+\text{Na}]^+$ : 347.2228, found: 347.2227.

=====  
Spectrum/Peak Report

Date 3/9/2020 Time 15:58:49 Page 1 of 1  
=====

Method file : <method not saved>  
Information : Default Method  
Data File : <data not saved>

Overlaid Spectra:



#	Name	Peaks (nm)	Abs (AU)
1		233.0	0.71396

**Figure 5.27** UV-Vis chromatogram of 17-OH-3-oxa DPA (**183**).

## Elemental Analysis Report

**Analysis Info**  
Sample Name  
Method

Acquisition Date 3/11/2020 8:03:32 AM  
Analysis Name D:\Data\maxis2020\16571.d

ESI\_neg\_50\_1500\_os.m

### Acquisition Parameter

Source Type	ESI	Ion Polarity	Negative	Set Nebulizer	0.4 Bar
Focus	Not active	Set Capillary	3500 V	Set Dry Heater	200 °C
Scan Begin	50 m/z	Set End Plate Offset	-500 V	Set Dry Gas	4.0 l/min
Scan End	1500 m/z	Set Charging Voltage	0 V	Set Divert Valve	Source
		Set Corona	0 nA	Set APCI Heater	0 °C

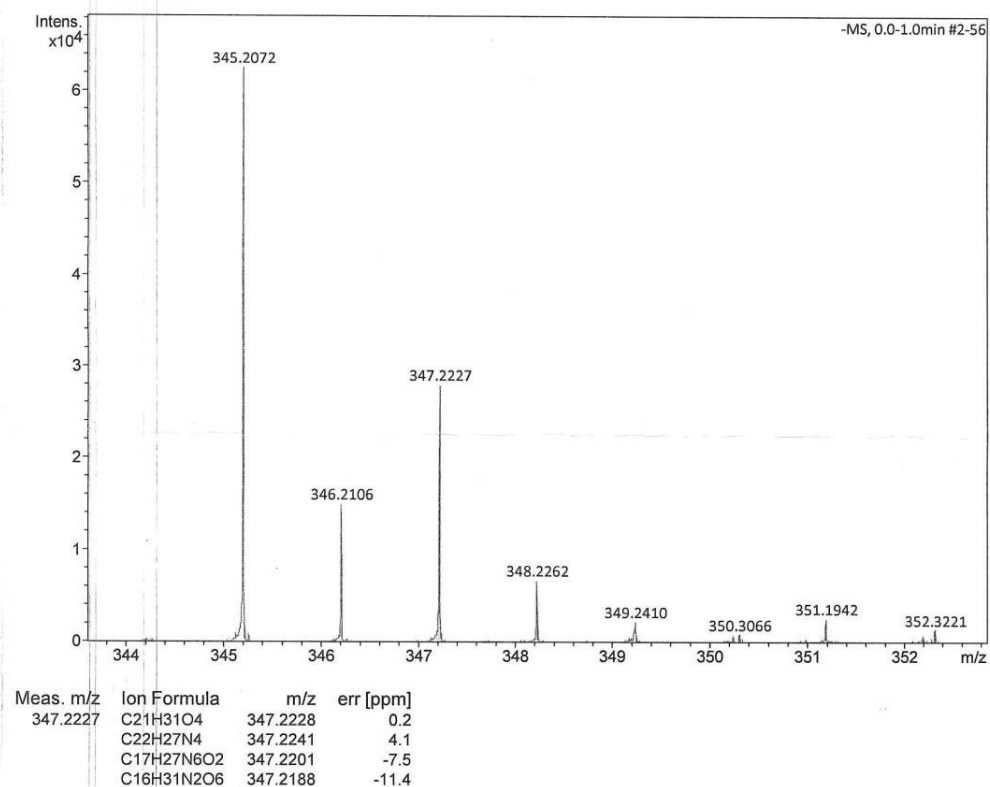


Figure 5.28 HRMS spectra of 17-OH-3-oxa DPA (183).





## Appendix



**Paper I:**

*Synthesis, Structural Confirmation, and Biosynthesis of 22-OH-PDI<sub>n-3</sub> DPA*



Jannicke Irina Nesman, Karoline Gangestad Primdahl, Jørn Eivind Tungen, Fransesco Palmas, Jesmond Dalli and Trond Vidar Hansen.

*Molecules*, **2019**, *24* (18), 3228-3240.



Article

# Synthesis, Structural Confirmation, and Biosynthesis of 22-OH-PD1<sub>n-3</sub> DPA<sup>†</sup>

Jannicke Irina Nesman<sup>1</sup>, Karoline Gangestad Primdahl<sup>1</sup>, Jørn Eivind Tungen<sup>1</sup>,  
Francesco Palmas<sup>2</sup> , Jesmond Dalli<sup>2,3</sup> and Trond Vidar Hansen<sup>1,\*</sup> 

<sup>1</sup> Department of Pharmacy, Section of Pharmaceutical Chemistry, University of Oslo, P.O. Box 1068 Blindern, N-0316 Oslo, Norway

<sup>2</sup> Lipid Mediator Unit, William Harvey Research Institute, Barts and The London School of Medicine, Queen Mary University of London, Charterhouse Square, London EC1M 6BQ, UK

<sup>3</sup> Centre for Inflammation and Therapeutic Innovation, Queen Mary University of London, London E1 4NS, UK

\* Correspondence: t.v.hansen@farmasi.uio.no; Tel.: +47-9326-5077

† Dedicated to professor Dieter Schinzer on the occasion of his 65th birthday.

Academic Editor: Ari Koskinen

Received: 26 August 2019; Accepted: 3 September 2019; Published: 5 September 2019



**Abstract:** PD1<sub>n-3</sub> DPA belongs to the protectin family of specialized pro-resolving lipid mediators. The protectins are endogenously formed mediators that display potent anti-inflammatory properties and pro-resolving bioactivities and have attracted interest in drug discovery. However, few studies have been reported of the secondary metabolism of the protectins. To investigate the metabolic formation of the putative C22 mono-hydroxylated product, coined 22-OH-PD1<sub>n-3</sub> DPA, a stereoselective synthesis was performed. LC/MS-MS data of synthetic 22-OH-PD1<sub>n-3</sub> DPA matched the data for the biosynthetic formed product. Cellular studies revealed that 22-OH-PD1<sub>n-3</sub> DPA is formed from n-3 docosapentaenoic acid in human serum, and we confirmed that 22-OH-PD1<sub>n-3</sub> DPA is a secondary metabolite produced by  $\omega$ -oxidation of PD1<sub>n-3</sub> DPA in human neutrophils and in human monocytes. The results reported are of interest for enabling future structure–activity relationship studies and provide useful molecular insight of the metabolism of the protectin class of specialized pro-resolving mediators.

**Keywords:** natural products; stereoselective synthesis; structural elucidation; biosynthesis; protectins; 22-OH-PD1<sub>n-3</sub> DPA; specialized pro-resolving mediators; polyunsaturated fatty acids; omega oxidation

## 1. Introduction

Inflammation is divided into acute inflammation, which by nature is self-resolving, and chronic inflammation, which occurs over an extended time period and does not resolve [1]. Uncontrolled, excessive acute and chronic unresolved inflammation may develop into several diseases, such as cardiovascular disease, cancer, rheumatoid arthritis, and neurological disorders, e.g., Parkinson's disease and Alzheimer's disease [2]. Over the last century, inflammation has been the topic of numerous studies at the biomolecular and the cellular levels [3]. These efforts have resulted in the identification of several chemical mediators, such as peptides, oxygenated polyunsaturated fatty acids (PUFAs), chemokines, and cytokines that initiate, modulate, and reduce acute inflammatory processes [4]. Today, various drugs—mostly inhibitors—that reduce the effects of inflammatory processes are available [2,5]. Resolution of inflammation was earlier believed to be a passive process [1,2]. However, recent studies have established that the resolution phase of inflammation and the return to physiology (homeostasis) are regulated by active and enzymatic formation of several novel families of oxygenated PUFAs [4,6]. These endogenously formed compounds have been coined specialized pro-resolving mediators (SPMs)

and are biosynthesized in the presence of cyclooxygenase and lipoxygenase enzymes from the dietary n-3 PUFAs eicosapentaenoic acid (EPA) and docosahexaenoic acid (DHA) (Figure 1) [6]. The E-series resolvins originate from EPA, the D-series resolvins, protectins and maresins, as well as the recently described sulfido-conjugates of resolvins (RCTRs), protectins (PCTRs), and maresins (MCTRs), are all biosynthesized from DHA [4]. Lipoxins are biosynthetically formed from arachidonic acid (AA) [3,5]. SPMs and their bioactions are considered to constitute a biomedical paradigm shift [5,7] with numerous interesting bioactivities reported [8].

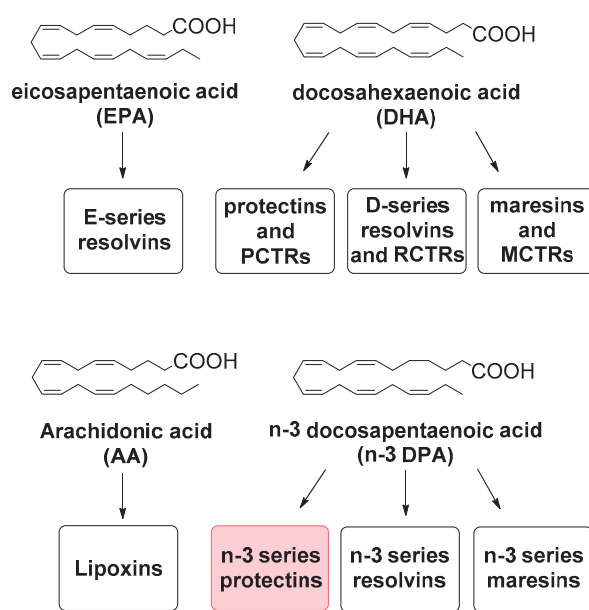


**Figure 1.** Overview of families of specialized pro-resolving mediators (SPMs) derived from eicosapentaenoic acid (EPA), docosahexaenoic acid (DHA), arachidonic acid (AA), and n-3 docosapentaenoic acid (DPA).

SPMs display highly potent agonist effects *in vivo*, often in the low nanomolar range, by acting as ligands on individual G-protein coupled receptors (GPCRs) [9]. Approximately 35% of all approved non-biological drugs target GPCRs [10]. Moreover, SPMs are excellent biomolecular templates for the development of new, small molecular anti-inflammatory drugs and immunoresolvents [5,9], and some SPMs have entered initial clinical trial programs [9].

New SPMs biosynthesized from the PUFA n-3 docosapentaenoic acid (n-3 DPA, **1**) were recently reported (Figure 2) [11,12]. N-3 DPA is formed from EPA and is also an intermediate in the biosynthesis of DHA [13]. Among these novel SPMs, PD1<sub>n-3 DPA</sub> (**2**) has been the topic of detailed biological investigations [11,14–19].

The biosynthesis of **2** [11] was recently established [20,21], as presented in Scheme 1. First, a 17-lipoxygenation of n-3 DPA produces 17(*S*)-hydroperoxy-7*Z*,10*Z*,13*Z*,15*E*,19*Z*-docosapentaenoic acid [17(*S*)-HpDPA, **3**] that is converted into the epoxide intermediate 16(*S*),17(*S*)-epoxy PD<sub>n-3 DPA</sub> (**4**), named ePD<sub>n-3 DPA</sub>. Epoxide **4** is then hydrolyzed to PD1<sub>n-3 DPA</sub> (**2**) by an unknown hydrolase (Scheme 1). Further metabolism of **2** should result in the formation of 22-OH-PD1<sub>n-3 DPA</sub> (**5**).

PUFAs and their oxygenated products undergo oxidative metabolism by eicosanoid reductase and cytochrome P450 (CYP) enzymes [6,22,23]. The  $\omega$ -oxidative metabolism has been reported for protectin D1 (PD1) [24–26]. Of interest, in contrast to the  $\omega$ -oxidation product of leukotriene B<sub>4</sub> (LTB<sub>4</sub>), 20-OH-LTB<sub>4</sub> [22,23], the PD1 metabolite 22-OH-PD1 [24] exhibited potent pro-resolving and anti-inflammatory bioactions in the nanomolar range [25]. Hence, we became interested in synthesizing **5** in a stereoselective manner and utilizing the synthetic material in biosynthetic investigations of the conversion of **1** and **2** into **5**.

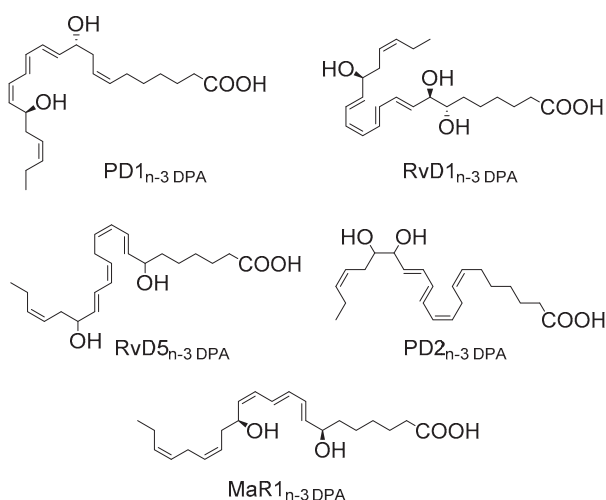
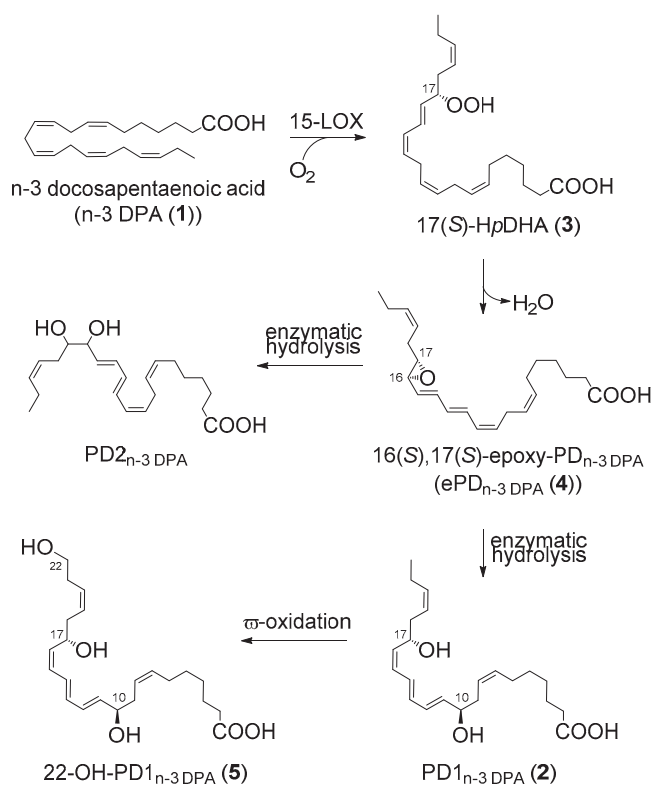


**Figure 2.** Chemical structures of some n-3 DPA derived SPMs. Where known, the absolute configuration is included.



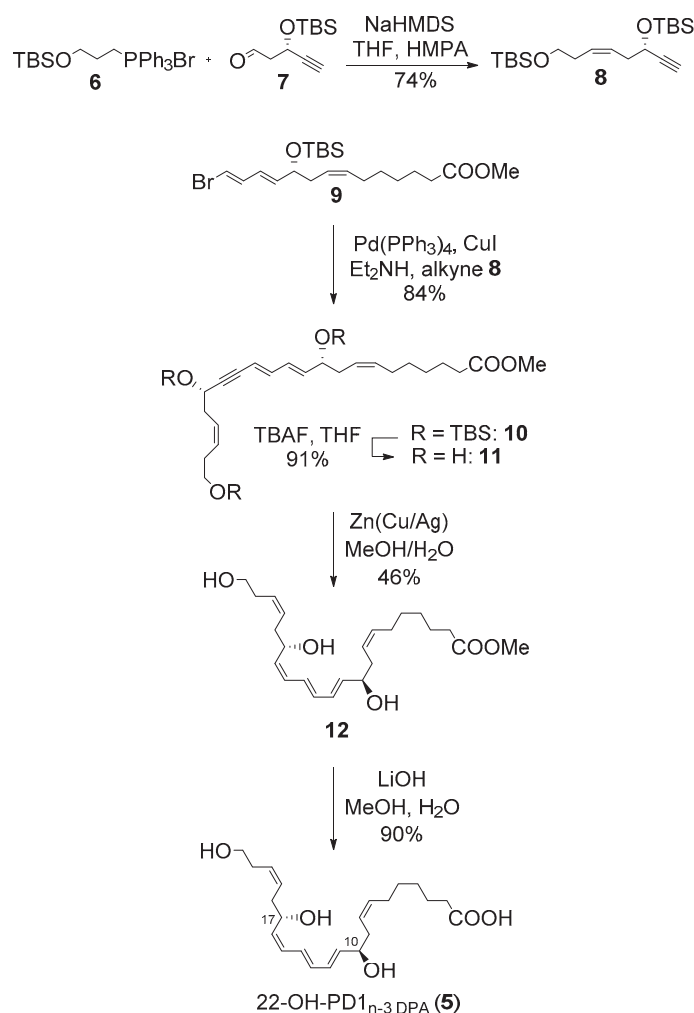
**Scheme 1.** Established biosynthesis of **2** [20,21] and putative formation of 22-OH-PD1<sub>n-3</sub> DPA (**5**).

## 2. Results and Discussion

### 2.1. Synthesis of 22-OH-PD1<sub>n-3</sub> DPA

To obtain stereochemically pure **5**, we first synthesized the Wittig-salt **6** from commercially available (3-bromopropoxy)-*tert*-butyldimethylsilane. The ylide of **6** was produced in the presence of sodium *bis*(trimethylsilyl)amide (NaHMDS) in THF/hexamethylphosphoric acid triamide (HMPA) and then reacted with the known aldehyde **7** [27] in a highly *Z*-selective Wittig reaction [28–32] (Scheme 2). This afforded *bis*-protected diol **8** in 74% isolated yield. The known vinylic bromide **9** was synthesized as earlier reported [14]. The two fragments **8** and **9** were then reacted in a Sonogashira reaction

[(Pd(PPh<sub>3</sub>)<sub>4</sub> (3 mol%) in Et<sub>2</sub>NH and in the presence of CuI (5 mol%)]. After column chromatography, isomeric pure **10** was obtained in 84% yield. Global deprotection using tetrabutylammonium fluoride (TBAF) (7.5 eq.) in THF at −78 °C afforded the triol **11** in 91% isolated yield. The *Z*-selective reduction of the internal alkyne in **11** proved challenging compared to similar systems [14,33,34]. Gratifyingly, the Boland reduction method [35] afforded the methyl ester **12** in 46% isolated yield after careful and repeated purifications by column chromatography. The chemical purity and the stereochemical integrity of **12** were validated using NMR and HPLC analyses, reaching > 95% purity (Supporting Information). Finally, mild saponification of the methyl ester in **12** afforded the target compound **5** in 90% isolated yield and in > 94% chemical purity based on NMR and HPLC analyses (Supporting Information). The geometrical configuration of the *E,E,Z*-triene moiety in **5** was assigned based on <sup>1</sup>H NMR and UV experiments as well as by analogy with literature [14]. The coupling constants from the <sup>1</sup>H NMR data were determined as 14.3 Hz, 13.9 Hz, and 11.4 Hz. The UV spectra of synthetic material of **5** showed absorbance peaks (λ<sub>max</sub><sup>EtOH</sup>) at 262, 271, and 282 nm, which is in agreement with the UV absorption profile of a conjugated triene double bond system [11].



**Scheme 2.** Synthesis of 22-OH-PD1<sub>n-3</sub> DPA (**5**).

## 2.2. Matching of Synthetic 22-OH-PD1<sub>n-3</sub> DPA with Material Formed in Human Serum

In order to obtain evidence that our synthetic material matched the authentic product of 22-OH-PD1<sub>n-3</sub> DPA (**5**), we assessed whether the physical properties of synthetic (**5**) matched with those of the product found in human serum [36]. Using liquid chromatography tandem mass spectrometry (LC/MS-MS) [37], we found that endogenous 22-OH-PD1<sub>n-3</sub> DPA (**5**) gave a retention time (T<sub>R</sub>-value) of



10.4 min using multiple reaction monitoring (MRM) (Figure 3A). Of note, synthetic **5** displayed the similar chromatographic behavior as the endogenous material (Figure 3B), and when these products were co-injected, they gave one peak in the MRM chromatogram with  $T_R = 10.4$  min (Figure 3C).

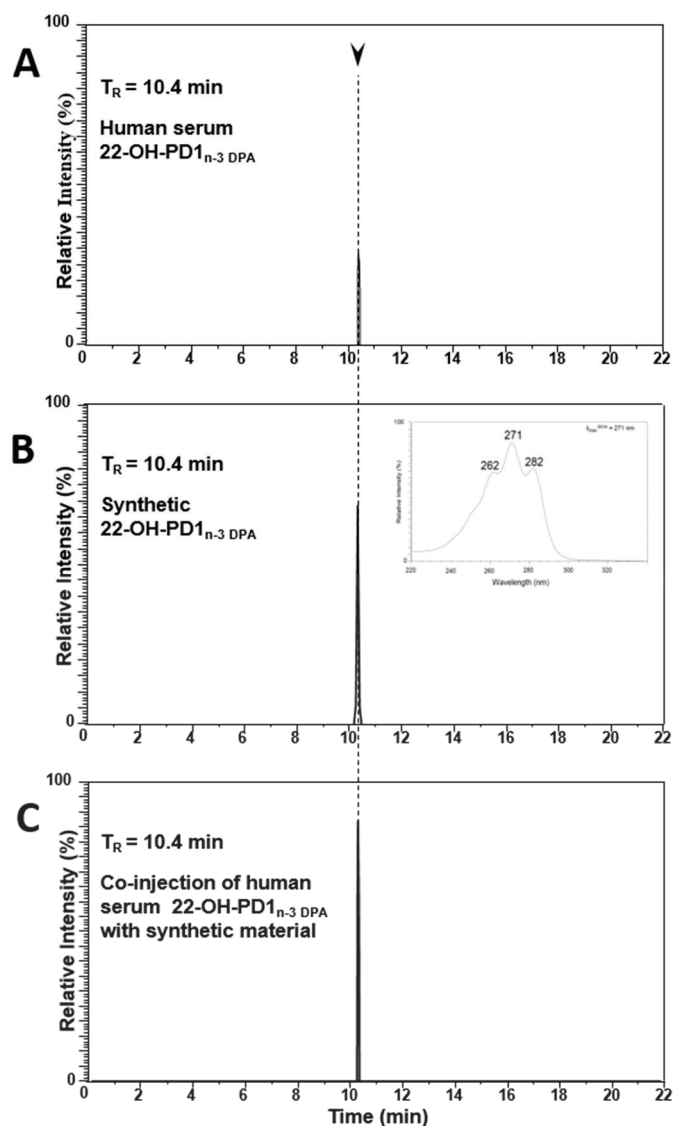


**Figure 3.** Multiple reaction monitoring (MRM) chromatogram of the products from (A) endogenous 22-OH-PD1<sub>n-3</sub> DPA (**5**) produced in human serum; (B) synthetic material of **5**; (C) co-injection of endogenous and synthetic material.

The MS-MS spectra obtained from both endogenous **5** and synthetic **5** displayed essentially identical MS-MS fragmentation spectra with the following fragments assigned:  $m/z$  377 = M – H,  $m/z$  359 = M – H – H<sub>2</sub>O,  $m/z$  341 = M – H – 2H<sub>2</sub>O,  $m/z$  323 = M – H – 3H<sub>2</sub>O,  $m/z$  297 = M – H – 2H<sub>2</sub>O – CO<sub>2</sub>,  $m/z$  245 = 263 – H<sub>2</sub>O,  $m/z$  165 = 183 – H<sub>2</sub>O and  $m/z$  139 = 183 – CO<sub>2</sub> (Supporting Information).

Overall, these results confirmed the structure of **5**, as depicted in Scheme 2, to be (7Z,10R,11E,13E,15Z,17S,19Z)-10,17,22-trihydroxydocosa-7,11,13,15,19-pentaenoic acid.

### 2.3. PD1<sub>n-3</sub> DPA is A Precursor in the Biosynthesis of 22-OH-PD1<sub>n-3</sub> DPA in Human Neutrophils

First, we investigated if human neutrophils produced 22-OH-PD1<sub>n-3</sub> DPA (**5**) (Figure 4A). Human neutrophils were isolated from whole blood and profiled by means of LC/MS-MS. The MRM-chromatogram displayed a peak with  $T_R = 10.4$  min (Figure 4A), and an MS/MS spectrum

for the product under this peak matched that of the material identified in human serum and synthetic **5** (Supporting Information). Next, we determined whether PD1<sub>n-3</sub> DPA (**2**) was a precursor of 22-OH-PD1<sub>n-3</sub> DPA (**5**). The latter was obtained from earlier synthetic work [14]. For this purpose, we incubated **2** (10 nM) with human neutrophils, and the resulting product(s) profile was assessed using LC-MS/MS, searching targeting ion pairs with  $m/z$  377 > 261 [36] in the MRM chromatogram. Here, we found that the intensity of the peak at  $T_R = 10.4$  min corresponding to 22-OH-PD1<sub>n-3</sub> DPA was markedly increased when compared to the intensity of the peak obtained with human neutrophils alone (Figure 4B). Furthermore, the co-injection of samples from both experiments gave one single sharp peak at  $T_R = 10.4$  min (Figure 4C). Overall, these experiments proved that PD1<sub>n-3</sub> DPA (**2**) was converted to 22-OH-PD1<sub>n-3</sub> DPA (**5**) by human neutrophils.

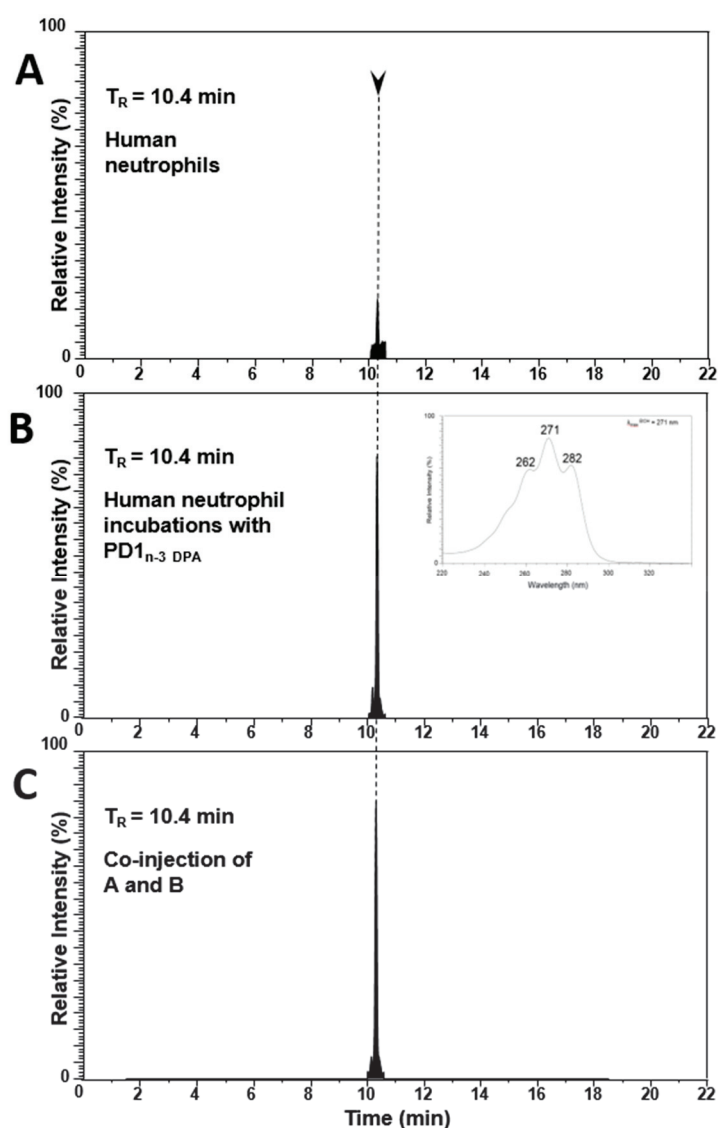


**Figure 4.** MRM chromatogram of the products from (A) human neutrophils incubated with vehicle; (B) human neutrophils incubated with PD1<sub>n-3</sub> DPA (**2**); (C) co-injection of samples obtained from (A,B).

#### 2.4. Biosynthesis of 22-OH-PD1<sub>n-3</sub> DPA from PD1<sub>n-3</sub> DPA in Human Monocytes

In order to gain additional confidence for the direct biosynthetic formation of 22-OH-PD1<sub>n-3</sub> DPA (**5**) from PD1<sub>n-3</sub> DPA (**2**), SPM **2** was incubated (10 nM) with human monocytes. Again, data from LC/MS-MS experiments showed that 22-OH-PD1<sub>n-3</sub> DPA (**5**) was indeed formed from PD1<sub>n-3</sub> DPA (**2**) by human monocytes, since identical retention times were observed (Figure 5). In addition, the MS/MS-data

of 5 from this experiment were in agreement with the data obtained from synthetic material of 5 (Supporting Information).

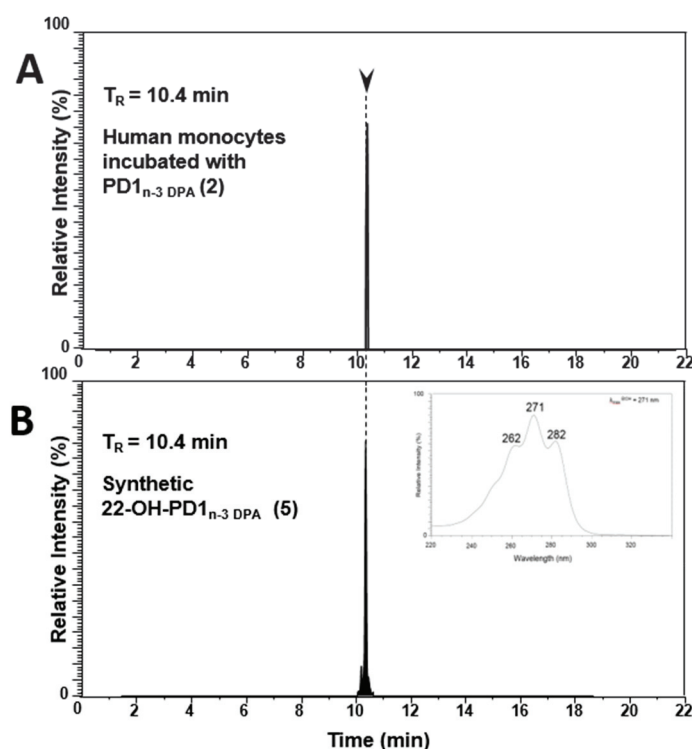


**Figure 5.** PD1<sub>n-3</sub> DPA (2) was converted to 22-OH-PD1<sub>n-3</sub> DPA (5) by human monocytes. Multiple reaction monitoring chromatograms for  $m/z$  377 > 361 of the products obtained from (A) human monocytes incubated with PD1<sub>n-3</sub> DPA; (B) synthetic 22-OH-PD1<sub>n-3</sub> DPA.

### 3. Materials and Methods

General: Unless otherwise stated, all commercially available reagents and solvents were used in the form they were supplied without any further purification. The stated yields were based on isolated material. All reactions were performed under an argon atmosphere using Schlenk techniques. Reaction flasks were covered with aluminum foil during reactions and storage to minimize exposure to light. Thin layer chromatography was performed on silica gel 60 F<sub>254</sub> aluminum-backed plates fabricated by Merck, Darmstadt, Germany. Flash column chromatography was performed on silica gel 60 (40–63  $\mu$ m) produced by Merck. NMR spectra were recorded on a Bruker AVI600 by Bruker, Billerica, MA, USA, a Bruker AVII400, or a Bruker DPX300 spectrometer at 600 MHz, 400 MHz, or 300 MHz, respectively, for <sup>1</sup>H NMR and at 150 MHz, 100 MHz, or 75 MHz, respectively, for <sup>13</sup>C NMR. Coupling constants ( $J$ ) are reported in hertz, and chemical shifts are reported in parts per million ( $\delta$ ) relative to the central residual protium solvent resonance in <sup>1</sup>H NMR (CDCl<sub>3</sub> =  $\delta$  7.26, DMSO-*d*<sub>6</sub> =  $\delta$  2.50, and MeOD =  $\delta$  3.31) and the central carbon solvent resonance in <sup>13</sup>C NMR (CDCl<sub>3</sub> =  $\delta$  77.00 ppm, DMSO-*d*<sub>6</sub> =  $\delta$  39.43, and MeOD =  $\delta$  49.00). Optical rotations were measured using a 1 mL cell with a 1.0 dm path length on a Perkin Elmer 341 polarimeter by Perkin Elmer, Waltham, MA, USA. Mass spectra were recorded at 70 eV on Micromass Prospec Q or Micromass QTOF 2 W spectrometer by Miltham, MA, USA, using electrospray ionization (ESI) as the method of ionization. High-resolution mass spectra were recorded at 70 eV on Micromass Prospec Q or Micromass QTOF 2W spectrometer using ESI as the method of ionization. HPLC analyses were performed using a C18 stationary phase (Eclipse XDB-C18, 4.6  $\times$  250 mm, particle size 5  $\mu$ m, from Agilent Technologies, Santa Clara, CA, USA), applying the conditions stated. The UV/VIS spectra were recorded using an Agilent Technologies Cary 8485 UV-VIS spectrophotometer using quartz cuvettes.

### 3.1. Synthesis of Compounds

#### 3.1.1. Bromo(3-((*tert*-butyldimethylsilyl)oxy)propyl)triphenyl- $\lambda^1$ 5-phosphane (6)

Commercially available (3-bromopropoxy)-*tert*-butyldimethylsilane (1.09 g, 4.32 mmol, 1.00 eq.) and PPh<sub>3</sub> (1.25 g, 4.75 mmol, 1.10 eq.) in toluene (5.0 mL) were heated to reflux for 16 h. The reaction mixture was cooled to rt and extracted with Et<sub>2</sub>O (3 × 25 mL). The solvent was removed in vacuo to give a white, cloudy liquid. This liquid was purified by column chromatography on silica using pure dichloromethane as eluent until all excess PPh<sub>3</sub> was eluted and there was 7% MeOH in CH<sub>2</sub>Cl<sub>2</sub>. The purified product was concentrated in vacuo to afford the title compound as a white solid in 76% yield (1.70 g). All spectroscopic and physical data were in agreement with those reported in the literature [38]. <sup>1</sup>H NMR (400 MHz, CDCl<sub>3</sub>)  $\delta$  7.89–7.75 (m, 9H), 7.74–7.64 (m, 6H), 3.96–3.80 (m, 4H), 1.97–1.83 (m, 2H), 0.85 (s, 9H), 0.03 (s, 6H); <sup>13</sup>C NMR (101 MHz, CDCl<sub>3</sub>)  $\delta$  135.1 (d, <sup>4</sup>J<sub>CP</sub> = 3.0 Hz), 133.9 (d, <sup>3</sup>J<sub>CP</sub> = 9.9 Hz), 130.6 (d, <sup>2</sup>J<sub>CP</sub> = 12.5 Hz), 118.6 (d, <sup>1</sup>J<sub>CP</sub> = 86.1 Hz), 61.9 (d, <sup>3</sup>J<sub>CP</sub> = 16.9 Hz), 26.2 (d, <sup>2</sup>J<sub>CP</sub> = 4.1 Hz), 26.1 (3C), 19.1 (d, <sup>1</sup>J<sub>CP</sub> = 52.6 Hz), 18.3, 5.2 (2C); thin layer chromatography (TLC) (MeOH/CH<sub>2</sub>Cl<sub>2</sub> 1:20, KMnO<sub>4</sub> stain) R<sub>f</sub> = 0.18; Mp: 137–139 °C.

#### 3.1.2. (*S,Z*)-5-Ethynyl-2,2,3,12,12,13,13-octamethyl-4,11-dioxo-3,12-disilatetradec-7-ene (8)

Wittig salt 6 (298 mg, 0.578 mmol, 1.00 eq.) was dissolved in THF (8.0 mL) and HMPA (0.45 mL). The solution was cooled to –78 °C followed by dropwise addition of NaHMDS (0.6 M in toluene, 0.95 mL, 0.986 eq.). The reaction mixture was stirred for 50 min, upon which it was warmed to rt and re-cooled to –78 °C. Aldehyde 7 (145 mg, 0.683 mmol, 1.20 eq.) in THF (1.0 mL) was added dropwise to the reaction mixture. After two hours, the reaction mixture was slowly allowed to warm to rt and then quenched with phosphate buffer (4.7 mL, pH = 7.2). The phases were separated, and the aqueous layer was extracted with Et<sub>2</sub>O (2 × 4.0 mL). The combined organic layers were dried (Na<sub>2</sub>SO<sub>4</sub>), and the solvent was removed by rotary evaporation. The crude product was filtered through a silica plug (hexane/EtOAc, 9:1) and concentrated in vacuo to afford compound 8 as a clear oil in 74% yield (157 mg); [ $\alpha$ ]<sub>D</sub><sup>20</sup> = –15.0 (c = 1.33, CHCl<sub>3</sub>); <sup>1</sup>H NMR (400 MHz, CDCl<sub>3</sub>)  $\delta$  5.59–5.49 (m, 2H), 4.34 (td, J = 6.5, 2.1 Hz, 1H), 3.61 (t, J = 7.0 Hz, 2H), 2.45 (t, J = 6.0 Hz, 2H), 2.38 (d, J = 2.1 Hz, 1H), 2.30 (q, J = 6.7 Hz, 2H), 0.90 (d, J = 3.8 Hz, 18H), 0.13 (s, 3H), 0.11 (s, 3H), 0.05 (s, 6H); <sup>13</sup>C NMR (101 MHz, CDCl<sub>3</sub>)  $\delta$  128.7, 126.3, 85.4, 72.3, 63.0, 62.8, 36.8, 31.5, 26.1, 25.9, 18.5, 18.4, –4.5, –4.9, –5.1; TLC (hexane/EtOAc 95:5, KMnO<sub>4</sub> stain) R<sub>f</sub> = 0.75; HRMS: exact mass calculated for C<sub>20</sub>H<sub>40</sub>O<sub>2</sub>Si<sub>2</sub>Na [M + Na]<sup>+</sup>: 391.2459, found: 391.2459.

#### 3.1.3. Methyl (7*Z*,10*R*,11*E*,13*E*,17*S*,19*Z*)-10,17,22-tris((*tert*-butyldimethylsilyl)oxy)docosa-7,11,13,19-tetraen-15-ynoate (10)

To a solution of vinyl bromide 9 (182 mg, 0.409 mmol, 1.00 eq.) in Et<sub>2</sub>NH (0.8 mL) and benzene (0.3 mL) was added Pd(PPh<sub>3</sub>)<sub>4</sub> (16.0 mg, 0.0140 mmol, 3.00 mol%), and the reaction was stirred for 45 min in the dark. CuI (4.00 mg, 0.0210 mmol, 5.00 mol%) dissolved in a minimal amount of Et<sub>2</sub>NH was added, followed by dropwise addition of alkyne 8 (160 mg, 0.434 mmol, 1.06 eq.) in Et<sub>2</sub>NH (0.8 mL). After 20 h of stirring at ambient temperature, the reaction was quenched with saturated aqueous NH<sub>4</sub>Cl (10 mL). Et<sub>2</sub>O (15 mL) was added, and the phases were separated. The aqueous phase was extracted with Et<sub>2</sub>O (2 × 15 mL), and the combined organic layers were dried (Na<sub>2</sub>SO<sub>4</sub>) before being concentrated in vacuo. The crude product was purified by column chromatography on silica (hexane/EtOAc, 95:5) to afford the title compound 10 as a clear oil in 84% yield (239 mg); [ $\alpha$ ]<sub>D</sub><sup>25</sup> = –11.6 (c = 0.95, MeOH); <sup>1</sup>H NMR (400 MHz, CDCl<sub>3</sub>)  $\delta$  6.50 (dd, J = 10.9, 15.5 Hz, 1H), 6.18 (dd, J = 10.9, 15.5 Hz, 1H), 5.76 (dd, J = 6.0, 15.1 Hz, 1H), 5.61–5.49 (m, 3H), 5.47–5.30 (m, 2H), 4.47 (td, J = 6.5, 1.8 Hz, 1H), 4.20–4.12 (m, 1H), 3.66 (s, 3H), 3.61 (t, J = 7.0 Hz, 2H), 2.49–2.41 (m, 2H), 2.32–2.16 (m, 6H), 2.01 (q, J = 7.1 Hz, 2H), 1.68–1.53 (m, 2H), 1.39–1.24 (m, 5H), 0.91–0.88 (m, 27H), 0.13 (s, 3H), 0.11 (s, 3H), 0.06–0.01 (m, 12H); <sup>13</sup>C NMR (101 MHz, CDCl<sub>3</sub>)  $\delta$  174.4, 141.2, 139.3, 131.9, 128.6, 128.5, 126.6, 125.3, 110.6, 93.3, 83.2, 72.9, 63.6, 63.0, 51.6, 37.0, 36.4, 34.2, 31.5, 29.4, 29.0, 27.4, 26.1, 26.0, 26.0, 25.0, 18.5,

18.4, 18.4, -4.3, -4.3, -4.6, -4.8, -5.1; TLC (hexane/EtOAc 95:5, UV-VIS)  $R_f = 0.33$ ; HRMS: exact mass calculated for  $C_{41}H_{76}O_5Si_3Na [M + Na]^+$ : 755.4891, found: 755.4893.

#### 3.1.4. Methyl (7Z,10R,11E,13E,17S,19Z)-10,17,22-trihydrodocosa-7,11,13,19-tetraen-15-ynoate (**11**)

TBAF (1.0 M in THF, 1.07 mL, 1.07 mmol, 7.48 eq.) was added to a solution of TBS-protected alcohol **10** (105 mg, 0.143 mmol, 1.00 eq.) in THF (1.5 mL) at  $-78\text{ }^\circ\text{C}$ . The reaction was stirred for 21 h before it was quenched with phosphate buffer (pH = 7.2, 3.5 mL). Brine (15 mL) and EtOAc (15 mL) were added, and the phases were separated. The aqueous phase was extracted with EtOAc ( $2 \times 10\text{ mL}$ ), and the combined organic layer was dried ( $Na_2SO_4$ ) before being concentrated in vacuo. The crude product was purified by column chromatography on silica (hexane/EtOAc, 4:6) to afford the title compound as a clear oil. Yield: 51 mg (91%);  $[\alpha]_D^{25} = -24.4$  ( $c = 0.67$ , MeOH);  $^1H$  NMR (400 MHz, MeOD)  $\delta$  6.55 (dd,  $J = 15.5, 10.8\text{ Hz}$ , 1H), 6.27 (dd,  $J = 15.5, 10.8\text{ Hz}$ , 1H), 5.81 (dd,  $J = 15.3, 6.4\text{ Hz}$ , 1H), 5.69–5.63 (m, 1H), 5.60–5.53 (m, 2H), 5.51–5.36 (m, 2H), 4.44 (td,  $J = 6.6, 1.9\text{ Hz}$ , 1H), 4.12 (q,  $J = 7.0, 6.5\text{ Hz}$ , 1H), 3.65 (s, 3H), 3.56 (t,  $J = 6.8\text{ Hz}$ , 2H), 2.49–2.44 (m, 2H), 2.36–2.22 (m, 6H), 2.05 (q,  $J = 6.9\text{ Hz}$ , 2H), 1.61 (p,  $J = 7.4\text{ Hz}$ , 2H), 1.42–1.28 (m, 4H);  $^{13}C$  NMR (101 MHz, MeOD)  $\delta$  176.0, 142.5, 139.9, 132.9, 130.3, 129.7, 127.5, 126.1, 111.7, 93.8, 84.3, 72.8, 63.1, 62.6, 52.0, 37.0, 36.2, 34.8, 32.0, 30.3, 29.80, 28.2, 25.9; TLC (hexane/EtOAc 2:3, UV-VIS)  $R_f = 0.22$ ; HRMS: exact mass calculated for  $C_{23}H_{34}O_5Na [M + Na]^+$ : 413.2299, found: 413.2298.

#### 3.1.5. 22-OH-PD1<sub>n-3</sub> DPA Methyl Ester (**12**)

The Zn(Cu/Ag) mixture was prepared as described by Boland et al. [35]. Zinc dust (3.12 g) in degassed  $H_2O$  (18.8 mL, pH = 7.0) was stirred under argon for 15 min before  $Cu(OAc)_2$  (312 mg) was added and stirred for an additional 15 min.  $AgNO_3$  (312 mg) was then added, and the reaction mixture was stirred for 30 min. The mixture was filtered and washed successively with  $H_2O$ , MeOH, acetone, and  $Et_2O$  before it was transferred to a flask containing alkyne **11** (50.0 mg, 0.128 mmol) in MeOH/ $H_2O$  (1:3, 9.2 mL). The mixture was stirred at rt and monitored by TLC analysis. After 2 h, the reaction was judged complete, and the reaction mixture was filtered through a pad of Celite® by Merck, Darmstadt, Germany, with  $Et_2O$ . Water was added to the filtrate, and the layers were separated. The aqueous layer was extracted with  $Et_2O$  ( $2 \times 10\text{ mL}$ ). The combined organic layers were washed with brine and dried ( $Na_2SO_4$ ). The solvent was removed in vacuo, and the crude product was purified by column chromatography on silica gel (hexane/EtOAc/MeOH, 49:50:1) to afford the methyl ester **12** as a pale yellow oil in 46% yield (23 mg);  $[\alpha]_D^{25} = -20.0$  ( $c = 0.20$ , MeOH);  $^1H$  NMR (600 MHz, MeOD)  $\delta$  6.58–6.48 (m, 1H), 6.32–6.20 (m, 2H), 6.08 (t,  $J = 11.2\text{ Hz}$ , 1H), 5.75 (dd,  $J = 6.6, 14.5\text{ Hz}$ , 1H), 5.53–5.36 (m, 5H), 4.62–4.55 (m, 1H), 4.15–4.08 (m, 1H), 3.65 (s, 3H), 3.55 (t,  $J = 6.8\text{ Hz}$ , 2H), 2.43–2.36 (m, 1H), 2.35–2.18 (m, 7H), 2.09–1.99 (m, 2H), 1.61 (p,  $J = 7.4\text{ Hz}$ , 2H), 1.42–1.27 (m, 4H);  $^{13}C$  NMR (151 MHz, MeOD)  $\delta$  176.0, 138.1, 135.0, 134.8, 132.8, 131.4, 130.6, 129.1, 128.8, 128.1, 126.2, 73.1, 68.5, 62.6, 52.0, 36.6, 36.4, 34.8, 32.0, 30.3, 29.8, 28.2, 25.9; TLC (hexane/EtOAc/MeOH 49:50:1)  $R_f = 0.22$ ; HRMS: exact mass calculated for  $C_{23}H_{36}O_5Na [M + Na]^+$ : 415.2455, found: 415.2455; UV-VIS:  $\lambda_{max}$  (EtOH) = 269, 271, 282 nm. The purity (96%) was determined by HPLC analysis (Eclipse XDB-C18, MeOH/ $H_2O$  3:1, 1.0 mL/min);  $t_R = 32.6$ .

#### 3.1.6. 22-OH-PD1<sub>n-3</sub> DPA (**5**)

Solid LiOH (17.0 mg, 0.710 mmol, 31.0 eq.) was added to a solution of methyl ester **12** (9 mg, 0.0229 mmol, 1.00 eq.) dissolved in THF-MeOH- $H_2O$  (2:2:1, 2.8 mL) at  $0\text{ }^\circ\text{C}$ . The reaction mixture was stirred at  $0\text{ }^\circ\text{C}$  for three hours and then allowed to warm to rt. After 7.5 h, the solution was cooled to  $0\text{ }^\circ\text{C}$ , acidified with saturated aqueous  $NaH_2PO_4$  (4.0 mL), and then EtOAc (4.0 mL) was added. The layers were separated, and the water phase was extracted with EtOAc ( $2 \times 4.0\text{ mL}$ ). The combined organic layers were dried ( $Na_2SO_4$ ) before the solvent was removed in vacuo. Then, 22-OH-PD1<sub>n-3</sub> DPA (**5**) was obtained as a colorless oil after purification by column chromatography (MeOH/ $CH_2Cl_2$ , 1:9)  $R_f = 0.22$ ; yield: 10 mg (90%);  $[\alpha]_D^{25} = -25.4$  ( $c = 0.35$ , MeOH);  $^1H$  NMR  $\delta$  6.53 (dd,  $J = 13.9, 11.4\text{ Hz}$ , 1H),

6.32–6.21 (m, 2H), 6.08 (t,  $J = 11.4$  Hz, 1H), 5.74 (dd,  $J = 14.3, 6.5$  Hz, 1H), 5.56–5.44 (m, 3H), 5.43–5.36 (m, 2H), 4.63–4.55 (m, 1H), 4.12 (q,  $J = 6.6$  Hz, 1H), 3.55 (t,  $J = 6.8$  Hz, 2H), 2.44–2.36 (m, 1H), 2.36–2.20 (m, 7H), 2.06 (q,  $J = 7.0$  Hz, 2H), 1.60 (p,  $J = 7.4$  Hz, 2H), 1.41–1.32 (m, 4H);  $^{13}\text{C}$  NMR (151 MHz, MeOD)  $\delta$  178.0, 138.1, 135.0, 134.8, 132.9, 131.4, 130.6, 129.1, 128.8, 128.1, 126.2, 73.1, 68.5, 62.6, 36.6, 36.4, 35.3, 32.0, 30.4, 29.9, 28.3, 26.1; HRMS: exact mass calculated for  $\text{C}_{22}\text{H}_{34}\text{O}_5\text{Na}$   $[\text{M} + \text{Na}]^+$ : 401.2298, found: 401.2298; UV-VIS:  $\lambda_{\text{max}}$  (EtOH) = 269, 271, 282 nm. The purity (94%) was determined by HPLC analysis (Eclipse XDB-C18, MeOH/H<sub>2</sub>O/10mM acetic acid 65:20:20, 1.0 mL/min);  $T_{\text{R}} = 18.1$ .

### 3.2. Lipid Mediator Profiling

MeOH—two and four volumes, respectively—containing deuterium-labeled synthetic internal standards of  $d_4$ -LTB<sub>4</sub> (500 pg) and  $d_5$ -RvE1 (100 pg) were added to cell incubations and human serum. Samples were stored at  $-40$  °C until extraction. Prior to extraction, samples were centrifuged at 2500 rpm, 4 °C, for 10 min. Supernatants were then collected and concentrated to  $\sim 1.0$  mL of MeOH content using a gentle stream of nitrogen gas (TurboVap LV system, Biotage, Uppsala, Sweden). Solid phase extraction was performed by means of the ExtraHera (Biotage) automated extraction system as follows. Aqueous HCl solution (pH = 3.5, 9.0 mL) was added to the samples, and the acidified solutions were loaded onto conditioned C18 500 mg 200-0050-B cartridges (Biotage). Prior to extraction, solid phase C18 cartridges were equilibrated with MeOH (3.0 mL) and H<sub>2</sub>O (6.0 mL). The extraction products were washed with H<sub>2</sub>O (4.0 mL) and hexane (5.0 mL) followed by product elution with 4.0 mL of methyl formate. Products were brought to dryness with a gentle stream of nitrogen (TurboVap LV, Biotage) and suspended in MeOH:H<sub>2</sub>O (50:50, *v/v*). Samples were centrifuged (2500 rpm, 4.0 °C, 5 min), and the supernatant was collected and centrifuged (9900 rpm, 4.0 °C, 10 sec). The collected supernatant was then subjected to LC/MS-MS, as described in reference [39].

### 3.3. Human Neutrophil Incubations

Human peripheral blood neutrophils were isolated from healthy volunteers using density-gradient Ficoll-Histopaque isolation. Volunteers gave written consent in accordance with a Queen Mary Research Ethics Committee (QMREC 2014:61) and the Helsinki declaration. Isolated neutrophils were suspended in PBS<sup>+/+</sup> containing 10% bovine serum albumin (BSA) and incubated for 10 min (37 °C, pH = 7.45) prior to the addition of the indicated concentrations of n-3 DPA (**1**) and *Escherichia coli* ( $2.5 \times 10^8$  cells/mL). Incubations were quenched using two volumes ice-cold methanol containing deuterium-labeled internal standards to facilitate quantification and identification. Products were extracted using C18 columns and quantified by LC/MS-MS metabololipidomics, as detailed above. The same experiment was repeated with synthetic **2**.

### 3.4. Human Serum Incubations

Human pool serum was purchased from Sigma-Aldrich (Poole, UK). Four volumes of methanol containing deuterium-labeled standards were added, and products were extracted using C18 column and profiled using LC/MS-MS metabololipidomics, as detailed above [39].

## 4. Conclusions

To summarize, 22-OH-PD1<sub>n-3</sub>DPA (**5**) was stereoselectively synthesized in six steps and with 38% yield from commercially available (3-bromopropoxy)-*tert*-butyldimethylsilane and known (S)-3-((*tert*-butyldimethylsilyloxy)pent-4-ynal (**7**). We herein established the exact configuration of the biomolecule **5**, and that **5** is an  $\omega$ -oxidation metabolic product of the SPM PD1<sub>n-3</sub>DPA (**2**). In addition, we showed that 22-OH-PD1<sub>n-3</sub>DPA (**5**) is formed in human serum, human neutrophils, and by human monocytes. The results reported contribute to additional information and knowledge of the growing number of members of the SPM family of endogenously formed lipid mediators and their metabolism, which is of interest in regard to developing new immunoresolvents without immunosuppressive effects [5,37].

**Supplementary Materials:** Electronic Supporting Information is available with  $^1\text{H}$ -,  $^{13}\text{C}$ -NMR, HPLC-chromatograms, UV-VIS, MS/MS and HRMS data of 5 and intermediates 6–11 and methyl ester 12. See <http://www.mdpi.com/1420-3049/24/18/3228/s1>.

**Author Contributions:** T.V.H., J.E.T. and J.D. designed the concept of the study. J.I.N. performed all the synthetic experiments with supervision by K.G.P. and J.E.T. K.G.P. performed purification of compounds and analyzed data with J.I.N., F.P. and J.I.N. performed lipid mediator profiling. J.I.N. performed human serum- and human neutrophil incubations. J.I.N. and T.V.H. wrote the paper. K.G.P., J.E.T., J.D. and F.P. reviewed and edited the paper.

**Funding:** The School of Pharmacy, University of Oslo is gratefully acknowledged for a Ph.D.-scholarship to J.I.N. We appreciate the funding for a travel grant to J.I.N. from The Norwegian Research School in Pharmacy (N.F.I.F.). The Norwegian Research Council is gratefully acknowledged for funding to T.V.H. (BIOTEK2021 224811 and FRIPRO-FRINATEK 230470). J.D. received funding from the European Research Council (ERC) under the European Union's Horizon 2020 research and innovation program (grant no: 677542) and the Barts Charity (grant no: MGU0343). J.D. is also supported by a Sir Henry Dale Fellowship jointly funded by the Wellcome Trust and the Royal Society (grant 107613/Z/15/Z).

**Acknowledgments:** T.V.H. is most grateful towards Dieter Schinzer, University of Magdeburg, Germany, for all discussions, interactions and fun, socially as well as professionally. Let the "Dolce Vita" live on!

**Conflicts of Interest:** The authors declare no conflict of interest.

## References

1. Rather, L.J. Disturbance of function (function laesa): The legendary fifth cardinal sign of inflammation, added by Galen to the four cardinal signs of Celsus. *Bull. N. Y. Acad. Med.* **1971**, *47*, 303–322. [[PubMed](#)]
2. Libby, P. Inflammatory mechanisms: The molecular basis of inflammation and disease. *Nutr. Rev.* **2007**, *65*, 140–146. [[CrossRef](#)]
3. Levy, B.D.; Clish, C.B.; Schmidt, B.; Gronert, K.; Serhan, C.N. Lipid mediator class switching during acute inflammation: Signals in resolution. *Nat. Immunol.* **2001**, *2*, 612–619. [[CrossRef](#)] [[PubMed](#)]
4. Tabas, I.; Glass, C.K. Anti-inflammatory therapy in chronic disease: Challenges and opportunities. *Science* **2013**, *339*, 166–172. [[CrossRef](#)] [[PubMed](#)]
5. Fullerton, J.N.; Gilroy, D.W. Resolution of inflammation: A new therapeutic frontier. *Nat. Rev. Drug Discov.* **2016**, *15*, 551–567. [[CrossRef](#)] [[PubMed](#)]
6. Serhan, C.N.; Petasis, N.A. Resolvins and protectins in inflammation resolution. *Chem. Rev.* **2011**, *111*, 5922–5943. [[CrossRef](#)] [[PubMed](#)]
7. Van Dyke, T.E.; Serhan, C.N. Resolution of inflammation: A new paradigm for the pathogenesis of periodontal disease. *J. Dent. Res.* **2003**, *82*, 82–90. [[CrossRef](#)]
8. Serhan, C.N. Treating inflammation and infection in the 21<sup>st</sup> century: New hints from decoding resolution mediators and mechanisms. *FASEB J.* **2017**, *31*, 1273–1288. [[CrossRef](#)] [[PubMed](#)]
9. Serhan, C.N.; Chiang, N. Resolution phase lipid mediators of inflammation: Agonists of resolution. *Curr. Opin. Pharmacol.* **2013**, *13*, 632–640. [[CrossRef](#)]
10. Lappano, R.; Maggiolini, M. G protein-coupled receptors: Novel targets for drug discovery in cancer. *Nat. Rev. Drug Discov.* **2011**, *10*, 47–60. [[CrossRef](#)]
11. Dalli, J.; Colas, R.A.; Serhan, C.N. Novel n-3 immunoresolvents: Structures and actions. *Sci. Rep.* **2013**, *3*, 1940. [[CrossRef](#)] [[PubMed](#)]
12. Dalli, J.; Chiang, N.; Serhan, C.N. Elucidation of novel 13-series resolvins that increase with atorvastatin and clear infections. *Nat. Med.* **2015**, *21*, 1071–1075. [[CrossRef](#)] [[PubMed](#)]
13. Kaur, G.; Cameron-Smith, D.; Garg, M.; Sinclair, A.J. Docosapentaenoic acid (22:5n-3): A review of its biological effects. *Prog. Lipid Res.* **2011**, *50*, 28–34. [[CrossRef](#)] [[PubMed](#)]
14. Aursnes, M.; Tungen, J.E.; Vik, A.; Colas, R.; Cheng, C.-Y.C.; Dalli, J.; Serhan, C.N.; Hansen, T.V. Total synthesis of the lipid mediator PD1<sub>n-3</sub>DPA: Configural assignments and anti-inflammatory and pro-resolving actions. *J. Nat. Prod.* **2014**, *77*, 910–916. [[CrossRef](#)] [[PubMed](#)]
15. Hansen, T.V.; Vik, A.; Serhan, C.N. The protectin family of specialized pro-resolving mediators: Potent immunoresolvents enabling innovative approaches to target obesity and diabetes. *Front. Pharmacol.* **2019**, *9*, 1582–1598. [[CrossRef](#)] [[PubMed](#)]
16. Hansen, T.V.; Dalli, J.; Serhan, C.N. The novel lipid mediator PD1<sub>n-3</sub>DPA: An overview of the structural elucidation, synthesis, biosynthesis and bioactions. *Prostaglandins Other Lipid Mediat.* **2017**, *133*, 103–110. [[CrossRef](#)] [[PubMed](#)]

17. Vik, A.; Dalli, J.; Hansen, T.V. Recent advances in the chemistry and biology of anti-inflammatory and specialized pro-resolving mediators biosynthesized from n-3 docosapentaenoic acid. *Bioorg. Med. Chem. Lett.* **2017**, *27*, 2259–2266. [[CrossRef](#)] [[PubMed](#)]
18. Gobetti, T.; Dalli, J.; Colas, R.A.; Canova, D.F.; Aursnes, M.; Bonnet, D.; Alric, L.; Vergnolle, N.; Deraison, C.; Hansen, T.V.; et al. Protectin D1<sub>n-3</sub>DPA and resolvin D5<sub>n-3</sub>DPA are novel effectors of intestinal protection. *Proc. Natl. Acad. Sci. USA* **2017**, *114*, 3963–3968. [[CrossRef](#)] [[PubMed](#)]
19. Frigerio, F.; Pasqualini, G.; Craparotta, I.; Marchini, S.; Van Vliet, E.A.; Foerch, P.; Vandenplas, C.; Leclercq, K.; Aronica, E.; Porcu, L.; et al. n-3 Docosapentaenoic acid-derived protectin D1 promotes resolution of neuroinflammation and arrests epileptogenesis. *Brain* **2018**, *141*, 3130–3143. [[CrossRef](#)] [[PubMed](#)]
20. Pistorius, K.; Souza, P.R.; De Matteis, R.; Austin-Williams, S.; Primdahl, K.G.; Vik, A.; Mazzacuva, F.; Colas, R.A.; Marques, R.M.; Hansen, T.V.; et al. PD<sub>n-3</sub>DPA pathway regulates human monocyte differentiation and macrophage function. *Cell Chem. Biol.* **2018**, *25*, 749–760. [[CrossRef](#)]
21. Primdahl, K.G.; Tungen, J.E.; De Souza, P.R.S.; Colas, R.A.; Dalli, J.; Hansen, T.V.; Vik, A. Stereocontrolled synthesis and investigation of the biosynthetic transformations of 16(S), 17(S)-epoxy-PD<sub>n-3</sub>DPA. *Org. Biomol. Chem.* **2017**, *15*, 8606–8613. [[CrossRef](#)] [[PubMed](#)]
22. Sumimoto, H.; Minakami, S. Oxidation of 20-hydroxy leukotriene B<sub>4</sub> by human neutrophil microsomes. Role of aldehyde dehydrogenase and leukotriene B<sub>4</sub> ω-hydroxylase (cytochrome P-450<sub>LTB4</sub>) in leukotriene B<sub>4</sub> ω-oxidation. *J. Biol. Chem.* **1990**, *265*, 4348–4353. [[PubMed](#)]
23. Divanovic, S.; Dalli, J.; Jorge-Nebert, L.F.; Flick, L.M.; Gálvez-Peralta, M.; Boespflug, N.D.; Stankiewicz, T.E.; Fitzgerald, J.M.; Somarathna, M.; Karp, C.L.; et al. Contributions of the three CYP1 monooxygenases to pro-inflammatory and inflammation-resolution lipid mediator pathways. *J. Immunol.* **2013**, *191*, 3347–3357. [[CrossRef](#)] [[PubMed](#)]
24. Serhan, C.N.; Hong, S.; Gronert, K.; Colgan, S.P.; Devchand, P.R.; Mirick, G.; Moussignac, R.-L. Resolvins. A family of bioactive products of omega-3 fatty acid transformation circuits initiated by aspirin treatment that counter proinflammation signals. *J. Exp. Med.* **2002**, *196*, 1025–1037. [[CrossRef](#)] [[PubMed](#)]
25. Tungen, J.E.; Aursnes, M.; Vik, A.; Colas, R.A.; Dalli, J.; Serhan, C.N.; Hansen, T.V. Synthesis, anti-inflammatory and pro-resolving activities of 22-OH-PD1, a mono-hydroxylated metabolite of protectin D1. *J. Nat. Prod.* **2014**, *77*, 2241–2247. [[CrossRef](#)] [[PubMed](#)]
26. Tungen, J.E.; Aursnes, M.; Ramon, S.; Colas, R.A.; Serhan, C.N.; Olberg, D.E.; Nuruddin, S.; Willoch, F.; Hansen, T.V. Synthesis of protectin D1 analogs: Novel pro-resolution and radiotracer agents. *Org. Biomol. Chem.* **2018**, *16*, 6818–6823. [[CrossRef](#)]
27. Tungen, J.E.; Aursnes, M.; Dalli, J.; Arnardottir, H.; Serhan, C.N.; Hansen, T.V. Total synthesis of the anti-inflammatory and pro-resolving lipid mediator MaR<sub>n-3</sub>DPA. *Chem. Eur. J.* **2014**, *20*, 14575–14578. [[CrossRef](#)]
28. Ramon, S.; Dalli, J.; Sanger, J.M.; Winkler, J.W.; Aursnes, M.; Tungen, J.E.; Hansen, T.V.; Serhan, C.N. The protectin PCTR1 is produced by human M2 macrophages and enhances resolution of infectious inflammation. *Am. J. Pathol.* **2016**, *186*, 962–973. [[CrossRef](#)]
29. Primdahl, K.G.; Aursnes, M.; Tungen, J.E.; Hansen, T.V.; Vik, A. An efficient synthesis of leukotriene B<sub>4</sub>. *Org. Biomol. Chem.* **2015**, *13*, 5412–5417. [[CrossRef](#)]
30. Tungen, J.E.; Aursnes, M.; Hansen, T.V. Stereoselective synthesis of maresin 1. *Tetrahedron Lett.* **2015**, *56*, 1843–1846. [[CrossRef](#)]
31. Nolsøe, J.M.; Aursnes, M.; Tungen, J.E.; Hansen, T.V. Dienals derived from pyridinium salts and their subsequent application in natural product synthesis. *J. Org. Chem.* **2015**, *80*, 5377–5385. [[CrossRef](#)] [[PubMed](#)]
32. Aursnes, M.; Tungen, J.E.; Vik, A.; Dalli, J.; Hansen, T.V. Stereoselective synthesis of protectin D1: A potent anti-inflammatory and pro-resolving lipid mediator. *Org. Biomol. Chem.* **2014**, *12*, 432–437. [[CrossRef](#)] [[PubMed](#)]
33. Primdahl, K.G.; Aursnes, M.; Walker, M.E.; Colas, R.A.; Serhan, C.N.; Dalli, J.; Hansen, T.V.; Vik, A. Synthesis of 13(R)-Hydroxy-7Z,10Z,13R,14E,16Z,19Z docosapentaenoic acid (13R-HDPA) and its biosynthetic conversion to the 13-series resolvins. *J. Nat. Prod.* **2016**, *79*, 2693–2702. [[CrossRef](#)] [[PubMed](#)]
34. Tungen, J.E.; Gerstmann, L.; Vik, A.; De Mates, R.; Colas, R.A.; Dalli, J.; Chiang, N.; Serhan, C.N.; Kalesse, M.; Hansen, T.V. Resolving inflammation: synthesis, configurational assignment, and biological evaluations of RvD1<sub>n-3</sub>DPA. *Chem. Eur. J.* **2019**, *25*, 1476–1480. [[CrossRef](#)] [[PubMed](#)]



35. Boland, W.; Schroer, C.N.; Sieler, C.M.; Feigel, M. Stereospecific syntheses and spectroscopic properties of isomeric 2,4,6,8-undecatetraenes. New hydrocarbons from the marine brown alga *Giffordia mitchellae*. Part IV. *Helv. Chim. Acta.* **1987**, *70*, 1025–1040. [[CrossRef](#)]
36. Dalli, J.; Serhan, C.N. Specific lipid mediator signatures of human phagocytes: Microparticles stimulate macrophage efferocytosis and pro-resolving mediators. *Blood* **2012**, *120*, e60–e72. [[CrossRef](#)] [[PubMed](#)]
37. Dalli, J. Does promoting resolution instead of inhibiting inflammation represent the new paradigm in treating infections? *Mol. Aspects Med.* **2017**, *58*, 12–20. [[CrossRef](#)] [[PubMed](#)]
38. Loiseau, F.; Simone, J.-M.; Carcache, D.; Bobal, P.; Neier, R. Radical couplings as key steps for the preparation of derivatives of nonactic acid. *Montash. Chem.* **2007**, *138*, 121–129. [[CrossRef](#)]
39. Dalli, J.; Colas, R.A.; Walker, M.E.; Serhan, C.N. Lipid mediator metabolomics via LC-MS/MS profiling and analysis. *Methods Mol. Biol.* **2018**, *1730*, 59–72. [[PubMed](#)]

**Sample Availability:** Samples of the compounds **6**, **8**, **12** and **5** are available from the authors.



© 2019 by the authors. Licensee MDPI, Basel, Switzerland. This article is an open access article distributed under the terms and conditions of the Creative Commons Attribution (CC BY) license (<http://creativecommons.org/licenses/by/4.0/>).



## Supporting Information for

### Synthesis, Structural Confirmation and Biosynthesis of 22-OH-PD1<sub>n-3</sub> DPA

Jannicke I. Nesman<sup>†</sup>, Karoline G. Primdahl<sup>†</sup>, Jørn E. Tungen<sup>†</sup>, Francesco Palmas<sup>‡</sup>, Jesmond Dalli<sup>‡c</sup> and Trond V. Hansen<sup>†\*</sup>

<sup>†</sup>*School of Pharmacy, Department of Pharmaceutical Chemistry, University of Oslo, PO Box 1068 Blindern, N-0316 Oslo, Norway*

<sup>‡</sup>*Lipid Mediator Unit, William Harvey Research Institute, Barts and The London School of Medicine, Queen Mary University of London, Charterhouse Square, London EC1 M 6BQ, UK*

\**E-mail: [t.v.hansen@farmasi.uio.no](mailto:t.v.hansen@farmasi.uio.no)*

<sup>c</sup> *Centre for Inflammation and Therapeutic Innovation, Queen Mary University of London, London, UK*

#### Contents

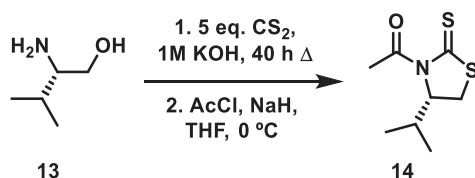
General Information .....	2
Experimental Details .....	2
<sup>1</sup> H-NMR and <sup>13</sup> C-NMR spectra.....	7
HPLC Chromatograms .....	17
Lipid Mediator Metabololipidomics.....	18
Matching of synthetic 22-OH-PD1 <sub>n-3</sub> DPA with material formed in human monocytes incubated with PD1 <sub>n-3</sub> DPA .....	18
MS-MS fragmentation spectra of 22-OH-PD1 <sub>n-3</sub> DPA .....	19
UV-Vis Spectra .....	20
References .....	20

## General Information

Unless otherwise stated, all commercially available reagents and solvents were used in the form in which they were supplied without any further purification. The stated yields are based on isolated material. All reactions were performed under an argon atmosphere using Schlenk techniques. Reaction flasks were covered with aluminum foil during reactions and storage to minimize exposure to light. Thin layer chromatography was performed on silica gel 60 F<sub>254</sub> aluminum-backed plates fabricated by Merck. Flash column chromatography was performed on silica gel 60 (40-63  $\mu\text{m}$ ) produced by Merck. NMR spectra were recorded on a Bruker AVI600, Bruker AVII400 or a Bruker DPX300 spectrometer at 600 MHz, 400 MHz or 300 MHz respectively for  $^1\text{H}$  NMR and at 150 MHz, 100 MHz or 75 MHz respectively for  $^{13}\text{C}$  NMR. Coupling constants ( $J$ ) are reported in hertz and chemical shifts are reported in parts per million ( $\delta$ ) relative to the central residual protium solvent resonance in  $^1\text{H}$  NMR ( $\text{CDCl}_3 = \delta$  7.26,  $\text{DMSO-}d_6 = \delta$  2.50 and  $\text{MeOD} = \delta$  3.31) and the central carbon solvent resonance in  $^{13}\text{C}$  NMR ( $\text{CDCl}_3 = \delta$  77.00 ppm,  $\text{DMSO-}d_6 = \delta$  39.43 and  $\text{MeOD} = \delta$  49.00). Optical rotations were measured using a 1 mL cell with a 1.0 dm path length on a Perkin Elmer 341 polarimeter. Mass spectra were recorded at 70 eV on a Micromass Prospec Q or Micromass QTOF 2 W spectrometer using ESI as the method of ionization. High-resolution mass spectra were recorded at 70 eV on a Micromass Prospec Q or Micromass QTOF 2W spectrometer using ESI as the method of ionization. HPLC-analyses were performed using a C18 stationary phase (Eclipse XDB-C18, 4.6 x 250 mm, particle size 5  $\mu\text{m}$ , from Agilent Technologies), applying the conditions stated. The UV/Vis spectra was recorded using an Agilent Technologies Cary 8485 UV-VIS spectrophotometer using quartz cuvettes.

## Experimental Details

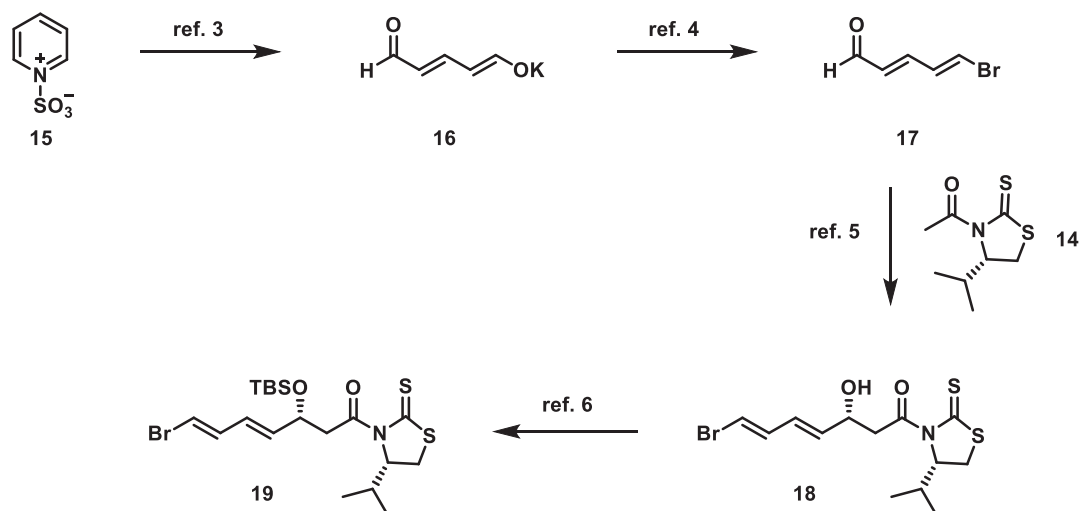
### (*S*)-4-isopropylthiazolidine-2-thione (**14**)



Nagao's chiral auxiliary **14**, was prepared from commercially available (*S*)-(+)-2-amino-3-methyl-1-butanol (**13**) as previously reported in the literature.<sup>1,2</sup> Yield: 67% over the two steps. All spectroscopic and physical data were in agreement with those reported in the literature.<sup>2</sup>  $[\alpha]_D^{20} = 434$  ( $c = 0.26$ ,  $\text{CHCl}_3$ );  $^1\text{H}$  NMR (400 MHz,  $\text{CDCl}_3$ )  $\delta$  5.15 (ddd,  $J = 7.6, 6.2, 1.2$  Hz, 1H), 3.50 (dd,  $J = 11.5, 8.0$  Hz, 1H), 3.02 (dd,  $J = 11.5, 1.2$  Hz, 1H), 2.77 (s, 3H), 2.45 – 2.28 (m, 1H), 1.06 (d,  $J = 6.8$  Hz, 3H), 0.97

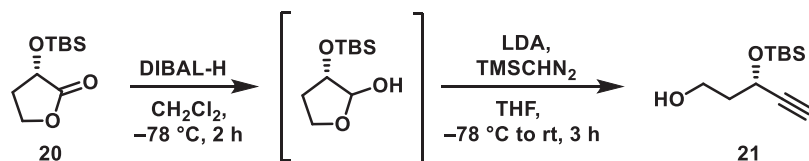
(d,  $J = 6.9$  Hz, 3H);  $^{13}\text{C}$  NMR (101 MHz,  $\text{CDCl}_3$ )  $\delta$  203.4, 170.9, 71.40, 30.9, 30.5, 27.1, 19.2, 17.9; TLC (hexane/ $\text{Et}_2\text{O}$  9:1,  $\text{KMnO}_4$ -stain)  $R_f = 0.25$ .

**(*R,4E,6E*)-7-bromo-3-((*tert*-butyldimethylsilyl)oxy)-1-((*R*)-4-isopropyl-2-thioxothiazolidin-3-yl)hepta-4,6-dien-1-one (19)**



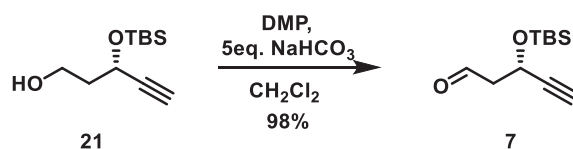
Thiazolidinethione **19** was prepared in four steps from commercially available pyridinium-1-sulfonate **15** as previously reported in the literature.<sup>3-6</sup> **Yield:** 28% over the four steps. All spectroscopic and physical data were in agreement with those reported in the literature.<sup>6</sup>  $[\alpha]_D^{20} = 265$  ( $c = 0.40$ ,  $\text{CHCl}_3$ );  $^1\text{H}$  NMR (400 MHz,  $\text{CDCl}_3$ )  $\delta$  6.69 (dd,  $J = 13.5, 10.9$  Hz, 1H), 6.31 (d,  $J = 13.5$  Hz, 1H), 6.15 (dd,  $J = 15.3, 10.9$  Hz, 1H), 5.79 (dd,  $J = 15.4, 6.3$  Hz, 1H), 5.08 – 4.98 (m, 1H), 4.79 – 4.69 (m, 1H), 3.64 (dd,  $J = 16.6, 7.9$  Hz, 1H), 3.47 (dd,  $J = 11.5, 7.8$  Hz, 1H), 3.21 (dd,  $J = 16.6, 4.5$  Hz, 1H), 3.03 (dd,  $J = 11.4, 1.1$  Hz, 1H), 2.43 – 2.29 (m,  $J = 6.9$  Hz, 1H), 1.05 (d,  $J = 6.8$  Hz, 3H), 0.97 (d,  $J = 7.0$  Hz, 3H), 0.86 (s, 9H), 0.05 (s, 3H), 0.03 (s, 3H);  $^{13}\text{C}$  NMR (101 MHz,  $\text{CDCl}_3$ )  $\delta$  203.0, 171.0, 136.9, 127.5, 109.1, 71.8, 69.9, 46.3, 31.0, 30.9, 26.0 (3C), 19.3, 18.2, 18.0, -4.2, -4.8; TLC (hexane/ $\text{EtOAc}$ , 7:3,  $\text{KMnO}_4$ -stain)  $R_f = 0.56$ .

**(S)-3-((tert-butyldimethylsilyl)oxy)pent-4-yn-1-ol (21)**



To a solution of TBS-lactone **20** (1.50 g, 6.90 mmol, 1.00 equiv.) in  $\text{CH}_2\text{Cl}_2$  (75 mL) was added DIBAL-H (1.0 M in  $\text{CH}_2\text{Cl}_2$ , 8.30 mL, 8.30 mmol, 1.20 equiv.) at  $-78\text{ }^\circ\text{C}$ . The reaction mixture was stirred for 2 h at this temperature and then quenched by addition of MeOH (10 mL). The solution was poured into a saturated aq. solution of Rochelle salt (potassium sodium tartrate) (100 mL) and vigorously stirred for 3 hours at room temperature. The layers were separated and the aq. layer was extracted ( $\text{CH}_2\text{Cl}_2$ , 3 x 50 mL). The combined organic layers were washed with brine (50 mL), dried ( $\text{MgSO}_4$ ), filtered, and the solvent removed *in vacuo* to yield the crude lactol. Next, to a solution of LDA (1.0 M in hexane/THF, 16.6 mL, 16.6 mmol, 2.40 equiv.) in THF (18 mL) was added  $\text{TMSCHN}_2$  (2.0 M in  $\text{Et}_2\text{O}$ , 4.14 mL, 8.28 mmol, 1.20 equiv.) at  $-78\text{ }^\circ\text{C}$  and the reaction mixture was stirred for 30 min at the same temperature. The crude lactol in THF (20 mL) was carefully added and stirring was continued for 2 h. The reaction was warmed to rt, stirred for 30 min.<sup>1</sup> and then quenched by careful addition of a saturated aq. solution of  $\text{NH}_4\text{Cl}$  (15 mL). The layers were separated and the aqueous layer was extracted with  $\text{Et}_2\text{O}$  (3 x 50 mL). The combined organic layers were washed with brine (20 mL), dried ( $\text{MgSO}_4$ ), filtered, and the solvent removed *in vacuo*. Alcohol **21** (832 mg, 3.88 mmol, 46%) was obtained after purification by column chromatography (heptane/ $\text{EtOAc}$ , 8:2) as a colorless oil.  $[\alpha]_D^{20} = -55$  ( $c = 0.11$ ,  $\text{CHCl}_3$ );  $^1\text{H NMR}$  (400 MHz,  $\text{CDCl}_3$ )  $\delta$  4.61 (ddd,  $J = 7.0, 5.1, 2.1$  Hz, 1H), 3.89 (ddd,  $J = 11.8, 7.6, 4.2$  Hz, 1H), 3.75 (ddd,  $J = 10.9, 6.1, 4.5$  Hz, 1H), 2.47 (bs, 1H), 2.42 (d,  $J = 2.1$  Hz, 1H), 2.02 – 1.82 (m, 2H), 0.88 (s, 9H), 0.14 (s, 3H), 0.12 (s, 3H);  $^{13}\text{C NMR}$  (101 MHz,  $\text{CDCl}_3$ )  $\delta$  84.8, 73.2, 61.8, 59.8, 40.2, 25.8 (3C), 18.2, -4.5, -5.1; TLC (hexane/ $\text{EtOAc}$  8:2,  $\text{KMnO}_4$  stain)  $R_f = 0.21$ .

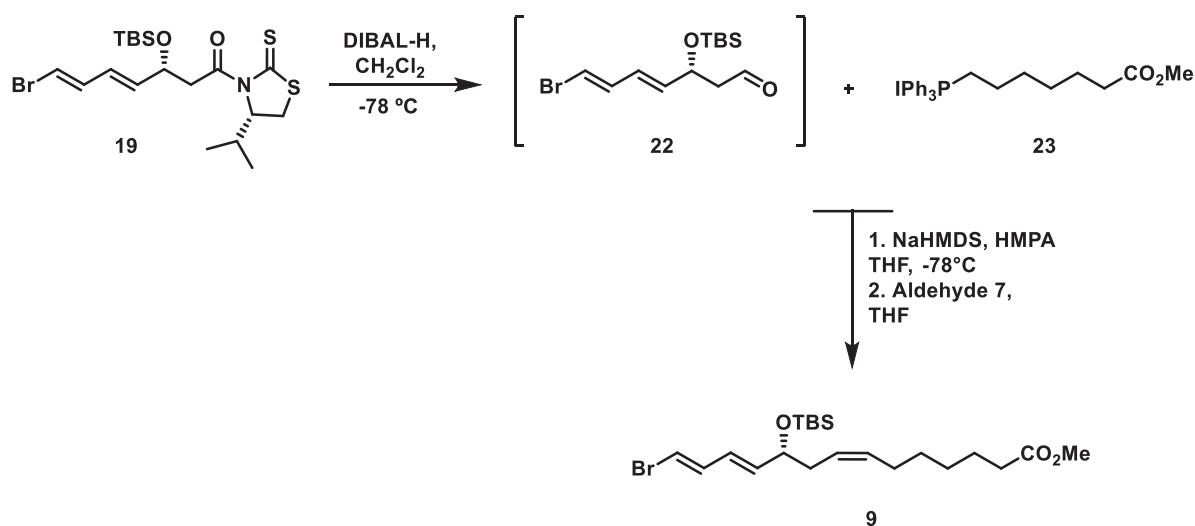
**(S)-3-((tert-butyldimethylsilyl)oxy)pent-4-ynal (7)**



Alcohol **21** (529 mg, 2.47 mmol, 1.00 equiv.) dissolved in dry  $\text{CH}_2\text{Cl}_2$  (22 mL) was added Dess-Martin periodinane (1.27 g, 2.99 mmol, 1.21 equiv.) and  $\text{NaHCO}_3$  (s) (972 mg, 11.6 mmol, 4.69 equiv.). After

6 hours, the reaction mixture was quenched with a saturated solution of  $\text{Na}_2\text{S}_2\text{O}_3$  (aq) (16 mL) and  $\text{NaHCO}_3$  (aq) (16 mL). The layers were separated and the aqueous layer was extracted with  $\text{Et}_2\text{O}$  ( $3 \times 10$  mL). The combined organic extracts were washed with brine (10 mL) dried ( $\text{Na}_2\text{SO}_4$ ) and concentrated *in vacuo*. The crude product was passed through a silica plug with hexane/ $\text{EtOAc}$  8:2 as eluent to afford the title compound **7** as a colorless oil. **Yield:** 515 mg (98%). All spectroscopic and physical data were in agreement with those reported in the literature.<sup>7</sup>  $^1\text{H NMR}$  (400 MHz,  $\text{CDCl}_3$ )  $\delta$  9.84 – 9.81 (m, 1H), 4.86 (ddd,  $J = 7.0, 4.9, 2.2$  Hz, 1H), 2.84 – 2.66 (m, 2H), 2.49 (d,  $J = 2.1$  Hz, 1H), 0.88 (s, 9H), 0.17 (s, 3H), 0.13 (s, 3H);  $^{13}\text{C NMR}$  (101 MHz,  $\text{CDCl}_3$ )  $\delta$  200.2, 83.9, 73.9, 58.2, 51.5, 25.8, 18.2, -4.5, -5.1; TLC ( $\text{EtOAc}$ /hexane 1:4,  $\text{KMnO}_4$  stain)  $R_f = 0.62$ .

**Methyl (*R,7Z,11E,13E*)-14-bromo-10-((*tert*-butyldimethylsilyl)oxy)tetradeca-7,11,13-trienoate (**9**)**

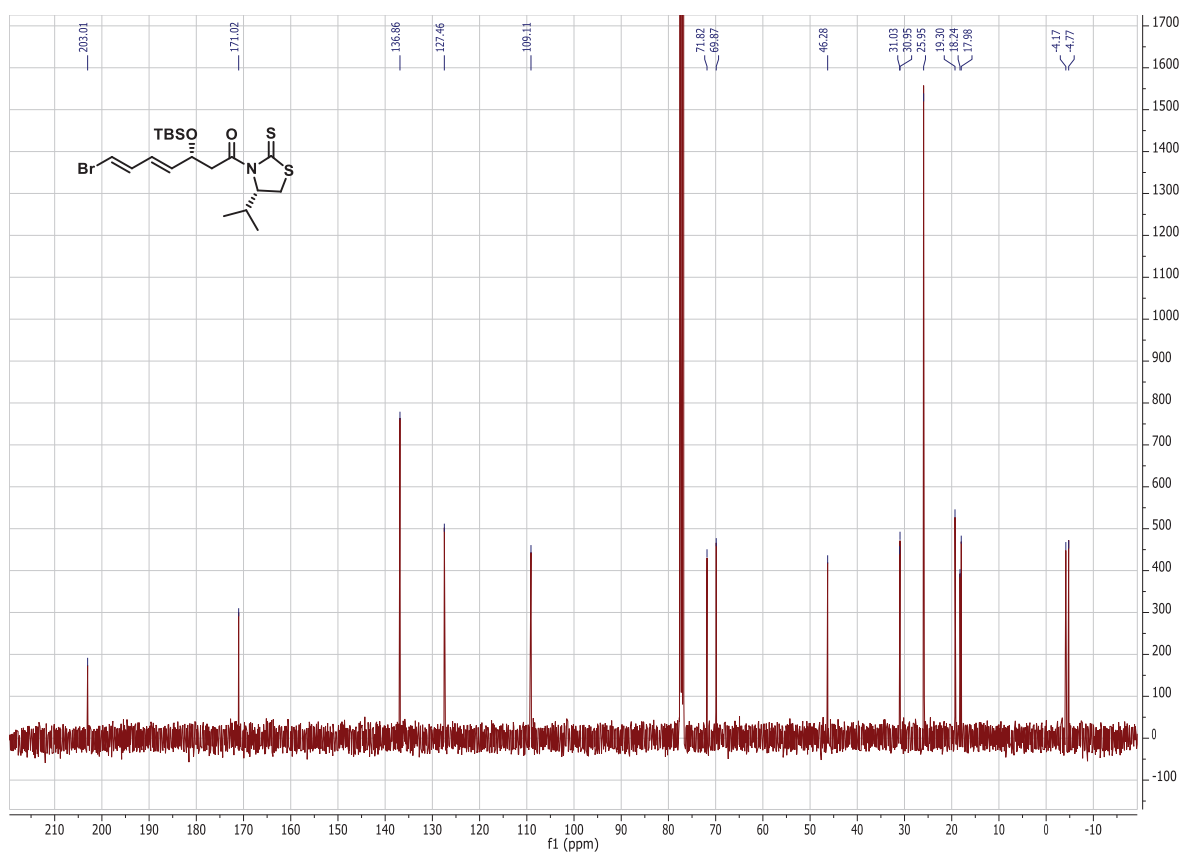
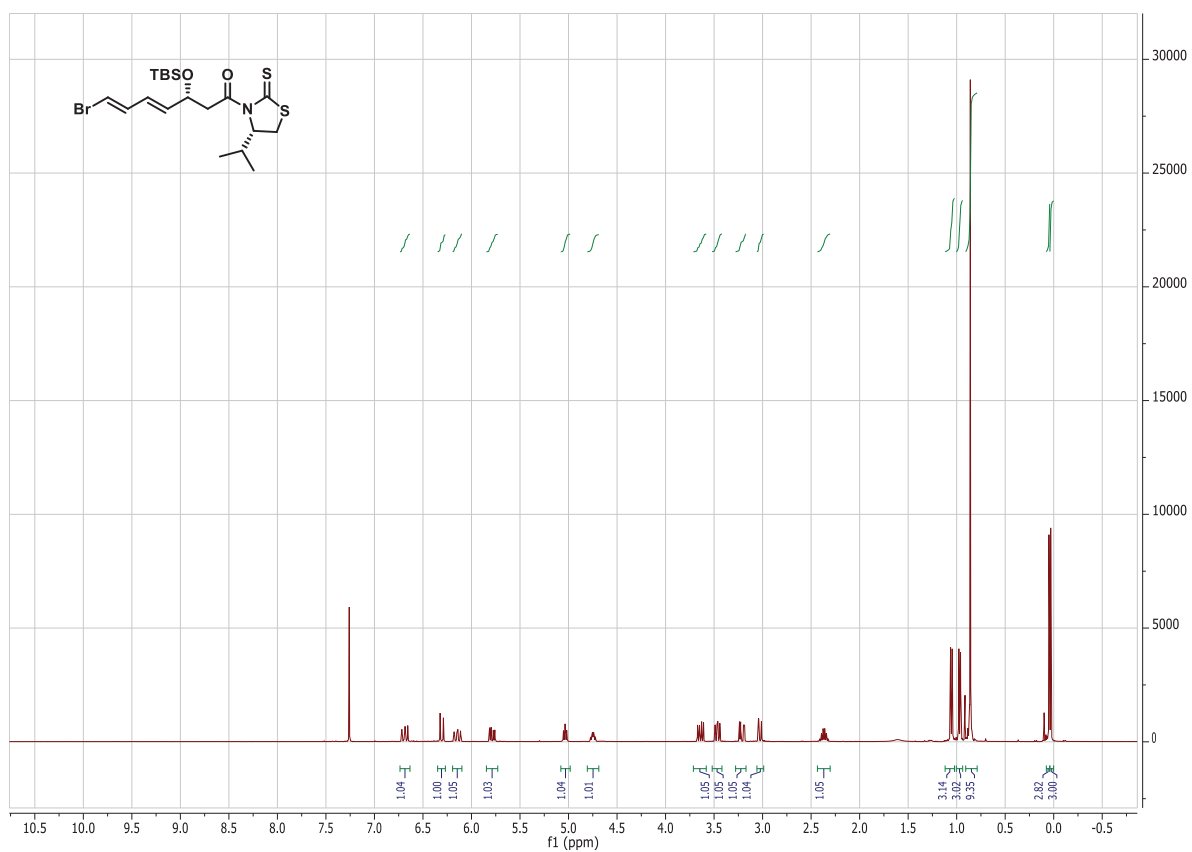


Following the procedure reported by Olivo and coworkers,<sup>8</sup> the protected thiazolidinethione **19** (578 mg, 1.21 mmol, 1.00 equiv.) was dissolved in  $\text{CH}_2\text{Cl}_2$  (23 mL) followed by dropwise addition of DIBAL-H (1.0 M in  $\text{CH}_2\text{Cl}_2$ , 1.45 mmol, 1.20 equiv.) at  $-78^\circ\text{C}$ . After three h., additional DIBAL-H was added (1.0 M in  $\text{CH}_2\text{Cl}_2$ , 0.240 mmol, 0.198 equiv.). The mixture was allowed to stir for 30 min and then quenched with saturated  $\text{NaHCO}_3$  (aq) (14 mL). The cooling bath was removed and solid Na-K tartrate (~ 0.400 g) (Rochelle salt) was added and stirring was continued for another 45 min.  $\text{Et}_2\text{O}$  (35 mL) was added. The layers were separated and the aq. layer was extracted with  $\text{Et}_2\text{O}$  ( $3 \times 30$  mL). The combined organic layers were dried ( $\text{Na}_2\text{SO}_4$ ) and concentrated *in vacuo*. The residue was purified by column chromatography on silica gel (hexane/ $\text{EtOAc}$  95:5)  $R_f = 0.24$ , and concentrated *in vacuo*, but not to dryness. Commercially available Wittig salt **23** (670 mg, 1.26 mmol, 1.00 equiv.) in THF (16 mL) and HMPA (1.7 mL) was slowly added NaHMDS (0.6 M in THF, 2.1 mL, 1.04 equiv.) at  $-78^\circ\text{C}$  and then stirred for 15 min at  $0^\circ\text{C}$ . The purified aldehyde **22** was added. The solution was allowed to slowly

warm up to room temperature in the dry ice/acetone bath for 24 h before it was quenched with phosphate buffer (12 mL, pH = 7.2). Et<sub>2</sub>O (15 mL) was added and the phases were separated. The aqueous phase was extracted with Et<sub>2</sub>O (2 × 15 mL) and the combined organic layers were dried (Na<sub>2</sub>SO<sub>4</sub>), before concentrated *in vacuo*. The crude product was purified by column chromatography on silica (hexane/EtOAc 95:5) to afford the title compound **9** as a clear oil. **Yield:** 386 mg (45-72% over two steps). All spectroscopic and physical data were in agreement with those reported in the literature.<sup>9</sup> [ $\alpha$ ]<sub>D</sub><sup>20</sup> = -18.0 (c = 0.090, MeOH); <sup>1</sup>H NMR (400 MHz, CDCl<sub>3</sub>)  $\delta$  6.68 (dd, *J* = 13.4, 10.9 Hz, 1H), 6.27 (d, *J* = 13.5 Hz, 1H), 6.09 (dd, *J* = 15.2, 10.9 Hz, 1H), 5.71 (dd, *J* = 15.3, 9.6 Hz, 1H), 5.48–5.29 (m, 2H), 4.17 – 4.11 (m, 1H), 3.67 (s, 3H), 2.34 – 2.16 (m, 4H), 2.00 (q, *J* = 6.8 Hz, 2H), 1.62 (p, *J* = 7.5 Hz, 2H), 1.41 – 1.26 (m, 4H), 0.89 (s, 9H), 0.04 (s, 3H), 0.02 (s, 3H); <sup>13</sup>C NMR (101 MHz, CDCl<sub>3</sub>)  $\delta$  174.4, 138.1, 137.2, 131.9, 126.6, 125.2, 108.2, 72.7, 51.6, 36.3, 34.2, 29.4, 29.0, 27.4, 26.0 (3C), 25.0, 18.4, -4.4, -4.6; TLC (hexane/EtOAc 95:5, KMnO<sub>4</sub> stain) *R*<sub>f</sub> = 0.33.



## **$^1\text{H}$ -NMR and $^{13}\text{C}$ -NMR spectra**



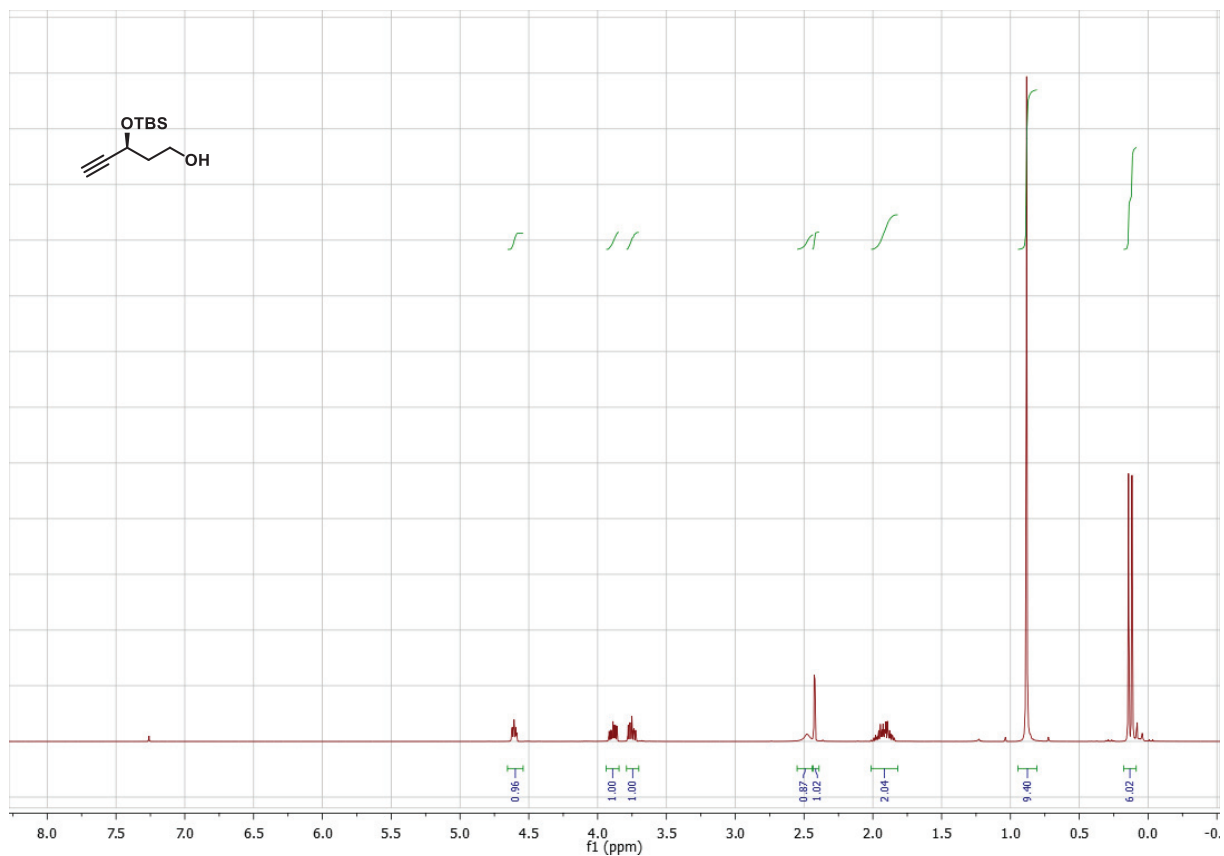


Figure S-3. <sup>1</sup>H-NMR spectrum of compound 21.

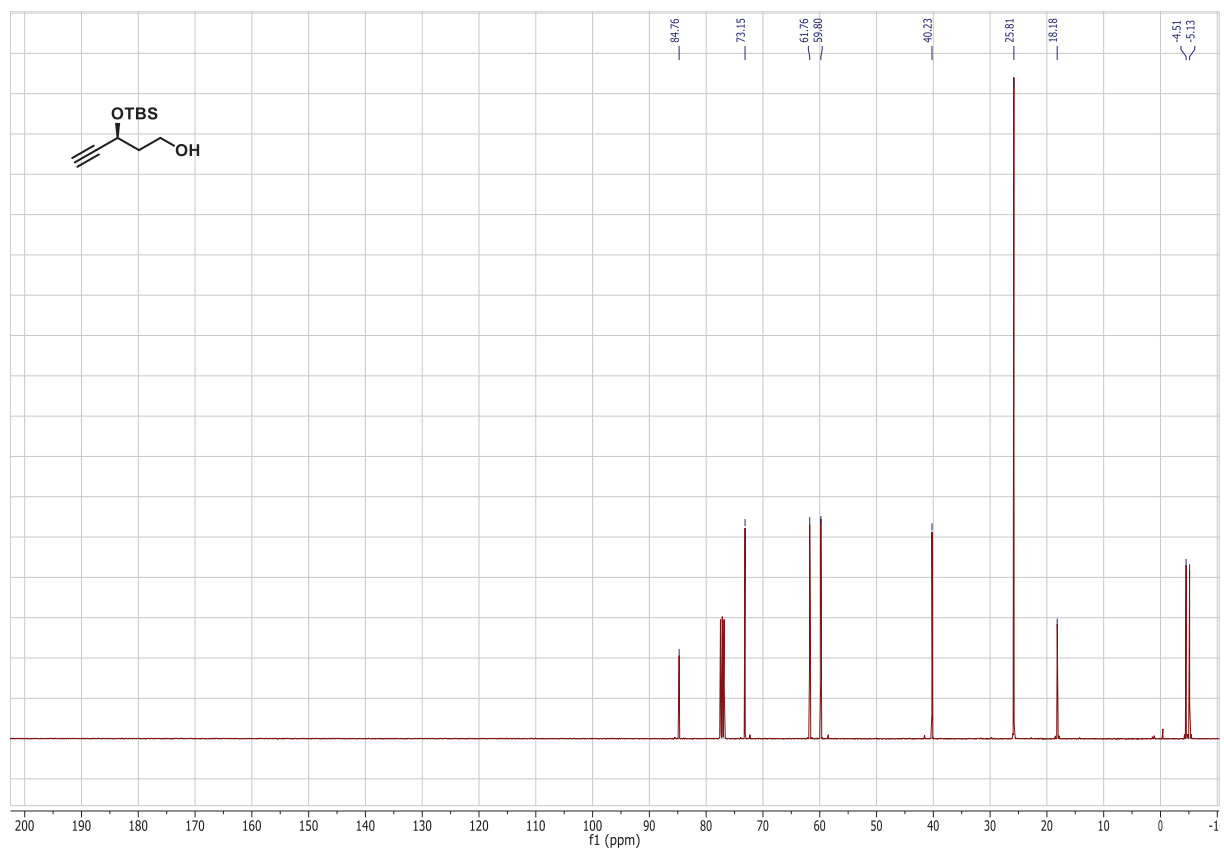
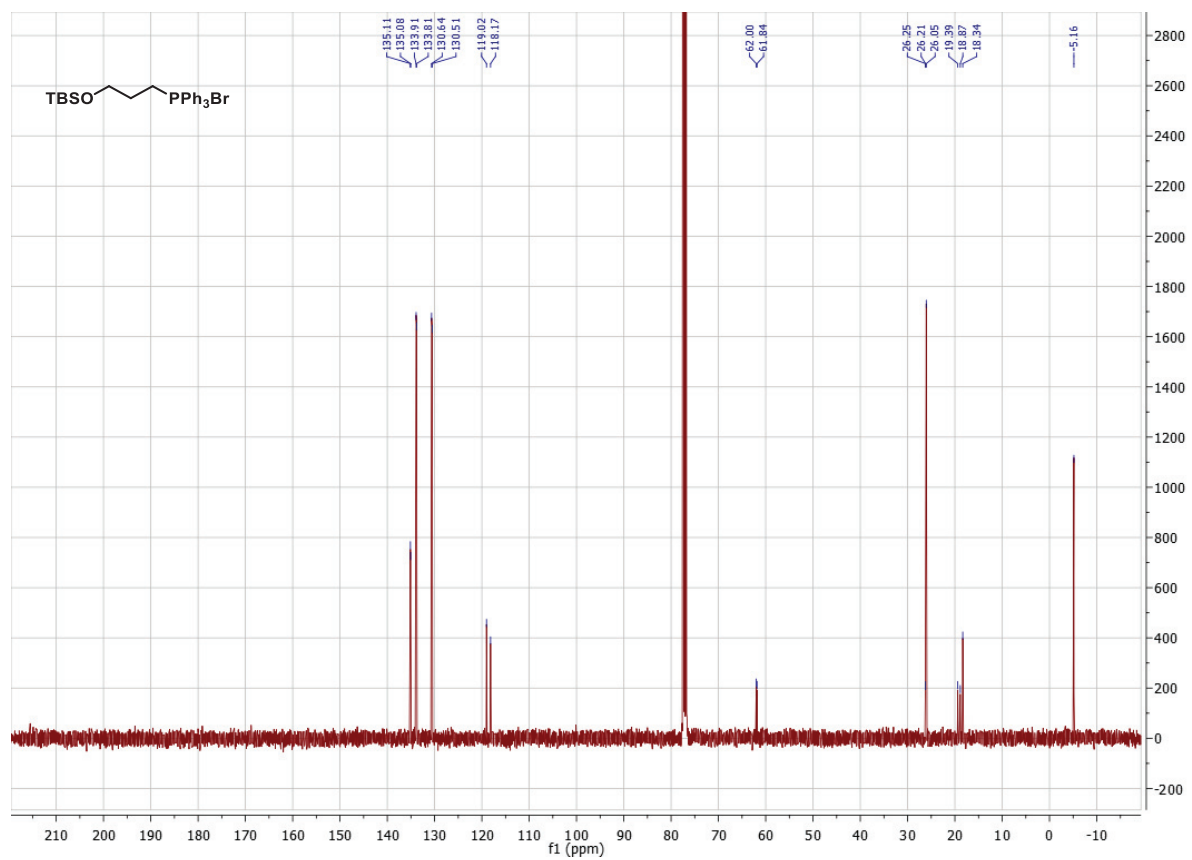
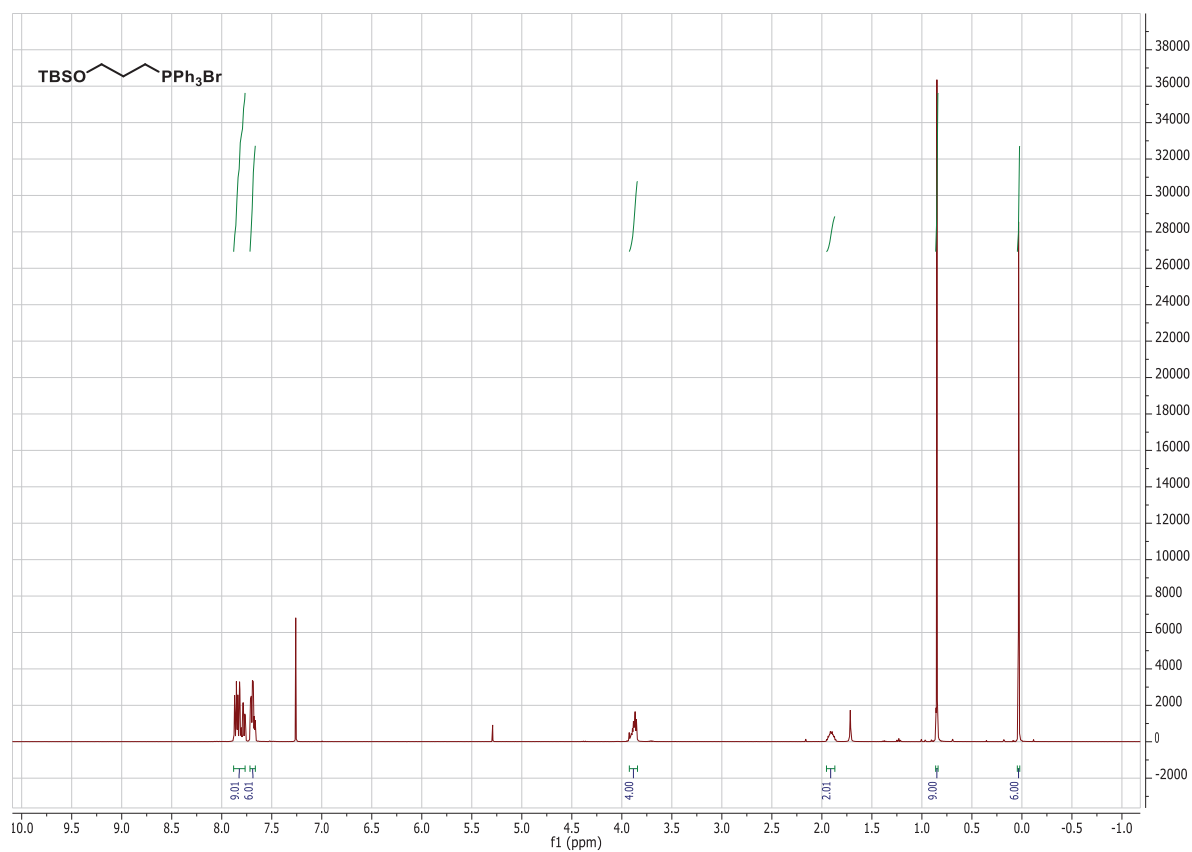


Figure S-4. <sup>13</sup>C-NMR spectrum of compound 21.



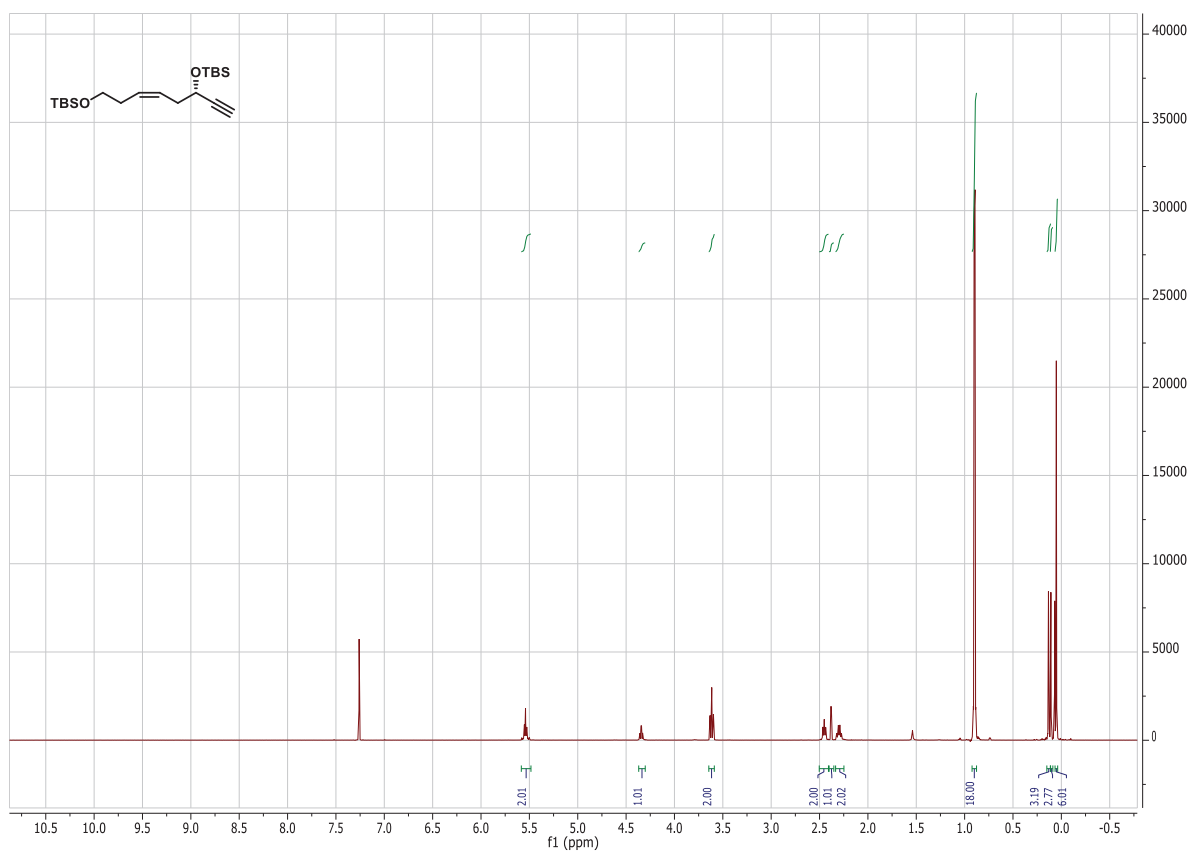


Figure S-7. <sup>1</sup>H-NMR spectrum of compound 8.

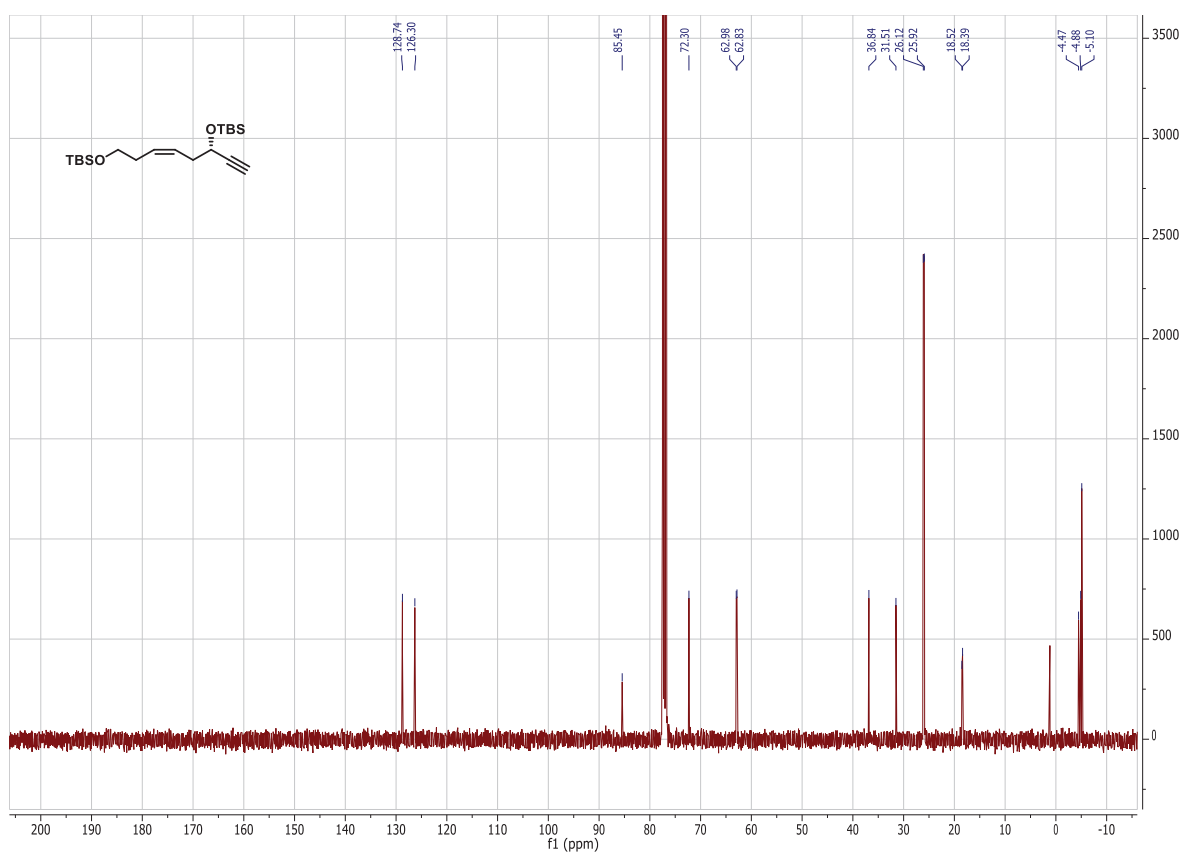


Figure S-8. <sup>13</sup>C-NMR spectrum of compound 8.

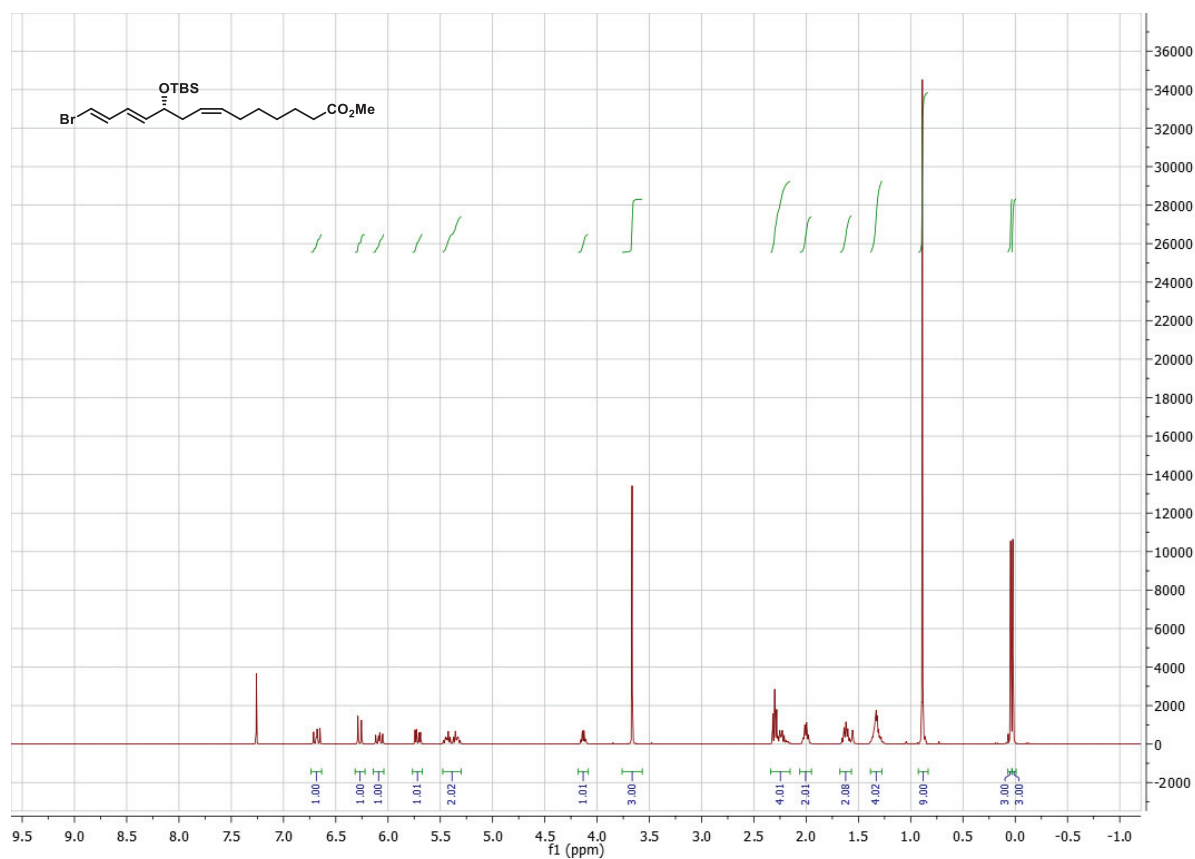


Figure S-9. <sup>1</sup>H-NMR spectrum of compound 9.

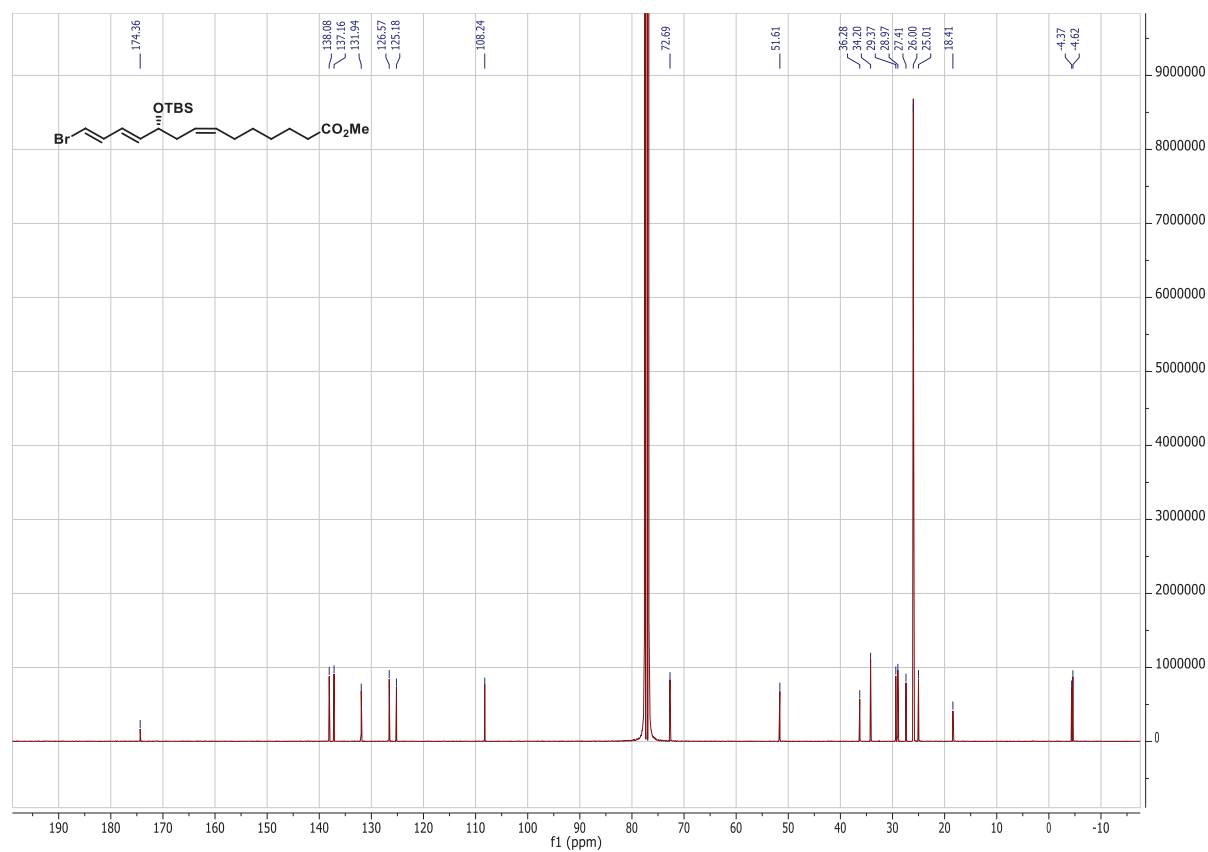


Figure S-10. <sup>13</sup>C-NMR spectrum of compound 9.

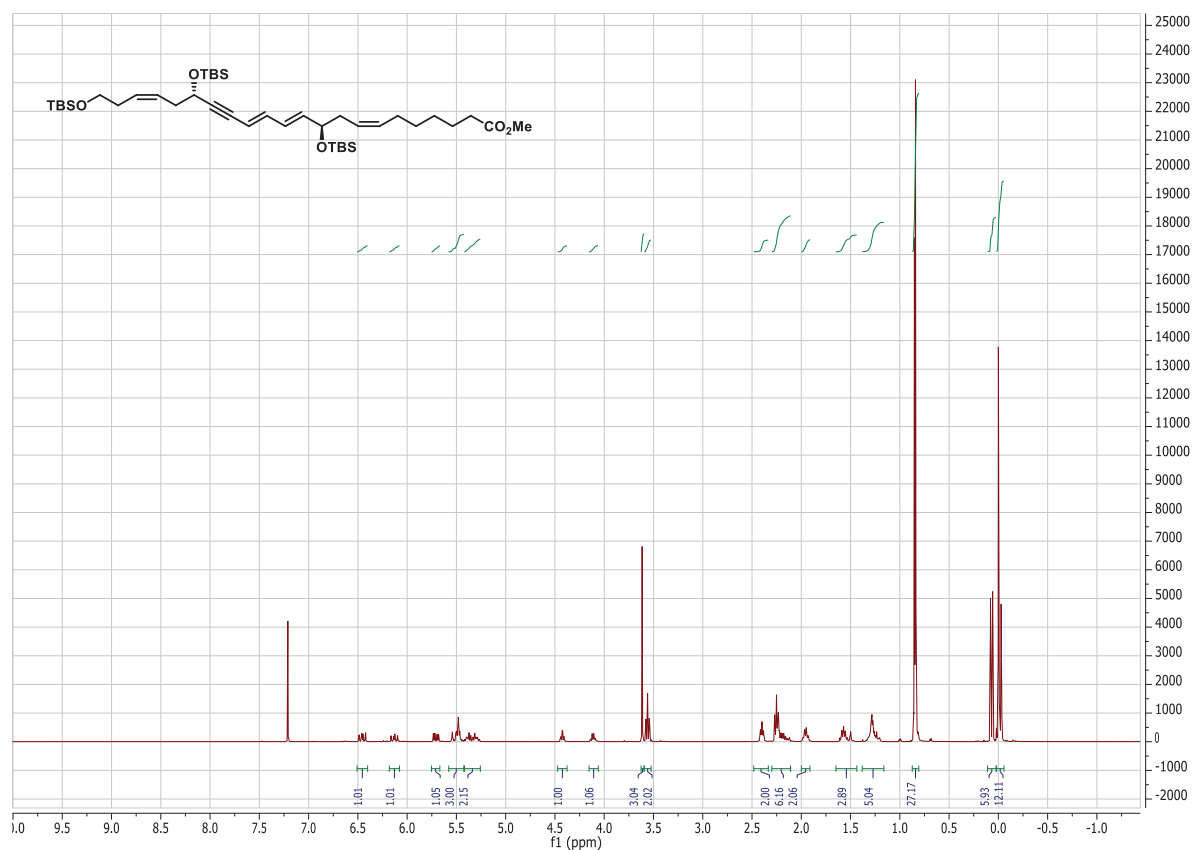


Figure S-11. <sup>1</sup>H-NMR spectrum of compound 10.

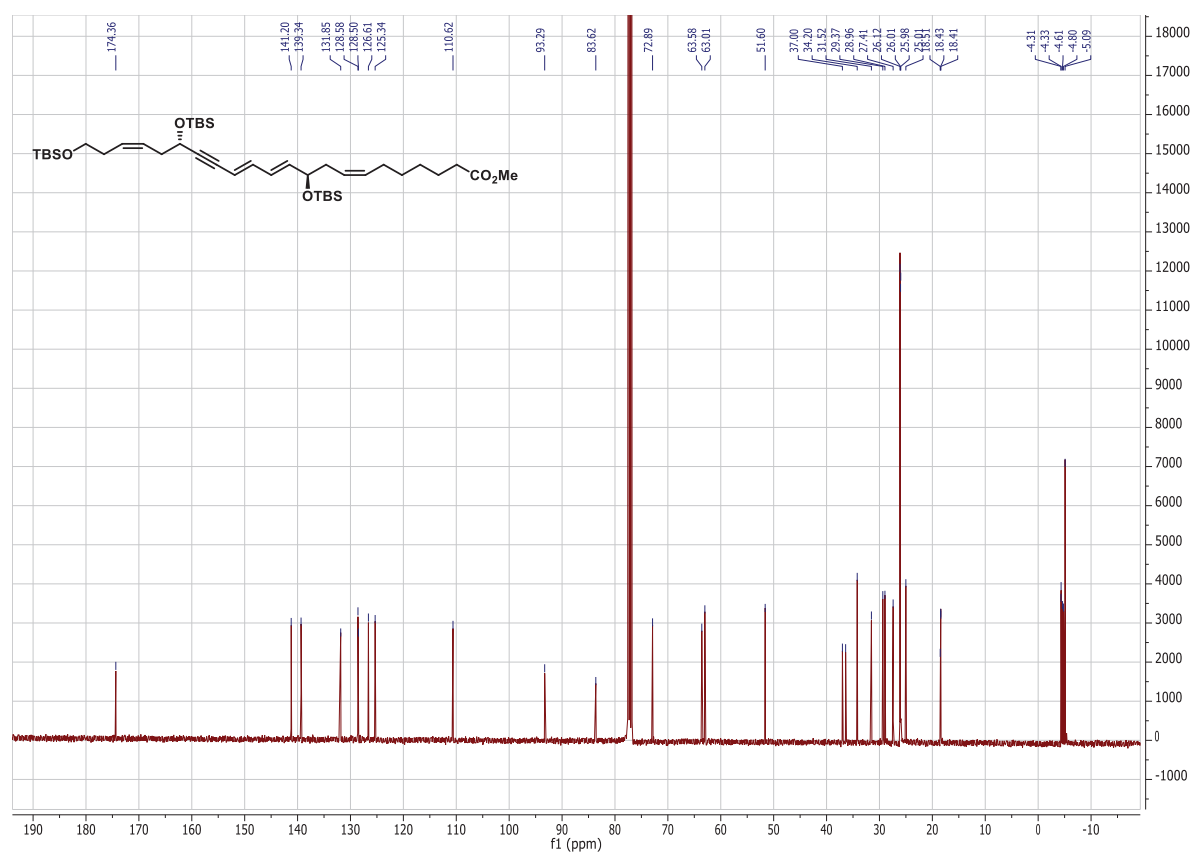


Figure S-12. <sup>13</sup>C-NMR spectrum of compound 10.

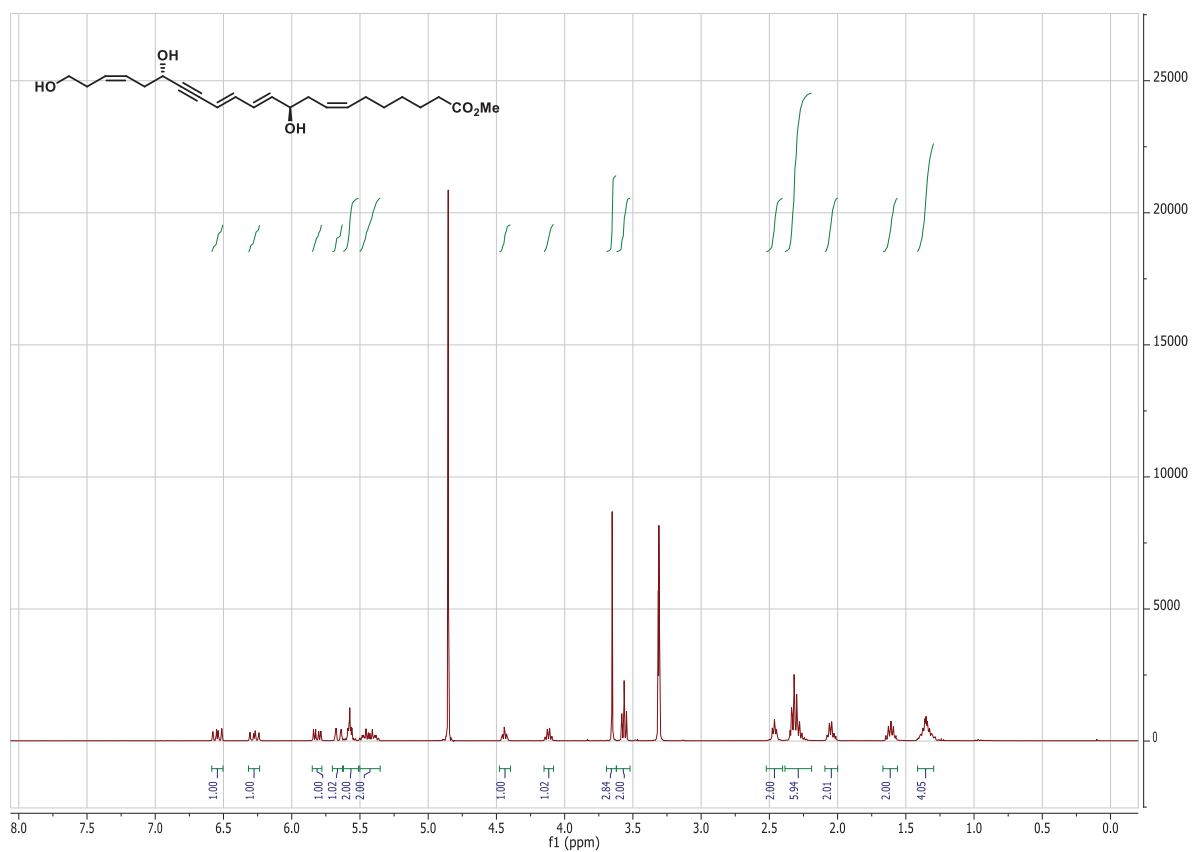


Figure S-13. <sup>1</sup>H-NMR spectrum of compound 11.

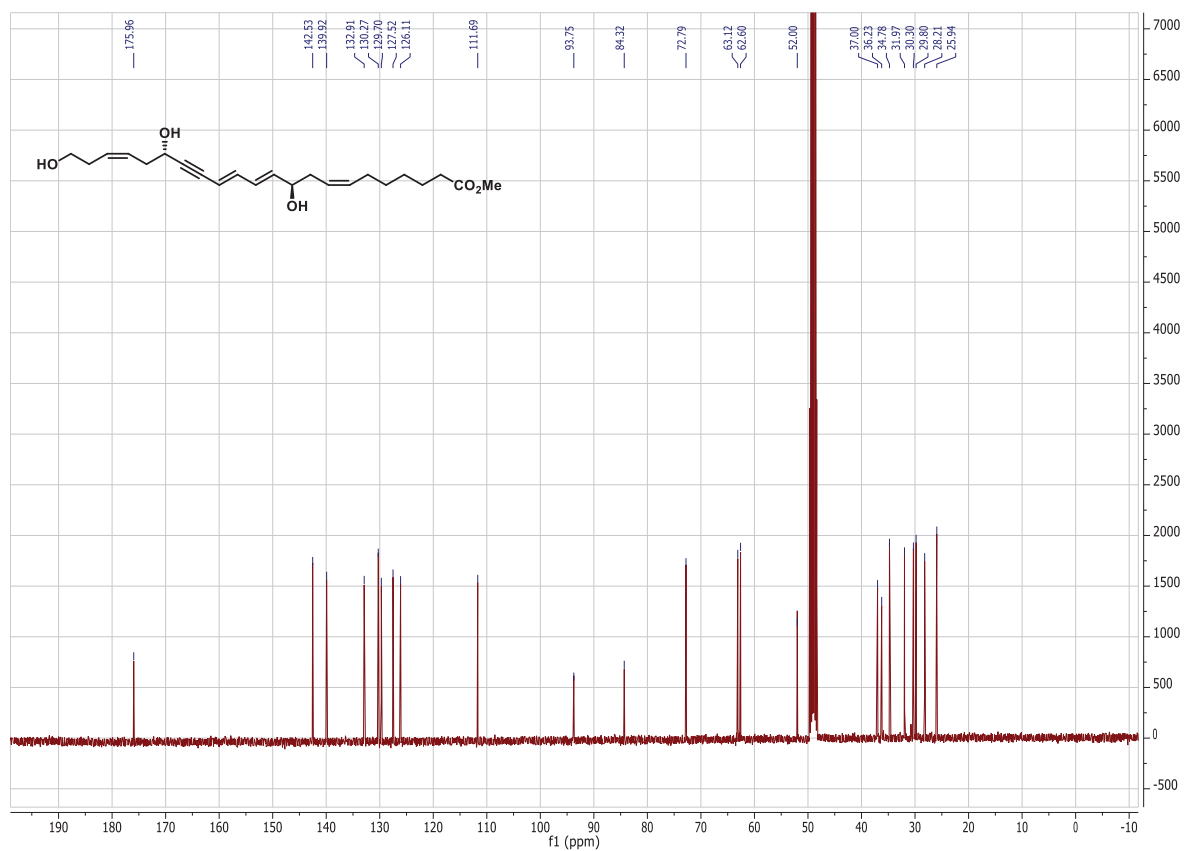


Figure S-14. <sup>13</sup>C-NMR spectrum of compound 11.



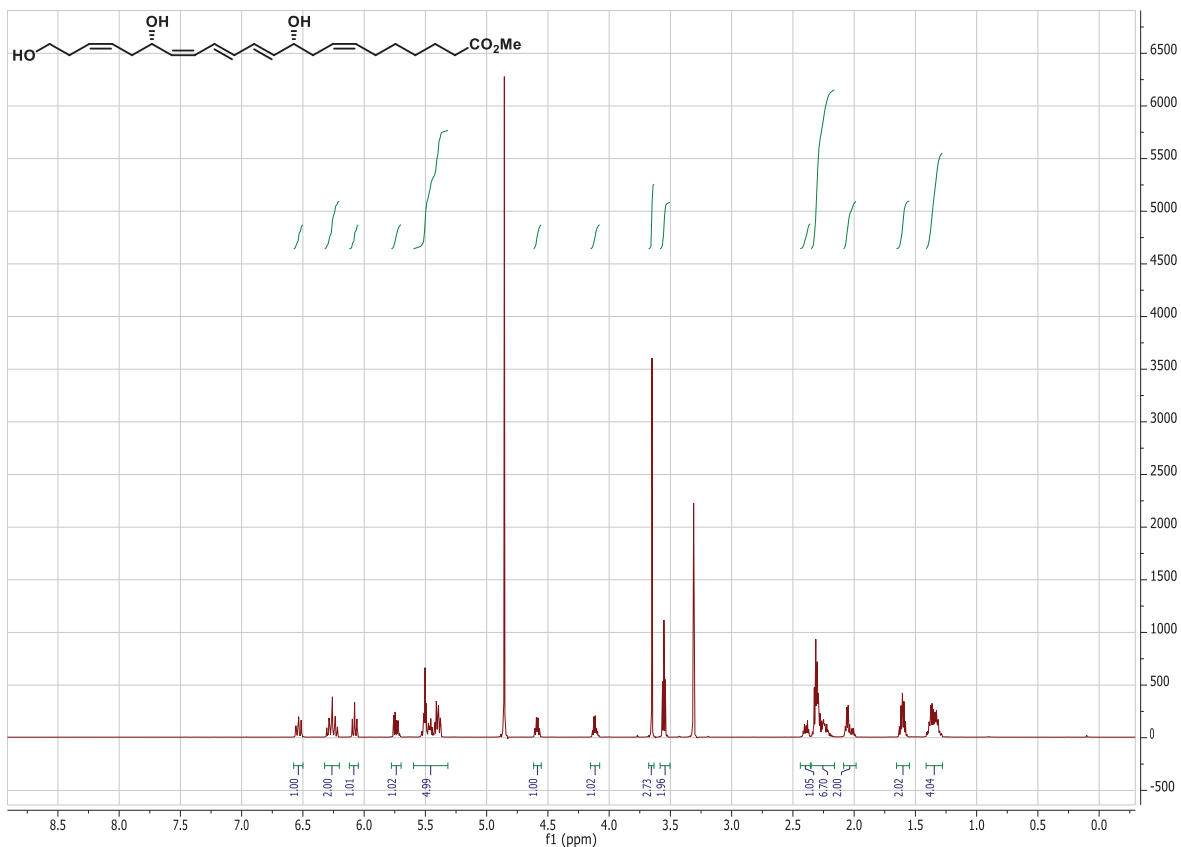


Figure S-15. <sup>1</sup>H-NMR spectrum of 22-OH-PD<sub>1n-3</sub> DPA methyl ester (**12**).

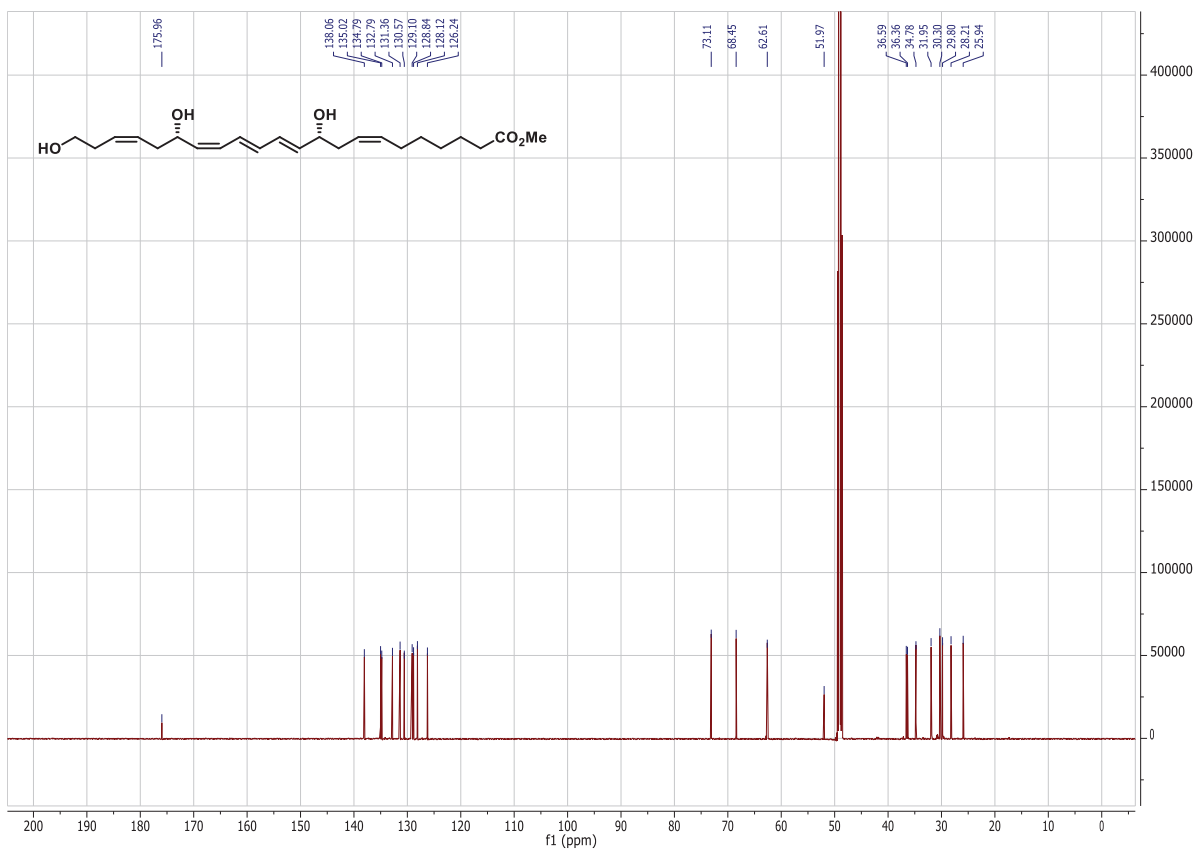


Figure S-16. <sup>13</sup>C-NMR spectrum of 22-OH-PD<sub>1n-3</sub> DPA methyl ester (**12**).

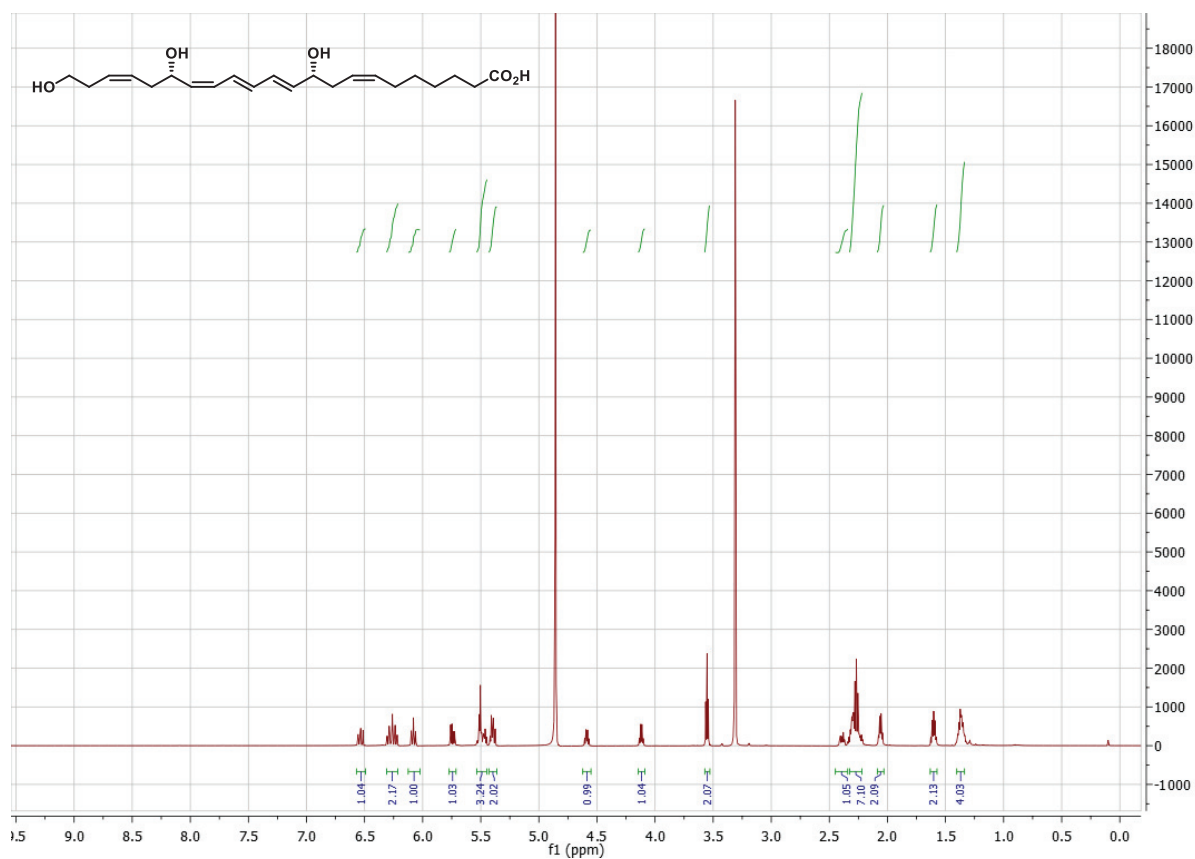


Figure S-17. <sup>1</sup>H-NMR spectrum of 22-OH-PD1<sub>n-3</sub> DPA (5).

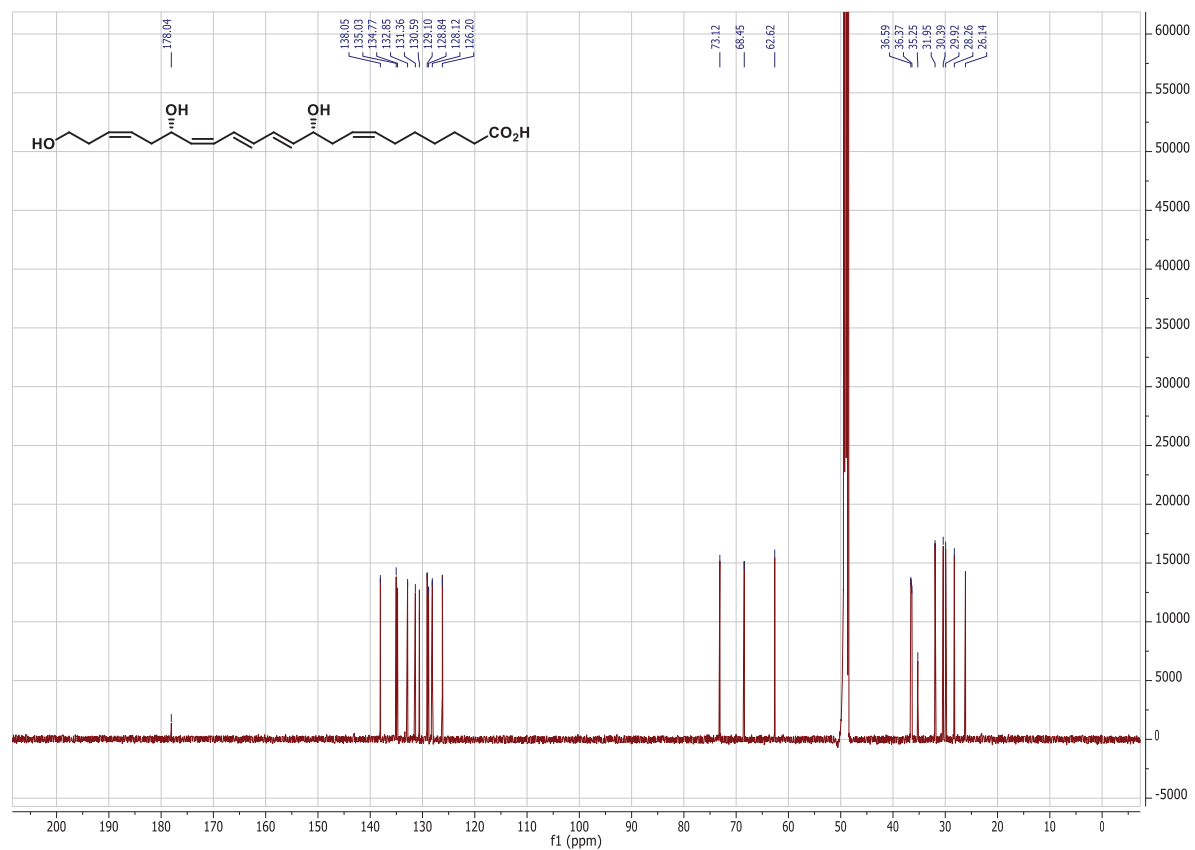
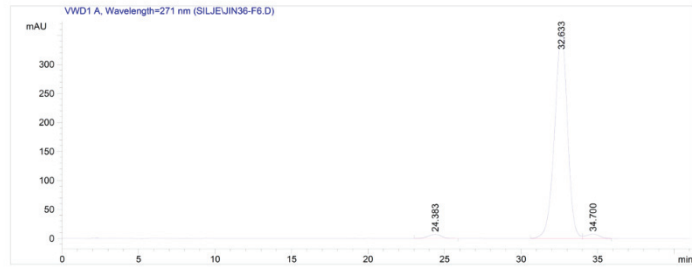


Figure S-18. <sup>13</sup>C-NMR spectrum of 22-OH-PD1<sub>n-3</sub> DPA (5).

# HPLC Chromatograms

Data File C:\CHEM32\1\DATA\SILJE\JIN36-F6.D  
 Sample Name: JIN36-F6  
 =====  
 Acq. Operator : Silje  
 Acq. Instrument : Instrument 1 Location : Vial 1  
 Injection Date : 24.05.2018 13:13:24 Inj Volume : 15 µl  
 Method : C:\CHEM32\1\METHODS\DGTHMTST.M  
 Last changed : 24.05.2018 10:40:55 by Silje  
 (modified after loading)  
 Method Info : Column thermostat functional test method  
 =====  
 Sample Info : Flash 5 metylester 22-OH-PD1n-3. 60:40, MeOH:H2O. 1ml/m  
 in, 271 nm, C-18 kolonne  
 =====



=====  
 Area Percent Report  
 =====

Sorted By : Signal  
 Multiplier : 1.0000  
 Dilution : 1.0000  
 Sample Amount : 1.00000 [ng/ul] (not used in calc.)  
 Use Multiplier & Dilution Factor with ISTDs

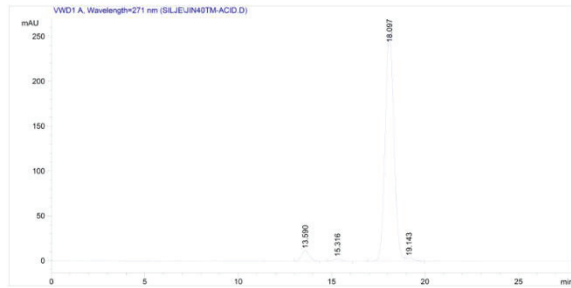
Signal 1: VWD1 A, Wavelength=271 nm

Peak #	RetTime [min]	Type	Width [min]	Area mAU *s	Height [mAU]	Area %
1	24.383	BB	0.6846	390.51266	6.71915	1.7983
2	32.633	BV	0.8864	2.08952e4	356.39899	96.2198
3	34.700	VB	0.6923	430.39163	7.44101	1.9819

Totals : 2.17161e4 370.55914

Figure S-19. HPLC chromatogram of 22-OH-PD1<sub>n-3</sub> DPA methyl ester (12).

Data File C:\CHEM32\1\DATA\SILJE\JIN40TM-ACID.D  
 Sample Name: JIN40TM-ACID  
 =====  
 Acq. Operator : silje  
 Acq. Instrument : Instrument 1 Location : Vial 1  
 Injection Date : 20.06.2018 16:04:13 Inj Volume : 10 µl  
 Acq. Method : C:\CHEM32\1\METHODS\DGTHMTST.M  
 Last changed : 20.06.2018 15:55:44 by silje  
 (modified after loading)  
 Analysis Method : C:\CHEM32\1\METHODS\DGTHMTST.M  
 Last changed : 21.06.2018 13:42:34 by Jonn  
 (modified after loading)  
 Method Info : Column thermostat functional test method  
 =====  
 Sample Info : JIN40TM-ACIDsyre, maämolekyl 271 nm, 1 mL/min, 65:20:20  
 metanol vann, 10ml maursyre, C-18, 10mlkolliter injeka  
 jon



=====  
 Area Percent Report  
 =====

Sorted By : Signal  
 Multiplier : 1.0000  
 Dilution : 1.0000  
 Sample Amount : 1.00000 [ng/ul] (not used in calc.)  
 Use Multiplier & Dilution Factor with ISTDs

Signal 1: VWD1 A, Wavelength=271 nm

Peak #	RetTime [min]	Type	Width [min]	Area mAU *s	Height [mAU]	Area %
1	13.590	BB	0.4379	350.90503	11.84972	3.9367
2	15.316	BB	0.3532	77.37843	2.83119	0.8681
3	18.097	BV	0.5033	8372.52051	257.37936	93.9286
4	19.143	VB	0.3589	112.90607	3.70745	1.2667

Figure S-20. HPLC chromatogram of 22-OH-PD1<sub>n-3</sub> DPA (5).

## Lipid Mediator Metabololipidomics

Matching of synthetic **5** with endogenous products was conducted as previously reported.<sup>10</sup> Summarily, biological samples were subject to C18 solid-phase extraction. Prior to sample extraction, d<sub>4</sub>-LTB<sub>4</sub>, (500 pg), d<sub>5</sub>-RvE1 (100 pg), were added as internal standards. Extracted samples were analyzed using QTrap 6500+ (ABSciex) MS system, coupled with a Shimadzu SIL-20AC HT autosampler and LC-20AD LC pumps. Agilent C18 Poroshell column (150 mm × 4.6 mm × 2.7 μm) was used to profile lipid mediators. The gradient was initiated at 20:80:0.01 (vol/vol/vol) methanol/water/acetic acid for 0.2 min this was ramped to 50:50:0.01 (vol/vol/vol) over 12 s, maintained for 2 min, then ramped to 80:20:0.01 (vol/vol/vol) over 9 min, and maintained for 3.5 min. The ratio was then ramped to 98:2:0.01 (vol/vol/vol) for 5.5 min. The flow rate was kept at 0.5 mL/min throughout elution.

Mediator identity was established using multiple reaction monitoring (MRM) using signature parent ion (Q1) and characteristic daughter ion (Q3) pairs to match retention time of the biological material to synthetic material (**5**). Then, using an Enhanced Product Ion (EPI) scan a minimum of six diagnostic ions were used to confirm identity, in accordance with published criteria.<sup>10</sup>

### Matching of synthetic 22-OH-PD1<sub>n-3</sub> DPA with material formed in human monocytes incubated with PD1<sub>n-3</sub> DPA

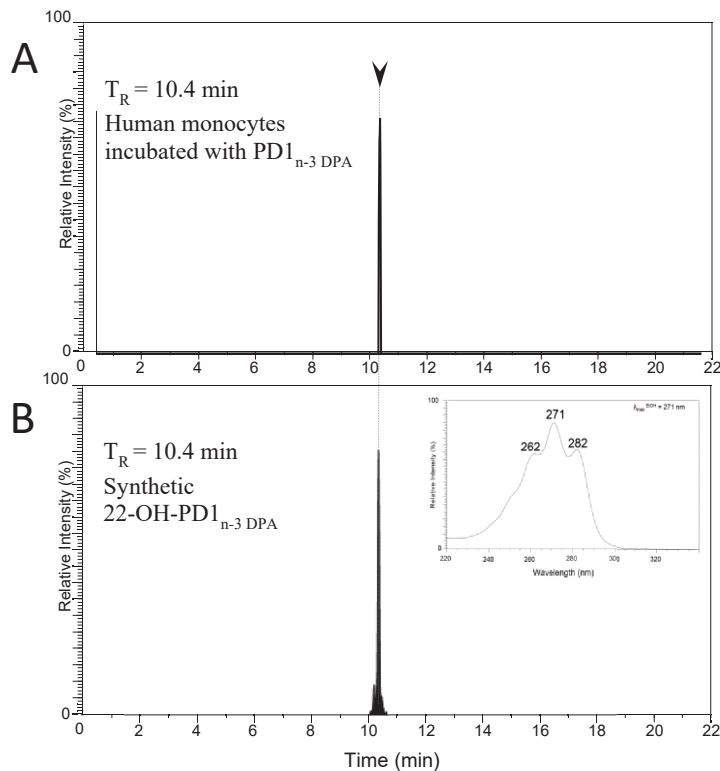


**Figure S-21.** PD1<sub>n-3</sub> DPA is converted to 22-OH-PD1<sub>n-3</sub> DPA by human monocytes. Multiple reaction monitoring chromatograms for  $m/z$  377>361 of the products obtained from (A) Human monocytes incubated with PD1<sub>n-3</sub> DPA. (B) Synthetic 22-OH-PD1<sub>n-3</sub> DPA.

### MS-MS fragmentation spectra of 22-OH-PD1<sub>n-3</sub> DPA

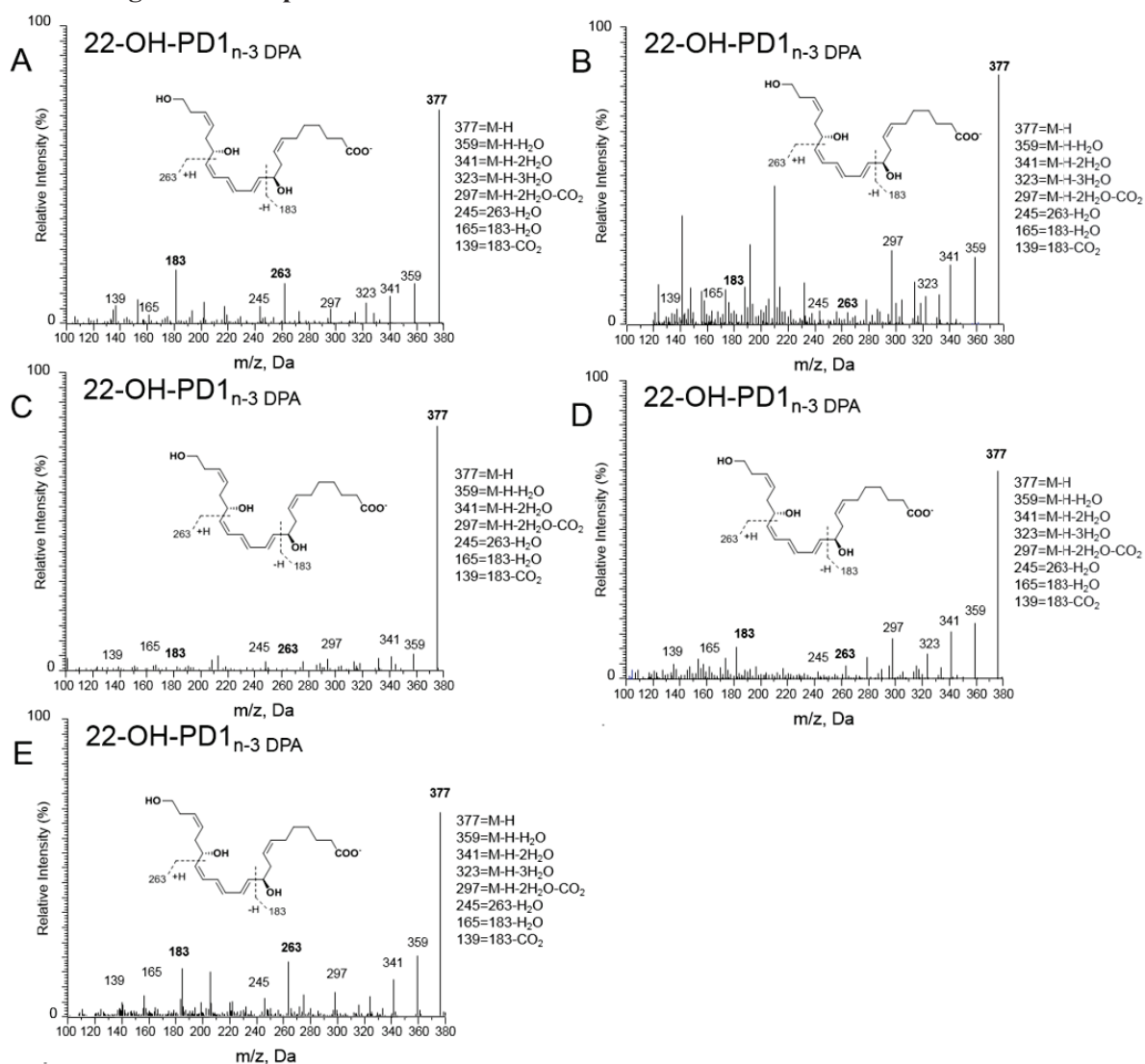


**Figure S-22.** MS-MS spectra employed for identification of **5** obtained from (A) Synthetic material, (B) Human serum, (C) Human neutrophils, (D) Human monocytes, (E) Human neutrophils incubated with **2**.

## UV-Vis Spectra

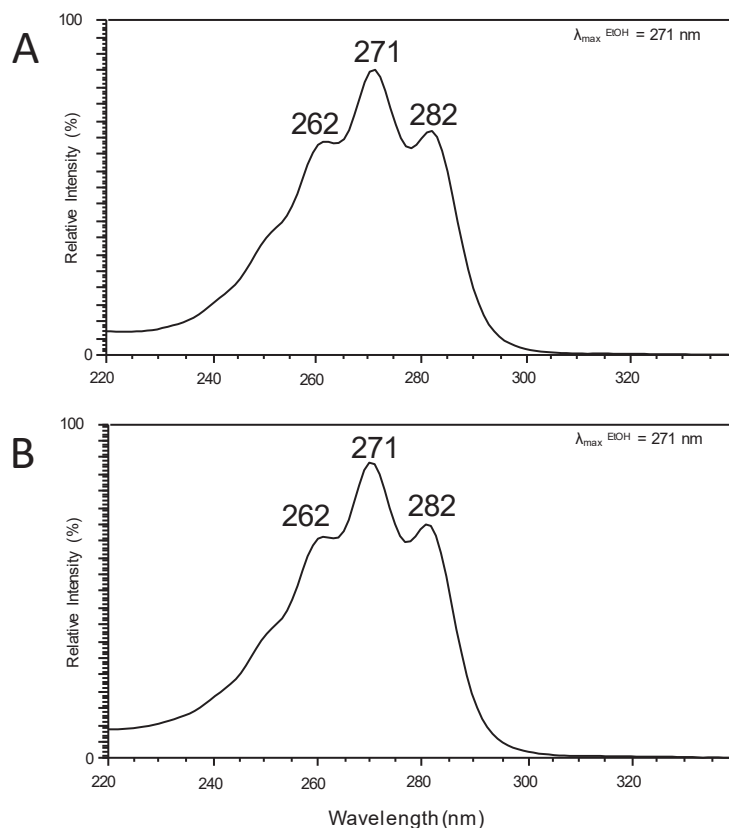


Figure S-23. UV-Vis chromatogram of (A) synthetic 22-OH-PD1<sub>n-3</sub> DPA and (B) PD1<sub>n-3</sub> DPA in ethanol.

## References

1. Delaunay, D.; Toupet, L.; Corre, M. L., *J. Org. Chem.* **1995**, *60* (20), 6604.
2. Nagao, Y.; Dai, W. M.; Ochiai, M.; Tsukagoshi, S.; Fujita, E., *J. Org. Chem.* **1990**, *55* (4), 1148.
3. Becher, J., *Org. Synth.* **1979**, *59*, 79.
4. Soullez, D.; Plé, G.; Duhamel, L., *J. Chem. Soc. Perkin Transactions 1.* **1997**, (11), 1639.
5. Romero-Ortega, M.; Colby, D. A.; Olivo, H. F., *Tetrahedron Lett.* **2002**, *43*, 6439.
6. Corey, E. J.; Cho, H.; Rucker, C.; Hua, D. H., *Tetrahedron Lett.* **1981**, *22*, 3455.
7. Tungen, J. E.; Aursnes, M.; Dalli, J.; Arnadottir, H.; Serhan, C. N.; Hansen, T. V., *Chem. Eur. J.* **2014**, *20*, 14575.
8. Tello-Aberto, R.; Ochoa-Teran, A.; Olivo, H. F., *Tetrahedron Lett.* **2006**, *47*, 5915.
9. Aursnes, M.; Tungen, J. E.; Vik, A.; Colas, R.; Cheng, C. Y.; Dalli, J.; Serhan, C.N.; Hansen, T.V., *J. Nat. Prod.* **2014**, *77* (4), 910.
10. Dalli, J.; Winkler, J. W.; Colas, R. A.; Arnadottir, H.; Cheng, C. Y.; Chiang, N.; Petasis, N. A.; Serhan, C. N., *Chem. Biol.* **2013**, *20* (2), 188.

**Paper III:**

*Stereoselective synthesis of the specialized pro-resolving and anti-inflammatory mediator  
resolvin E1*

Jannicke Irina Nesman, Jørn Eivind Tungen, Anders Vik and Trond Vidar Hansen.

*Tetrahedron*, **2020**, 76 (3), 130821-130826.







# Stereoselective synthesis of the specialized pro-resolving and anti-inflammatory mediator resolvin E1

Jannicke Irina Nesman, Jørn Eivind Tungen, Anders Vik, Trond Vidar Hansen\*

Department of Pharmacy, Section for Pharmaceutical Chemistry, University of Oslo, PO Box 1068 Blindern, N-0316 Oslo, Norway

## ARTICLE INFO

### Article history:

Received 8 October 2019  
Received in revised form  
21 November 2019  
Accepted 22 November 2019  
Available online 25 November 2019

### Keywords:

Resolvin E1  
Oxygenated polyunsaturated fatty acid  
Stereoselective synthesis  
Specialized pro-resolving mediator  
Anti-inflammatory  
Resolution of inflammation

## ABSTRACT

The n-3 polyunsaturated fatty acids eicosapentaenoic acid, docosahexaenoic acid and n-3 docosapentaenoic acid, act as substrates for the biosynthesis of specialized pro-resolving lipid mediators. Resolvin E1, produced from eicosapentaenoic acid, was the first specialized pro-resolving lipid mediator reported. This oxygenated polyunsaturated fatty acid displays a plethora of interesting biological activities, and has entered initial clinical trial development programs. The Evans-Nagao aldol reaction, a stereoselective alkyne reduction and a Z-selective Wittig reaction, were utilized for the stereocontrolled synthesis of resolvin E1 presented herein. In addition, results from HPLC analysis revealed that the synthetic material matched authentic resolvin E1.

© 2019 The Authors. Published by Elsevier Ltd. This is an open access article under the CC BY-NC-ND license (<http://creativecommons.org/licenses/by-nc-nd/4.0/>).

## 1. Introduction

Polyunsaturated fatty acids (PUFAs) such as eicosapentaenoic acid (EPA) and docosahexaenoic acid (DHA), see Fig. 1, play a major role in human physiology by dampening the negative effects of inflammatory processes [1]. These two omega-3 PUFAs are abundant in marine organisms, fat fish and commercial fish oil products that are widely used as dietary supplements [1]. Furthermore, the potential health benefits of EPA and DHA have been linked to prevention of several human diseases [2,3]. More recently, n-3 docosapentaenoic acid (n-3 DPA) has also attracted interest from the biomedical community [4]. For a long period of time it was believed that EPA and DHA exhibited anti-inflammatory properties [5] by competing with arachidonic acid (AA) in the suppression of inflammatory responses and thereby reducing the biosynthesis of pro-inflammatory eicosanoids derived from AA [6]. Examples of classical eicosanoids are the prostaglandins, thromboxanes and leukotrienes [7]. Recent efforts have shown that lipoxygenase (LOX) enzymes and cyclooxygenase-2 (COX-2) in resolving inflammatory exudates use EPA, DHA and n-3 DPA as substrates in the biosynthesis of individual families of oxygenated PUFA products that are

collectively named specialized pro-resolving lipid mediators (SPMs), see Fig. 1 [8].

SPMs are resolution agonists [8] acting on individual G-protein coupled receptors (GPCRs) [9] that display very potent pro-resolution and anti-inflammatory bioactions *in vivo* [10]. These exciting biological activities have spurred a great interest using SPMs as biotemplates in drug development efforts - aiming at providing new anti-inflammatory agents without immunosuppressive effects [11]. The pro-resolution and anti-inflammatory bioactions that SPMs possess have been coined a biomedical paradigm shift due to the active role SPMs play in the return to physiology [11,12].

In 1998, Serhan and co-workers reported the isolation, structural elucidation and biological activities of resolvin E1 (RvE1, **1**) and resolvin E2 (**2**) [13], see Fig. 1. More recently, resolvin E3 (**3**) has been reported [14].

In connection with our ongoing projects related to total synthesis [15] and biological evaluations [16] of SPMs, we needed to secure multi-mg amounts of resolvin E1 (**1**). As of today, a few syntheses have been presented [17].

The sensitive *E,E,Z*-triene connecting the two secondary allylic alcohols in **1** must be synthesized in a highly stereoselective manner, since SPMs' pro-resolution and anti-inflammatory bioactions is highly dependent of stereospecific receptor interactions, we envisioned that RvE1 could be prepared from Wittig-salt **4**,

\* Corresponding author.

E-mail address: [t.v.hansen@farmasi.uio.no](mailto:t.v.hansen@farmasi.uio.no) (T.V. Hansen).

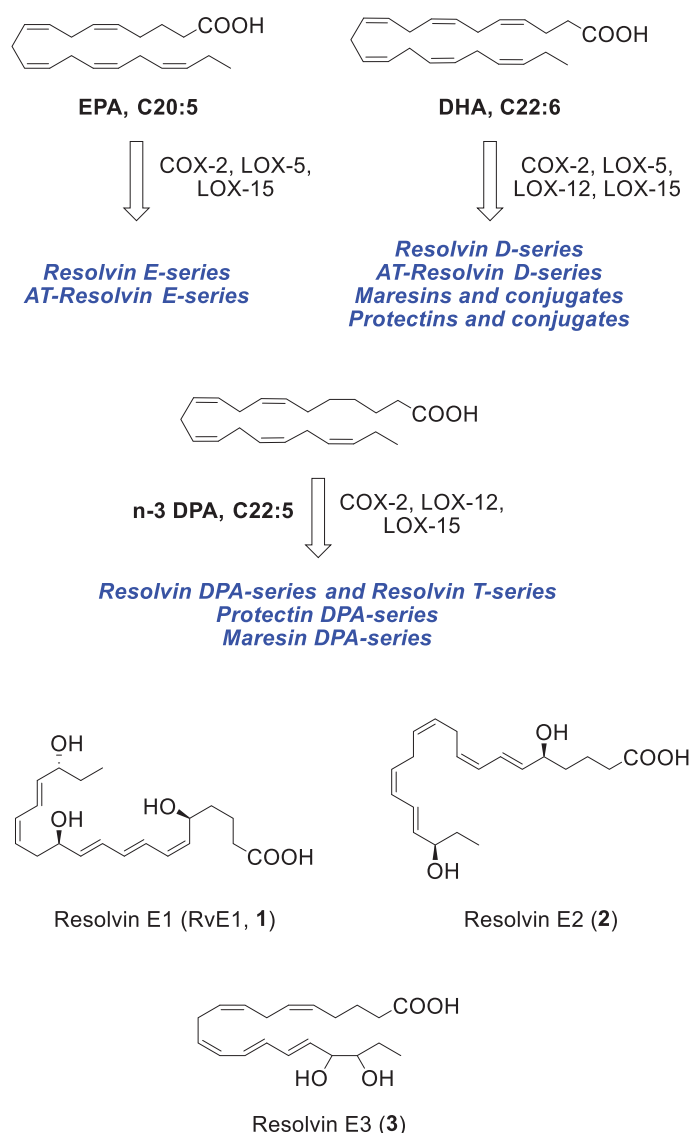


**Fig. 1.** Outline of the individual families of SPMs and the chemical structures of EPA, DHA, n-3 DPA and resolvins E1-E3.

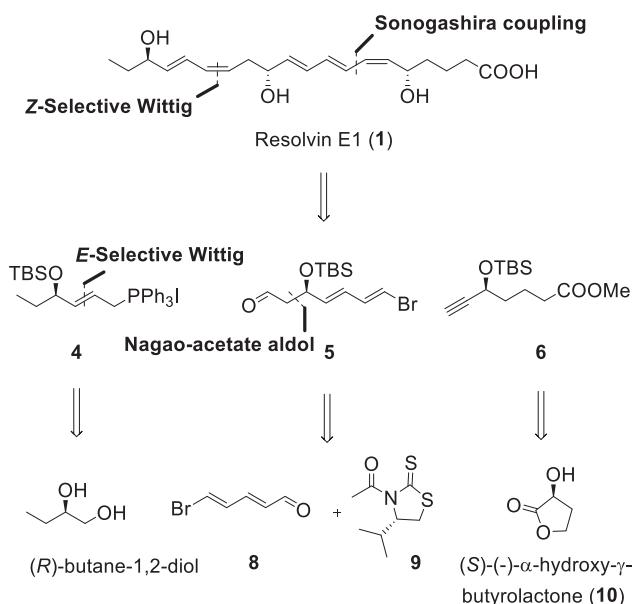
aldehyde **5** and alkyne **6**. The configurations at C17 and C5 in RvE1 would arrive from commercially available chiral pool starting materials. The aldehyde **5** can be made from the synthetically versatile compound 5-bromo-2*E*,4*E*-pentadienal (**8**) [18] and thiazolidine-thione **9**, see [Scheme 1](#).

## 2. Results and discussion

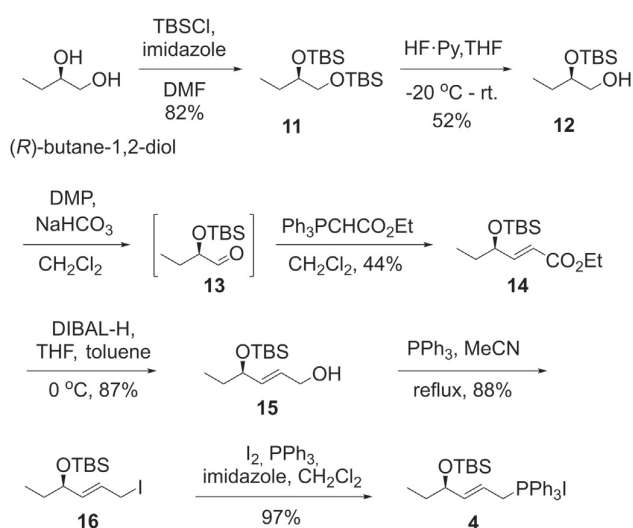
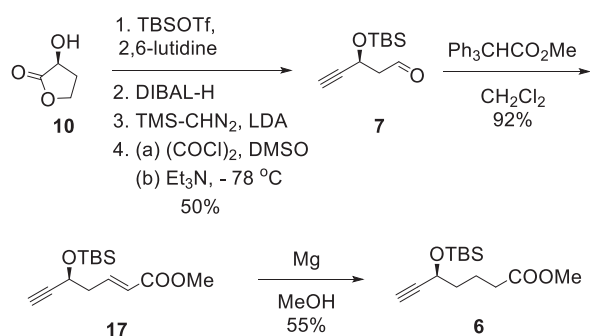
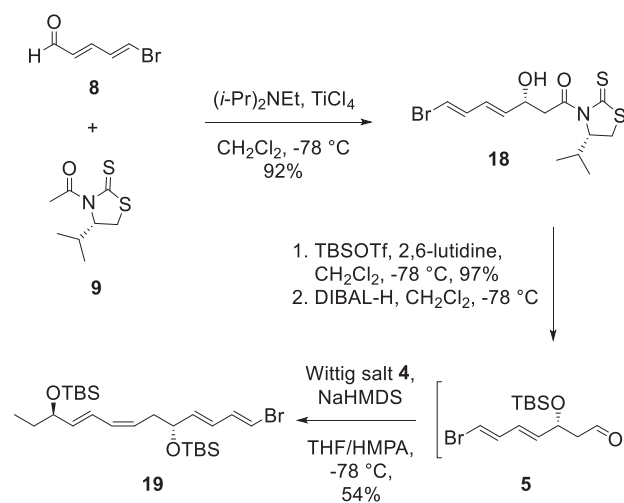
The synthesis of **1** commenced with the preparation of Wittig-salt **4** from (*R*)-butane-1,2-diol that was *bis*-protected with TBSCl to afford **11** in 82% yield. Then, regioselective deprotection with HF·pyridine in THF at  $-20$  °C gave alcohol **12** that was oxidized with Dess-Martin periodinane to afford aldehyde **13**. This aldehyde was immediately subjected to an *E*-selective Wittig reaction to produce ester **14**. The ester functionality in **14** was reduced with DIBAL-H to give alcohol **15**, which was reacted in an Appel reaction to yield the corresponding iodide that was converted to the Wittig-salt **4**. The overall yield of **4** was 14% from commercially available (*R*)-butane-1,2-diol over the seven steps presented in [Scheme 2](#).

Alkyne **6** was synthesized from commercially available (*S*)-(-)- $\alpha$ -hydroxy- $\gamma$ -butyrolactone (**10**) as outlined in [Scheme 3](#). First, a four-step procedure (silyl protection, DIBAL-H reduction, Colvin rearrangement [19], and oxidation) produced aldehyde **7** [15g]. This aldehyde was subjected to a highly *E*-selective Wittig-reaction to form ester **17**. A chemoselective reduction using magnesium in methanol [20] afforded alkyne ester **6** in 25% yield from lactone **10**, see [Scheme 3](#).

Next, we synthesized 5-bromo-2*E*,4*E*-pentadienal (**8**) [21] that was subjected to an Evans-Nagao aldol reaction with chiral auxiliary **9** [22] using our earlier reported conditions [15k]. This afforded alcohol **18** in a 15.3:1 diastereomeric ratio of the favored isomer depicted ([Supporting information](#)). Protection of the alcohol as TBS-ether followed by reduction with DIBAL-H gave aldehyde **5** that was reacted immediately with the ylide of Wittig-salt **4**. The ylide was formed after reaction with NaHMDS at  $-78$  °C in THF and HMPA ([Scheme 4](#)). The desired vinylic bromide **19** was formed in a 3.5:1 ratio compared to its *all E*-isomer and was isolated as one diastereomer in 54% yield after chromatography ([Supporting information](#)).



Scheme 1. Retrosynthetic analysis of RvE1.

Scheme 2. Synthesis of Wittig-salt **4**.Scheme 3. Synthesis of alkyne **6**.Scheme 4. Synthesis of bromide **19**.

The Sonogashira-coupling reaction between alkyne **6** and vinylic bromide **19** under classical conditions [23] produced the internal alkyne **20** in 91% yield. Removal of the three TBS-groups using TBAF in THF followed by a *Z*-selective Boland-reduction gave the methyl ester of resolvin E1 (**22**) in 59% over the two steps. Hydrolysis (LiOH, MeOH, H<sub>2</sub>O) yielded the SPM **1** in 83% yield for the last step (Scheme 5). The spectroscopic data (Supporting information) were in agreement with literature [17].

SPMs, including resolvin E1 (**1**), are biosynthesized in nanogram amounts *in vivo* [10]. Hence, matching synthetic material with endogenously formed SPMs is therefore essential. HPLC experiments revealed that synthetic **1** co-elutes with naturally occurring **1** [24], since identical retention times ( $T_R = 14.2$  min) were observed for both synthetic and biologically produced **1**, see Fig. 2.

### 3. Conclusions

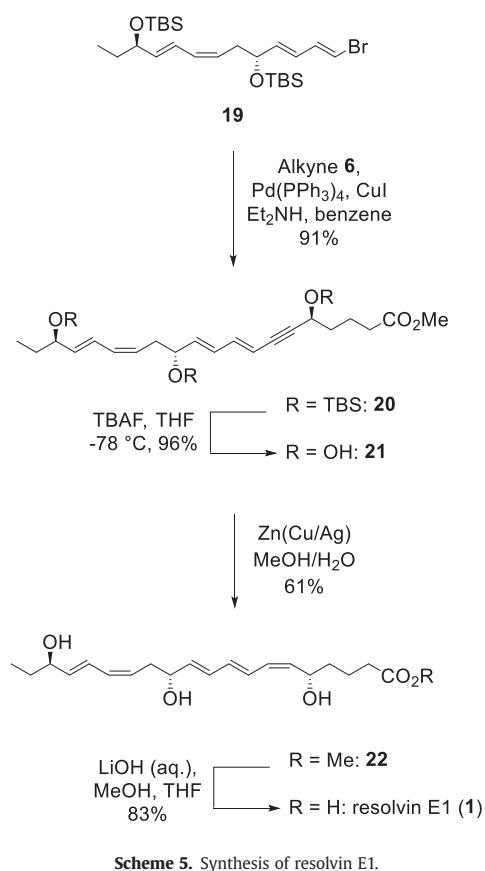
Individual SPMs possess several chiral secondary alcohols and conjugated *E*- and *Z*-double bonds. This reflects the biochemical origin of each SPM, but also their functions as stereospecific agonists towards individual GPCRs [9–11]. Herein, multi-mg amounts of resolvin E1 (**1**) has been stereoselectively prepared in 3% yield over 12 steps (longest linear sequence). This SPM has attracted a great interest towards developing new anti-inflammatory drugs and in particular targeting periodontal disease [25]. As of today, no effective drug treatment is available against this inflammatory driven disease [26]. Endogenously formed and non-toxic resolvin E1 displays nanomolar agonist effects against the ERV1/ChemR23 and the BLT1/GPR16 receptors [8,9,27]. These receptors are interesting biological targets towards developing remedies against the many inflammatory conditions resulting in periodontal disease [24]. Our collaborative efforts towards such aims will be presented in due time.

Supporting information available: <sup>1</sup>H, <sup>13</sup>C NMR, HPLC-chromatograms, UV/VIS, MS/MS and HRMS data of **1** and all intermediates, see DOI: (to be added/)

### 4. Experimental

#### 4.1. General procedures

Unless otherwise stated, all commercially available reagents and



solvents were used in the form they were supplied without any further purification. The stated yields are based on isolated material. All reactions were performed under an argon atmosphere using Schlenk techniques. Reaction flasks were covered with aluminium foil during reactions and storage to minimize exposure to light. Thin layer chromatography was performed on silica gel 60 F254 aluminum-backed plates fabricated by Merck. Flash column chromatography was performed on silica gel 60 (40–63 μm) produced by Merck. NMR spectra were recorded on a Bruker AVI600, Bruker AVI400 or a Bruker DPX300 spectrometer at 600 MHz, 400 MHz or 300 MHz respectively for  $^1\text{H}$  NMR and at 150 MHz, 100 MHz or 75 MHz respectively for  $^{13}\text{C}$  NMR. Coupling constants ( $J$ ) are reported in hertz and chemical shifts are reported in parts per million ( $\delta$ ) relative to the central residual protium solvent resonance in  $^1\text{H}$  NMR ( $\text{CDCl}_3 = \delta$  7.26,  $\text{DMSO}-d_6 = \delta$  2.50 and  $\text{MeOD}-d_4 = \delta$  3.31) and the central carbon solvent resonance in  $^{13}\text{C}$  NMR ( $\text{CDCl}_3 = \delta$  77.00 ppm,  $\text{DMSO}-d_6 = \delta$  39.43 and  $\text{MeOD}-d_4 = \delta$  49.00). Optical rotations were measured using a 1 mL cell with a 1.0 dm path length on a PerkinElmer 341 polarimeter. Mass spectra were recorded at 70 eV on Micromass Prospec Q or Micromass QTOF 2 W spectrometer using ESI as the method of ionization. High-resolution mass spectra were recorded at 70 eV on Micromass Prospec Q or Micromass QTOF 2W spectrometer using ESI as the method of ionization. HPLC-analyses were performed using a C18 stationary phase (Eclipse XDB-C18,  $4.6 \times 250$  mm, particle size 5 μm, from Agilent Technologies), applying the conditions stated. The UV/Vis spectrum was recorded using an Agilent Technologies Cary 8485 UV-VIS spectrophotometer using quartz cuvettes.

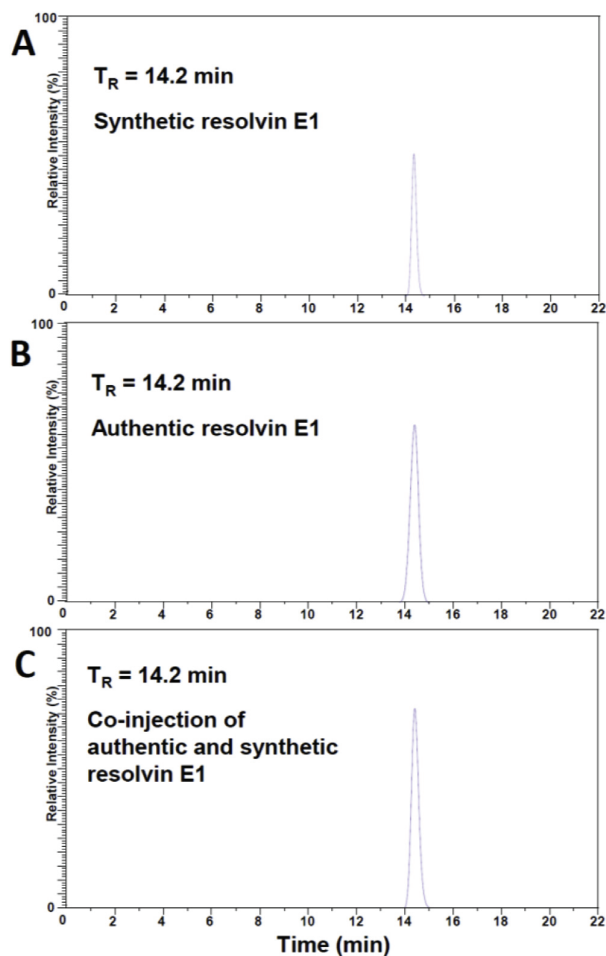


**Fig. 2.** HPLC chromatograms obtained from the matching experiments.

#### 4.2. (*R*)-5-ethyl-2,2,3,3,8,8,9,9-octamethyl-4,7-dioxo-3,8-disiladecane (11)

(*R*)-Butane-1,2-diol (1.35 g, 15.0 mmol) was dissolved in DMF (40 mL) and added imidazole (4.49 g, 66.0 mmol, 4.40 eq.) and *tert*-butyldimethylsilyl chloride (6.78 g, 45.0 mmol, 3.00 eq.). The mixture was stirred overnight (22 h). Next, the mixture was transferred to a separatory funnel and added sat. aq.  $\text{NH}_4\text{Cl}$  (200 mL) and hexane (50 mL). The layers were separated and the aq. layer was extracted with additional hexane ( $2 \times 30$  mL). The organic layers were combined, washed with sat. aq.  $\text{NH}_4\text{Cl}$  ( $2 \times 30$  mL) and water ( $3 \times 30$  mL), dried ( $\text{MgSO}_4$ ) and evaporated. The residue was purified by flash chromatography on silica gel (2–3% EtOAc in hexane) to afford the desired *bis*-protected diol as a colorless oil. Yield: 3.93 g (82%).  $[\alpha]_D^{25} = +15.2$  ( $c = 1.8$ ,  $\text{CH}_2\text{Cl}_2$ );  $^1\text{H}$  NMR (400 MHz,  $\text{CDCl}_3$ )  $\delta$  3.64–3.55 (m, 1H), 3.51 (dd,  $J = 9.9, 5.5$  Hz, 1H), 3.41 (dd,  $J = 9.9, 6.4$  Hz, 1H), 1.65–1.54 (m, 1H), 1.45–1.32 (m, 1H), 0.89 (s, 9H), 0.89 (s, 9H), 0.89 (m, 3H), 0.06 (s, 6H), 0.05 (s, 3H) and 0.04 (s, 3H);  $^{13}\text{C}$  NMR (101 MHz,  $\text{CDCl}_3$ )  $\delta$  74.4, 67.2, 27.2, 26.2, 26.1, 18.6, 18.4, 9.7, –4.1, –4.6, –5.1, –5.2. TLC (EtOAc/hexane, 1:19,  $\text{KMnO}_4$ -stain)  $R_f = 0.58$ ; HRMS: Exact mass calculated for  $\text{C}_{16}\text{H}_{38}\text{NaO}_2\text{Si}_2$   $[M+\text{Na}]^+$ : 341.2303, found: 341.2301.

4.3. (*R*)-2-((*tert*-butyldimethylsilyloxy)butan-1-yl) (12)

The *bis*-protected alcohol **11** (3.60 g, 11.3 mmol) was dissolved in dry THF (200 mL) and pyridine (15.8 mL). Then, hydrogen fluoride pyridine (13.0 mL, pyridine ca. 30%, HF ca. 70%) was added at 0 °C. The mixture was stirred for 1 h at 0 °C before the ice bath was removed and the mixture was stirred for an additional 1.5 h at rt. The mixture was cooled on an ice bath and poured over a solution of sat. aq. NaHCO<sub>3</sub> (400 mL). After stirring vigorously for a few minutes, the mixture was added water (200 mL) and hexane (100 mL) and the layers were separated. The aq. layer was extracted with additional hexane (2 × 50 mL). Next, the organic layers were combined, washed with water (50 mL) and brine (50 mL), dried (MgSO<sub>4</sub>) and evaporated. The residue was purified by flash chromatography on silica gel (10–20% EtOAc in hexane) to afford the desired primary alcohol as a colorless oil. Yield: 1.19 g (52%);  $[\alpha]_D^{25} = -4.8$  ( $c = 1.1$ , CH<sub>2</sub>Cl<sub>2</sub>); <sup>1</sup>H NMR (400 MHz, CDCl<sub>3</sub>) δ 3.71–3.62 (m, 1H), 3.56 (dd,  $J = 11.0$ , 3.7 Hz, 1H), 3.45 (dd,  $J = 11.0$ , 5.4 Hz, 1H), 1.88 (d,  $J = 0.9$  Hz, 1H), 1.56–1.48 (m, 2H), 0.90 (s, 9H), 0.88 (t,  $J = 7.6$  Hz, 3H), 0.08 (s, 6H); <sup>13</sup>C NMR (101 MHz, CDCl<sub>3</sub>) δ 74.2, 66.0, 26.9, 26.0, 18.3, 9.9, -4.3, -4.5; TLC (EtOAc/hexane, 1:4, KMnO<sub>4</sub>-stain) R<sub>f</sub> = 0.36; HRMS: Exact mass calculated for C<sub>10</sub>H<sub>24</sub>NaO<sub>2</sub>Si [M+Na]<sup>+</sup>: 227.1438, found: 227.1437.

4.4. Ethyl (*R,E*)-4-((*tert*-butyldimethylsilyloxy)hex-2-enoate) (14)

The primary alcohol **12** (1.16 g, 5.68 mmol, 1.00 eq.) was dissolved in CH<sub>2</sub>Cl<sub>2</sub> (25 mL) and added NaHCO<sub>3</sub> (2.63 g, 31.3 mmol, 5.50 eq.) and Dess-Martin periodinane (3.37 g, 7.95 mmol, 1.40 eq.). After stirring for 2 h, hexane was added and the resulting precipitate was removed by filtration through a pad of Celite®. The mixture was transferred to a separatory funnel and washed with sat. aq. Na<sub>2</sub>S<sub>2</sub>O<sub>3</sub> (50 mL) and brine (50 mL), dried (Na<sub>2</sub>SO<sub>4</sub>) and filtered quickly through a pad of silica gel. The pad was washed with 10% EtOAc in hexane and the filtrate was evaporated to give the crude aldehyde (0.880 g) as a colorless oil (R<sub>f</sub> = 0.49 in EtOAc:hexane 1:4, KMnO<sub>4</sub>-stain). The crude aldehyde was immediately dissolved in dry CH<sub>2</sub>Cl<sub>2</sub> and added (carboxymethylene)triphenylphosphorane (2.28 g, 6.55 mmol) in one portion at 0 °C. After stirring for 1 h, the mixture was evaporated and added hexane (80 mL). The precipitate was removed by filtration through a pad of Celite that was washed with 5% EtOAc in hexane. The residue was purified by flash chromatography on silica gel (3–5% EtOAc in hexane) to give the desired product as a colorless oil. Yield: 0.687 g (44%) over the two steps;  $[\alpha]_D^{25} = +5.1$  ( $c = 1.1$ , CH<sub>2</sub>Cl<sub>2</sub>); <sup>1</sup>H NMR (400 MHz, CDCl<sub>3</sub>) δ 6.91 (dd,  $J = 15.6$  and 4.6 Hz, 1H), 5.97 (dd,  $J = 15.6$  and 1.7 Hz, 1H), 4.28–4.14 (m, 3H), 1.67–1.50 (m, 2H), 1.29 (t,  $J = 7.1$  Hz, 3H), 9.91 (s, 9H), 0.89 (t,  $J = 7.6$  Hz, 3H), 0.05 (s, 3H) and 0.03 (s, 3H); <sup>13</sup>C NMR (101 MHz, CDCl<sub>3</sub>) δ 166.9, 151.0, 120.1, 72.7, 60.4, 30.3, 26.0, 18.4, 14.4, 9.3, -4.5, -4.8; TLC (EtOAc/hexane, 95:5, KMnO<sub>4</sub>-stain) R<sub>f</sub> = 0.29; HRMS: Exact mass calculated for C<sub>14</sub>H<sub>28</sub>NaO<sub>3</sub>Si [M+Na]<sup>+</sup>: 295.1700, found: 295.1699.

4.5. (*R,E*)-4-((*tert*-butyldimethylsilyloxy)hex-2-en-1-yl) (15)

The ester (**14**) (0.672 g, 2.47 mmol, 1.00 eq.) was dissolved in dry toluene (6.0 mL) under argon. DIBAL-H (1.0 M in THF 6.20 mmol, 2.50 eq.) was added dropwise at 0 °C. After stirring for 50 min at 0 °C, the mixture was quenched by slow addition of 10% aq. Rochelle salt (40 mL) and diluted with hexane (20 mL) and diethyl ether (20 mL). The turbid mixture was then stirred vigorously until the top layer was clear (approx. 1 h), so that the layers could be separated in a separatory funnel. The aq. layer was extracted with EtOAc (2 × 20 mL), the organic layers were combined and washed with brine (20 mL), dried (Na<sub>2</sub>SO<sub>4</sub>) and evaporated. The residue

was purified by flash chromatography on silica gel (EtOAc/hexane 8:2) to afford the desired allylic alcohol as a colorless oil. Yield: 0.494 g (87%);  $[\alpha]_D^{25} = +5.5$  ( $c = 1.7$ , CH<sub>2</sub>Cl<sub>2</sub>); <sup>1</sup>H NMR (400 MHz, CDCl<sub>3</sub>) δ 5.76 (dt,  $J = 15.6$  and 5.5 Hz, 1H), 5.66 (dd,  $J = 15.6$  and 5.7 Hz, 1H), 4.13 (d,  $J = 5.4$  Hz, 2H), 4.05 (q,  $J = 6.1$  Hz, 1H), 1.56–1.41 (m, 3H), 0.89 (s, 9H), 0.87 (t, 7.4 Hz, 3H), 0.05 (s, 3H) and 0.02 (s, 3H); <sup>13</sup>C NMR (101 MHz, CDCl<sub>3</sub>) δ 135.2, 128.5, 74.0, 63.4, 31.1, 26.0, 18.4, 9.7, -4.2, -4.6; TLC (hexane/EtOAc, 4:1, KMnO<sub>4</sub>-stain) R<sub>f</sub> = 0.27; HRMS: Exact mass calculated for C<sub>12</sub>H<sub>26</sub>NaO<sub>2</sub>Si [M+Na]<sup>+</sup>: 253.1594, found: 253.1594.

4.6. (*R,E*)-*tert*-butyl((6-iodohex-4-en-3-yl)oxy)dimethylsilane (16)

Triphenylphosphine (811 mg, 3.09 mmol, 1.50 eq.) and imidazole (221 mg, 3.25 mmol, 1.58 eq.) were added to a stirring solution of alcohol **15** (475 mg, 2.06 mmol, 1.00 eq.) in CH<sub>2</sub>Cl<sub>2</sub> (22 mL). The reaction flask was placed in a cooling bath (ice-water/NaCl) and stirred for 15 min before iodine (816 mg, 1.47 mmol, 3.19 mmol, 1.55 eq.) was added in one portion with rapid stirring. After stirring for 50 min, the mixture was quenched by slow addition of sat. aq. Na<sub>2</sub>SO<sub>3</sub> (2.5 mL) and added distilled water (15 mL). The phases were separated and the aq. phase was extracted with CH<sub>2</sub>Cl<sub>2</sub> (2 × 15 mL). The combined organic extracts were dried (Na<sub>2</sub>SO<sub>4</sub>) and evaporated followed by purification by flash chromatography on silica gel (hexane-10% EtOAc) to give the title compound as a pale yellow oil. Yield: 617 mg (88%);  $[\alpha]_D^{25} = -8.9$  ( $c = 0.40$ , CH<sub>2</sub>Cl<sub>2</sub>); <sup>1</sup>H NMR (400 MHz, CDCl<sub>3</sub>) δ 5.90–5.79 (m, 1H), 5.66 (dd,  $J = 15.1$ , 6.0 Hz, 1H), 4.02 (q,  $J = 6.0$  Hz, 1H), 3.88 (d,  $J = 8.0$  Hz, 2H), 1.53–1.44 (m, 2H), 0.90 (s, 9H), 0.86 (t,  $J = 7.4$  Hz, 3H), 0.05 (s, 3H), 0.04 (s, 3H); <sup>13</sup>C NMR (101 MHz, CDCl<sub>3</sub>) δ 137.4, 127.3, 73.6, 31.0, 26.1 (3C), 18.4, 9.6, 5.8, -4.1, -4.7; TLC (hexane, KMnO<sub>4</sub>-stain) R<sub>f</sub> = 0.46; HRMS: Exact mass calculated for C<sub>12</sub>H<sub>25</sub>INO<sub>2</sub>Si [M+Na]<sup>+</sup>: 363.0611, found: 363.0612.

4.7. (*R,E*)-4-((*tert*-butyldimethylsilyloxy)hex-2-en-1-yl) iodotriphenyl-λ<sup>5</sup>-phosphane (4)

Iodine **16** (603 mg, 1.77 mmol, 1.00 eq.) in dry MeCN (18.5 mL) was added triphenylphosphine (937 mg, 3.57 mmol, 2.02 eq.) and heated to reflux for 16 h. Next, the reaction mixture was cooled to ambient temperature and concentrated *in vacuo*. The residual was purified by flash chromatography (CH<sub>2</sub>Cl<sub>2</sub> – 5% MeOH) to give Wittig salt **4** as a white solid. Yield: 1.036 g (97%);  $[\alpha]_D^{25} = +0.40$  ( $c = 0.50$ , MeOH); <sup>1</sup>H NMR (400 MHz, CDCl<sub>3</sub>) δ 7.82–7.76 (m, 9H), 7.71–7.65 (m, 6H), 6.23–6.16 (m, 1H), 5.55–5.45 (m, 1H), 4.73 (td,  $J = 15.0$ , 7.8 Hz, 1H), 4.51 (td,  $J = 15.3$ , 7.0 Hz, 1H), 4.10–4.02 (m, 1H), 1.44–1.27 (m, 2H), 0.73 (s, 9H), 0.67 (t,  $J = 7.4$  Hz, 3H), -0.06 (s, 3H), -0.19 (s, 3H); <sup>13</sup>C NMR (101 MHz, CDCl<sub>3</sub>) δ 145.0 (d, <sup>2</sup> $J = 13.1$  Hz), 135.2 (d, <sup>4</sup> $J = 3.0$  Hz), 134.1 (d, <sup>3</sup> $J = 9.1$  Hz), 130.5 (d, <sup>2</sup> $J = 12.1$  Hz), 118.1 (d, <sup>1</sup> $J = 85.5$  Hz), 112.6 (d, <sup>3</sup> $J = 9.1$  Hz), 72.6 (d, <sup>4</sup> $J = 2.0$  Hz), 30.4 (d, <sup>5</sup> $J = 3.0$  Hz), 27.9 (d, <sup>1</sup> $J = 50.3$  Hz), 25.8 (3C), 18.1, 9.0, -4.7, -4.7; TLC (MeOH/CH<sub>2</sub>Cl<sub>2</sub> 5:95, UV-vis.) R<sub>f</sub> = 0.46; HRMS: Exact mass calculated for C<sub>30</sub>H<sub>40</sub>NaOPSi [M+Na]<sup>+</sup>: 475.2580, found: 475.2581.

4.8. (5*R*,6*E*,8*Z*,11*R*)-11-((1*E*,3*E*)-4-bromobuta-1,3-dien-1-yl)-5-ethyl-2,2,3,3,13,13,14,14-octamethyl-4,12-dioxo-3,13-disilapentadeca-6,8-diene (19)

Following the procedure reported by Olivo and coworkers [22d], the protected thiazolidinethione obtained from compound **18** (335 mg, 0.700 mmol, 1.00 eq.) was dissolved in CH<sub>2</sub>Cl<sub>2</sub> (13 mL) followed by dropwise addition of DIBAL-H (1.0 M in CH<sub>2</sub>Cl<sub>2</sub>, 0.870 mmol, 1.20 eq.) at -78 °C. After 3 h, additional DIBAL-H was added (1.0 M in CH<sub>2</sub>Cl<sub>2</sub>, 0.140 mmol, 0.200 eq.). The mixture was

allowed to stir for 30 min and then quenched with sat. aq. NaHCO<sub>3</sub> (10 mL). The cooling bath was removed and solid Na–K tartrate (–0.300 g) (Rochelle salt) was added and stirring was continued for another 45 min. Et<sub>2</sub>O (10 mL) was added. The layers were separated and the aq. layer was extracted with Et<sub>2</sub>O (3 × 10 mL). The combined organic layers were dried (Na<sub>2</sub>SO<sub>4</sub>) and the solvent evaporated. The residue was purified by column chromatography on silica gel (hexane/Et<sub>2</sub>O 95:5) R<sub>f</sub> = 0.24, and concentrated *in vacuo*. Wittig salt **4** (281 mg, 0.466 mmol, 1.00 eq.) in THF (15 mL) and HMPA (2.5 mL) was slowly added NaHMDS (0.6 M in THF, 0.444 mmol, 0.950 eq.) at –78 °C and then stirred for 1 h at that temperature. The purified aldehyde **5** dissolved in a minimum amount THF was added dropwise with cooling on syringe. The reaction was stirred at –78 °C for 12 h before it was quenched with phosphate buffer (8 mL, pH = 7.2). The phases were separated and the aq. phase was extracted with Et<sub>2</sub>O (3 × 10 mL). The combined organic layers were dried (Na<sub>2</sub>SO<sub>4</sub>) and the solvent evaporated. The crude product was purified by column chromatography on silica gel (8% EtOAc in hexane) to afford the title compound **19** as a pale yellow oil. Yield: 236 mg (54% over two steps); [α]<sub>D</sub><sup>20</sup> = –21.7 (c = 0.60, CHCl<sub>3</sub>); <sup>1</sup>H NMR (400 MHz, CDCl<sub>3</sub>) δ 6.67 (dd, *J* = 13.4, 10.9 Hz, 1H), 6.40–6.32 (m, 1H), 6.27 (d, *J* = 13.5 Hz, 1H), 6.14–6.01 (m, 2H), 5.71 (dd, *J* = 15.3, 5.7 Hz, 1H), 5.63 (dd, *J* = 15.1, 6.2 Hz, 1H), 5.41–5.33 (m, 1H), 4.18 (q, *J* = 6.0 Hz, 1H), 4.08 (q, *J* = 6.0 Hz, 1H), 2.42–2.33 (m, 2H), 1.53–1.46 (m, 2H), 0.91–0.85 (m, 21H), 0.06–0.02 (m, 12H); <sup>13</sup>C NMR (101 MHz, CDCl<sub>3</sub>) δ 137.9, 137.6, 137.2, 130.3, 126.8, 126.5, 124.6, 108.3, 74.6, 72.5, 36.7, 31.3, 26.1 (3C), 26.0 (3C), 18.4, 18.4, 9.8, –4.2, –4.4, –4.6, –4.6; TLC (8% EtOAc in hexane, UV–Vis.) R<sub>f</sub> = 0.28; HRMS: Exact mass calculated for C<sub>25</sub>H<sub>47</sub>Br NaO<sub>2</sub>Si<sub>2</sub> [M+Na]<sup>+</sup>: 537.2190, found: 537.2190; d.r.: 1:3.5 (E/Z, based on isolated yields).

#### 4.9. Methyl (5*S*,8*E*,10*E*,12*R*,14*Z*,16*E*,18*R*)-5,12,18-tris((tert-butyl)dimethylsilyloxy)icosa-8,10,14,16-tetraen-6-ynoate (**20**)

To a solution of vinyl bromide **19** (122 mg, 0.236 mmol, 1.00 eq.) in Et<sub>2</sub>NH (0.55 mL) and benzene (0.25 mL) was added Pd(PPh<sub>3</sub>)<sub>4</sub> (9.00 mg, 0.00788 mmol, 3.00 mol%), and the reaction was stirred for 45 min in the dark. CuI (3.00 mg, 0.0158 mmol, 7.00 mol%) dissolved in a minimum amount of Et<sub>2</sub>NH was added, followed by dropwise addition of alkyne **6** (68.0 mg, 0.251 mmol, 1.06 eq.) in Et<sub>2</sub>NH (0.5 mL). After 20 h of stirring at ambient temperature, the reaction was quenched with sat. aq. NH<sub>4</sub>Cl (7.0 mL). Et<sub>2</sub>O (7.0 mL) was added and the phases were separated. The aq. phase was extracted with Et<sub>2</sub>O (2 × 7.0 mL), and the combined organic layers were dried (Na<sub>2</sub>SO<sub>4</sub>), before being concentrated *in vacuo*. The crude product was purified by column chromatography on silica gel (hexane/EtOAc, 95:5) to afford the title compound **20** as a pale yellow oil in 91% yield (153 mg); [α]<sub>D</sub><sup>20</sup> = –57.4 (c = 0.35, CHCl<sub>3</sub>); <sup>1</sup>H NMR (400 MHz, CDCl<sub>3</sub>) δ 6.50 (dd, *J* = 15.6, 10.8 Hz, 1H), 6.37 (dd, *J* = 15.1, 11.0 Hz, 1H), 6.19 (dd, *J* = 15.0, 10.8 Hz, 1H), 6.04 (t, *J* = 11.0 Hz, 1H), 5.76 (dd, *J* = 15.2, 6.0 Hz, 1H), 5.63 (dd, *J* = 15.2, 6.2 Hz, 1H), 5.57 (d, *J* = 15.6 Hz, 1H), 5.38 (dt, *J* = 10.8, 7.7 Hz, 1H), 4.52–4.47 (m, 1H), 4.21 (q, *J* = 6.0 Hz, 1H), 4.08 (q, *J* = 6.1 Hz, 1H), 3.67 (s, 3H), 2.46–2.29 (m, 4H), 1.85–1.65 (m, 4H), 1.54–1.43 (m, 2H), 0.93–0.82 (m, 30H), 0.13 (s, 3H), 0.11 (s, 3H), 0.03 (dd, *J* = 8.8, 3.7 Hz, 12H); <sup>13</sup>C NMR (101 MHz, CDCl<sub>3</sub>) δ 174.4, 141.2, 139.3, 131.9, 128.6, 128.5, 126.6, 125.3, 110.6, 93.3, 83.2, 72.9, 63.6, 63.0, 51.6, 37.0, 36.4, 34.2, 31.5, 29.4, 29.0, 27.4, 26.1, 26.0, 26.0, 25.0, 18.5, 18.4, 18.4, –4.3, –4.3, –4.6, –4.8, –5.1; TLC (hexane/EtOAc 95:5, KMnO<sub>4</sub>-stain) R<sub>f</sub> = 0.42; HRMS: Exact mass calculated for C<sub>39</sub>H<sub>72</sub>NaO<sub>5</sub>Si<sub>3</sub> [M+Na]<sup>+</sup>: 727.4580, found: 727.4578.

#### 4.10. Methyl (5*S*,8*E*,10*E*,12*R*,14*Z*,16*E*,18*R*)-5,12,18-trihydroxyicosa-8,10,14,16-tetraen-6-ynoate (**21**)

TBAF (1.0 M in THF, 0.27 mL, 0.270 mmol, 4.00 eq.) was added to

a solution of TBS-protected triol **20** (48.0 mg, 0.0682 mmol, 1.00 eq.) in THF (3.0 mL) at –78 °C. The reaction was stirred for 21 h before it was quenched with phosphate buffer (pH = 7.2, 5.0 mL). Brine (6.0 mL) and EtOAc (6.0 mL) were added, and the phases were separated. The aq. phase was extracted with EtOAc (3 × 6.0 mL), and the combined organic layers were dried (Na<sub>2</sub>SO<sub>4</sub>) and the solvent evaporated. The crude product was purified by column chromatography on silica gel (hexane/EtOAc, 4:6) to afford the title compound as a pale yellow oil. Yield: 24 mg (96%); [α]<sub>D</sub><sup>25</sup> = –23.0 (c = 0.10, MeOH); <sup>1</sup>H NMR (400 MHz, MeOD) δ 6.62–6.43 (m, 2H), 6.31 (dd, *J* = 15.2, 10.7 Hz, 1H), 6.11 (t, *J* = 10.9 Hz, 1H), 5.84 (dd, *J* = 15.2, 6.2 Hz, 1H), 5.72–5.64 (m, 2H), 5.46 (dt, *J* = 11.0, 7.6 Hz, 1H), 4.50–4.42 (m, 1H), 4.19 (q, *J* = 6.3 Hz, 1H), 4.03 (q, *J* = 6.6 Hz, 1H), 3.68 (s, 3H), 2.49–2.42 (m, 2H), 2.46–2.35 (m, 2H), 1.90–1.63 (m, 4H), 1.62–1.47 (m, 2H), 0.93 (t, *J* = 7.4 Hz, 3H); <sup>13</sup>C NMR (101 MHz, MeOD) δ 175.6, 142.5, 139.7, 137.9, 131.2, 130.4, 127.8, 126.6, 111.8, 93.7, 84.4, 74.7, 72.7, 62.9, 52.1, 38.2, 36.6, 34.4, 31.2, 21.9, 10.2; TLC (hexane/EtOAc 4:6, KMnO<sub>4</sub>-stain) R<sub>f</sub> = 0.28; HRMS: Exact mass calculated for C<sub>21</sub>H<sub>30</sub>NaO<sub>5</sub> [M+Na]<sup>+</sup>: 385.1985, found: 385.1986.

#### 4.11. Methyl (5*S*,8*E*,10*E*,12*R*,14*Z*,16*E*,18*R*)-5,12,18-trihydroxyicosa-8,10,14,16-tetraen-6-ynoate (**22**)

The Zn(Cu/Ag) mixture was prepared as described by Boland et al. [28] Zinc dust (1.57 g) in degassed H<sub>2</sub>O (9.5 mL, pH = 7.0) was stirred under argon for 15 min before Cu(OAc)<sub>2</sub> (158 mg) was added and stirred for an additional 15 min AgNO<sub>3</sub> (157 mg) was then added and the reaction mixture was stirred for 30 min. The mixture was filtered and washed successively with H<sub>2</sub>O, MeOH, acetone and Et<sub>2</sub>O before it was transferred to a flask containing alkyne **21** (22.0 mg, 60.7 μmol) in MeOH/H<sub>2</sub>O (3:1, 4.6 mL). The mixture was stirred at room temperature and monitored by TLC analysis. After 4.5 h, the reaction mixture was filtered through a pad of Celite® and washed with Et<sub>2</sub>O. Water was added to the filtrate and the layers were separated. The aq. layer was extracted with Et<sub>2</sub>O (2 × 6.0 mL). The combined organic layers were washed with brine (10 mL) and dried (Na<sub>2</sub>SO<sub>4</sub>). The solvent was evaporated and the crude product was purified by column chromatography on silica gel (50–60% EtOAc in hexane) to afford the title compound as a pale yellow oil. Yield: 14.2 mg (61%) with purity > 91% determined by HPLC analysis; [α]<sub>D</sub><sup>25</sup> = –10.0 (c = 0.20, MeOH); <sup>1</sup>H NMR (600 MHz, MeOD) δ 6.89–6.77 (m, 2H), 6.66–6.52 (m, 2H), 6.39 (t, *J* = 11.4 Hz, 2H), 6.06 (dd, *J* = 14.8, 6.5 Hz, 1H), 5.96 (dd, *J* = 15.1, 6.6 Hz, 1H), 5.75 (dt, *J* = 10.8, 7.6 Hz, 1H), 5.66 (t, *J* = 9.9 Hz, 1H), 4.89–4.84 (m, 1H), 4.47 (q, *J* = 6.4 Hz, 1H), 4.32 (q, *J* = 6.4 Hz, 1H), 3.96 (s, 3H), 2.80–2.70 (m, 2H), 2.66 (t, *J* = 7.1 Hz, 2H), 2.03–1.89 (m, 3H), 1.88–1.79 (m, 2H), 1.78–1.70 (m, 2H), 1.22 (t, *J* = 7.5 Hz, 2H); <sup>13</sup>C NMR (151 MHz, MeOD) δ 175.8, 137.9, 137.8, 135.1 (2C), 131.5, 131.1, 130.6, 128.8, 128.0, 126.6, 74.7, 73.0, 68.1, 52.1, 37.9, 36.7, 34.6, 31.2, 22.0, 10.3; TLC (Hexane/EtOAc 4:6, UV–vis.) R<sub>f</sub> = 0.21; HRMS: Exact mass calculated for C<sub>21</sub>H<sub>32</sub>NaO<sub>5</sub> [M+Na]<sup>+</sup>: 387.2142, found: 387.2142; UV–vis: λ<sub>max</sub> = 262, 271, 282 nm. After additional purification using Biotage® Select Purification system (Biotage® Sfär-C-18, MeOH/H<sub>2</sub>O 60:40, 4 mL/min) the purity (97%) of product **22** was determined by HPLC analysis (Eclipse XDB-C18, MeOH/H<sub>2</sub>O 3:1, 1.0 mL/min); t<sub>r</sub> = 13.7.

#### 4.12. Resolvin E1 (**1**)

Solid LiOH (2.30 mg, 83.5 μmol, 30.5 eq.) was added to a solution of methyl ester **22** (1.00 mg, 2.74 μmol, 1.00 eq.) dissolved in THF–MeOH–H<sub>2</sub>O (2:2:1, 0.34 mL) at 0 °C. The reaction mixture was stirred at 0 °C for 3 h and then allowed to warm to rt. After 4.5 h, the solution was acidified with sat. aq. NaH<sub>2</sub>PO<sub>4</sub> (0.5 mL), and then added EtOAc (0.5 mL). The layers were separated and the water

phase was extracted with EtOAc (2 × 0.5 mL). The combined organic layers were dried (Na<sub>2</sub>SO<sub>4</sub>) before the solvent was removed *in vacuo*. RvE1 (**1**) was obtained as a pale yellow oil after filtration through a plug of silica gel (Hexane/MeOH/EtOAc 3:1:6). TLC (EtOAc/hexane 7:3, UV–vis.) R<sub>f</sub> = 0.26; Yield: 0.80 mg (83%);  $[\alpha]_D^{25} = +8.0$  (c = 0.12, MeOH); <sup>1</sup>H NMR (600 MHz, MeOD) δ 6.56 (dd, J = 14.6, 11.4 Hz, 1H), 6.50 (dd, J = 15.2, 11.1 Hz, 1H), 6.31 (dd, J = 15.1, 10.7 Hz, 1H), 6.23 (dd, J = 14.7, 10.7 Hz, 1H), 6.07 (q, J = 10.5 Hz, 2H), 5.74 (dd, J = 15.0, 6.6 Hz, 1H), 5.66 (dd, J = 15.1, 6.7 Hz, 1H), 5.45 (dt, J = 11.0, 7.6 Hz, 1H), 5.37 (t, J = 9.9 Hz, 1H), 4.61–4.53 (m, 1H), 4.16 (q, J = 6.7 Hz, 1H), 4.01 (q, J = 6.5 Hz, 1H), 2.50–2.38 (m, 2H), 2.25 (t, J = 7.0 Hz, 2H), 1.59–1.44 (m, 6H), 0.91 (t, J = 7.2 Hz, 3H); HRMS: Exact mass calculated for C<sub>20</sub>H<sub>30</sub>NaO<sub>5</sub> [M+Na]<sup>+</sup>: 373.1985, found: 373.1985; UV–vis: λ<sub>max</sub> (EtOH) = 262, 271, 282 nm. The purity (94%) was determined by HPLC analysis (Eclipse XDB-C18, MeOH/3.3 mM aq. acetic acid 55:45, 1.0 mL/min); t<sub>r</sub> = 14.2 min.

### Acknowledgment

The Department of Pharmacy, University of Oslo is gratefully acknowledged for a Ph.D.-scholarship to J. I. N. We appreciate the funding for a travel grant to J. I. N. from The Norwegian Research School in Pharmacy (N. F. I. F.). The Norwegian Research Council is gratefully acknowledged for funding to T. V. H. (BIOTEK2021 224811 and FRIPRO-FRINATEK 230470).

### Appendix A. Supplementary data

Supplementary data to this article can be found online at <https://doi.org/10.1016/j.tet.2019.130821>.

### References

- P.C. Calder, L.E.M. Willemsen, *Eur. J. Pharmacol.* 785 (2016) 1.
- J.W. Fetterman Jr., M.M. Zdanowicz, *Am. J. Health Syst. Pharm.* 66 (2009) 1169–1179.
- A.P. Simopoulos, *J. Am. Coll. Nutr.* 21 (2002) 495–505.
- (a) G. Kaur, D. Cameron-Smith, M. Garg, A.J. Sinclair, *Prog. Lipid Res.* 50 (2011) 28–34; (b) G. Kaur, X.-F. Guo, A.J. Sinclair, *Curr. Opin. Clin. Nutr. Metab. Care* 19 (2016) 88–91.
- P.C. Calder, *Br. J. Clin. Pharmacol.* 75 (2013) 645–662.
- W.R. Leonard, In *Lifestyle, Diet, and Disease: Comparative Perspectives on the Determinants of Chronic Health Risks*, second ed., University Press, New York: Oxford, 2008, pp. 265–276.
- B. Samuelsson, *J. Biol. Chem.* 287 (2012) 10070–10080.
- C.N. Serhan, N.A. Petasis, *Chem. Rev.* 111 (2011) 5922–5943, and references cited therein.
- C.N. Serhan, N. Chiang, *Curr. Opin. Pharmacol.* 13 (2013) 632–640.
- C.N. Serhan, Pro-resolving lipid mediators are leads for resolution physiology, *Nature* 510 (2014) 92–101.
- J.N. Fullerton, D.W. Gilroy, *Nat. Rev. Drug Discov.* 15 (2016) 551–567.
- J. Dallii, *Mol. Asp. Med.* 58 (2017) 12–20.
- (a) C.N. Serhan, C.B. Clish, J. Brannon, S.P. Colgan, N. Chiang, K. Gronert, *J. Exp. Med.* 192 (2000) 1197–1204; (b) M. Arita, M. Yoshida, S. Hong, E. Tjonahen, J.N. Glickman, N.A. Petasis, R.S. Blumberg, C.N. Serhan, *Proc. Natl. Acad. Sci.* 102 (2005) 7671–7676.
- Y. Isobe, M. Arita, S. Matsueda, R. Iwamoto, T. Fujihara, H. Nakanishi, R. Taguchi, K. Masuda, K. Sasaki, D. Urabe, M. Inoue, H. Arai, *J. Biol. Chem.* 23 (2012) 10525–10534.
- (a) M. Aursnes, J.E. Tungen, A. Vik, R. Colas, C.Y.C. Cheng, J. Dallii, C.N. Serhan, T.V. Hansen, *J. Nat. Prod.* 77 (2014) 910–916; (b) T.V. Hansen, A. Vik, C.N. Serhan, *Front. Pharmacol.* 9 (2019) 1582–1598; (c) T.V. Hansen, J. Dallii, C.N. Serhan, *Prostaglandins Other Lipid Mediat.* 133 (2017) 103–110; (d) A. Vik, J. Dallii, T.V. Hansen, *Bioorg. Med. Chem. Lett.* 27 (2017) 2259–2266; (e) J.E. Tungen, M. Aursnes, I. Vlasakov, R.A. Colas, J. Dallii, C.N. Serhan, T.V. Hansen, *J. Nat. Prod.* 78 (2015) 2924–2931; (f) J.E. Tungen, M. Aursnes, S. Ramon, R.A. Colas, C.N. Serhan, D.E. Olberg, S. Nuruddin, F. Willoch, T.V. Hansen, *Org. Biomol. Chem.* 16 (2018) 6818–6823; (g) J.E. Tungen, M. Aursnes, J. Dallii, H. Arnardottir, C.N. Serhan, T.V. Hansen, *Chem. Eur. J.* 20 (2014) 14575–14578; (h) S. Ramon, J. Dallii, J.M. Sanger, J.W. Winkler, M. Aursnes, J.E. Tungen, T.V. Hansen, C.N. Serhan, *Am. J. Pathol.* 186 (2016) 962–973; (i) K.G. Primdahl, M. Aursnes, J.E. Tungen, T.V. Hansen, A. Vik, *Org. Biomol. Chem.* 13 (2015) 5412–5417; (j) J.E. Tungen, M. Aursnes, T.V. Hansen, *Tetrahedron Lett.* 56 (2015) 1843–1846; (k) M. Aursnes, J.E. Tungen, A. Vik, J. Dallii, T.V. Hansen, *Org. Biomol. Chem.* 12 (2014) 432–437; (l) K.G. Primdahl, M. Aursnes, M.E. Walker, R.A. Colas, C.N. Serhan, J. Dallii, T.V. Hansen, A. Vik, *J. Nat. Prod.* 79 (2016) 2693–2702; (m) J.E. Tungen, L. Gerstmann, A. Vik, R. De Mateis, R.A. Colas, J. Dallii, N. Chiang, C.N. Serhan, M. Kalesse, T.V. Hansen, *Chem. Eur. J.* 25 (2019) 1476–1480.
- (a) T. Gobbe, J. Dallii, R.A. Colas, R.F. Canova, M. Aursnes, D. Bonnet, N. Alric l'Vergnolle, C. Deraison, T.V. Hansen, C.N. Serhan, M. Perretti, *Proc. Natl. Acad. Sci. U.S.A.* 114 (2017) 3963–3968; (b) F. Frigerio, G. Pasqualini, I. Craparotta, S. Marchini, E.A. Van Vliet, P. Foerch, C. Vandenplas, K. Leclercq, E. Aronica, L. Porcu, K. Pistorius, R.A. Colas, T.V. Hansen, M. Perretti, R.M. Kaminski, J. Dallii, A. Vezzani, *Brain* 141 (2018) 3130–3143; (c) K. Pistorius, P.R. Souza, R. De Matteis, S. Austin-Williams, K.G. Primdahl, A. Vik, F. Mazzacava, R.A. Colas, R.M. Marques, T.V. Hansen, J. Dallii, *Cell Chem. Biol.* 25 (2018) 749–760; (d) K.G. Primdahl, J.E. Tungen, P.R.S. De Souza, R.A. Colas, J. Dallii, T.V. Hansen, A. Vik, *Org. Biomol. Chem.* 15 (2017) 8606–8613; (e) Y. Tian, M. Aursnes, T.V. Hansen, J.E. Tungen, J.D. Galpin, L. Leisle, C.A. Ahern, R. Xu, S.H. Heinemann, T. Hoshi, *Proc. Natl. Acad. Sci. U.S.A.* 113 (2016) 13905–13910.
- (a) M. Arita, F. Bianchini, J. Aliberti, A. Sher, N. Chiang, S. Hong, R. Yang, N.A. Petasis, C.N. Serhan, *J. Exp. Med.* 201 (2005) 713–722; (b) Petasis N.A. U.S. Pat. Appl. Publ. 2005; 20050228047; (c) N. Ogawa, Y. Kobayashi, *Tetrahedron Lett.* 50 (2009) 6079; (d) M. Allard, K. Barnes, X. Chen, Y.Y. Cheung, B. Duffy, C. Heap, J. Inthavongsay, M. Johnson, R. Krishnamoorthy, C. Manely, S. Steffke, D. Varughese, R. Wang, Y. Wang, C.E. Schwartz, *Tetrahedron Lett.* 52 (2011) 2623–2626; (e) Prakash J. PCT Int. Appl. 2016; WO 2017064701.
- J.M. Nolsøe, M. Aursnes, J.E. Tungen, T.V. Hansen, *J. Org. Chem.* 80 (2015) 5377–5385.
- E.W. Colvin, B.J.J. Hamill, *Chem. Soc. Chem. Commun.* (1973) 151–152; (b) D. Habrant, V. Rauhala, A. Koskinen, *Chem. Soc. Rev.* 39 (2010) 2007–2017.
- I.K. Youn, G.H. Yon, C.S. Pak, *Tetrahedron Lett.* 27 (1986) 2409–2410.
- (a) J. Becher, *Org. Synth.* 59 (1980) 79–84; (b) D. Soulez, G. Ple, L. Duhame, P. Duhamel, *J. Chem. Soc. Perkin Trans. 1* (11) (1997) 1639–1646.
- (a) D.A. Evans, J. Bartroli, T.L. Shih, *J. Am. Chem. Soc.* 103 (1981) 2127–2129; (b) Y. Nagao, W.M. Dai, M. Ochiai, S. Tsukagoshi, E. Fujita, *J. Org. Chem.* 54 (1989) 5211–5217; (c) M. Romero-Ortega, D.F. Colby, H.F. Olivio, *Tetrahedron Lett.* 43 (2002) 6349–6356; (d) R. Tello-Aburto, A. Ochoa-Teran, H.F. Olivio, *Tetrahedron Lett.* 47 (2006) 5915–5917.
- K. Sonogashira, Y. Tohda, N. Hagihara, *Tetrahedron Lett.* 16 (1975) 4467–4470.
- Resolvin E1 was purchased from cayman chemicals, see <https://www.caymanchem.com/product/10007848>.
- M.G. Balta, B.G. Loos, E.A. Nicu, *Front. Immunol.* 8 (2017) 1682.
- T.E. Van Dyke, *J. Clin. Periodontol.* 38 (2011) 119–125.
- (a) M. Arita, T. Ohira, Y.P. Sun, S. Elangovan, N. Chiang, C.N. Serhan, *J. Immunol.* 178 (2007) 3912–3917; (b) M. Arita, F. Bianchini, J. Aliberti, A. Sher, N. Chiang, S. Hong, R. Yang, N.A. Petasis, C.N. Serhan, *J. Exp. Med.* 201 (2005) 713–722.
- W. Boland, N. Schroer, C. Sieler, M. Feigel, *Helv. Chim. Acta* 70 (1987) 1025–1040.





## Supporting Information for

# Stereoselective Synthesis of the Specialized Pro-resolving and Anti-inflammatory Mediator Resolvin E1

**Jannicke I. Nesman<sup>†</sup>, Jørn E. Tungen<sup>†</sup>, Anders Vik<sup>†</sup> and Trond V. Hansen<sup>†\*</sup>**

<sup>†</sup>*Department of Pharmacy, Section for Pharmaceutical Chemistry, University of Oslo, PO Box 1068 Blindern, N-0316 Oslo, Norway*

\**E-mail: [t.v.hansen@farmasi.uio.no](mailto:t.v.hansen@farmasi.uio.no)*

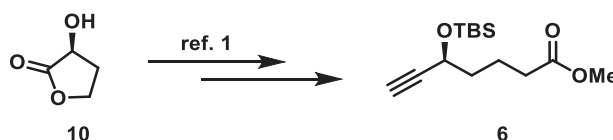
General Information .....	2
Experimental details .....	2
<sup>1</sup> H-NMR and <sup>13</sup> C-NMR Spectra .....	5
HPLC Chromatograms .....	17
UV-Vis spectra .....	19
References .....	20

## General Information

Unless otherwise stated, all commercially available reagents and solvents were used in the form in which they were supplied without any further purification. The stated yields are based on isolated material. All reactions were performed under an argon atmosphere using Schlenk techniques. Reaction flasks were covered with aluminium foil during reactions and storage to minimize exposure to light. Thin layer chromatography was performed on silica gel 60 F254 aluminum-backed plates fabricated by Merck. Flash column chromatography was performed on silica gel 60 (40-63  $\mu\text{m}$ ) produced by Merck. NMR spectra were recorded on a Bruker AVI600, Bruker AVII400 or a Bruker DPX300 spectrometer at 600 MHz, 400 MHz or 300 MHz respectively for  $^1\text{H}$  NMR and at 150 MHz, 100 MHz or 75 MHz respectively for  $^{13}\text{C}$  NMR. Coupling constants ( $J$ ) are reported in hertz and chemical shifts are reported in parts per million ( $\delta$ ) relative to the central residual protium solvent resonance in  $^1\text{H}$  NMR ( $\text{CDCl}_3 = \delta 7.26$ ,  $\text{DMSO}-d_6 = \delta 2.50$  and  $\text{MeOD}-d_4 = \delta 3.31$ ) and the central carbon solvent resonance in  $^{13}\text{C}$  NMR ( $\text{CDCl}_3 = \delta 77.00$  ppm,  $\text{DMSO}-d_6 = \delta 39.43$  and  $\text{MeOD}-d_4 = \delta 49.00$ ). Optical rotations were measured using a 1 mL cell with a 1.0 dm path length on a Perkin Elmer 341 polarimeter. Mass spectra were recorded at 70 eV on a Micromass Prospec Q or Micromass QTOF 2 W spectrometer using ESI as the method of ionization. High-resolution mass spectra were recorded at 70 eV on a Micromass Prospec Q or Micromass QTOF 2W spectrometer using ESI as the method of ionization. HPLC-analyses were performed using a C18 stationary phase (Eclipse XDB-C18, 4.6 x 250 mm, particle size 5  $\mu\text{m}$ , from Agilent Technologies), applying the conditions stated. The UV/Vis spectrum was recorded using an Agilent Technologies Cary 8485 UV-VIS spectrophotometer using quartz cuvettes.

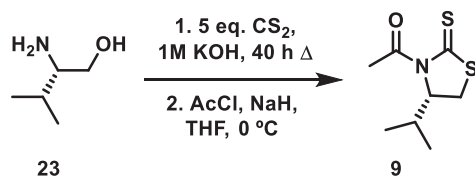
## Experimental details

### Methyl (*S*)-5-((*tert*-butyldimethylsilyl)oxy)hept-6-ynoate (**6**)



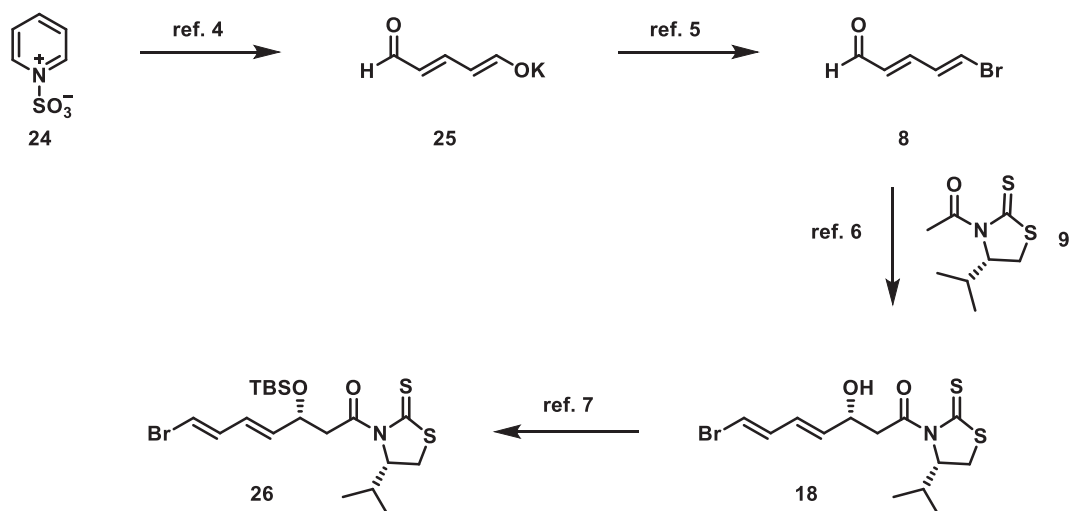
The terminal alkyne **6**, was prepared from commercially available (*S*)-(-)- $\alpha$ -hydroxy- $\gamma$ -butyrolactone **10** as previously reported in the literature.<sup>1</sup> Yield: 24% over the 6 steps. All spectroscopic and physical data were in agreement with those reported in the literature.<sup>1</sup>  $[\alpha]_D^{20} = -36$  ( $c = 0.20$ , MeOH);  $^1\text{H}$  NMR (400 MHz,  $\text{CDCl}_3$ )  $\delta$  4.37 (td,  $J = 6.0, 2.1$  Hz, 1H), 3.67 (s, 3H), 2.39-2.32 (m, 3H), 1.83-1.66 (m, 4H), 0.9 (s, 9H), 0.13 (s, 1H), 0.10 (s, 3H);  $^{13}\text{C}$  NMR (101 MHz,  $\text{CDCl}_3$ )  $\delta$  174.0, 85.3, 72.5, 62.5, 51.6, 37.9, 33.8, 25.9 (3C), 20.8, 18.3, -4.4, -5.0; TLC (hexane/Et<sub>2</sub>O 9:1,  $\text{KMnO}_4$ -stain)  $R_f = 0.48$ .

**(S)-4-isopropylthiazolidine-2-thione (9)**



Nagao's chiral auxiliary **9**, was prepared from commercially available (S)-(+)-2-amino-3-methyl-1-butanol (**23**) as previously reported in the literature.<sup>2-3</sup> Yield: 67% over the two steps. All spectroscopic and physical data were in agreement with those reported in the literature.<sup>3</sup>  $[\alpha]_D^{20} = +434$  (c = 0.26, CHCl<sub>3</sub>); <sup>1</sup>H NMR (400 MHz, CDCl<sub>3</sub>) δ 5.15 (ddd, *J* = 7.6, 6.2, 1.2 Hz, 1H), 3.50 (dd, *J* = 11.5, 8.0 Hz, 1H), 3.02 (dd, *J* = 11.5, 1.2 Hz, 1H), 2.77 (s, 3H), 2.45 – 2.28 (m, 1H), 1.06 (d, *J* = 6.8 Hz, 3H), 0.97 (d, *J* = 6.9 Hz, 3H); <sup>13</sup>C NMR (101 MHz, CDCl<sub>3</sub>) δ 203.4, 170.9, 71.40, 30.9, 30.5, 27.1, 19.2, 17.9; TLC (hexane/Et<sub>2</sub>O 9:1, KMnO<sub>4</sub>-stain) *R<sub>f</sub>* = 0.25.

**(R,4E,6E)-7-bromo-3-((tert-butyldimethylsilyl)oxy)-1-((R)-4-isopropyl-2-thioxothiazolidin-3-yl)hepta-4,6-dien-1-one (26)**



Thiazolidinethione **26** was prepared in four steps from commercially available pyridinium-1-sulfonate **24** as previously reported in the literature.<sup>4-7</sup> Yield: 28% over the four steps. Stereoselectivity obtained for compound **18**: dr 15.3:1 (*R*:*S*). All spectroscopic and physical data were in agreement with those reported in the literature.<sup>7</sup>  $[\alpha]_D^{20} = +265$  (c = 0.40, CHCl<sub>3</sub>); <sup>1</sup>H NMR (400 MHz, CDCl<sub>3</sub>) δ 6.69 (dd, *J* =

13.5, 10.9 Hz, 1H), 6.31 (d,  $J = 13.5$  Hz, 1H), 6.15 (dd,  $J = 15.3, 10.9$  Hz, 1H), 5.79 (dd,  $J = 15.4, 6.3$  Hz, 1H), 5.08 – 4.98 (m, 1H), 4.79 – 4.69 (m, 1H), 3.64 (dd,  $J = 16.6, 7.9$  Hz, 1H), 3.47 (dd,  $J = 11.5, 7.8$  Hz, 1H), 3.21 (dd,  $J = 16.6, 4.5$  Hz, 1H), 3.03 (dd,  $J = 11.4, 1.1$  Hz, 1H), 2.43 – 2.29 (m,  $J = 6.9$  Hz, 1H), 1.05 (d,  $J = 6.8$  Hz, 3H), 0.97 (d,  $J = 7.0$  Hz, 3H), 0.86 (s, 9H), 0.05 (s, 3H), 0.03 (s, 3H);  $^{13}\text{C}$  NMR (101 MHz,  $\text{CDCl}_3$ )  $\delta$  203.0, 171.0, 136.9, 127.5, 109.1, 71.8, 69.9, 46.3, 31.0, 30.9, 26.0 (3C), 19.3, 18.2, 18.0, -4.2, -4.8; TLC (hexane/EtOAc, 7:3,  $\text{KMnO}_4$ -stain)  $R_f = 0.56$ .

## **$^1\text{H}$ -NMR and $^{13}\text{C}$ -NMR Spectra**

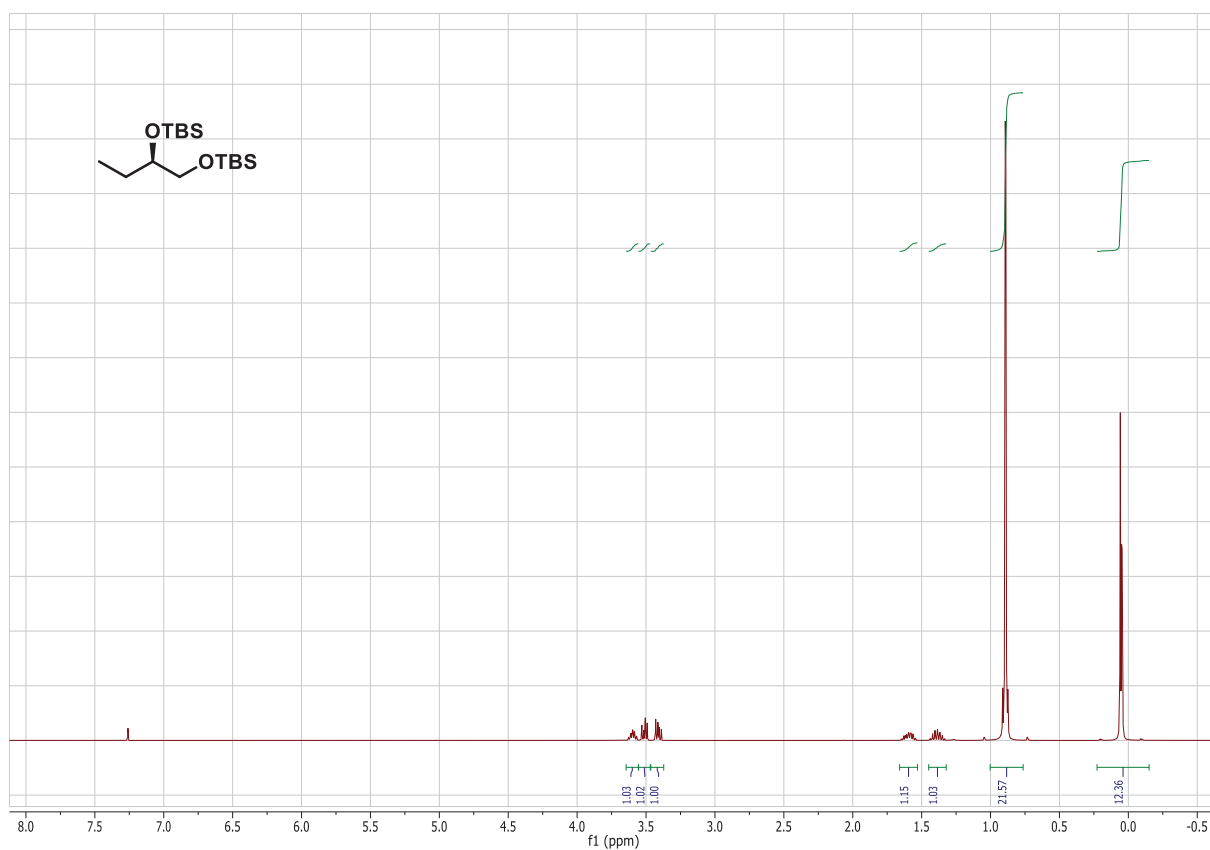


Figure S-1  $^1\text{H-NMR}$  spectrum of compound 11.

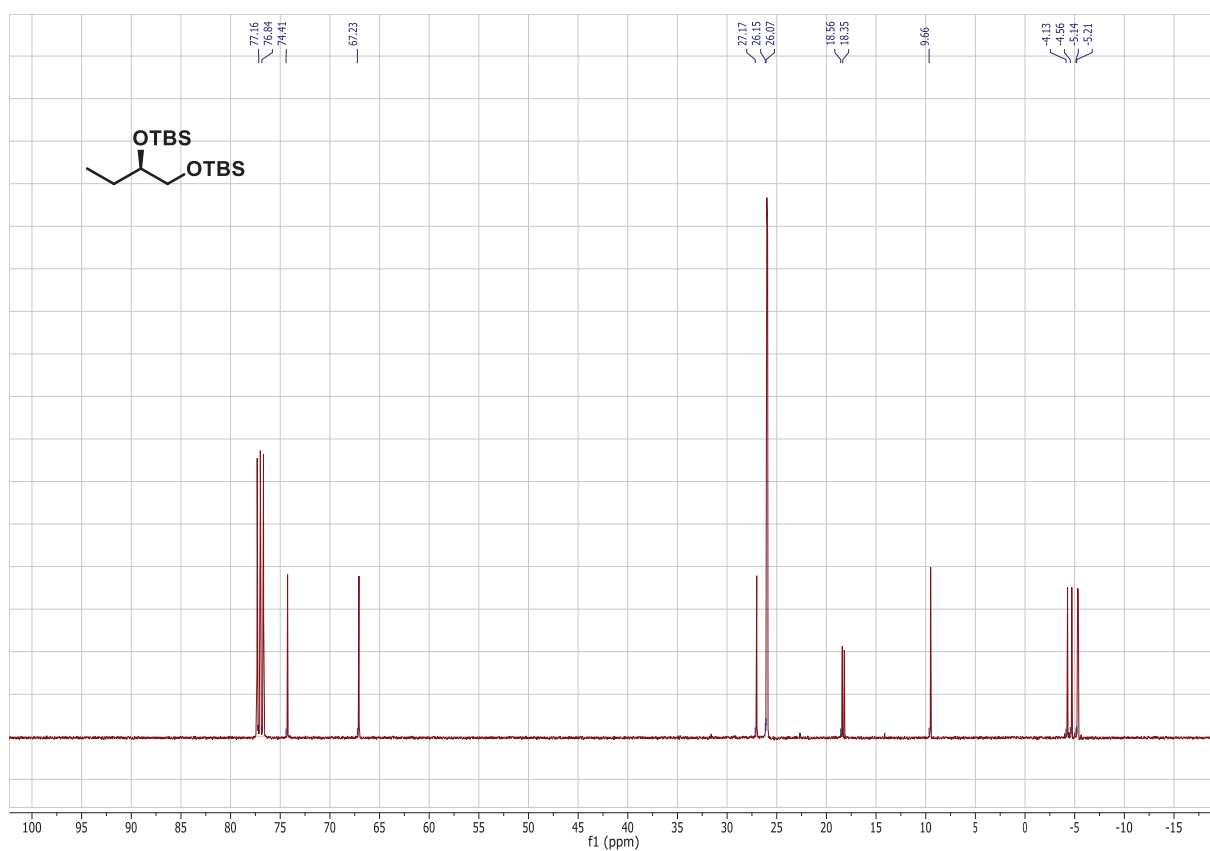


Figure S-2  $^{13}\text{C-NMR}$  spectrum of compound 11.

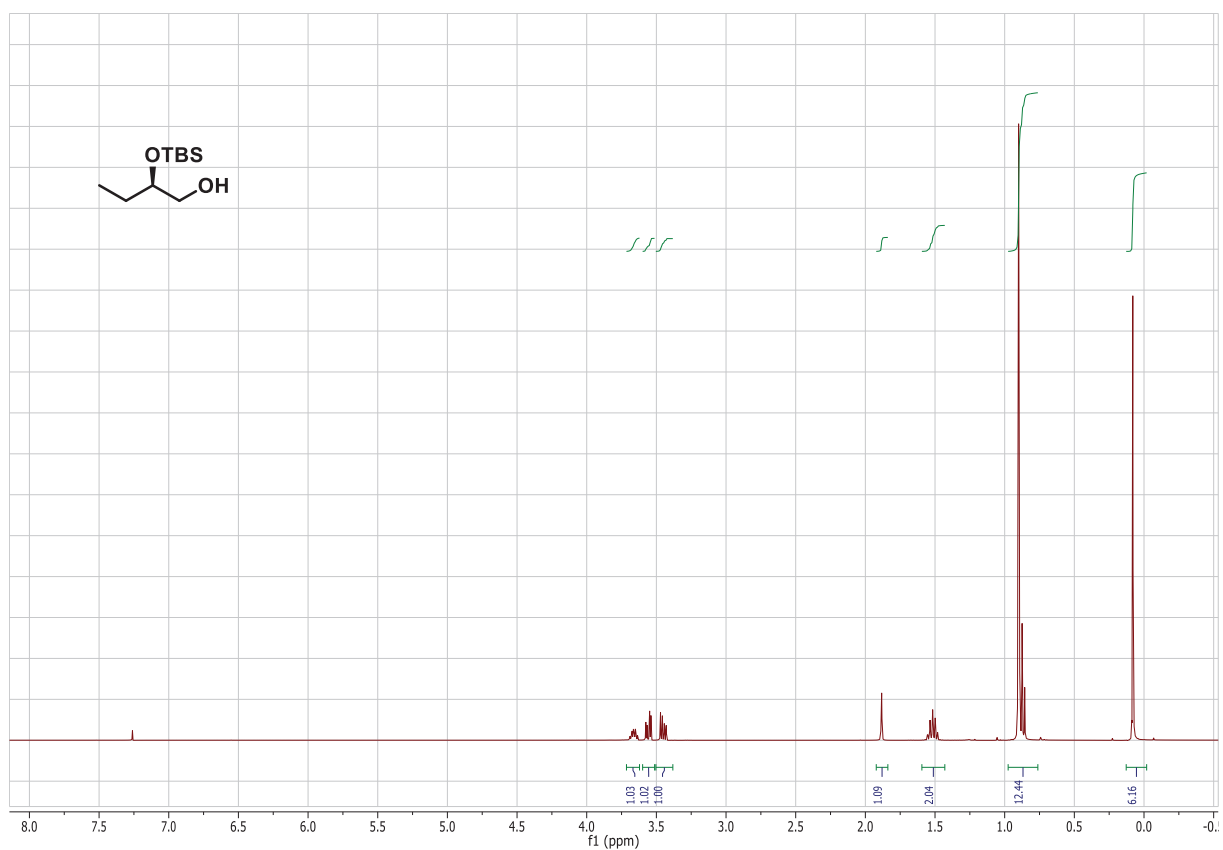


Figure S-3 <sup>1</sup>H-NMR spectrum of compound 12.

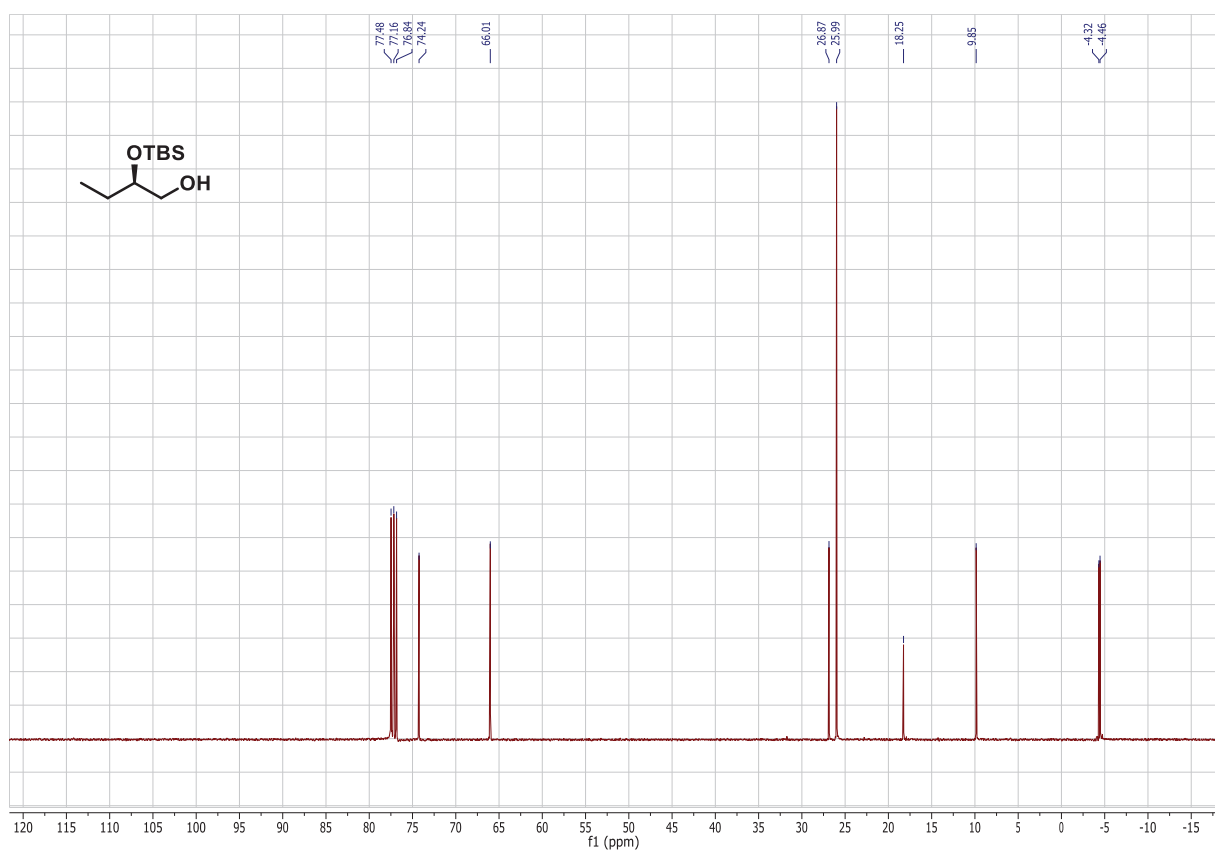


Figure S-4 <sup>13</sup>C-NMR spectrum of compound 12.

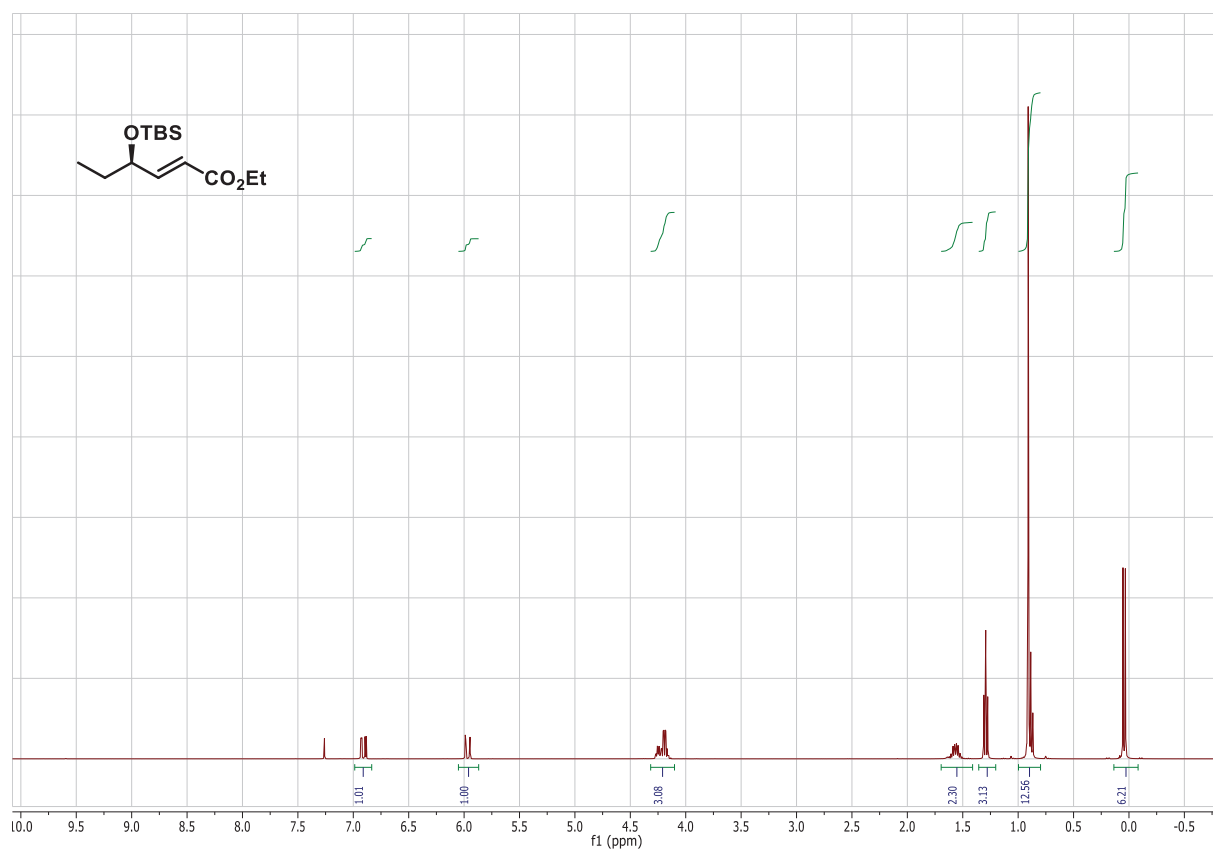


Figure S-5  $^1\text{H-NMR}$  spectrum of compound 14.

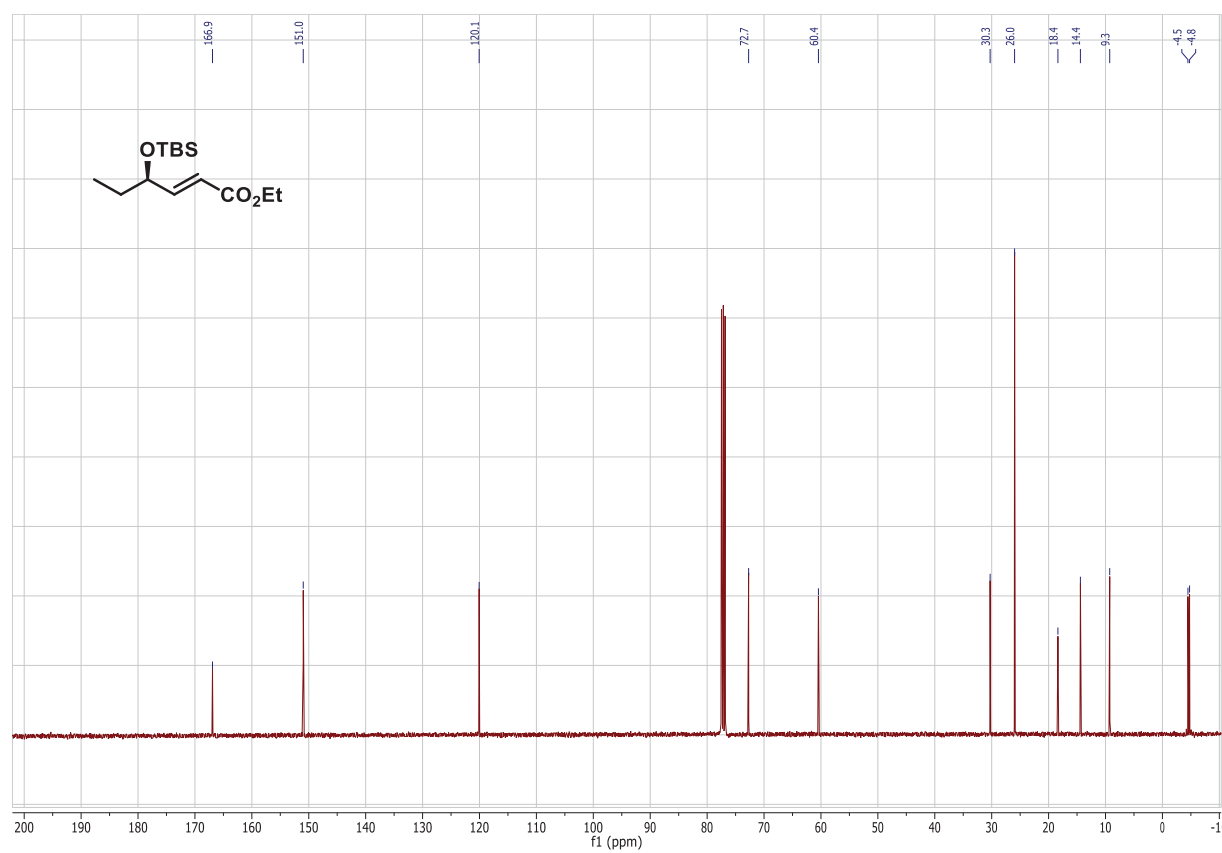


Figure S-6  $^{13}\text{C-NMR}$  spectrum of compound 14.



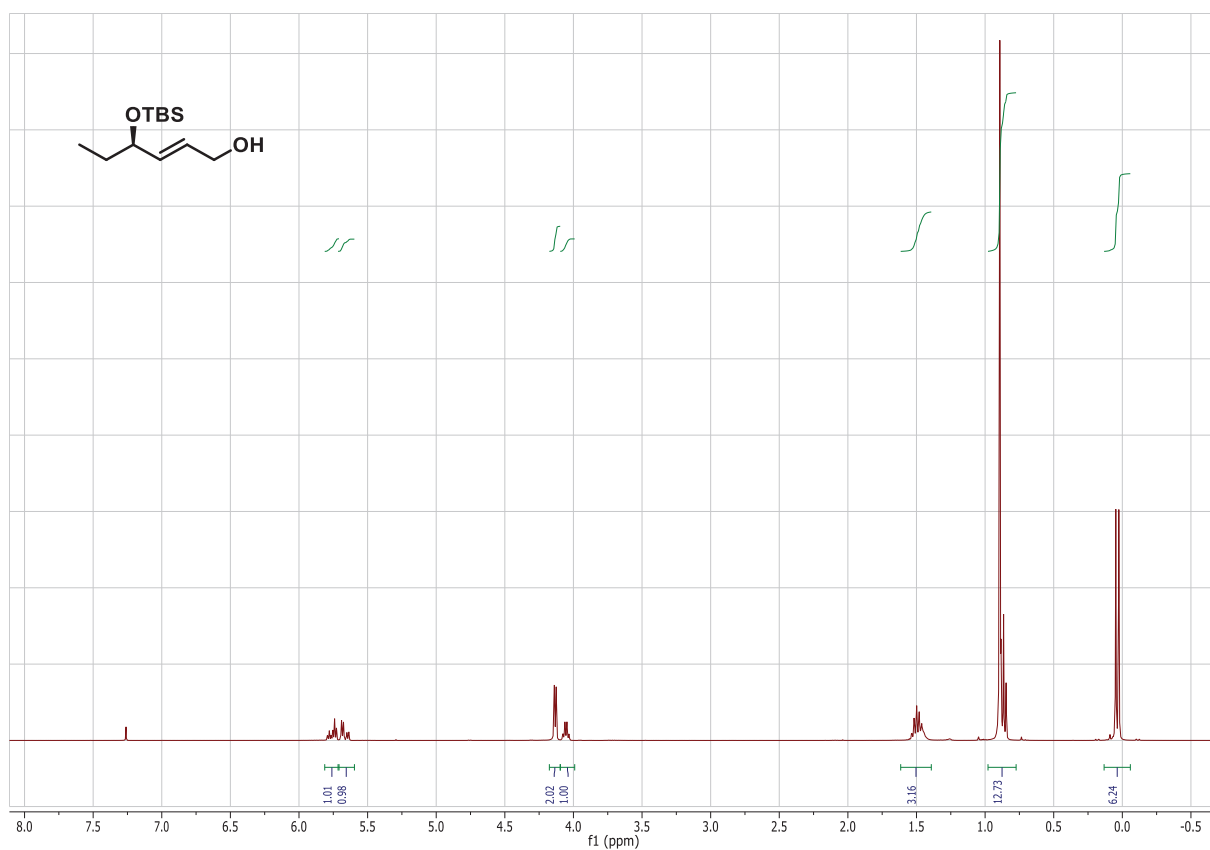


Figure S-7 <sup>1</sup>H-NMR spectrum of compound 15.

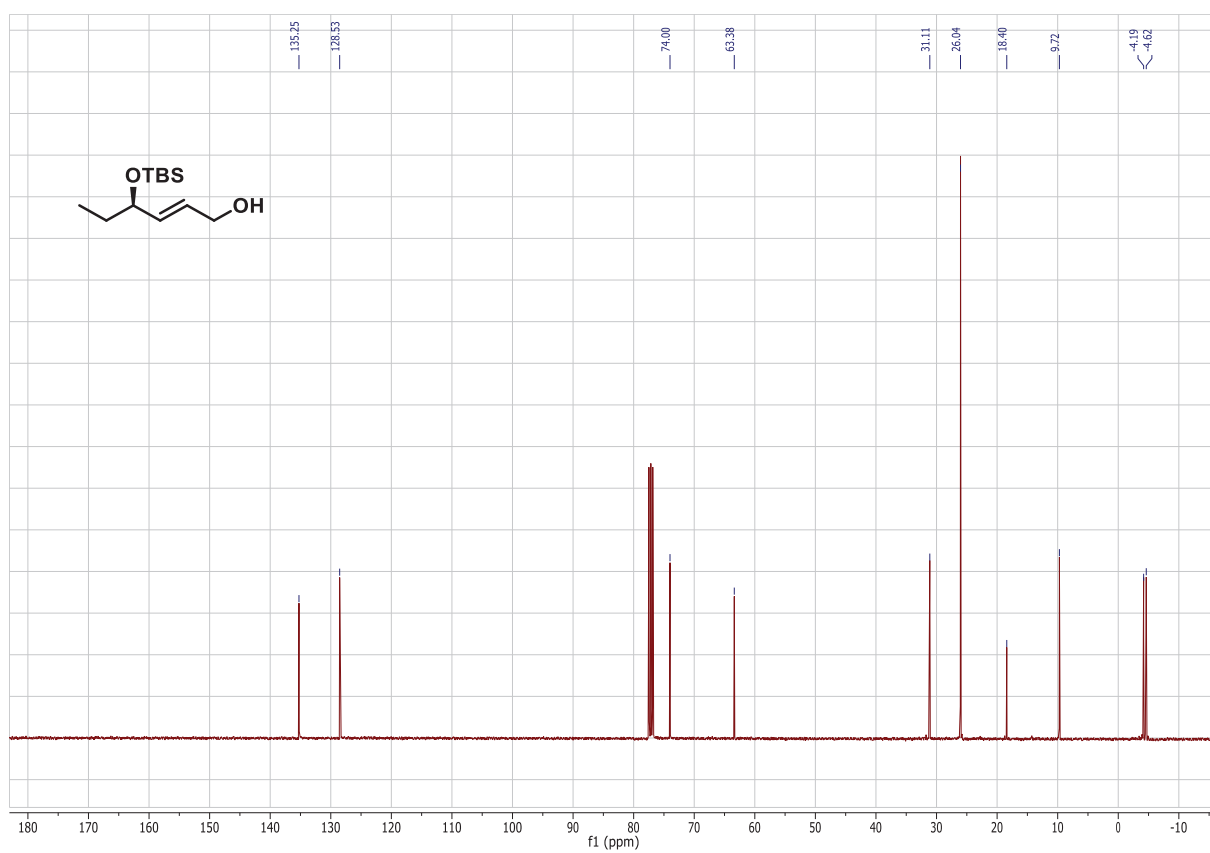


Figure S-8 <sup>13</sup>C-NMR spectrum of compound 15.

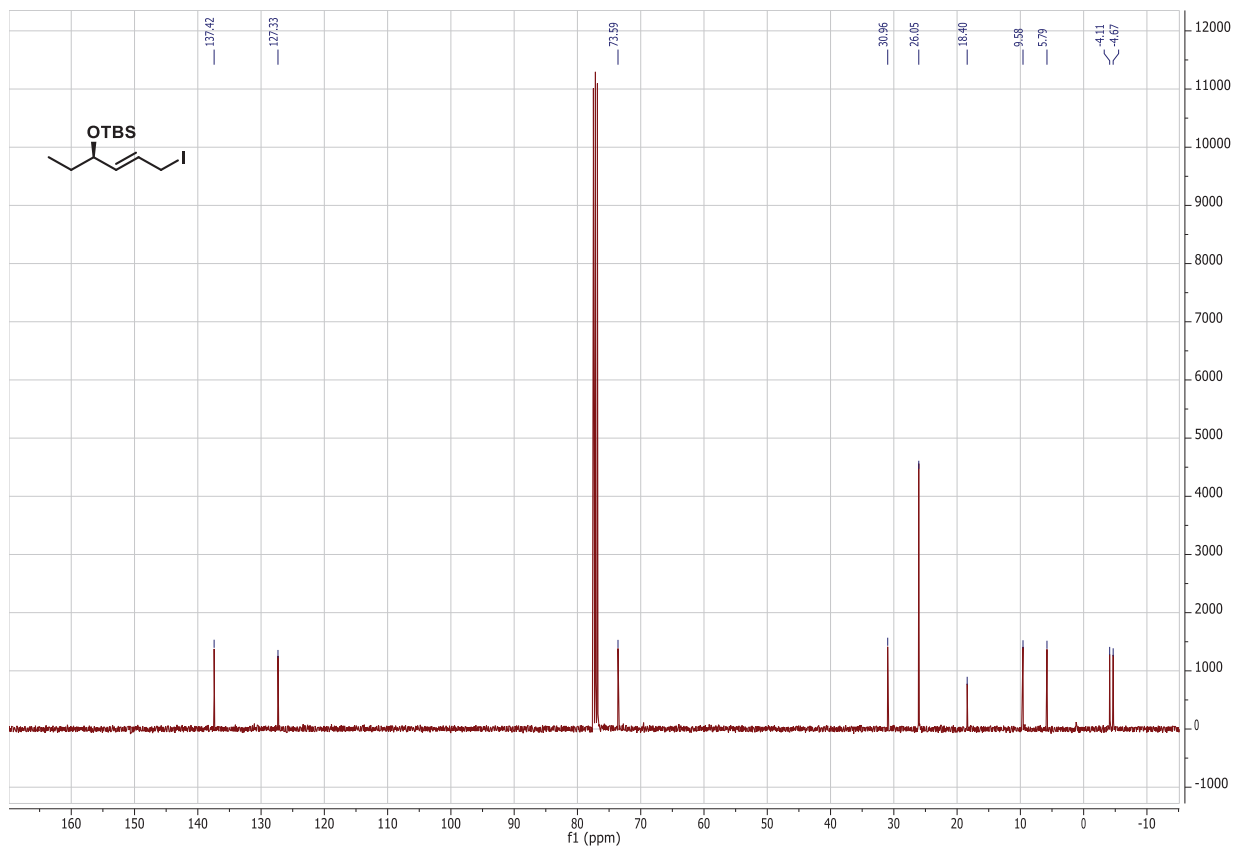


Figure S-9 <sup>1</sup>H-NMR spectrum of compound 16.

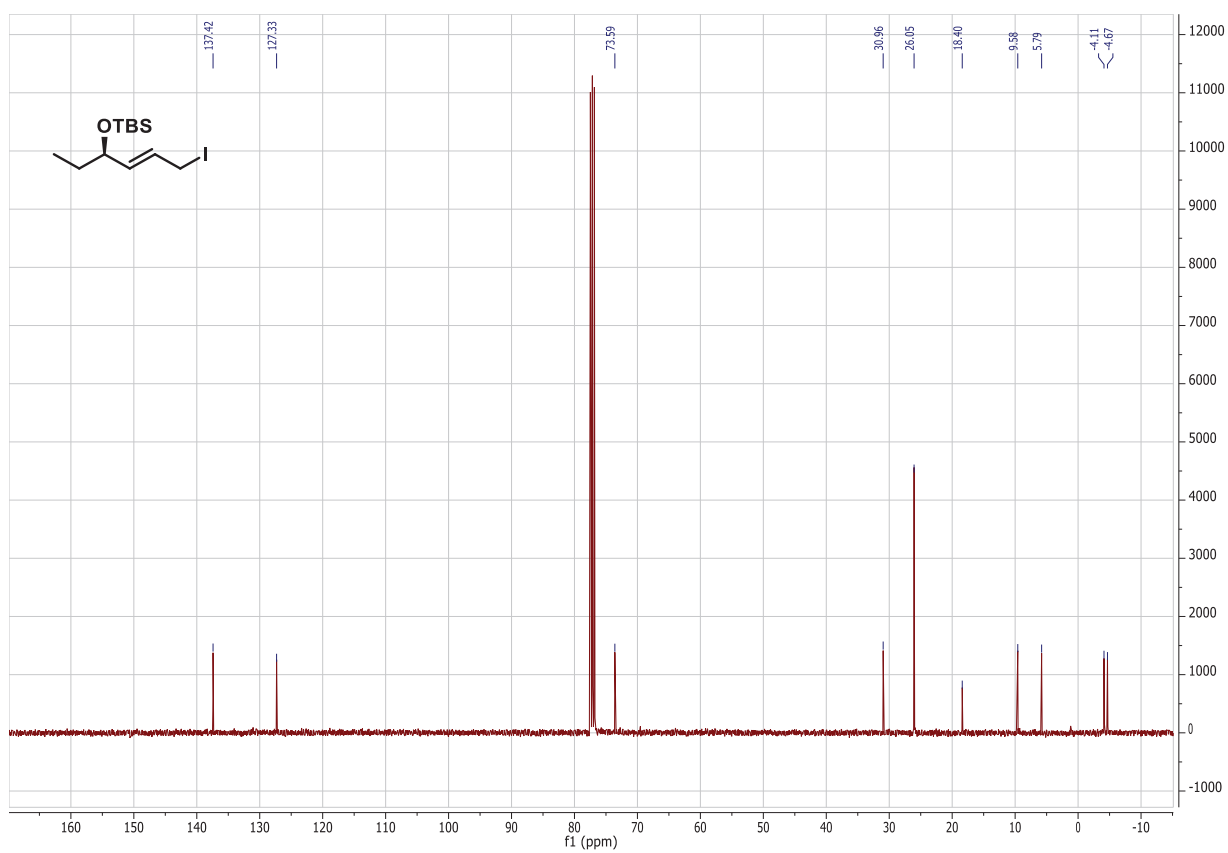
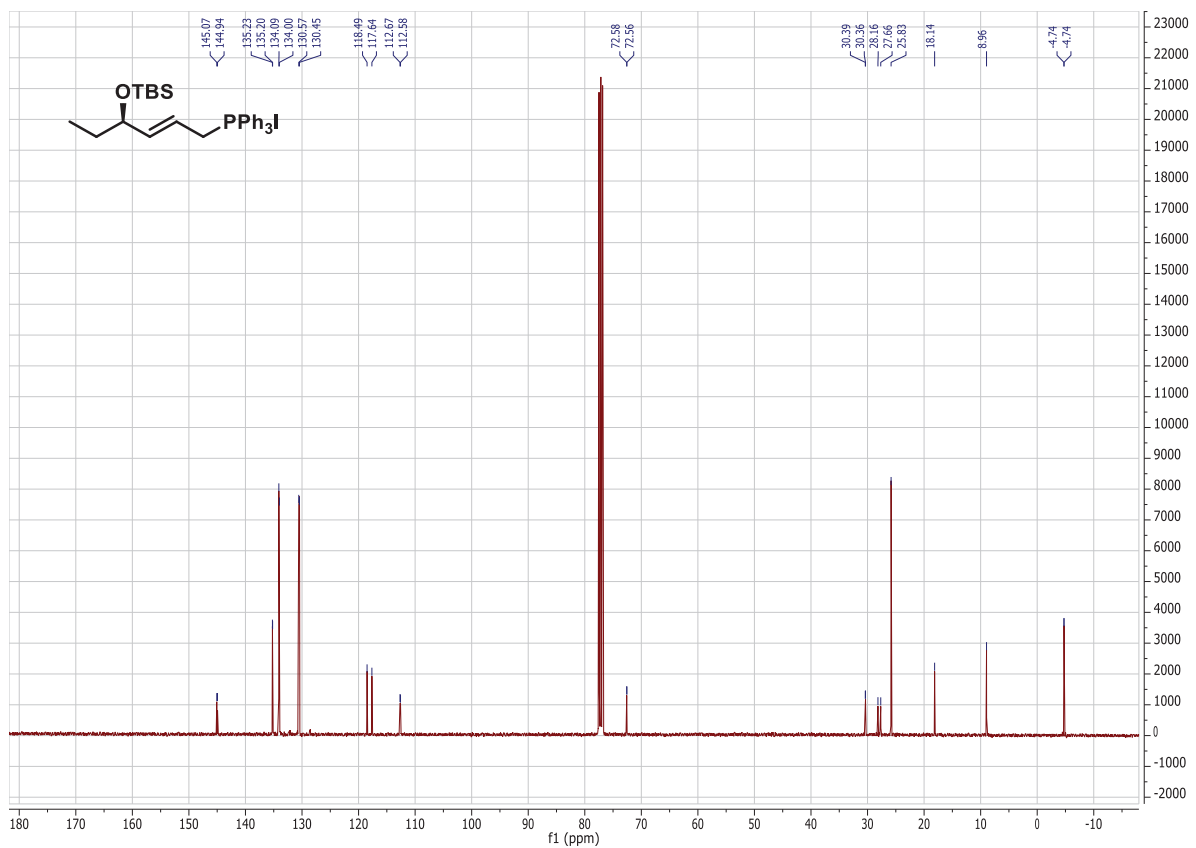
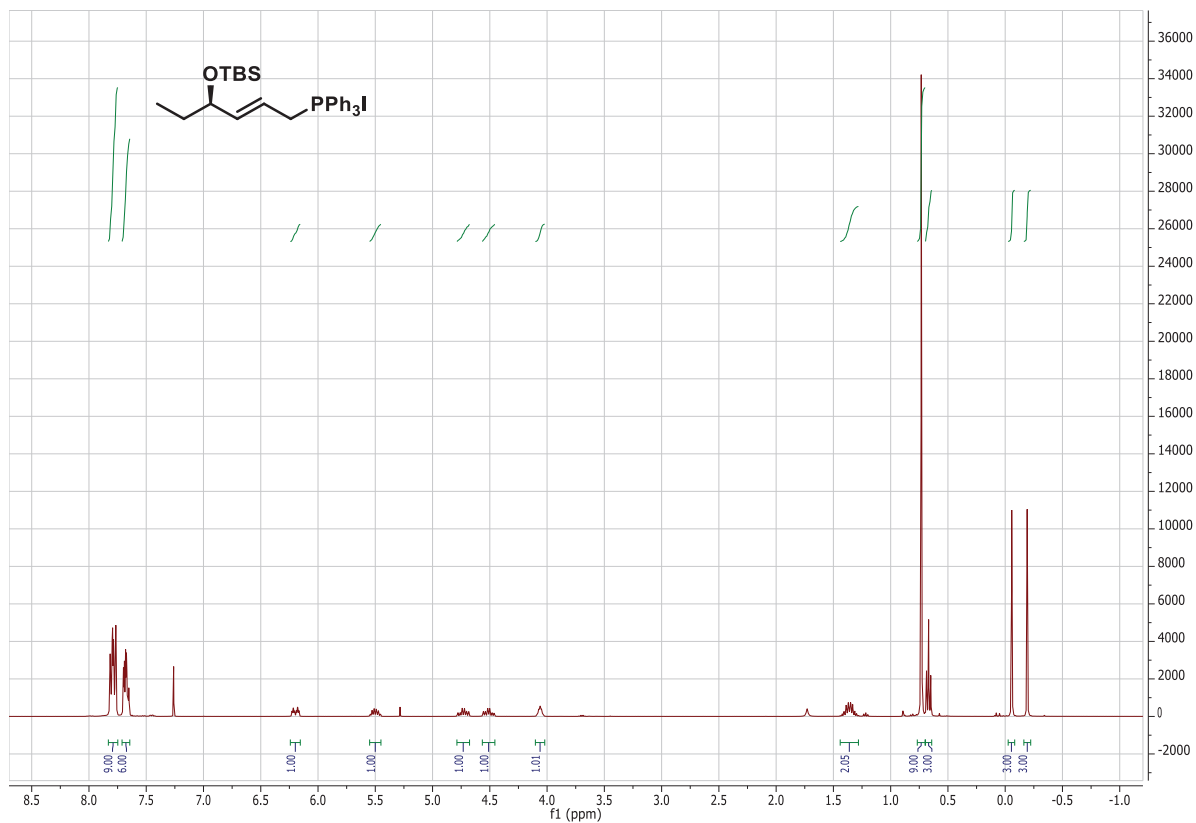


Figure S-10 <sup>13</sup>C-NMR spectrum of compound 16.



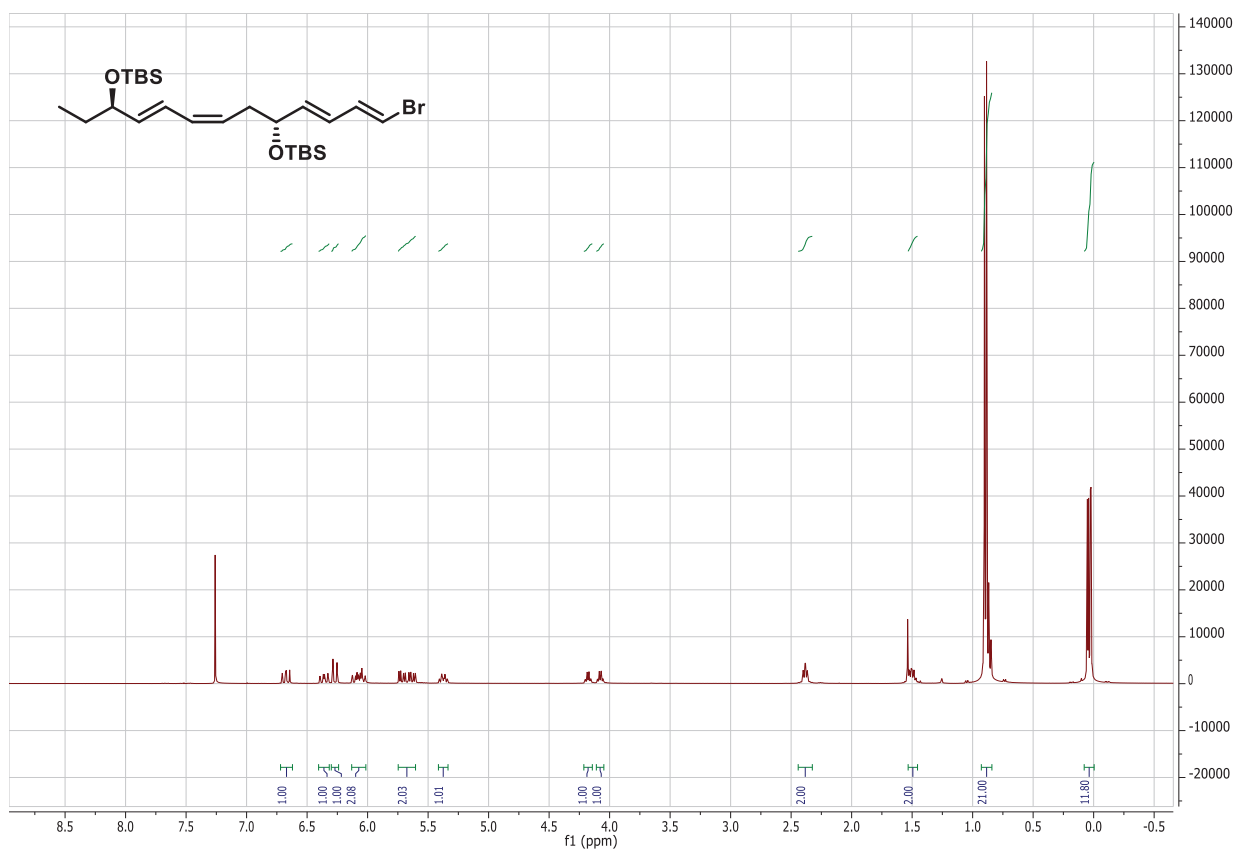


Figure S-13 <sup>1</sup>H-NMR spectrum of compound 19.

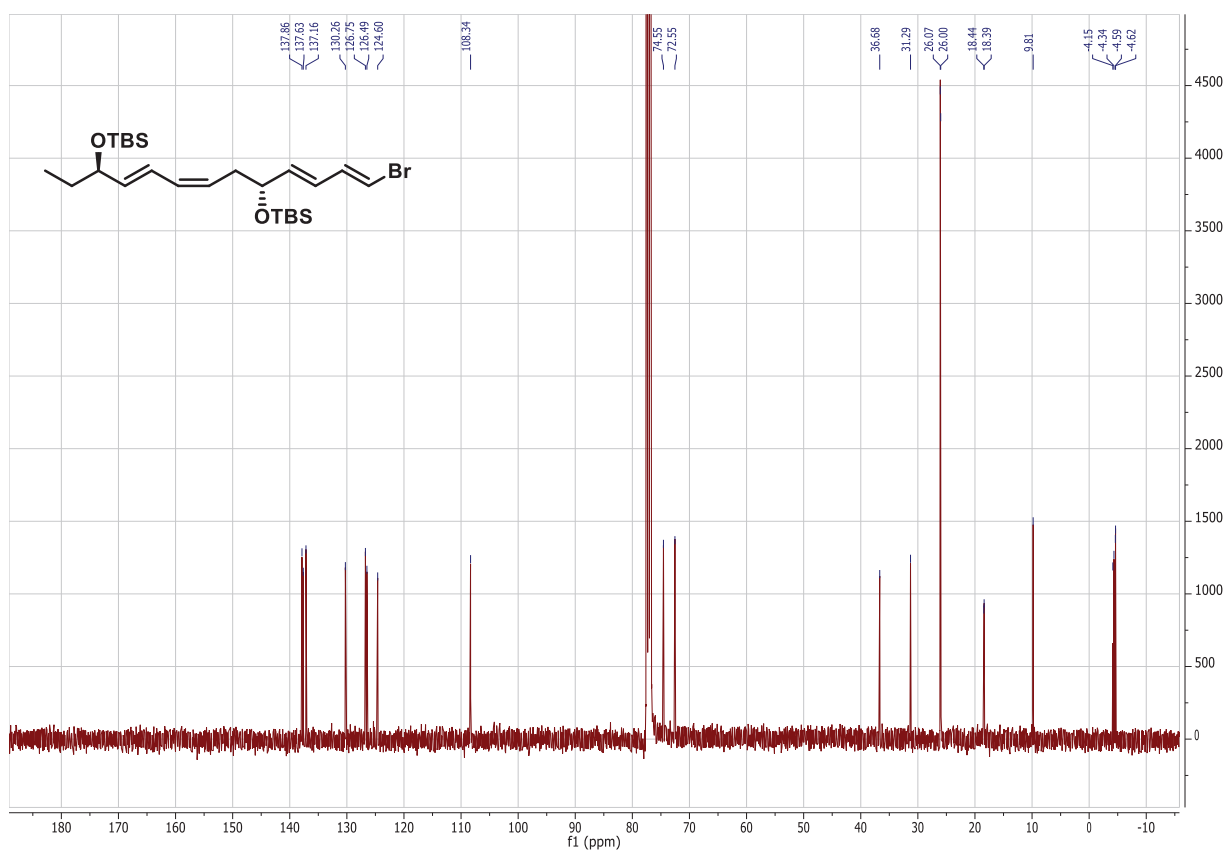


Figure S-14 <sup>13</sup>C-NMR spectrum of compound 19.



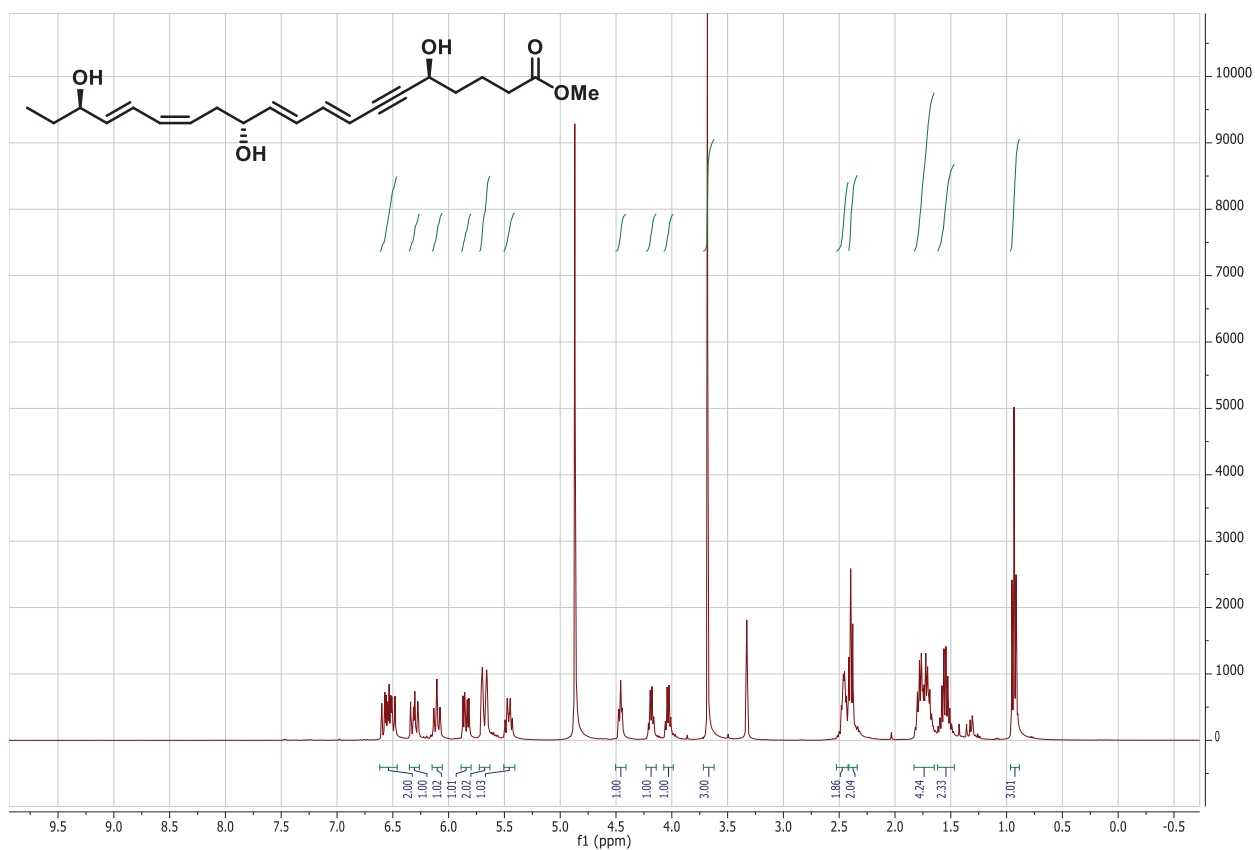


Figure S-17  $^1\text{H-NMR}$  spectrum of compound 21.

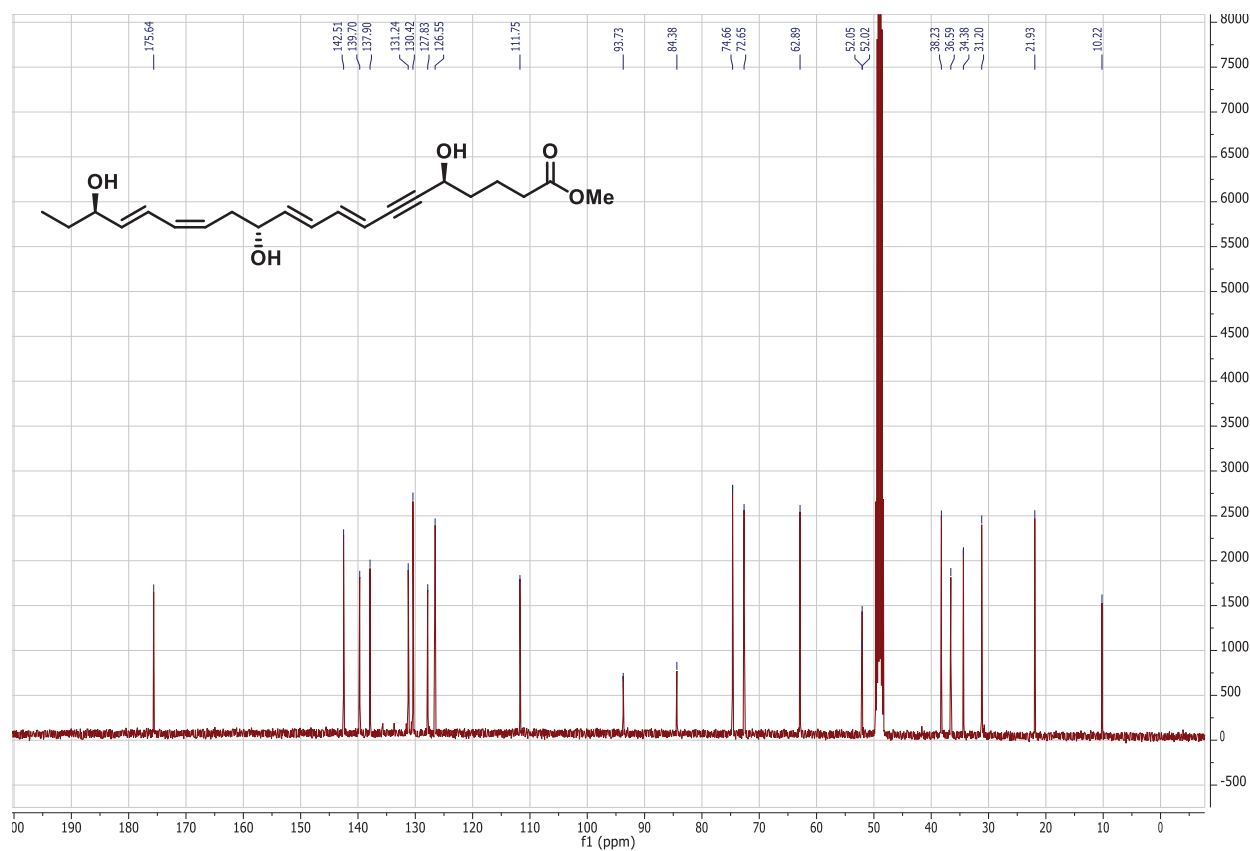


Figure S-18  $^{13}\text{C-NMR}$  spectrum of compound 21.

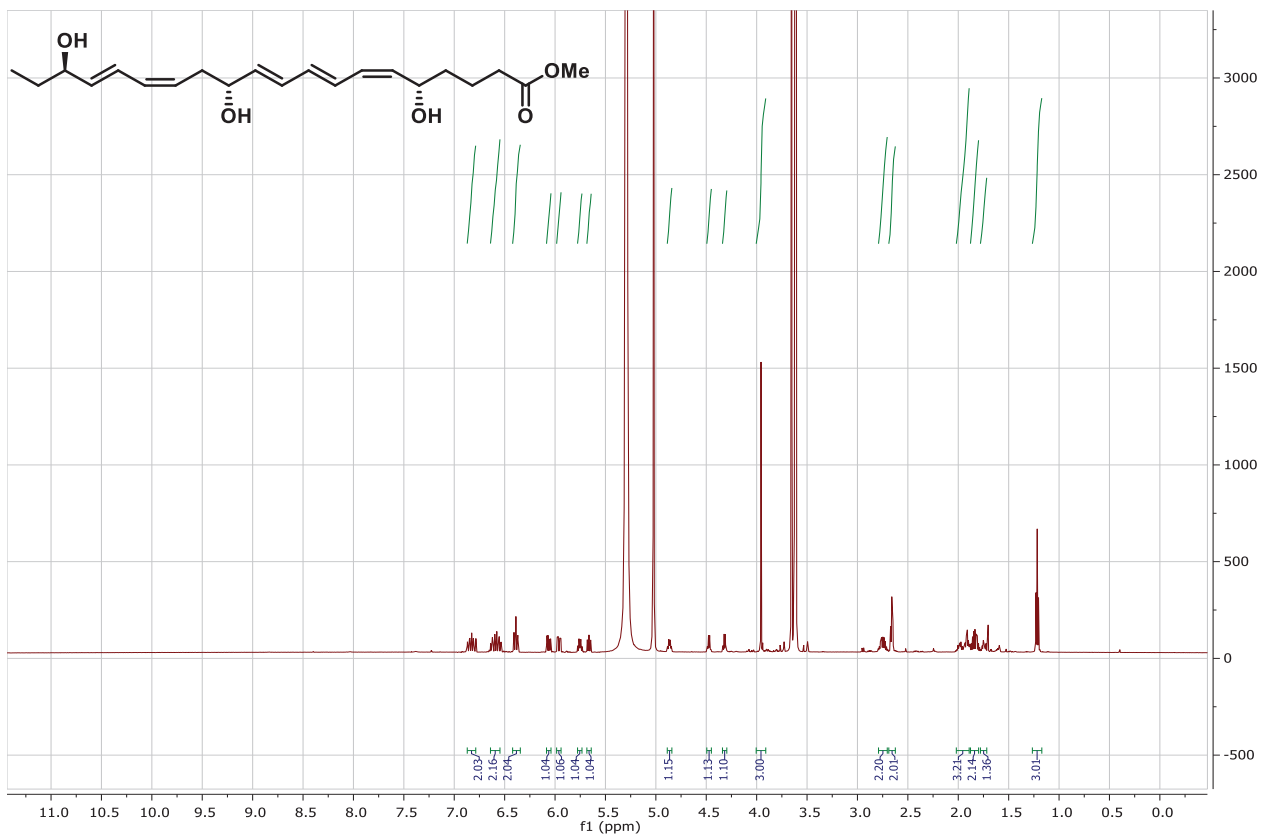


Figure S-19  $^1\text{H-NMR}$  spectrum of compound 22.

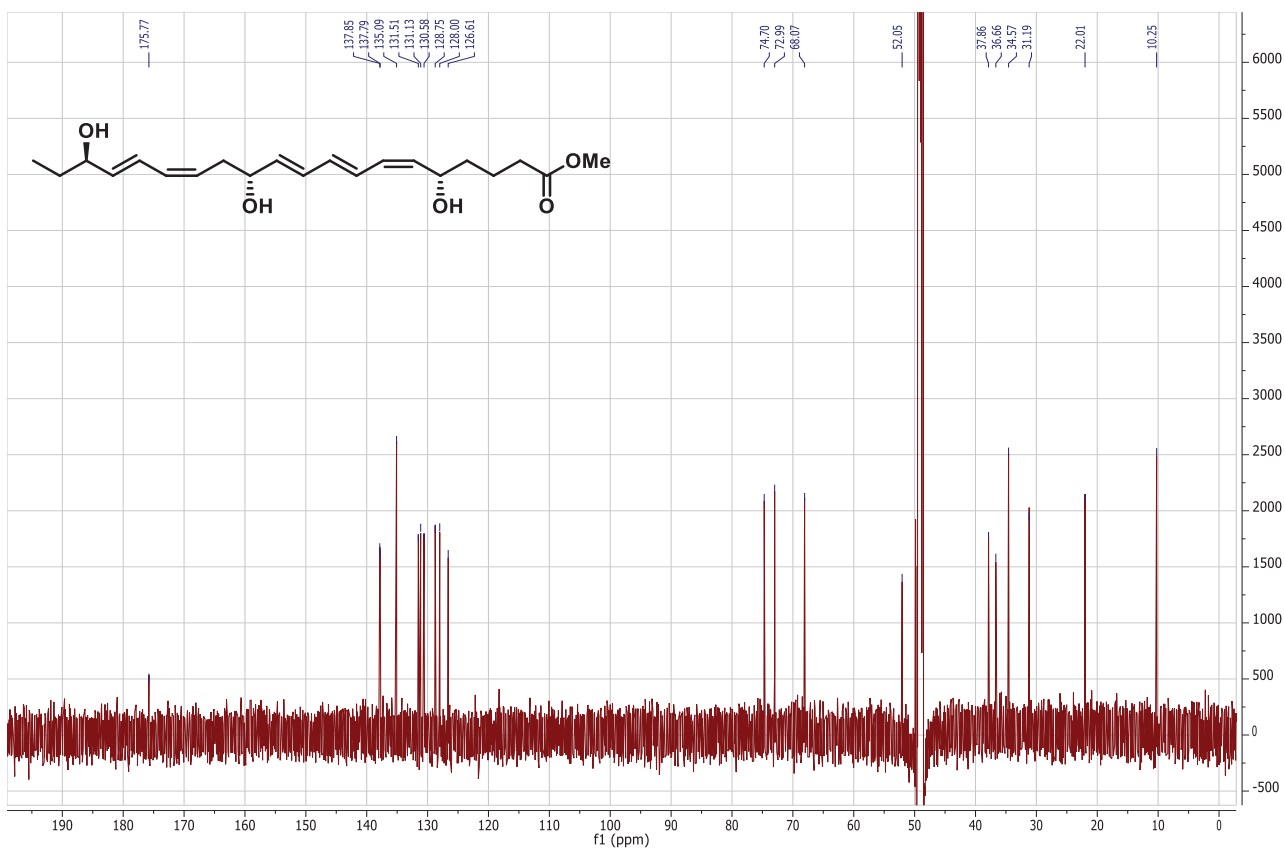


Figure S-20  $^{13}\text{C-NMR}$  spectrum of compound 22.

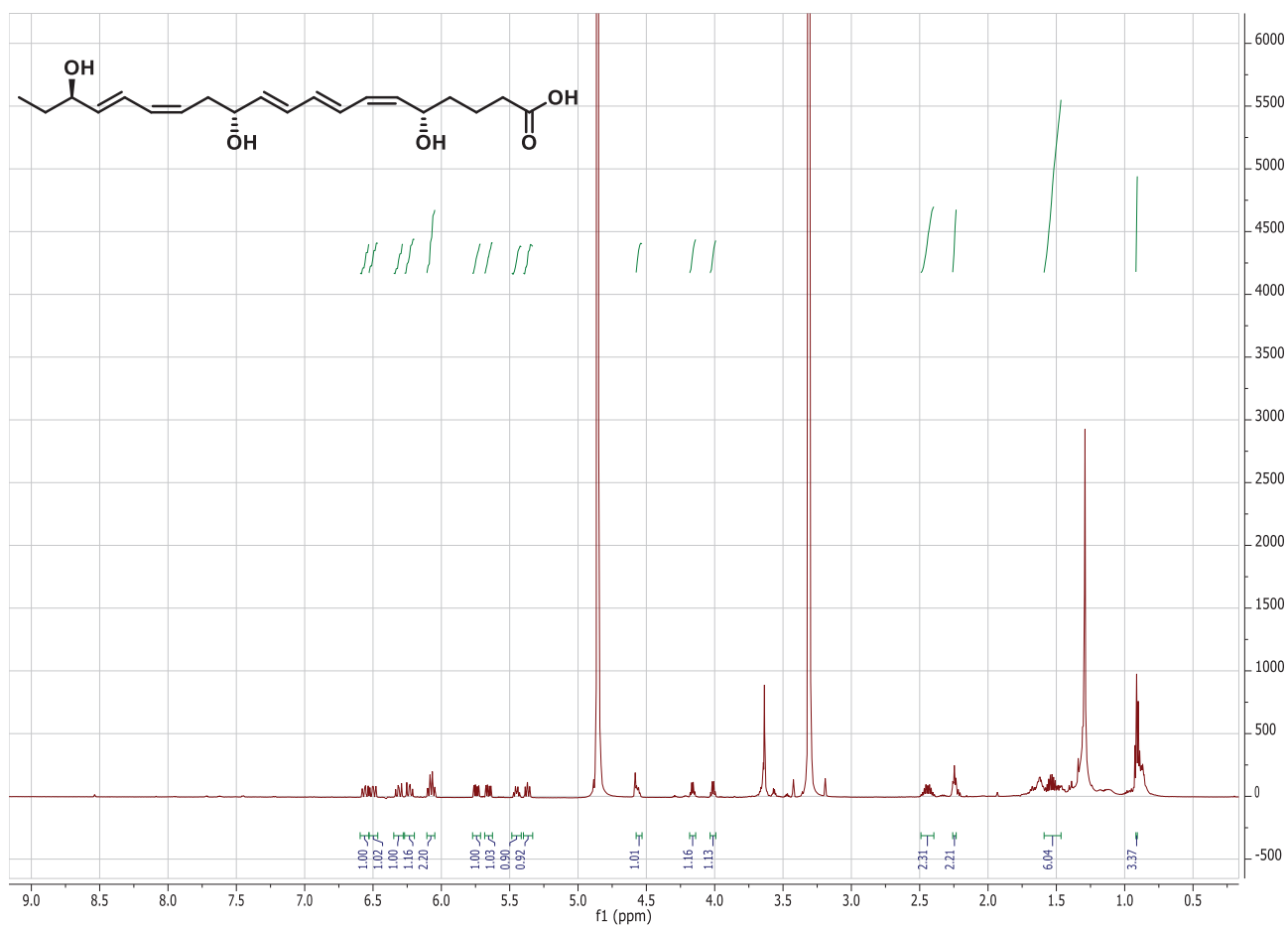
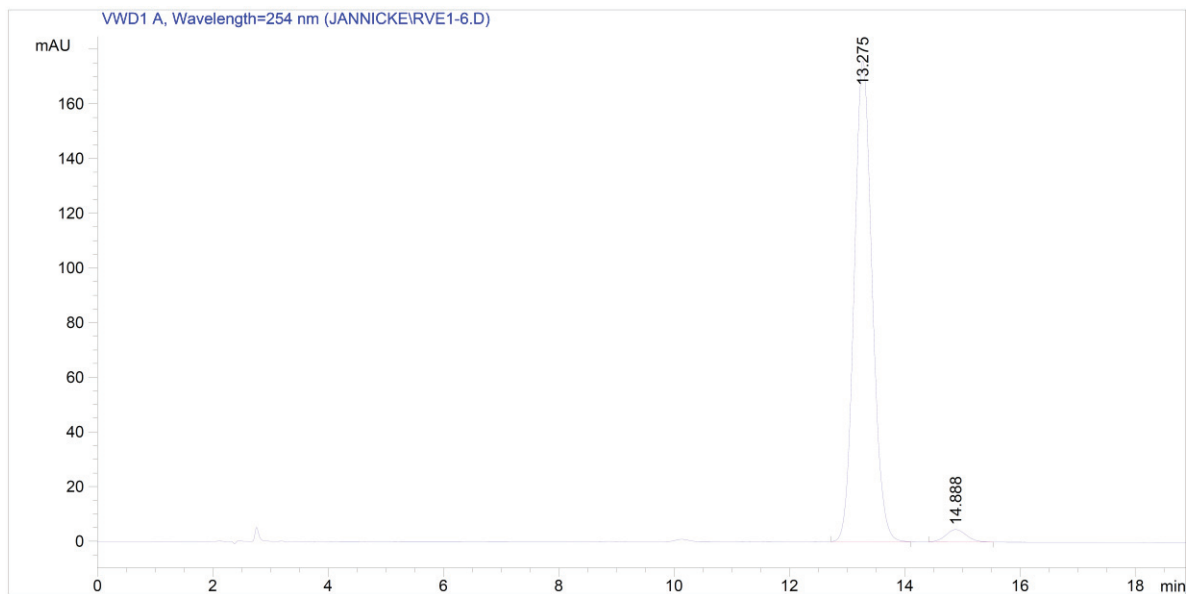


Figure S-21 <sup>1</sup>H-NMR spectrum of Resolvin E1 (1).



## HPLC Chromatograms



=====  
Area Percent Report  
=====

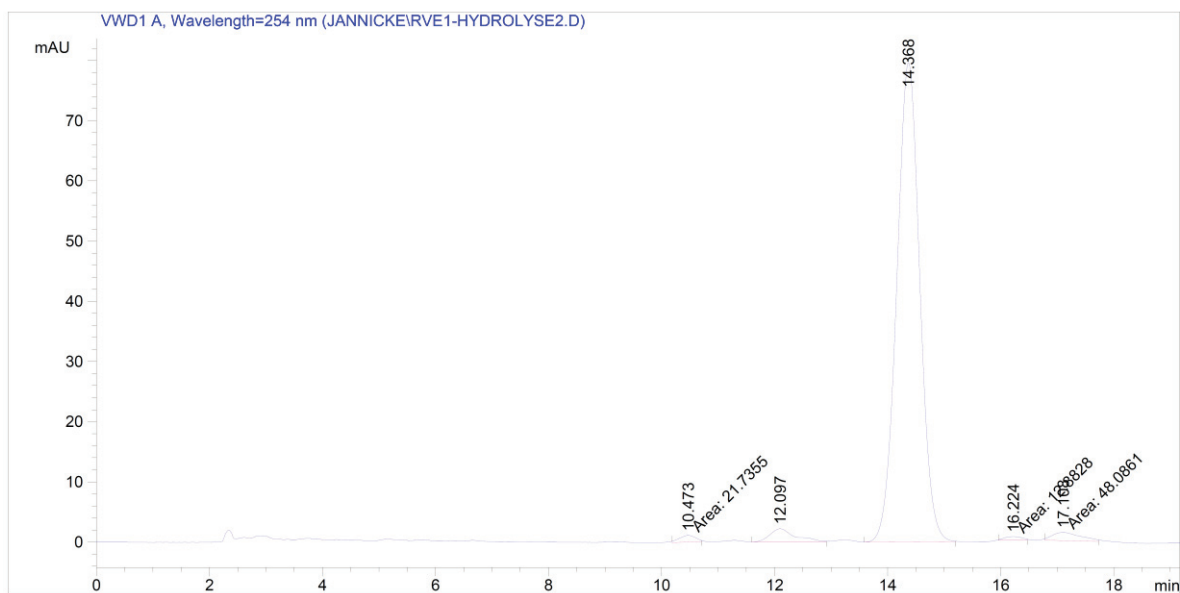
Sorted By : Signal  
Multiplier : 1.0000  
Dilution : 1.0000  
Use Multiplier & Dilution Factor with ISTDs

Signal 1: VWD1 A, Wavelength=254 nm

Peak #	RetTime [min]	Type	Width [min]	Area mAU *s	Height [mAU]	Area %
1	13.275	BB	0.3341	3808.83154	175.94061	97.1350
2	14.888	BB	0.3778	112.34075	4.55906	2.8650

Totals : 3921.17229 180.49967

**Figure S-22** HPLC chromatogram of compound **22**.



=====  
 Area Percent Report  
 =====

Sorted By : Signal  
 Multiplier : 1.0000  
 Dilution : 1.0000  
 Use Multiplier & Dilution Factor with ISTDs

Signal 1: WVD1 A, Wavelength=254 nm

Peak #	RetTime [min]	Type	Width [min]	Area mAU *s	Height [mAU]	Area %
1	10.473	MM	0.3327	21.73546	1.08892	0.9036
2	12.097	BV	0.4538	70.02503	2.21212	2.9112
3	14.368	VB	0.4364	2252.63916	79.60614	93.6505
4	16.224	MM	0.3554	12.88284	6.04135e-1	0.5356
5	17.108	MM	0.5844	48.08612	1.37139	1.9991

Totals : 2405.36861 84.88270

**Figure S-23** HPLC chromatogram of resolin E1 (1).

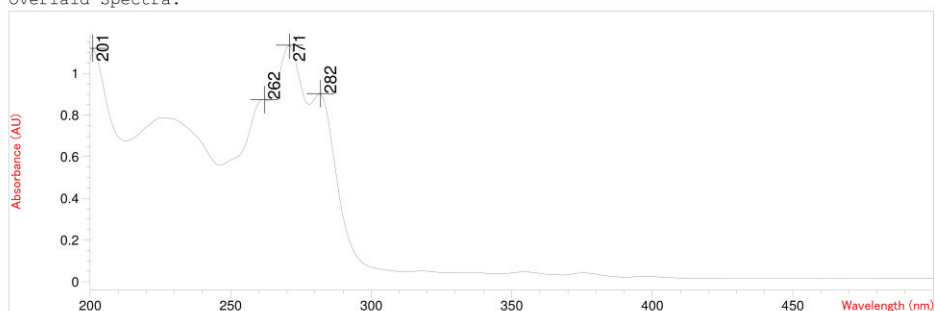
## UV-Vis spectra

Spectrum/Peak Report

Date 6/25/2019 Time 17:26:29 Page 1 of 1

Method file : <method not saved>  
Information : Default Method  
Data File : <data not saved>

Overlaid Spectra:



#	Name	Peaks (nm)	Abs (AU)	#	Name	Peaks (nm)	Abs (AU)
1		271.0	1.13620	1		282.0	0.90360
1		201.0	1.12110	1		262.0	0.87457

Report generated by :

Signature: .....

\*\*\* End Spectrum/Peak Report \*\*\*

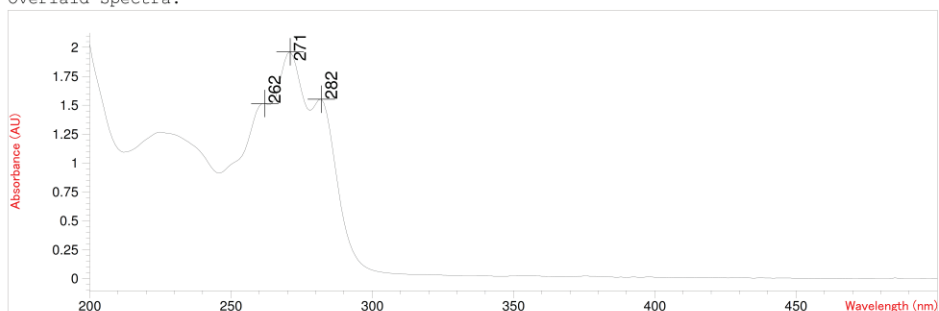
**Figure S-24 UV-Vis chromatogram of compound 22.**

Spectrum/Peak Report

Date 6/11/2019 Time 16:51:17 Page 1 of 1

Method file : <method not saved>  
Information : Default Method  
Data File : <data not saved>

Overlaid Spectra:



#	Name	Peaks (nm)	Abs (AU)	#	Name	Peaks (nm)	Abs (AU)
1		271.0	1.96230	1		262.0	1.51550
1		282.0	1.55260				

Report generated by :

Signature: .....

\*\*\* End Spectrum/Peak Report \*\*\*

**Figure S-25 UV-Vis chromatogram of compound Resolvin E1 (1).**

## References

1. Primdahl, K. G.; Tungen, J. E.; Aursnes, M.; Hansen, T. V.; Vik, A., *Org. Biomol. Chem.* **2015**, *13* (19), 5412.
2. Delaunay, D.; Toupet, L.; Corre, M. L., *J. Org. Chem.* **1995**, *60* (20), 6604.
3. Nagao, Y.; Dai, W. M.; Ochiai, M.; Tsukagoshi, S.; Fujita, E., *J. Org. Chem.* **1990**, *55* (4), 1148.
4. Becher, J., *Org. Synth.* **1979**, *59*, 79.
5. Soullez, D.; Plé, G.; Duhamel, L., *J. Chem. Soc., Perkin Transactions 1.* **1997**, (11), 1639.
6. Romero-Ortega, M.; Colby, D. A.; Olivo, H. F., *Tetrahedron Lett.* **2002**, *43*, 6439.
7. Corey, E. J.; Cho, H.; Rucker, C.; Hua, D. H., *Tetrahedron Lett.* **1981**, *22*, 3455.